



**Royal
HaskoningDHV**
Enhancing Society Together

Section 5 Appendix 5.2 Model Calibration and Validation

[Blank Page]

Northern Gateway Container Terminal

Hydrodynamic and sedimentation studies



Report EX 5250
Release 2.0
May 2006

Document Information

Project	Northern Gateway Container Terminal
Report title	Hydrodynamic and sedimentation studies
Client	Haskoning UK
Client Representative	Matt Simpson
Project No.	DDR 3855
Report No.	EX 5250
Doc. ref.	EX 5250 - Teesport Container Terminal Extension r2-0.doc
Project Manager	J V Baugh
Project Sponsor	Dr M P Dearnaley

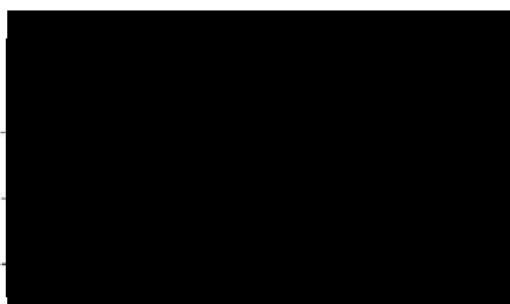
Document History

Date	Release	Prepared	Approved	Authorised	Notes
05/05/06	2.0	jvb	tjc	mpd	Final report
19/01/06	1.0	jvb	mpd		Draft final report
12/01/06	0.1	jvb	mpd		Revisions to draft and further inputs identified
07/12/05	0.0	jvb	mpd		First, incomplete draft

Prepared

Approved

Authorised



© HR Wallingford Limited

HR Wallingford accepts no liability for the use by third parties of results or methods presented in this report. The Company also stresses that various sections of this report rely on data supplied by or drawn from third party sources. HR Wallingford accepts no liability for loss or damage suffered by the client or third parties as a result of errors or inaccuracies in such third party data.

Summary

Teesport Container Terminal Extension

Northern Gateway Container Terminal - Hydrodynamic and sedimentation studies

Report EX 5250

May 2006

PD Teesport is proposing to construct a deep sea container terminal on the site of the existing Container Terminal No. 1, the redundant ex-Shell jetty and the Riverside Ro-Ro No. 3 at Teesport. The construction phase of the scheme comprises capital dredging works in the Tees estuary, reclamation, land-side development and disposal of dredged material. HR Wallingford were commissioned by Royal Haskoning to supply specialist input to address the hydrodynamic and sedimentological effects of the construction on the Tees Estuary and Tees Bay as part of the environmental impact assessment (EIA) of the development.

The findings of the study in terms of the predicted impacts of the development were:

During the construction phase

The sediment plumes resultant from the operation of cutter suction and trailer suction hopper dredgers at the main dredging locations were simulated. For all the dredger simulations the largest rise in peak concentrations and deposition were in the immediate vicinity of the dredger, centred either at the location of the barge loading pontoon or along the line of the trailer dredger track.

Disposal operations during the construction phase were not predicted to lead to enhanced deposition of fine material greater outside the boundary of the disposal areas. The suspended fine sediment concentrations increases were predicted to be less than 5mg/l further than 2km from the boundary of the disposal areas. A short term accumulation of the sand sized fraction within the disposed material at the disposal sites was predicted. However in the medium term the deposited material is predicted to be dispersed from the offshore disposal sites by the tidal currents, a process which would be strongly enhanced by wave effects.

During the operational phase

The scheme is predicted to have a very small effect on water levels with tidal range increased by less than 2mm adjacent to the development and less than 4mm at the Barrage.

Currents were predicted to generally decrease in the deepened areas however an increase in the near bed net landward flow associated with the density driven, gravitational circulation present in the area was also predicted.

The wind waves generated in the estuary are affected by the proposed changes in reflective properties of the Teesport Container Terminal, but are unaffected by the changes to dredging at depth, as they are short period waves.

The modelling of incoming swell waves showed that the deepened channel reflects more wave energy from these long period waves, slightly increasing the significant wave height on the eastern side of the Norse Oil Terminal. This increased reflection within the channel leads to a slight decrease in significant wave height on North Gare Sands and Bran Sands. The pattern of change was similar for all return periods modelled and showed only a slight dependence on the direction of incoming swell. The swell waves do not reach as far up the estuary as the Teesport Container Terminal, and so are unaffected by the reclamation itself.

Summary continued

The predicted volumes of infill of sandy material in the dredged areas for the the existing situation and for the proposed scenario do not change significantly. This is because the seaward parts of the development include only minor dredging (an increase in depth from a currently declared -14.1m CD to -14.5m CD). Deposition in the Estuary system from fine material (clay and silt) was predicted to increase by an average of about 60,000 m³/year due to the enhanced net near bed landward current due to the deepening of the channel.

The dispersion of suspended solids released into Dabholm Gut at Teesport is predicted to be similar after the development. The centre of the plume of suspended particles is predicted to be closer to the east bank of the River Tees than under existing conditions, so that deposition is enhanced near the shore to the north of Dabholm Gut. Some enhancement of deposition from the plume in the upstream turning circle is predicted for larger tide ranges particularly under high freshwater flow conditions.

The tested scheme was further simulated in combination with the proposed deepening of the Seaton Channel to -9m CD. The in combination simulation showed the speed decrease in Seaton Channel would result in deposition of approximately a third of the extra sediment imported due to the Approach Channel deepening.

The sensitivity of the simulation results to a change to the detail of the Approach channel and Seaton Turning circle was tested. This sensitivity test demonstrated no significant difference in the hydrodynamic effects compared to the original scheme.

Contents

<i>Title page</i>	<i>i</i>
<i>Document Information</i>	<i>ii</i>
<i>Summary</i>	<i>iii</i>
<i>Contents</i>	<i>v</i>
1. Introduction.....	1
1.1 During the construction phase.....	1
1.2 During the operational phase.....	1
1.2.1 Effect on tidal propagation.....	1
1.2.2 Effect on current speeds.....	1
1.2.3 Effect on infill rates in dredged areas.....	1
1.2.4 Effect on wave energy.....	2
1.3 Structure of report.....	2
2. Flow modelling.....	3
2.1 Introduction.....	3
2.2 Model set-up.....	3
2.3 Model calibration.....	4
2.4 Impact of scheme.....	7
3. Wave modelling.....	11
3.1 Background.....	11
3.2 The SWAN wave transformation model.....	11
3.3 Application of SWAN model to the Tees Estuary.....	11
3.3.1 Representation of Reflection.....	12
3.4 Wind and wave forcing of the model.....	12
3.4.1 Wind Climate.....	12
3.4.2 Wave Climate.....	14
3.4.3 Results of the wave modelling.....	14
4. Sediment transport.....	21
4.1 Introduction and sediment sources.....	21
4.1.1 Fluvial input.....	21
4.1.2 Industrial input.....	21
4.1.3 Marine input.....	22
4.2 Sand transport.....	22
4.2.1 Introduction.....	22
4.2.2 Methodology.....	23
4.2.3 Selection of conditions modelled.....	23
4.2.4 Existing conditions.....	25
4.2.5 Post construction conditions.....	25
4.2.6 Channel infill prediction due to tidal action with wave enhancement.....	26
4.2.7 Impact on sand transport and morphology.....	27
4.2.8 Conclusions.....	27
4.3 Mud transport.....	28
4.3.1 Introduction.....	28
4.3.2 Methodology.....	28
4.3.3 Existing conditions.....	29
4.3.4 Sensitivity to sediment resuspension.....	29
4.3.5 Post construction conditions.....	30

Contents continued

5.	Sediment dispersion	33
5.1	Introduction.....	33
5.2	Existing maintenance disposal practice	33
5.3	DISPERSION from Dredging operations.....	34
5.3.1	Methodology	34
5.3.2	Dredge parameters used	34
5.3.3	Simulation results.....	36
5.3.4	Conclusions	36
5.4	Dispersion from disposal area(s)	37
5.4.1	Particle size distribution of material to be disposed.....	37
5.4.2	Release of fine material at the offshore disposal sites.....	37
5.4.3	Dispersion of fine sand from the offshore disposal sites.....	38
5.4.4	Behaviour of coarser material at offshore disposal sites.....	39
5.5	Dabholm Gut	39
5.5.1	Methodology	39
5.5.2	Existing conditions.....	40
5.5.3	Proposed layout.....	41
5.5.4	Conclusions	41
6.	In-combination effects for Northern Gateway and Seaton Channel deepening.	43
6.1	Introduction.....	43
6.2	Hydrodynamics.....	43
6.3	Sedimentation	43
7.	Sensitivity test for Tees Approach Channel and Seaton Turning Circle.....	45
7.1	Introduction.....	45
7.2	Simulations undertaken.....	45
8.	Summary and conclusions.....	47
9.	References	49

Tables

Table 2.1	Tidal conditions at the River Tees Entrance	4
Table 2.2	Dates of wet season transects and points extracted.....	5
Table 2.3	Tidal ranges and freshwater discharge on the days relevant to ADCP transects	5
Table 2.4	Description of comparisons made in Figures 9 to 39.....	6
Table 2.5	Impact of scheme on height and timing of high and low waters	9
Table 3.1	Reflection Coefficients used in the SWAN model of Teesport, derived from the formulation of Allsop (1990).....	12
Table 3.2	Observed Wind Climate at South Gare, 1999-2005	13
Table 3.3	Wind conditions used in model runs.....	14
Table 3.4	Offshore swell conditions used in model runs.....	14
Table 3.5	Offshore wave climate: Significant wave height estimated from observations at the waverider buoy, 400m north of Tees North Buoy	15
Table 3.6	Parameters of SWAN model sensitivity tests	17
Table 3.7	Parameters of SWAN model runs for the accompanying sand modelling study	18
Table 3.8	Model results: significant wave height, H _s , at points in the Tees Estuary.....	19
Table 3.9	Locations of output points for model results quoted in Table 3.6	20

Contents continued

Table 4.1	Wave conditions used for wave stirring simulations	24
Table 4.2	Water levels at various tidal states	24
Table 4.3	Wave conditions used for storm simulations	24
Table 4.4	Predicted volumes of channel infill due to tidal action with wave enhancement	26
Table 4.5	Sand percentage composition	26

Figures

Figure 1.1	Study area
Figure 1.2	Proposed development
Figure 2.1	Model domain and bathymetry
Figure 2.2	Model mesh (existing and scheme)
Figure 2.3	Details of proposed scheme
Figure 2.4	Existing and scheme model bathymetry, and change in bathymetry
Figure 2.5	Locations of observations
Figure 2.6	Calibration: dry season
Figure 2.7	Calibration: observation wet season ebb velocity
Figure 2.8	Calibration: observation wet season flood velocity
Figure 2.9	Calibration: observation wet season, mean spring tide at Location M
Figure 2.10	Calibration: observation wet season, mean spring tide at Location N
Figure 2.11	Calibration: observation wet season, mean spring tide at Location O
Figure 2.12	Calibration: observation wet season, mean spring tide at Location P
Figure 2.13	Calibration: observation wet season, mean spring tide at Location Q
Figure 2.14	Calibration: observation wet season, mean spring tide at Location A
Figure 2.15	Calibration: observation wet season, mean spring tide at Location B
Figure 2.16	Calibration: observation wet season, mean spring tide at Location C
Figure 2.17	Calibration: observation wet season, mean spring tide at Location D
Figure 2.18	Calibration: observation wet season, mean spring tide at Location E
Figure 2.19	Calibration: observation wet season, mean spring tide at Location F
Figure 2.20	Calibration: observation wet season, mean spring tide at Location G
Figure 2.21	Calibration: observation wet season, mean spring tide at Location H
Figure 2.22	Calibration: observation wet season, mean spring tide at Location I
Figure 2.23	Calibration: observation wet season, mean spring tide at Location J
Figure 2.24	Calibration: observation wet season, mean spring tide at Location K
Figure 2.25	Calibration: observation wet season, mean spring tide at Location L
Figure 2.26	Calibration: observation wet season, mean tide at Location E
Figure 2.27	Calibration: observation wet season, mean tide at Location F
Figure 2.28	Calibration: observation wet season, mean tide at Location G
Figure 2.29	Calibration: observation wet season, mean tide at Location H
Figure 2.30	Calibration: observation wet season, mean tide at Location I
Figure 2.31	Calibration: observation wet season, mean tide at Location J
Figure 2.32	Calibration: observation wet season, mean tide at Location K
Figure 2.33	Calibration: observation wet season, mean tide at Location L
Figure 2.34	Calibration: observation wet season, mean tide at Location K
Figure 2.35	Calibration: observation wet season, mean tide at Location L
Figure 2.36	Calibration: observation wet season, mean tide at Location M
Figure 2.37	Calibration: observation wet season, mean tide at Location N
Figure 2.38	Calibration: observation wet season, mean tide at Location P
Figure 2.39	Calibration: observation wet season, mean tide at Location Q
Figure 2.40	Dry spring conditions: depth-mean ebb speed – existing, scheme, difference
Figure 2.41	Dry spring conditions: depth-mean flood speed – existing, scheme, difference

Contents continued

- Figure 2.42 Wet spring conditions: depth-mean ebb speed – existing, scheme, difference
Figure 2.43 Wet spring conditions: depth-mean flood speed – existing, scheme, difference
Figure 2.44 Dry neap conditions: depth-mean ebb speed – existing, scheme, difference
Figure 2.45 Dry neap conditions: depth-mean flood speed – existing, scheme, difference
Figure 2.46 Wet neap conditions: depth-mean ebb speed – existing, scheme, difference
Figure 2.47 Wet neap conditions: depth-mean flood speed – existing, scheme, difference
Figure 2.48 Dry spring conditions at Location 1: existing and scheme
Figure 2.49 Dry spring conditions at Location 2: existing and scheme
Figure 2.50 Dry spring conditions at Location 3: existing and scheme
Figure 2.51 Wet spring conditions at Location 1: existing and scheme
Figure 2.52 Wet spring conditions at Location 2: existing and scheme
Figure 2.53 Wet spring conditions at Location 3: existing and scheme
Figure 2.54 Dry neap conditions at Location 1: existing and scheme
Figure 2.55 Dry neap conditions at Location 2: existing and scheme
Figure 2.56 Dry neap conditions at Location 3: existing and scheme
Figure 2.57 Wet neap conditions at Location 1: existing and scheme
Figure 2.58 Wet neap conditions at Location 2: existing and scheme
Figure 2.59 Wet neap conditions at Location 3: existing and scheme
Figure 2.60 Dry spring conditions: ebb velocity near surface and bed – existing, scheme
Figure 2.61 Dry spring conditions: flood velocity near surface and bed – existing, scheme
Figure 2.62 Wet spring conditions: ebb velocity near surface and bed – existing, scheme
Figure 2.63 Wet spring conditions: flood velocity near surface and bed – existing, scheme
Figure 2.64 Dry neap conditions: ebb velocity near surface and bed – existing, scheme
Figure 2.65 Dry neap conditions: flood velocity near surface and bed – existing, scheme
Figure 2.66 Wet neap conditions: ebb velocity near surface and bed – existing, scheme
Figure 2.67 Wet neap conditions: flood velocity near surface and bed – existing, scheme
Figure 3.1 Model bathymetry – existing layout
Figure 3.2 Model Bathymetry – proposed layout (mark on waverider buoy)
Figure 3.3 Model Layout – existing and proposed, map of output points
Figure 3.4 Model results: Significant wave height for 20 m/s winds from 225°N
Figure 3.5 Model results: Significant wave height for 20 m/s winds from 0°N
Figure 3.6 Model results: Significant wave height for 6m swell from 15°N
Figure 3.7 Model results: Significant wave height for 6m swell from 15°N with channel dredged to declared depth of -14.1m CD
Figure 4.1 Dredged volumes for the period 1973 to 2001
Figure 4.2 Chart areas
Figure 4.3 Particle size distribution, 1991 data (after Bridgland (1991))
Figure 4.4 Net tidal deposition for existing condition under representative wave conditions
Figure 4.5 Net tidal sediment transport for existing condition under representative wave conditions
Figure 4.6 Net tidal deposition for existing condition under an extreme wave condition
Figure 4.7 Net tidal sediment transport for existing condition under an extreme wave condition
Figure 4.8 Net tidal deposition for proposed scheme under representative wave conditions
Figure 4.9 Net tidal sediment transport for proposed scheme under representative wave conditions
Figure 4.10 Net tidal deposition for proposed scheme under an extreme wave condition
Figure 4.11 Net tidal sediment transport for proposed scheme under an extreme wave condition
Figure 4.12 Modelled channel infill volumes comparison
Figure 4.13 Significant wave height for existing and scheme. Offshore wave conditions
 $H_s=6.03$, $T_m=9.5s$, $0^\circ N$

Contents continued

- Figure 4.14 Significant wave height differences. Offshore wave conditions $H_s=6.03$, $T_m=9.5s$, $0^\circ N$
- Figure 4.15 Significant wave height for existing and scheme. Offshore wave conditions $H_s=6.03$, $T_m=9.5s$, $15^\circ N$
- Figure 4.16 Significant wave height differences. Offshore wave conditions $H_s=6.03$, $T_m=9.5s$, $15^\circ N$
- Figure 4.17 Significant wave height for existing and scheme. Offshore wave conditions $H_s=6.03$, $T_m=9.5s$, $30^\circ N$
- Figure 4.18 Significant wave height differences. Offshore wave conditions $H_s=6.03$, $T_m=9.5s$, $30^\circ N$
- Figure 4.19 Simulated total annual accretion depths for existing conditions
- Figure 4.20 Sensitivity of accretion predictions to resuspension processes in the Estuary
- Figure 4.21 Simulated total annual accretion depths after development
- Figure 5.1 Simulated dredge locations and sensitive receiver points
- Figure 5.2 Peak concentration and peak deposition for cutter dredger at location 1, spring tide, low flow
- Figure 5.3 Peak concentration and peak deposition for cutter dredger at location 2, spring tide, low flow
- Figure 5.4 Peak concentration and deposition for trailer in approach channel, spring tide, low flow conditions
- Figure 5.5 Time histories of deposition in Seaton Channel (Locations 1 and 2) and Seal Sands (Locations 3 and 4) for TSHD dredging sand in the approach channel, spring tide, low flow conditions
- Figure 5.6 Time histories of concentration in Seaton Channel (Locations 1 and 2) and Seal Sands (Locations 3 and 4) for TSHD dredging sand in the approach channel, spring tide, low flow conditions
- Figure 5.7 Time histories of concentration at Bran and North Gare Sands for TSHD dredging sand in approach channel, spring tide low flow conditions
- Figure 5.8 Simulated peak concentration for disposal operations at present maintenance disposal site
- Figure 5.9 Simulated peak deposition for disposal operations at present maintenance disposal site
- Figure 5.10 Simulated peak concentration for disposal operations at present capitol disposal site
- Figure 5.11 Simulated peak deposition for disposal operations at present capitol disposal site
- Figure 5.12 Conceptual sediment transport diagram at disposal sites
- Figure 5.13 Location of Dabholm Gut
- Figure 5.14 Depth-averaged suspended particle concentrations. Existing layout, spring tide, summer condition
- Figure 5.15 Increase in deposits over a tidal cycle – Existing layout, spring tide, summer conditions
- Figure 5.16 Distribution of maximum deposits over the tidal cycle. Existing layout, spring tide, summer conditions
- Figure 5.17 Depth-averaged suspended particle concentrations. Existing layout, spring tide, winter condition
- Figure 5.18 Increase in deposits over a tidal cycle – Existing layout, spring tide, winter conditions
- Figure 5.19 Distribution of maximum deposits over the tidal cycle. Existing layout, spring tide, winter conditions
- Figure 5.20 Depth-averaged suspended particle concentrations. Existing layout, neap tide, summer condition

Contents continued

- Figure 5.21 Increase in deposits over a tidal cycle – Existing layout, neap tide, summer condition
- Figure 5.22 Distribution of maximum deposits over the tidal cycle. Existing layout, neap tide, summer conditions
- Figure 5.23 Depth-averaged suspended particle concentrations. Existing layout, neap tide, winter condition
- Figure 5.24 Increase in deposits over a tidal cycle – Existing layout, neap tide, winter conditions
- Figure 5.25 Distribution of maximum deposits over the tidal cycle. Existing layout, neap tide, winter conditions
- Figure 5.26 Depth-averaged suspended particle concentrations. Proposed layout, spring tide, summer condition
- Figure 5.27 Increase in deposits over a tidal cycle – Proposed layout, spring tide, summer conditions
- Figure 5.28 Distribution of maximum deposits over the tidal cycle. Proposed layout, spring tide, summer conditions
- Figure 5.29 Depth-averaged suspended particle concentrations, proposed layout, spring tide, winter condition
- Figure 5.30 Increase in deposits over a tidal cycle – Proposed layout, spring tide, winter conditions
- Figure 5.31 Distribution of maximum deposits over the tidal cycle. Proposed layout, spring tide, winter conditions
- Figure 5.32 Depth-averaged suspended particle concentrations. Proposed layout, neap tide, summer condition
- Figure 5.33 Increase in deposits over a tidal cycle – Proposed layout, neap tide, summer conditions
- Figure 5.34 Distribution of maximum deposits over the tidal cycle. Proposed layout, neap tide, summer conditions
- Figure 5.35 Depth-averaged suspended particle concentrations. Proposed layout, neap tide, winter conditions
- Figure 5.36 Increase in deposits over a tidal cycle – Proposed layout, neap tide, winter conditions
- Figure 5.37 Distribution of maximum deposits over the tidal cycle. Proposed layout, neap tide, winter conditions
- Figure 6.1 Model bathymetry for in-combination test
- Figure 6.2 Peak ebb tidal currents before and after Seaton Channel deepening
- Figure 6.3 Peak flood tidal currents before and after Seaton Channel deepening
- Figure 6.4 Peak ebb tidal current patterns before and after Seaton Channel deepening
- Figure 6.5 Peak flood tidal current patterns before and after Seaton Channel deepening
- Figure 6.6 Time series of 3D currents at entrance to Seaton Channel before and after Seaton Channel deepening
- Figure 6.7 Time series of 3D currents near power station intake to Seaton Channel before and after Seaton Channel deepening
- Figure 7.1 Model bathymetries used for sensitivity test
- Figure 7.2 Sensitivity of peak ebb current magnitude to amended dredging
- Figure 7.3 Sensitivity of peak flood current magnitude to amended dredging
- Figure 7.4 Sensitivity of peak tidal current pattern to amended dredging

1. Introduction

PD Teesport is proposing to construct a deep sea container terminal on the site of the existing Container Terminal No. 1, the redundant ex-Shell jetty and the Riverside Ro-Ro No. 3 at Teesport. The construction phase of the scheme comprises capital dredging works in the Tees Estuary, reclamation, land-side development and disposal of dredged material. HR Wallingford were commissioned by Royal Haskoning to supply specialist input to address the hydrodynamic and sedimentological effects of the construction on the Tees Estuary and Tees Bay as part of the environmental impact assessment (EIA) of the development. The issues for the Estuary and Bay as identified by the Environmental scoping report (Haskoning (2005)) are described below. Figures 1.1 and 1.2 from the scoping report show the study area and the proposed layout of the development.

1.1 DURING THE CONSTRUCTION PHASE

The key effects related to the sedimentary regime of the estuary system arising during the construction phase are the suspension of sediment into the water column during the capital dredging, from run-off from the reclamation and disposal activities, its dispersion and subsequent temporary and/or permanent deposition on the seabed. The volume of material requiring dredging during the capital works is estimated to be about 5.5 million cubic metres.

1.2 DURING THE OPERATIONAL PHASE

1.2.1 *Effect on tidal propagation*

The manner in which the tide propagates into an estuary system is partly dependant on the cross sectional area of the estuary. Changes to the cross sectional area arising from, for example, capital dredging and reclamation works therefore have the potential to affect tidal propagation with the possibility of changes to tidal range, levels of high and low waters etc.

1.2.2 *Effect on current speeds*

The deepening of the approach channel and the terminal construction has the potential to changes current speeds and/or current directions at certain stages in the tidal cycle. Changes to flow patterns can have an important influence on navigation and manoeuvring operations within the estuary and at nearby berths. Changes to the flow regime can also result in changes to sediment transport processes which in turn can effect morphological change in the area.

1.2.3 *Effect on infill rates in dredged areas*

Dredged channels and berthing pockets, or certain parts of such areas, are commonly depositional areas for sediment; hence the need for maintenance dredging of such navigational areas at intervals in order to maintain the required depth. When channels are deepened or realigned through capital dredging, the flow and sediment regimes can be changed to result in changes in infill rates with consequential change in maintenance dredging requirement.

As part of the assessment of potential changes to maintenance dredging any change to the dispersion and deposition of potentially contaminated material emerging from Dabholm Gut was investigated.

1.2.4 *Effect on wave energy*

Channel dredging and reclamation works can influence wave activity in the estuary in a number of possible ways. For example, allowing larger waves generated offshore to propagate closer to the coastline or further into the estuary or changing the distribution of wave energy as the changed bathymetry alters the way the waves are refracted as they approach the coastline. Within an estuary waves generated by wind action can be reflected from new quay faces leading to changed patterns of energy in the vicinity of the scheme.

1.3 STRUCTURE OF REPORT

The studies relating to the above mentioned issues for the proposed development are described in this report as follows: Section 2 describes the establishment of the flow model and the evaluation of the changes to tidal propagation and current speeds from the development. Section 3 describes the study of wave conditions in the area both before and after the development. Section 4 covers the studies related to sediment transport and is divided between studies related to non-cohesive (sand) and cohesive (mud) sediment. Section 5 describes the studies of the dispersion of sediment plume from the capital dredging operations, from reclamation run-off and from disposal of dredged arisings. This chapter also describes the studies of the dispersion of sediment emerging from Dabholm Gut. The studies are summarised in Section 6 and the main conclusions of the studies presented.

2. Flow modelling

2.1 INTRODUCTION

A TELEMAC-3D flow model was set up to simulate currents in the Tees Estuary. TELEMAC-3D is a state-of-the-art finite element flow model, originally developed by LNHE Paris, which uses a completely unstructured grid enabling the accurate simulation of water movement in complex shaped areas. TELEMAC-3D also includes vertical layers, enabling three-dimensional flow structures in the river to be accurately represented. Distribution of salinity, and its evolution, can be modelled. Further details of the TELEMAC-3D model are provided in Malcherek et al (1996).

The geometry of the model for the existing layout, and the proposed scheme, is described in Section 2.2. The model was first run simulating some periods of observations, in order to establish its calibration (see Section 2.3). Once the model had shown a satisfactory match to observations, four runs were undertaken for both the existing and scheme layouts, to simulate different tidal conditions (mean spring and mean neap) and different freshwater conditions (dry and wet: 0 cumecs and 60 cumecs). Section 2.4 discusses these results and the predicted impact of the scheme on flow in the area.

2.2 MODEL SET-UP

The model domain for this study is shown in Figure 2.1. The model has its upstream limit at the Tees Barrage, and extends to 6.5km offshore in Tees Bay, covering an area of approximately 80km². The horizontal co-ordinates of the model are OSGB36.

Figure 2.1 also shows the model bathymetry (for the existing layout). The model coastline and bathymetry were obtained from the following sources:

- A 2004/2005 bathymetry survey supplied by PD Teesport covering most of the Estuary
- Admiralty Charts, including Chart 2566 (Tees and Hartlepool Bays)
- Photographic evidence for depths in Dabholm Gut

Side slopes of 1:5 were included for the berth area at Phillips Inset Dock and adjacent main river channel. Training banks near the river entrance were included with crests at mid-tide level.

Boundary conditions are applied at the upstream and downstream ends of the model, as indicated in Figure 2.1.

UPSTREAM – a discharge of freshwater is introduced to the model, with a salinity of zero in contrast to a background salinity of 32ppt;

DOWNSTREAM – tidal elevations are imposed at the open sea boundary, based on mean spring, mean, and mean neap tides as shown in Table 2.1. The mean spring and mean neap tide levels in Table 2.1 are taken from the Admiralty Tide Tables; the mean tide is inferred.

Table 2.1 Tidal conditions at the River Tees Entrance

Tidal conditions	HW (mCD)	LW (mCD)	Range (m)
Mean spring (ATT)	5.5	0.9	4.6
Mean	4.9	1.5	3.4
Mean neap (ATT)	4.3	2.0	2.3

The model mesh is shown in Figure 2.2. The mesh resolution varies from 800m at the seaward model boundary, to 50 m over most of the estuary, and 30m in narrow sections. Figure 2.2 shows the detail of the mesh at Teesport, for both the existing layout and the proposed scheme. With the exception of the removal of the reclamation area from the model domain, the mesh is identical for both layouts.

The proposed scheme for inclusion in the model is shown in Figure 2.3. Its features are:

- a reclamation at Teesport (covering approximately 90,000m²);
- an adjacent berth pocket dredged to -16mCD;
- dredging of the main River Tees channel, with a slightly revised route, to -14.5mCD; and
- dredging of the two turning areas to -14.5m CD

The model bathymetry for the existing and proposed scheme layouts is shown in Figure 2.4. The change in bathymetry due to the scheme is also shown in Figure 2.4. The greatest changes in bathymetry occur where the channel or berth pocket adjoin existing inter-tidal banks.

2.3 MODEL CALIBRATION

The credibility of the model is assessed by comparison with observations made in the estuary. The model parameters are adjusted until the closest match between model and observations (i.e. calibration) is achieved. When the model is rerun with the same parameters but for a different set of conditions (e.g. a different tide/freshwater input), and a satisfactory match with corresponding observations is still achieved, the model is validated.

Various observations of currents in the River Tees are available for comparison with the model. Figure 2.5 shows the locations of current observations, for times of “dry” (negligible freshwater input through barrage) and “wet” (average 14 cumecs flow through barrage) conditions. The details of the observations are as follows:

Dry season observations were undertaken on 15th and 16th June 1995 (after the construction of the barrage) across two transects using ADCP. Six points have been extracted from those transects for time-history comparison with the model. See HR Wallingford (1995) for further detail about these observations. The large spring tidal range at the time of the observations was approximately 5.0m (compared to a mean spring tide range of 4.6m). Freshwater discharge at the time was negligible. The model was run for the existing layout with a 5m-tide and no freshwater input, and is compared with the depth-averaged observations in Figure 2.6, showing a reasonable match for both speeds and directions.

Wet season observations were undertaken between 22nd and 30th April 2005, during various tidal and freshwater conditions. Figure 2.5 shows the locations of the eleven

ADCP transects, together with seventeen points extracted for time-series comparison with the model. Tables 2.2 and 2.3 describe the dates, tides and freshwater discharges for the days of measurement.

Table 2.2 Dates of wet season transects and points extracted

Transect	Survey dates (April 2005)	Point data
1	22 nd , 28 th	E, F
2	22 nd , 28 th	G, H, I, J
3	22 nd , 28 th , 30 th	K, L
4	22 nd , 28 th	-
5	26 th , 29 th , 30 th	P, Q
6	26 th , 29 th	O
7	26 th , 29 th , 30 th	M, N
8	27 th	C
9	27 th	B
10	27 th	A
11	28 th	D

Table 2.3 Tidal ranges and freshwater discharge on the days relevant to ADCP transects

Date (April 2005)	Tidal range (m)	Barrage discharge (cumecs)		
		Min	Max	Mean
22 nd	3.5m	0.8	23.2	10.8
25 th	4.5m	0	131.5	36.4
26 th	4.6m	0	27.5	7.7
27 th	4.5m	0	64.1	11.3
28 th	4.1m	0	37.5	15.9
29 th	3.7m	0	41.2	11.6
30 th	3.2m	0	41.2	11.6

The model was run for mean spring and mean tide conditions. A typical average discharge for the period of observations – 14 cumecs – was discharged into the river at the barrage. Vectors of depth-averaged observations (Transects 1 to 4, 28th April) are shown with the equivalent model results (mean spring tide, 14 cumecs freshwater) in Figures 2.7 and 2.8, for four hours after and before HW respectively. The model is shown to capture well the qualitative nature of the flow on both the ebb and flood – the strength and direction of currents, and the presence and position of eddies in the depth-mean flow are well represented by the model.

Further comparison between the model and measurements can be made by considering time histories of speeds and directions at the selected points shown in Figure 2.5. The three-dimensional behaviour of the model is also assessed in the following figures, which show near-surface, mid-depth and near-bed currents. Table 2.4 lists the real and modelled tidal ranges, and modelled freshwater discharge for each comparison made in Figures 2.9 to 2.39.

Table 2.4 Description of comparisons made in Figures 9 to 39

Figure no	Point	Date of observations	Tidal range on date of observations	Model tide for comparison	Model FW discharge
9	M	26 th April	4.6m	Mean spring (4.6m range)	14 cumecs
10	N				
11	O				
12	P				
13	Q				
14	A	27 th April	4.5m	Mean spring (4.6m range)	14 cumecs
15	B				
16	C				
17	D	28 th April	4.1m	Mean spring (4.6m range)	14 cumecs
18	E				
19	F				
20	G				
21	H				
22	I				
23	J				
24	K				
25	L	22 nd April	3.5m	Mean tide (3.4m range)	14 cumecs
26	E				
27	F				
28	G				
29	H				
30	I				
31	J				
32	K	30 th April	3.2m	Mean tide (3.4m range)	14 cumecs
33	L				
34	K				
35	L				
36	M				
37	N				
38	P				
39	Q				

Observations plotted are all those within a 25m to 50m radius of the chosen location, giving an impression of the scatter of measurements. Figures 2.9 to 2.39 show a good match of the 3D model results to the observed speeds and directions.

The vertical structure of flow is particularly well reproduced by the model. On days where the freshwater has a significant impact on flow, a different vertical structure occurs during the ebb and flood (seen in 27th and 28th April):

- at the surface, ebb flow often exceeds flood, since the less dense, downstream-flowing freshwater, enhances the ebb flow whilst opposing the flood
- at the bed, flood flow often exceeds ebb, since the inflowing denser salty water is confined to the lower part of the water column, and must supply the unaltered tidal prism

The model has been shown to be calibrated and validated, having successfully simulated real flows under a range of tidal and freshwater conditions. The model is therefore established as a credible tool for examining the impacts of the proposed scheme. These impacts are shown in the following section.

2.4 IMPACT OF SCHEME

The model was run, for both the existing and scheme geometries, to simulate the following conditions:

- “dry” spring (mean spring tide, no freshwater input)
- “wet” spring (mean spring tide, 60 cumecs freshwater input)
- “dry” neap (mean neap tide, no freshwater input)
- “wet” neap (mean neap tide, 60 cumecs freshwater input).

A comparison of the dry spring peak ebb depth-mean speed for existing and proposed layouts is given in Figure 2.40. The general pattern of depth-mean flow – less than 0.5m/s and fastest in the channels – is the same before and after the scheme. The change in speed is also included in Figure 2.40 (orange represents an increase in speed due to the scheme; blue represents slower flow following the scheme). The impact is a reduction in depth-mean flow speed where the channel has been deepened (since the same tidal discharge is passing through an increased cross-sectional area), with some increase in depth-mean flow speed over the adjacent banks. Figure 2.41 shows the equivalent for dry spring peak flood flow, where similar patterns of depth-mean speed difference are modelled.

Figures 2.42 and 2.43 show the depth-mean existing and scheme speeds for the wet spring model run – again flow is slowed in some areas of the channel, and increased on some banks.

For both freshwater conditions during a spring tide, the impact on depth-mean speed is smaller than $\pm 0.2\text{m/s}$.

Figures 2.44, 2.45, 2.46 and 2.47 show impacts of the scheme on depth-mean neap tide flow for a dry ebb, dry flood, wet ebb and wet flood respectively. The impact on depth-mean flow speeds for a mean neap tide is shown to be smaller than $\pm 0.1\text{m/s}$.

To examine the impact of the scheme on the 3D nature of the flow, comparisons are made at the following three locations:

Location	Label	Easting	Northing
Tees Approach Channel	1	455427m	528348m
Tees River Channel (opp. Norsea Oil)	2	454582m	525505m
Adjacent to proposed quay	3	454633m	524113m

Figure 2.48 shows modelled current speeds and directions for Location 1, at near-surface, mid-depth and near-bed, for a dry mean-spring tidal cycle. Results for the existing layout (thick line/filled diamonds) are compared with the scheme layout (fine line/empty diamonds). Near the river entrance (Location 1), there is very little difference in flow at any depth due to the scheme. Figure 2.49 shows the dry spring results for Location 2, where the ebb flow is slightly reduced at all depths, due to the channel deepening. Dry spring results for Location 3 are shown, in Figure 2.50, to have

reduced speed and a slight change in direction throughout the water column, due to the scheme.

Figures 2.51, 2.52 and 2.53 show wet spring results at Locations 1, 2 and 3 respectively. At Location 1, there is again little impact on flow. At Location 2 (where a very distinctive freshwater-induced depth-variation in flow is seen) the surface flood is suppressed by the scheme, whilst the minimal deep ebb is enhanced. Location 3 experiences most impact on near-bed flows, where speeds are reduced and directions are altered.

The dry neap results for Locations 1, 2 and 3 are shown in Figures 2.54, 2.55 and 2.56. The smaller neap speeds are not significantly altered by the scheme at the downstream Locations 1 and 2; Location 3 shows slower flow and a slight change of direction.

Figures 2.57, 2.58 and 2.59 show wet neap results at Locations 1, 2 and 3. This flow regime shows the most influence of the freshwater input (due to the reduced tidal influence), with the surface always “ebbing”, and the bed always flooding at Locations 2 and 3. Mid-depth flows are shown to reverse with the tide. The scheme again has a small impact on flow speeds and directions at Locations 2 and 3, whilst the river entrance (Location 1) is relatively unaffected.

The nature of the flow near Teesport is examined further in Figures 2.60 to 2.67. In each figure, velocity vectors are shown near the surface (left panel) and near the bed (right panel), for existing (blue vectors) and post-scheme (red vectors) layouts. Figure 2.60 shows peak ebb flow for the dry spring model run: this condition has been shown to give depth-variation in flow, but the impact of the scheme is demonstrated. The reclamation and dredging have encouraged flow to veer eastward where the turning circle meets the main channel, and to flow over the bank north of Dabholm Gut. The flood flow, in Figure 2.61, also veers eastward as it encounters the reclamation.

Figures 2.62 and 2.63 show vectors for wet spring ebb and flood flows respectively. A more striking impact is seen on the flow pattern, with fast surface ebb flows favouring a straighter route around the channel bend adjacent to the reclamation, whilst deep ebb flows are slowed over much of the area. Surface flood flows, slow due to the opposition of tidal and freshwater influences, are slower north of the reclamation due to dredging; adjacent to the reclamation, the dredging effect on cross sectional area is offset by the reclamation, so flow is relatively unaffected. Near-bed flood flows show a larger, slower eddy at the turning circle.

Dry neap vectors (shown in Figures 2.64 and 2.65 for ebb and flood) echo the dry spring patterns, with smaller magnitudes. Wet neap vectors (Figures 2.66 and 2.67 for peak ebb and flood) show near-surface flow to be directed downstream at both times and near-bed flows always upstream. The scheme again shows a tendency for flow to be less deviated by the river bend.

The scheme is predicted to have a very small effect on water levels as shown in Table 2.5 – tidal range is increased by less than 4mm; the tide arrives up to 2 minutes earlier.

Table 2.5 Impact of scheme on height and timing of high and low waters

	Tees Approach Channel (Location 1)		Adjacent to proposed reclamation (Location 3)		Near barrage	
	<i>Elevation</i>	<i>Timing</i>	<i>Elevation</i>	<i>Timing</i>	<i>Elevation</i>	<i>Timing</i>
HW	No change	No change	0.001m higher	No change	0.002m higher	2 minutes earlier
LW	No change	No change	0.002m higher	1 minute earlier	0.002m lower	2 minutes earlier

3. *Wave modelling*

3.1 BACKGROUND

Wave conditions in the Tees Estuary are a combination of offshore swell and locally generated wind waves. The swell entering the estuary is limited in direction by the North Gare and South Gare Breakwaters. The majority of offshore swell in the region was found in a previous study (HR Wallingford (2002)) to come from a Northerly direction. The position of the proposed Container Terminal determines that it will have most effect on Northerly and South-Westerly wind-generated waves.

As part of the EIA studies the wave study has included the set up of a third generation wave model (SWAN) to predict wind-wave and swell conditions in the Tees Estuary. This model has been used to investigate the impact of the proposed scheme on wave conditions in the Tees Estuary, looking predominately at high water level with sensitivity studies at mid-tide and low water. The SWAN model is described in Section 3.2. The application of the SWAN model to the Tees Estuary is presented in Section 3.3. The results of the wave modelling are given in Section 3.4.

3.2 THE SWAN WAVE TRANSFORMATION MODEL

SWAN (acronym for **S**imulating **W**aves **N**earshore) was developed by the Technical University of Delft (TU Delft) in the Netherlands. SWAN is a 3rd generation wave model, which is a state-of-the-art spectral wave transformation model for coastal wave studies.

SWAN includes the effect of refraction and shoaling, friction, wave breaking and wave-wave interactions. The model is ideally suited to the transformation of wave energy spectra in relatively large coastal areas. This is particularly true where the features of the seabed, such as offshore banks, result in depth-induced wave breaking and wave-wave interactions.

The model also includes wave generation by wind within the model area. SWAN therefore is especially useful in regions such as lochs, fjords, partially enclosed bays or estuaries where wave conditions may be equally comprised of refracted offshore waves and those generated locally by winds (not necessarily correlated with the predominant offshore wave direction). SWAN also has the ability to model the effect of wave reflections from structures.

3.3 APPLICATION OF SWAN MODEL TO THE TEES ESTUARY

The SWAN model was used in this study to transform refracted waves from the North Sea and those generated locally within the estuary, accounting for refraction, shoaling, seabed friction, breaking and reflections. Complete directional spectra were transformed. The domain was chosen to include the fetch of all wind waves generated locally and incident upon the quay extension, and extended offshore as far as the location of the waverider buoy that is deployed by PD Teesport in Tees Bay, including all parts of the proposed dredging scheme. The model bathymetry used is shown in Figure 3.1 (existing layout) and Figure 3.2 (proposed layout). The bathymetry is based on the same sources of data used for the flow model studies. The horizontal resolution of the model is 50 metres. The model resolves a spectral range of wave periods from 0.25 to 40 seconds, with 10° resolution in direction.

Output from SWAN was used to investigate the impact of the proposed Teesport Container Terminal development and dredging on wave conditions in the area, and also to provide input for subsequent sediment transport studies (see Chapter 4).

3.3.1 Representation of Reflection

The reflection properties of the boundaries of the Estuary were represented in the SWAN model by assigning an appropriate reflection coefficient (k_r) to each of the boundary types. These reflection coefficients were calculated using a method developed at HR Wallingford, (Allsop (1990)), which takes into account the type of construction and slope of the boundary as well as the incident wave conditions. A reflection coefficient of 1.0 indicates that all the incident wave energy will be reflected, while a lower reflection coefficient indicates that some wave energy will be dissipated. The reflection boundaries were included in the SWAN model and the reflection coefficients assigned are shown in Table 3.1. The proposed extended quay is a piled structure above a slope faced with either rock armour or grouted mattress (yet to be specified). The option with highest reflection coefficient (grouted mattress) was included here for purposes of informing the EIA. The reflection coefficients for the quay extension area correspond to locally generated wind waves, with short periods. It was found that longer period swell waves do not reach this upstream area with any significant strength.

Table 3.1 Reflection Coefficients used in the SWAN model of Teesport, derived from the formulation of Allsop (1990)

Description of region of coastline	Reflection Coefficient
Beach (e.g. Coatham Sands, Seaton Sands)	0.1
Small rock, steep slope (e.g. much of banks of Tees between jetties)	0.4
Small rock, shallow slope	0.2
Smooth concrete, steep slope	0.6
Smooth concrete, shallow slope	0.3
Vertical wall	0.95
Riverside Ro-Ro and region of Shell Jetty	0.4
Piled frontage of existing Teesport Container Terminal	0.5
Proposed Teesport Container Terminal Quay with grouted mattress	0.4

3.4 WIND AND WAVE FORCING OF THE MODEL

The scope of this study is to consider the impact of the proposed scheme under a representative range of realistic wind and wave conditions. The conditions used were drawn from a survey of literature (HR Wallingford (1989b), (1997), (2002), ABPmer (2002), (2005)) and validated as representative against the observed data from South Gare (winds) and the waverider buoy in Tees Bay (waves).

3.4.1 Wind Climate

Table 3.2 is a frequency table of wind speed and direction, in parts per 100,000, derived from data observed at South Gare between 1999 and 2005. Each value represents a 5 minute average. Approximate percentage exceedences have been estimated for the winds used in the model runs (Table 3.3) considering the model winds to last for one hour, and converting from the five minute average wind speeds in the climate table using a technique developed by the Met Office.

Table 3.2 Observed Wind Climate at South Gare, 1999-2005

Data in parts per 100,000

Frequency Table	Wind Direction (°N)														Total
	0	30	60	90	120	150	180	210	240	270	300	330	360		
0	3358	3350	2751	3210	1817	1536	3593	6118	6361	2369	1423	1799	37685		
5	1875	2437	1916	3711	1352	1672	5400	8340	6281	2782	1650	939	38355		
10	851	991	751	1398	320	617	2101	4042	2789	1310	946	603	16718		
15	202	242	149	197	74	181	520	1061	728	335	356	213	4258		
20	22	23	14	60	6	22	92	198	145	79	71	43	776		
25	1	1	0	4	0	1	13	40	30	18	5	4	118		
30	0	0	0	0	0	0	1	7	9	6	1	2	27		
35	0	0	0	0	0	0	1	1	3	1	0	1	8		
40+	313	104	49	32	79	110	95	90	76	107	81	918	2056		
Total	6623	7149	5630	8612	3647	4140	11817	19897	16422	7008	4534	4522	100000		

(Note – due to an outstanding quality control issue, this climate includes some unrealistically high wind speeds and is not suitable for deriving extreme winds)

Table 3.3 Wind conditions used in model runs

Wind Direction (°N)	Wind Speed (m/s) Hourly average	Estimated percentage exceedences (%)
90	5	60
0	10	12
0	20	0.4
0	30	0.02*
225	10	27
225	20	1.2
225	30	0.04*

*Due to outstanding quality control issues, this climate includes some unrealistically high winds speeds and is not suitable for generating extreme winds, these estimates are illustrative.

3.4.2 Wave Climate

The offshore swell conditions used in the model runs (Table 3.4) consist of significant wave heights corresponding to return periods of between 0.1 and 50 years (Babtie (1998)) with corresponding mean wave periods taken from a nearby observed climate (HR Wallingford (1977)). The conditions used are consistent with the wave climate observed at the waverider buoy north of Tees North Buoy (Table 3.5), for which no directional information is available. Mean wave period (T_m) was converted to peak wave period (T_p) for input to the model assuming a standard JONSWAP spectrum. Significant wave height figures (H_s) quoted here were converted from 5 minute maximum wave height using a period dependent factor

$$\frac{H_{\max}}{H_s} = \frac{1}{\sqrt{2}} \left[(\ln N)^{\frac{1}{2}} + 0.2886(\ln N)^{\frac{-1}{2}} \right], \text{ where } N \text{ is the number of wave crests in each } 5 \text{ minute period (BSi (1984)).}$$

A $\cos^6 \theta$ directional spreading function was applied to the incoming swell to represent the spreading (Goda (1985)) following refraction of the offshore waves to the model boundary, at approximately 20m depth. Previous studies (HR (2002)) have shown the majority of swell to approach from a northerly direction. Taking into account refraction towards the coast, swell was tested at incoming angles of 0°N, 15°N and 30°N.

Table 3.4 Offshore swell conditions used in model runs

Return Period (years)	H _s (m)	T _m (s)	T _p (s)	Direction (°N)
0.1	3.87	7	9.0	15
1	6.03	9.5	12.2	0, 15, 30
10	8.63	11	14.1	15
50	10.69	12	15.4	15

3.4.3 Results of the wave modelling

The model was run to simulate high water conditions with northerly swell, northerly winds, and south-westerly winds. Extensive sensitivity tests were completed, including combinations of swell and wind waves, and swell conditions at mid-tide and low water. Table 3.6 lists the model parameters used in the sensitivity tests. Table 3.7 lists the model parameters used in runs to inform the accompanying sand modelling study.

Table 3.5 Offshore wave climate: Significant wave height estimated from observations at the waverider buoy, 400m north of Tees North Buoy

Frequency Table		Average wave period Tm (s)																Total	
Hs (m) from	From To	0	1	2	3	4	5	6	7	8	9	10	11	12	13	14	15	16	+
0	1	15295	0	1501	20162	19354	11939	7573	3522	1492	911	279	91	32	11	7	2	75	82247
1	2	0	0	0	336	2918	4207	3017	1613	741	281	96	33	8	4	1	5	24	13285
2	3	0	0	0	0	18	635	1068	598	301	140	44	14	24	9	2	8	204	3063
3	4	0	0	0	0	4	6	176	170	69	43	15	7	12	5	1	1	8	516
4	5	0	0	0	0	0	5	7	37	29	18	17	14	11	5	8	4	70	223
5	6	0	0	0	0	0	2	5	11	16	15	10	18	13	7	6	2	78	181
6	7	0	0	0	0	3	8	7	4	13	10	5	9	9	5	4	1	86	163
7	8	0	0	0	0	6	13	8	10	6	5	11	5	2	0	0	1	15	80
8	9	0	0	0	1	0	1	6	8	12	7	15	3	4	5	1	3	23	88
9	10	0	0	0	0	0	0	0	2	2	5	0	2	1	0	1	0	29	42
10	11	0	0	0	0	0	0	0	1	1	0	2	3	0	1	0	0	64	71
11	12	0	0	0	0	0	0	0	0	0	4	0	0	0	0	0	0	6	10
12	+	0	0	1	0	0	0	0	0	9	8	5	3	3	1	0	1	0	31
Total		15295	0	1503	20500	22303	16815	11866	5975	2690	1445	497	200	118	52	30	27	683	100000

NB Significant wave height figures (Hs) are converted from 5 minute maximum wave height using a period dependent factor

$$\frac{H_{\max}}{H_s} = \frac{1}{\sqrt{2}} \left[(\ln N)^{\frac{1}{2}} + 0.2886(\ln N)^{\frac{-1}{2}} \right]$$

where N is the number of wave crests in each 5 minute period (Reference 4).

The effects of the scheme are best illustrated by considering the wind and swell components separately. Model results for significant wave height, H_s , are shown in Figures 3.4, 3.5 and 3.6 and tabulated for selected points in Table 3.8, at locations specified in Table 3.9 and shown in Figure 3.3. The points were chosen to assess local impacts. The overall pattern of changes to wave height is best seen in the figure for each condition tested.

The wind waves generated in the estuary are affected by the proposed changes in reflective properties of the Teesport Container Terminal, but are unaffected by the changes to dredging at depth, as they are short period waves. The swell waves do not reach as far up the estuary as the Teesport Container Terminal, and so are unaffected by the reclamation, but are affected by the dredging at depth, as they have longer periods.

In the model tests it has been assumed that the reclamation and extended quay at Teesport Container Terminal will be faced with piles in front of grouted mattress. If the stated alternative of rock armour is used instead of grouted mattress, the reflection will be reduced. If a vertical wall was used, as originally stated, the reflections would increase significantly from those shown here.

The prevailing south-westerly winds run along the Tees and reflect northward off south bank of the Tees in the Teesport area. The wind speed applied here (20 m/s) has an exceedance of 1.2%. Figure 3.4 shows the reflection pattern, which extends as far as the North Gare breakwater. However, the change in significant wave height is small: less than 0.1m throughout. Tests with 30m/s south-westerly winds showed stronger waves, with the same pattern of change and a maximum increase in significant wave height of 0.1m.

Figure 3.5 shows the effect of the proposed scheme on northerly winds of 20m/s, with 0.4% exceedance. Reflection of the proposed quay increase the significant wave height in the river by up to 0.05m over an area adjacent to the extended quay and extending upstream. The pattern of change was found to be similar for other wind speeds and adjacent directions.

Figure 3.6 shows the effect of the proposed scheme on swell with significant wave height 6m approaching from 30°N. This condition has an estimated return period of 1 year. Long period waves are reflected on the side of the dredged channel and impact on the Norsesea Oil Terminal, increasing the significant wave height on the eastern side of the Norsesea Oil Terminal by up to 0.3m. The increased reflection is due to the deepening of the channel (surveyed to be shallower than the stated -14.1mCD in places) to -14.5mCD. The increased reflection within the channel leads to a slight decrease in significant wave height on North Gare Sands and Bran Sands. The pattern of change was similar for all return periods modelled, with increases of up to 0.5m in the 50 year return period case. There was only slight dependence on the direction of incoming swell.

Much of the predicted change in wave conditions at the mouth arises from the fact that there is presently a backlog of maintenance dredging at this location in the channel. A sensitivity test was undertaken to illustrate the effect of deepening the channel to the presently declared depth of -14.1m CD. This sensitivity test was run for 6 m swell from 15°N. The results showed that about half of the increase in wave height at Phillips Dock was due to the reestablishment of the channel edges to the declared depth. This redistribution of wave energy also resulted in most of the reduction in wave height over North Gare Sands and Bran Sands. The results of the sensitivity test are shown in Figure 3.7.

Table 3.6 Parameters of SWAN model sensitivity tests

Name	Wind direction (deg. N)	wind speed (m/s)	swell direction (deg. N)	Swell Hs (m)	Swell Tm (s)	swell Tp (s)	Water level (m CD)	Layout
A1	90	5	15	3.87	7	9.0	5.5	existing
A2	90	5	15	6.03	9.5	12.2	5.5	existing
A3	90	5	15	8.63	11	14.1	5.5	existing
A4	90	5	15	10.69	12	15.4	5.5	existing
A5	90	5	0	6.03	9.5	12.2	5.5	existing
A6	90	5	30	6.03	9.5	12.2	5.5	existing
A7	90	5	30	6.03	7	9.0	5.5	existing
A8	90	5	30	8.63	8	10.3	5.5	existing
A9	90	5	30	10.69	9	11.5	5.5	existing
A10	90	10	15	6.03	9.5	12.2	5.5	existing
A23	90	5	15	6.03	9.5	12.2	3.2	existing
A24	90	5	15	6.03	9.5	12.2	0.9	existing
B1	0	10	15	3.87	7	9.0	5.5	existing
B2	0	20	15	3.87	7	9.0	5.5	existing
B3	0	30	15	3.87	7	9.0	5.5	existing
B4	350	10	15	3.87	7	9.0	5.5	existing
B5	350	20	15	3.87	7	9.0	5.5	existing
B6	350	30	15	3.87	7	9.0	5.5	existing
B7	0	20	15	0	0	0.0	5.5	existing
B8	350	20	15	0	0	0.0	5.5	existing
C1	225	10	0	0	0	0	5.5	existing
C2	225	20	0	0	0	0	5.5	existing
C3	225	30	0	0	0	0	5.5	existing
C4	210	20	0	0	0	0	5.5	existing
C5	240	20	0	0	0	0	5.5	existing
D1	90	5	15	3.87	7	9.0	5.5	Proposed
D2	90	5	15	6.03	9.5	12.2	5.5	Proposed
D3	90	5	15	8.63	11	14.1	5.5	Proposed
D4	90	5	15	10.69	12	15.4	5.5	Proposed
D5	90	5	0	6.03	9.5	12.2	5.5	Proposed
D6	90	5	30	6.03	9.5	12.2	5.5	Proposed
D7	90	5	30	6.03	7	9.0	5.5	Proposed
D8	90	5	30	8.63	8	10.3	5.5	Proposed
D9	90	5	30	10.69	9	11.5	5.5	Proposed
D10	90	10	15	6.03	9.5	12.2	5.5	Proposed
D23	90	5	15	6.03	9.5	12.2	3.2	Proposed
D24	90	5	15	6.03	9.5	12.2	0.9	Proposed
E1	0	10	15	3.87	7	9.0	5.5	Proposed
E2	0	20	15	3.87	7	9.0	5.5	Proposed
E3	0	30	15	3.87	7	9.0	5.5	Proposed
E4	350	10	15	3.87	7	9.0	5.5	Proposed
E5	350	20	15	3.87	7	9.0	5.5	Proposed
E6	350	30	15	3.87	7	9.0	5.5	Proposed
E7	0	20	15	0	0	0	5.5	Proposed
E8	350	20	15	0	0	0	5.5	Proposed
F1	225	10	0	0	0	0	5.5	Proposed
F2	225	20	0	0	0	0	5.5	Proposed
F3	225	30	0	0	0	0	5.5	Proposed
F4	210	20	0	0	0	0	5.5	Proposed
F5	240	20	0	0	0	0	5.5	Proposed

Table 3.7 Parameters of SWAN model runs for the accompanying sand modelling study

Name	Wind direction (deg. N)	Wind speed (m/s)	Swell direction (deg. N)	Swell Hs (m)	Swell Tm (s)	swell Tp (s)	Water level (m CD)	Layout
G1a	270	0.1	15	1.81	4.78	6.1	5.5	Existing
G1b	270	0.1	15	1.81	4.78	6.1	4.35	Existing
G1c	270	0.1	15	1.81	4.78	6.1	3.2	Existing
G1d	270	0.1	15	1.81	4.78	6.1	2.05	Existing
G1e	270	0.1	15	1.81	4.78	6.1	0.9	Existing
G2a	270	0.1	45	1.57	4.48	5.7	5.5	Existing
G2b	270	0.1	45	1.57	4.48	5.7	4.35	Existing
G2c	270	0.1	45	1.57	4.48	5.7	3.2	Existing
G2d	270	0.1	45	1.57	4.48	5.7	2.05	Existing
G2e	270	0.1	45	1.57	4.48	5.7	0.9	Existing
G3a	270	0.1	75	2.03	5.06	6.5	5.5	Existing
G3b	270	0.1	75	2.03	5.06	6.5	4.35	Existing
G3c	270	0.1	75	2.03	5.06	6.5	3.2	Existing
G3d	270	0.1	75	2.03	5.06	6.5	2.05	Existing
G3e	270	0.1	75	2.03	5.06	6.5	0.9	Existing
G4a	270	0.1	105	1.83	4.81	6.2	5.5	Existing
G4b	270	0.1	105	1.83	4.81	6.2	4.35	Existing
G4c	270	0.1	105	1.83	4.81	6.2	3.2	Existing
G4d	270	0.1	105	1.83	4.81	6.2	2.05	Existing
G4e	270	0.1	105	1.83	4.81	6.2	0.9	Existing
H1a	270	0.1	15	1.81	4.78	6.1	5.5	Proposed
H1b	270	0.1	15	1.81	4.78	6.1	4.35	Proposed
H1c	270	0.1	15	1.81	4.78	6.1	3.2	Proposed
H1d	270	0.1	15	1.81	4.78	6.1	2.05	Proposed
H1e	270	0.1	15	1.81	4.78	6.1	0.9	Proposed
H2a	270	0.1	45	1.57	4.48	5.7	5.5	Proposed
H2b	270	0.1	45	1.57	4.48	5.7	4.35	Proposed
H2c	270	0.1	45	1.57	4.48	5.7	3.2	Proposed
H2d	270	0.1	45	1.57	4.48	5.7	2.05	Proposed
H2e	270	0.1	45	1.57	4.48	5.7	0.9	Proposed
H3a	270	0.1	75	2.03	5.06	6.5	5.5	Proposed
H3b	270	0.1	75	2.03	5.06	6.5	4.35	Proposed
H3c	270	0.1	75	2.03	5.06	6.5	3.2	Proposed
H3d	270	0.1	75	2.03	5.06	6.5	2.05	Proposed
H3e	270	0.1	75	2.03	5.06	6.5	0.9	Proposed
H4a	270	0.1	105	1.83	4.81	6.2	5.5	Proposed
H4b	270	0.1	105	1.83	4.81	6.2	4.35	Proposed
H4c	270	0.1	105	1.83	4.81	6.2	3.2	Proposed
H4d	270	0.1	105	1.83	4.81	6.2	2.05	Proposed
H4e	270	0.1	105	1.83	4.81	6.2	0.9	Proposed

Table 3.8 Model results: significant wave height, Hs, at points in the Tees Estuary

Run:	C2	F2	B7	E7	A2	D2
Figure	4	4	5	5	6	6
Wind Conditions:	Speed (m/s) 20	Dir (°N) 225	Speed (m/s) 20	Dir (°N) 0	Speed (m/s) 5	Dir (°N) 90
Offshore Wave Conditions:	Hs (m) 0	Dir (°N) 0	Hs (m) 0	Dir (°N) 0	Hs (m) 6.03 (1:1 year event)	Dir (°N) 15
Layout:	Existing	Change	Existing	Change	Existing	Change
Label	Hs (m)	Hs (m)	Hs (m)	Hs (m)	Hs (m)	Hs (m)
Adjacent to proposed quay	0.61	-0.03	0.70	-0.01	0.12	-0.01
Beach upstream	0.43	0.00	0.41	0.00	0.95	0.03
BASF Chemicals Terminal	0.38	-0.01	0.55	-0.01	0.14	0.00
Beach opposite proposed quay	0.42	0.00	0.52	-0.04	0.13	-0.01
Norsea Oil Terminal	0.56	0.01	0.82	0.00	0.73	0.14
Seal Sands Training Wall	0.54	0.00	0.39	0.00	0.16	0.00
North Gare Sands Training Wall	0.53	0.02	0.75	0.00	0.54	0.00
North Gare Sands	0.45	0.01	0.75	0.00	2.16	0.00
North Gare Sands (channel side)	0.61	-0.01	0.92	0.00	2.01	-0.05
South Gare Breakwater	0.69	0.00	0.95	0.00	3.26	0.00
Bran Sands	0.38	0.00	0.82	0.00	1.05	-0.01

Table 3.9 Locations of output points for model results quoted in Table 3.6

Location	Label	Easting	Northing
Adjacent to proposed quay	3	454633	524113
Beach upstream	4	452424	522037
BASF Chemicals Terminal	5	453945	523724
Beach opposite proposed quay	6	454423	524418
Norsea Oil Terminal	7	454280	526000
Seal Sands Training Wall	8	453601	526434
North Gare Sands Training Wall	9	454353	526902
North Gare Sands	10	454178	527662
North Gare Sands (channel side)	11	454740	527601
South Gare Breakwater	12	455597	528187
Bran Sands	13	455238	526771

4. *Sediment transport*

4.1 INTRODUCTION AND SEDIMENT SOURCES

Among the requirements for the study of the impacts of the proposed new container quay and deepened approach channel are the changes to sediment transport and deposition rates in the area, both in terms of changes to the maintenance dredging requirement and any resultant changes for the intertidal areas.

The present situation in the Tees for sediment transport have been summarised well in the Baseline Maintenance Dredging Document (ABPmer (2005)) and the Conceptual model of estuary processes Report (ABPmer (2002)) both written for PD Teesport. The data from these reports provided the baseline understanding of the sediment transport and deposition regime in the area.

The sources of material into the system are fluvial inputs coming through the Barrage, material entering from Tees Bay and any industrial inputs. These inputs are in addition to material eroded from the estuary bed. Within the system the driving forces for sediment transport are the tidal flows, density driven currents, wave induced currents, vessel induced forces and resuspension by dredging operations. These last two were postulated by HR Wallingford (1989a) as a means by which material entering the system from offshore can be resuspended and moved further upstream into the estuary.

4.1.1 *Fluvial input*

HR Wallingford (1989a) outlined the pre-barrage conditions for fluvial input with general very low concentrations (<10 ppm) which rose to about 200 ppm during occasional floods. The inputs were suggested to be closely linked to large fluvial events with about 8,000 dry tonnes entering the estuary during the 1:1 year flood (300 cumecs at Low Moor, 44 km up estuary of South Gare). The average total inputs were estimated at 40,000 dry tonnes per year. However the close link to high fluvial events would suggest that this could vary considerably from year to year. Most of this material is assumed to be trapped in the estuary.

At the time of construction the Tees Barrage was assumed to not greatly alter the input of fluvial sediment into the estuary. ABPmer (2005) reported that considerable siltation has occurred upstream of the barrage with the implication that fluvial sediment input to the estuary may have reduced for a period. Recent observed increases in fluvial material dredged by PD Teesport suggest that the area upstream of the barrage may be moving back to an equilibrium state. However even if the pre-barrage fluvial input was fully restored it would remain small (by a factor of 30) when compared to marine inputs described below.

4.1.2 *Industrial input*

ABPmer (2005) stated that up to 22,000 t/year (mostly limestone) may be discharged from ICI Wilton at Redcar. This material is discharged in the Dabholm Gut (directly downstream of the proposed development).

4.1.3 Marine input

Comparison of the above figures with the present knowledge of the dredging requirements in the area (770,000 – 670,000 m³ between 1996 and 2001, ABPmer (2005)) shows that the remaining source of material, from Tees Bay, is the predominant source of sediment in to the system. This material comes in on the flood tide, particularly during times when concentrations in Tees Bay are raised by the resuspension of material from the sea bed during storm events. The coarser material, mostly sand, is then able to settle out in the lower estuary. Once finer material is in the system the estuary hydrodynamics come into play. The combination of the density variation in the estuary, both longitudinal and vertical and the generally low tidal currents result in a significant gravitational circulation where the ebb tide is concentrated towards the surface flows and the flood tide is more flat. This variation in the vertical profile results in net landward near bed current. For some combinations of salinity and tide the near bed flows can be continuously landward with continual seaward flow at the surface.

Dredged volumes for the period 1973 to 2001 are shown in Figure 4.1 which includes the split of the volume between the various Chart areas defined in the area. The location of the chart areas is shown in Figure 4.2. A general reduction can be seen over the last 10 years linked to the response of the then THPA to a dredging review which was undertaken in 1991/2 (HR Wallingford (1992), Halcrow (1991)). These reports showed that the dredging was removing about 11% more material than that accreting. Further reduction is also shown following the construction of the Tees Barrage (commissioned in 1992). The study of the effect of the barrage (HR Wallingford 1989a) suggested that the 10% reduction in the tidal volumes of the estuary would cause a 10% reduction in tidal currents at the mouth of the Tees and change the gravitational circulation decreasing it near the estuary mouth and increasing it further upstream. The net predicted decrease in the long term average rate of siltation was about 10%.

Bed sampling undertaken by Bridgland (shown in Halcrow, (1991)) and reproduced in Figure 4.3 shows the mix of sands, clay and silt in the various chart areas. Over recent years the fines content (silts and clay) are of the order of 50-60% of the total siltation (of the order of 330,000-460,000 m³).

4.2 SAND TRANSPORT

4.2.1 Introduction

Sand transport within the Tees estuary is dependent on the effects of both tides and waves. Tidal action generates the large-scale transport due to bedload as a result of the stress generated by the tidal currents on the seabed, and suspended load as sand is carried by the water column. The effect of waves on sand transport is two-fold: firstly, they generate a stirring effect that enhances the suspension of sand from the seabed, and secondly they generate local currents in relatively shallow areas as a result of wave breaking.

Tidal currents are strongest in the offshore areas, and also through the Tees entrance, whereas along the coast the effects of wave breaking can generate significant wave-driven currents. The stirring effect of waves is greatest in shallow water.

4.2.2 Methodology

Sediment transport simulations were performed with the HR Wallingford model, SANDFLOW. SANDFLOW is a dynamic non-cohesive sediment (sand) transport model that simulates the advection and dispersion of suspended sediment due to the effects of both currents and waves. The sediment transport algorithm is based on a formula developed by Soulsby (1997).

SANDFLOW was used to simulate the sediment transport patterns throughout the Tees Estuary due to tidal conditions alone, and including the effects of wave stirring for typical (representative) waves and for storm waves. The resulting sediment transport patterns include only the *potential* for sediment transport, since the information on the actual availability of sediment is not incorporated.

SANDFLOW was run to simulate the present day scenario and the proposed scheme scenario.

The sediment grain size varies over the study area and although SANDFLOW is capable of simulating transport of mixed sediment grain sizes, the processes associated with the transport of mixed sediments is not well understood. Therefore, for the purposes of this study the more traditional approach of specification of a representative uniform median grain diameter was used, and a value of 0.1mm was defined which is consistent with previous information (HR Wallingford (2002), ABPmer (2002)). This assumption of D_{50} should be borne in mind in the assessment of the presented model results.

Output from SANDFLOW comprises the net residual potential sediment transport rate over the period simulated, and the corresponding patterns of erosion and deposition. Due to the non-linear nature of sediment transport (which means that increases in currents give rise to disproportionately higher sediment transport rates) the sediment flux patterns are presented on a logarithmic scale so that the full range of transport rates (especially those at the lower end) can be visualised. In the vector plots, the length of the vector is proportional to the magnitude of the sediment flux for each colour band, the colours representing the magnitude of transport.

Simulations were performed for spring tides, with and without the effect of wave stirring and for storm waves (both described in Chapter 3) during spring tide conditions.

4.2.3 Selection of conditions modelled

Representative conditions

Having established the offshore wave climate, specific wave conditions were selected on the basis of being representative of the total effects of wave stirring on the sediment transport within the Tees estuary. The approach used was based on experience from previous studies and research carried out by HR Wallingford (Chesher and Miles (1992)), from which a procedure has been devised that filters the full wave climate into a reduced set of representative conditions.

Using the approach described in Chesher and Miles (1992) representative wave conditions for each coastal-propagating wave direction were calculated, and are shown in Table 4.1 below.

Table 4.1 Wave conditions used for wave stirring simulations

Direction	15°N	45°N	75°N	105°N
Significant wave height, H_s	1.81m	1.57m	2.03m	1.83m
Mean period, T_m	4.78s	4.48s	5.06s	4.81s
Frequency of occurrence	22%	6.7%	6.2%	5.5%

SWAN was run for each of these conditions, for the five water levels given in Table 4.2 below.

Table 4.2 Water levels at various tidal states

Tide state	Tidal level (m CD)	Tidal level (m OD)
MHWS		2.65
MHWN		1.5
MWL		0.35
MLWN		-0.8
MLWS		-1.95

For each of the four wave conditions, the five wave orbital velocity fields (for each level) were merged to the flow model results. This information is then passed to the sediment transport model where, at runtime, the appropriate wave stirring field is calculated by interpolating between appropriate fields depending on the actual water level.

The results from the sediment transport model (from four wave conditions and tide only) are combined using the relative frequency of occurrence shown in Table 4.1 as weighting factors (note that calm conditions and offshore propagating waves would represent a frequency of 59.6%).

Storm conditions

Storm wave conditions were selected from the offshore wave climate, and are presented in Table 4.3 below. These waves were selected in order to identify the relative effect of infrequent (but not the most extreme) storms on the sediment transport regime, which may be important in some areas where sediment transport is only significant during storm periods. The waves shown in Table 4.3 have a return period of the order of 1:1 year.

Table 4.3 Wave conditions used for storm simulations

Direction (°N)	0	15	30
Significant wave height (m)	6.03	6.03	6.03
Mean period, T_m (s)	9.5	9.5	9.5

Although the wave model SWAN was run for the three conditions specified in Table 4.3, the sediment model SANDFLOW was run only for the middle storm wave condition (15° N) under spring tide conditions.

4.2.4 Existing conditions

Representative conditions

Figure 4.4 shows the predicted patterns of deposition due to the representative wave conditions. The existing bathymetry has been overlain on the results plots in order to aid with the representation of the results. It is clear from this figure that the net deposition for the different chart areas is very small (of the order of less than 1mm/tide). This confirms earlier findings (ABPmer (2005)) that channel infill by the mechanisms of tide (spring) only and including the effects of wave stirring, is relatively small. This would mean that the maintenance burden of sandy material is in fact due to storm events where wave-driven currents play a significant role. This was investigated by simulating storm conditions, the results of which are given in the next section.

Figure 4.5 shows the distribution of the sediment flux throughout the area of interest for these representative wave conditions.

Extreme conditions

Figure 4.6 shows the patterns of deposition due to the storm wave conditions of 6m (corresponding to 1:1 year offshore) in terms of the wave stirring process (i.e. not from the point of view of wave-generated currents). The net deposition for the different chart areas shown in this figure is of greater magnitude, particularly in the outer parts of the channel. For the Chart areas as shown in Figure 4.2 within Chart 9 deposition rates do not vary as much in comparison with those from representative wave conditions, being around less than 1mm/tide. Chart 10 and 11 show average deposition rates of around 40mm/tide with maximum of around 600mm/tide. Chart 12 shows an average deposition rate of around 10mm/tide, with a maximum of around 20mm/tide.

Figure 4.7 shows the distribution of the sediment flux throughout the area of interest for this extreme wave condition.

4.2.5 Post construction conditions

SANDFLOW was re-run to simulate the sediment transport patterns following the implementation of the proposed scheme. Both the representative conditions and the extreme condition were used.

Representative conditions

Figure 4.8 shows the patterns of deposition due to the representative wave conditions for the proposed scheme. The net deposition for the different chart areas is very small (of the order of less than 1mm/tide). When comparing it with the deposition patterns for the existing condition (Figure 4.1), it is seen that they are very similar.

Figure 4.9 shows the distribution of the sediment flux throughout the area of interest with the proposed dredging for these representative wave conditions. Comparing the existing sediment flux (Figure 4.5) it is difficult to ascertain any differences between them.

Extreme conditions

Figure 4.10 shows the patterns of deposition due to the storm wave conditions modelled on the proposed scheme. Chart 9 deposition rates are less than 1mm/tide. Chart 10 and 11 show average deposition rates of around 40mm/tide with maximum of around 600mm/tide. Chart 12 shows an average deposition rate of around 10mm/tide, with a

maximum of around 20mm/tide. These values are similar to those obtained for the existing case (Figure 4.6).

Figure 4.11 shows the sediment flux distribution throughout the area of interest for this extreme wave condition once the proposed scheme is in place.

4.2.6 Channel infill prediction due to tidal action with wave enhancement

In order to compare the results with the information available regarding the actual dredging in the estuary (HR (2002)), the volume of infill was calculated in the different Chart areas by integrating the deposition per area.

For the representative wave conditions, it was assumed that the infill in the dredged areas due to neap tides is very small, and the deposition per area shown in Figures 4.4 and 4.8 (for existing and proposed scheme relatively) was integrated.

For the storm condition, it was assumed that this condition would only happen once every year and the deposition per area shown in Figures 4.6 and 4.10 (for existing and proposed scheme relatively) was integrated.

On this basis, the predicted rates of infill of the channel are shown in Table 4.4 in m³ per year. This table also shows the details of the average dredging per chart area (since the barrier being in place in 1996) (HR Wallingford (2002)) for comparison purposes. Note that these chart areas are composed mainly of sand and gravel as shown in Table 4.5.

Table 4.4 Predicted volumes of channel infill due to tidal action with wave enhancement

Chart area	Average dredging (m ³ insitu)	Representative conditions		Extreme condition	
		Existing Infill (m ³ /year)	Scheme Infill (m ³ /year)	Existing Infill (m ³ /tide)	Scheme Infill (m ³ /tide)
9	291,268	251	20	10	22
10 and 11	252,113	53,488	55,156	23,191	22,956
12 and 13	49,998	0	28	1,976	2,195

Table 4.5 Sand percentage composition

Chart area	Sand and gravel composition (%)
9	78
10	97
11	63
12	90

The information shown in Table 4.4 for the predicted infill in the maintained areas is shown in graphical form in Figure 4.12. (Note that the scale in the graphs is logarithmic). Comparing the graphs on the left the comparison between the existing and proposed scheme is emphasised.

The predicted volumes of infill in the maintained areas due to the extreme condition are two to three orders of magnitude larger than those due to the representative conditions in the outer parts of the channel (Chart areas 12 and 13). In Chart areas 10 and 11 the

prediction for the extreme wave condition is half that predicted for the representative conditions.

The predicted volumes of channel infill for the existing and the proposed scenario do not change by a great amount. These results highlight that channel infill by sand material is only very slightly modified by the proposed dredging and therefore unlikely to give rise to any adjustment in the present maintenance figures.

When comparing the model figures with the average annual dredging figures, there is a considerable discrepancy. This is likely to be due to the fact that the modelling undertaken does not include the effects of wave-driven currents. However when comparing the rate of channel infill for existing conditions and with the predicted scheme this would not change the predicted effect of the channel. To further investigate the relative importance of wave energy in sand transport an analysis of the modelled changes in wave energy was carried out for storm conditions and is included in the next section of this report.

4.2.7 Impact on sand transport and morphology

A comparison of the wave energy levels with the existing and proposed scenario has been carried out by the means of comparing the predicted wave heights in the area of interest for the extreme wave conditions specified in Table 4.3.

Figures 4.13, 4.15 and 4.17 show the wave height field for the existing and proposed condition, whereas Figures 4.14, 4.16 and 4.18 show the actual differences in wave height between the scheme and the existing case (for the extreme condition from three different directions). These figures indicate decreased wave energy away from the channel and onto the intertidal zones at either side. This would suggest a small impact on these intertidal zones associated with the slight reduction in wave energy during storm conditions. It is assumed that this will not result in a significant increase in the channel infill. Whilst the changes are not large a further outcome of the reduction in wave energy on North Gare Sands is likely to be a small reduction in sand supply into the Turning Basin and from there into Seaton Channel and Seal Sands.

4.2.8 Conclusions

The conclusions from this analysis are that the proposed scheme simulated in this study would not have a significant effect on the potential sediment transport in the estuary. These results highlight that channel infill is only very slightly modified by the dredging and therefore unlikely to give rise to any adjustment in the maintenance figures.

Sand transport processes in the outer estuary over the intertidal areas at the mouth are unchanged for representative conditions. For storm wave conditions a small reduction in wave energy over the intertidal areas, particularly over North Gare, is predicted which would suggest an increase in the potential for deposition or a reduction in the rate of erosion. These small changes are unlikely to be significant in terms of the overall morphology of the intertidal areas within the variability of the number of storm events in any given year. A further potential effect is a reduction in sand transport from North Gare towards Seaton Channel and from there onto Seal Sands.

4.3 MUD TRANSPORT

4.3.1 Introduction

As described above the fines content (silts and clay) of materials dredged are of the order of 50-60% of the total accumulation (from Bridgland shown in Halcrow (1991)).

Mud transport modelling has been undertaken to examine the behaviour of the mud fraction with the expectation that the proposed deepened channel would alter the maintenance dredging requirement in the Estuary with possible consequences on the sediment dynamics near intertidal areas.

As described in the Section 4.1 the bulk of fine sediment is thought to enter the system during the flood tide having being resuspended from the sea bed in Tees Bay. Once within the estuary fine sediment would be pushed further landward by the gravitational circulation present possibly with resuspension by dredging activities or large vessel passage.

HR Wallingford (1989b) attempted a correlation between suspended sediment concentration and tides and waves. Although a strong dependence between concentration and bed shear stress and tide was established the work was restricted by the relatively short period of observations. This data was used in combination with longer term silt monitoring in Tees Bay to provide representative concentrations in Tees Bay for summer, winter and equinoctial conditions as required by the modelling for the Tees Barrage studies (HR, (1989a)). These representative concentrations were considered suitable for use in the present studies.

4.3.2 Methodology

The chosen model for the study of fine sediment transport was SUBIEF3D which is a post processing transport model within the TELEMAC system. SUBIEF3D uses the hydrodynamics generated by TELEMAC3D to transport fine sediment with allowance for the deposition and erosion of material on the bed. Full details for the software are given in Luck (2002).

The model was amended to represent the settling of sediment according to the algorithm defined by Manning (2004). The critical erosion velocity was taken as 0.12 m/s and the model was run without a critical velocity for deposition according to Winterwerp (2003). The model deposition volumes were calculated assuming a dry density of bed deposition of 500 kg/m.

The model was run for 5 repeating spring or neap tides for the defined conditions with the deposition volumes calculated over the 5th tide.

The conditions simulated were as used for the Tees Barrage study of the impact of the barrage on marine mud siltation in the estuary (HR Wallingford 1989a). For the winter and equinoctial conditions (October to April) the high fluvial flow case as hydrodynamically modelled above was used. This run would also be expected to include the most effect of the gravitational circulation and would therefore represent the greatest near bed import of material. For these conditions the model was run with concentrations in Tees Bay of 125, 250 and 600 ppm.

For the summer conditions the low flow (no fluvial flow) flow model results were used. These results would be expected to have the minimum effect of the gravitational circulation since it is directly related to the freshwater flow coming over the Barrage.

For these conditions the model was run for concentrations in Tees Bay of 125 and 250 ppm.

As the main import of sediment occurred during storm events near bed stresses in Tees Bay and in the mouth of the Estuary were enhanced by adding the wave induced bed stress from one of the runs of SWAN described in Chapter 3 (run A1, 3.87m significant wave height, 9s period).

4.3.3 Existing conditions

The volumes of sediment imported for the conditions simulated are shown below. The percentages used to combine the simulated volumes into an annual volume deposited in the estuary were as for the previous Tees Barrage studies.

Winter and Equinoctial period: 7 months

14.5%	30 days at 600 ppm	230,000 m ³ /year
21.4%	45 days at 250 ppm	110,000 m ³ /year
14.5%	30 days at 125 ppm	40,000 m ³ /year
50.0%	105 days negligible	negligible
	Sub-total	380,000 m ³ /year

Summer period: 5 months

14.5%	22.5 days at 250 ppm	70,000 m ³ /year
14.5%	22.5 days at 125 ppm	30,000 m ³ /year
71%	110 days negligible	negligible
	Sub-total	100,000 m ³ /year

Fluvial sediments 80,000 m³/year

TOTAL 560,000 m³/year

This total is of the right order compared to in situ dredged volumes (770,000-670,000m³, ABPmer (2005)) allowing for the fact that the prediction is for the whole estuary system not just the maintained areas and the modelled assumption of a large freshwater flow into the River Tees over the whole 7 month winter and equinoctial period and the consequent larger than average gravitational circulation. This simulation suggests approximately 80% of the deposition occurs during the 7 month winter/equinoctial period (assuming most of the fluvial input is in the winter). This proportionality approximately matches the findings of the Tees Barrage studies. The biggest single contribution to the total deposition by fine material in the estuary is the 30 days with a concentration of 600 ppm in Bay during periods of higher river flow.

Figure 4.19 shows the model distribution of the total predicted depths of annual accretion. It is clear that the model deposition is more concentrated in the estuary mouth than that observed.

4.3.4 Sensitivity to sediment resuspension

Although the above simulation was close to the correct total volume of fine material imported into the Tees Estuary further detail of which Chart areas the material eventually accumulated within was not possible without running long periods of simulation which was not feasible using a computationally intensive 3D model as applied and so the resultant depths of deposition were more concentrated in the estuary mouth. It was also the case that in general the currents further into the Estuary were not

great enough to re-suspend material allowing further transport with tidally or density driven currents. The barrage studies concluded that further resuspension of bed material was occurring due to dredging activity and the passage (and manoeuvring of) large ships. At the time of the Barrage studies it was practise to overflow the dredge hopper allowing finer dredged sediments to pass back into the estuary and removing only the coarse fraction. Although this overflow practice has been modified the action of the dredger in disturbing the bed remains.

A sensitivity test to this effect was undertaken by simulating the high flow conditions with a concentration of 125 ppm on Tees Bay but with bed stresses in the Channel within the Estuary to be increased such that they were above the critical stress for erosion for half of the flood and ebb tide period.

A comparison of the predicted infill for Chart area 7 shows the simulated infill for the 5th spring tide without enhanced resuspension as 30.9 m³/tide and the predicted infill with enhanced resuspension as 32.1 m³/tide. This result confirms the ability of increased bed stress within the Estuary to push more material landwards. This result is illustrated in Figure 4.20 which shows one tides worth of predicted deposition for high flow, spring tide conditions. Reductions are shown at the mouth of the Estuary with increases further into the estuary.

4.3.5 Post construction conditions

For the post construction case the same simulations were undertaken and the total volumes of deposition in the estuary calculated. It was assumed that the development will not alter the amount of fluvial input to the system.

Winter and Equinoctial period: 7 months

14.5%	30 days at 600 ppm	290,000 m ³ /year
21.4%	45 days at 250 ppm	140,000 m ³ /year
14.5%	30 days at 125 ppm	50,000 m ³ /year
50.0%	105 days negligible	negligible
	Sub-total	480,000 m ³ /year

Summer period: 5 months

14.5%	22.5 days at 250 ppm	40,000 m ³ /year
14.5%	22.5 days at 125 ppm	20,000 m ³ /year
71%	110 days negligible	negligible
	Sub-total	60,000 m ³ /year

Fluvial sediments 80,000 m³/year

TOTAL 620,000 m³/year

The simulated change in annual accretion of fine material is 60,000 m³/year which represents an increase of about 10% over the existing situation. The interesting result here is that the summer accretion volumes are predicted to decrease and the winter/equinoctial periods are predicted to increase. This suggests a balance between two effects with overall tidal currents reduced in the Estuary mouth due to the deepening but with enhanced gravitational circulation leading to larger near bed landwards residual flows.

Since the simulations undertaken covered more extreme freshwater flow conditions (60 cumecs for high flow and 0 for low flow) the predicted impacts (increase in winter period and decrease in summer period) are considered to be at the upper and lower limits of likely changes.

A calculation based on the first flood tide suggests less of an overall increase at 5% (30,000 m³/year) which would represent the changes from just the altered tidal dynamics before the gravitational circulation has a significant influence. A suitable upper estimate would assume the gravitational circulation associated with the average summer flow (long term average of about 11 cumecs at Low Moor during May-September) would be increased proportionally. This somewhat simplified assumption would give an increase in annual deposition of fine material (silts and clays) of the order of 25% (120,000 m³/year) within the Estuary system.

Since the bulk of the transport comes in from the Bay and enters the Estuary in the near bed layer very little effect would be expected on the intertidal areas (which are on the whole sandy around the estuary mouth. Further comparison of the existing and developed case is possible by comparing the distribution of the predicted depths of deposition in Figure 4.21 with the simulation of existing conditions shown in Figure 4.19. As mentioned above neither of the simulations include the effects of sediment resuspension within the estuary and so the increases are concentrated more in the estuary mouth than would be expected to occur in reality. Two indicative results from this plot are that increased deposition is to be expected in the immediate approaches to the proposed container terminal and that the general increase in the area of the Seaton Channel turning circle is predicted to result in some slight increases in Seaton Channel itself (order 10%). Since Seaton Channel is the main route for fine material supply onto Seal Sands this would indicate a potential for a slightly increased supply of fine material to Seal Sands. Within the material deposited on Seal Sands the proportion of fines is predicted to slightly increase.

5. *Sediment dispersion*

5.1 INTRODUCTION

This section describes an assessment of the dispersion of sediment associated with the capital dredging for the proposed development and the influence of the proposed works on discharge of sediment from Dabholm Gut.

The sources of sediment considered are:

- fine material released by dredging operations,
- material placed at disposal site, and
- fine material discharged into Dabholm Gut from industrial activities.

The HR Wallingford developed model SEDPLUME-RW(3D) was used to simulate the dispersion, deposition and resuspension of the fine sediment within the Tees Estuary and in Tees Bay at the proposed disposal sites. The dispersal of coarser sandy material placed at the disposal site was assessed using available current and wave observations at the disposal sites.

SEDPLUME-RW(3D) uses tidal currents to determine the advection of material within the water column and calculates areas in which suspended particles may settle on the bed, either temporarily (around slack water) or longer-term. In this way, areas where discharged solids are deposited may be identified. Dispersion in the direction of flow is simulated in the model by the shear action of differential speeds through the water column, while turbulent dispersion is parameterised using a random walk technique. The deposition and resuspension of particles at the seabed are modelled by assuming critical shear stresses for erosion and deposition.

The dispersion modelling undertaken does not include background concentrations but simulates the increase of suspended sediment concentrations over the background caused by sediment plumes.

In the Estuary the SEDPLUME model is driven by flows from the TELEMAC-3D model. In Tees Bay a series of near bed current measurements from a long term deployment of a CEFAS bed frame (HR Wallingford 1998b) were used to schematise the flow regime in the vicinity of the disposal sites as part of a detailed MAFF research project into the behaviour of dredged material.

5.2 EXISTING MAINTENANCE DISPOSAL PRACTICE

Presently the annual maintenance dredge in the Tees Estuary is about 700,000m³ of which 50-60% of this material can be deemed to be silt and clay.

During the MAFF research project a series of cores were taken from locations where maintenance dredging is undertaken in the estuary, from the hopper of the dredger and at the offshore disposal site. The results of the sampling are summarised below.

Location	Fines content (less than 63 microns) (%)	Median Grain Size (microns)
In estuary	87-97	7-17
In hopper	65-90	7-17
At disposal site	3-34	100-400

The cores taken from the disposal site generally comprised fine sand, silt and small particles of coal. Sectioning the cores clearly showed layers of fine sand separated by thinner layers of small granules of coal. It was assumed that the source of coal is a natural one rather than the dredgers transporting it to the site from the estuary.

Sampling of the disposal site was undertaken at locations where material had recently been placed by the Teesport TSHD dredgers. Only small amounts of fines were found in the cores suggesting that dispersion during disposal was very effective or that the strength of the placed material was very low so that it was washed off the surface of the cores during recovery.

Measurements of suspended solids concentrations close (~2.25km away) to the disposal site were rarely (if ever) influenced by the disposal activities. There exists a repeating pattern in terms of turbidity during the tidal cycle and concentrations during spring tides were typically higher than those during neaps. However, the major influence on near bed suspended solids concentrations was clearly demonstrated to be associated with wave conditions. The measurements illustrated a mechanism whereby storm waves generate a sediment source that remains available for resuspension by smaller waves for 3-4 weeks before either being dispersed from the site or having undergone sufficient consolidation to resist erosion (HR Wallingford, 2000)

5.3 DISPERSION FROM DREDGING OPERATIONS

5.3.1 Methodology

Using SEDPLUME-RW(3D) to disperse sediment from dredging operations there are a number of things that it is required to know about the dredging operations, such as dredger size, cycle time, overflow period etc which all feed to an understanding of the rate of sediment introduced to the water column. PD Teesport commissioned Dredging Research Ltd (DRL) to undertake a study of available dredging methods and suggest the various parameters which would act as input to the sediment plume study as well as providing further information on the likely construction process for the development.

It is proposed that a TSHD will be used for the dredging and reclamation of granular material (approximately 1 million m³) from the Seaton Channel Turning Circle and the downstream reaches of the Channel. It is proposed that a CSD loading into barges will be used for the bulk of the dredging of the mudstone (approximately 3.8 million m³). If mudstone is to be pumped ashore this can also be undertaken by the CSD when operating close to the reclamation area.

5.3.2 Dredge parameters used

The capital dredging operations are likely to be largely undertaken by trailer suction hopper dredger (TSHD), cutter suction dredger (CSD) and or backhoe dredgers. The last major capital dredging project on the Tees, 1998 at the Ro-Ro terminal was undertaken by CSD.

For the purposes of the EIA the backhoe dredger is not considered because whilst the total amount of material lost to the water column during the dredging is higher than for the CSD or TSHD the production rates are much lower and therefore the rates of release of fine material and the associated short term elevations in suspended solids concentration or temporary deposition of material will be smaller.

The trailer dredger sucks up a mixture of sediment and water from the sea bed and discharges this mixture into a hopper on the vessel. The cutter suction dredger involves an integrated cutter and suction device. The cut material (and water) is sucked to the dredger before being pumped either ashore or to a barge.

The proportion of solids loaded into the hopper (trailer) or barge (cutter) can be increased by continuing to dredge after the plant is filled. The excess water is discharged overboard and contains a proportion of the finer sediment fractions. This discharge, as well as the action of the dredger itself will lead to increases in suspended sediment concentrations. DRL used their hopper models to predict the nature of the overflow from different dredging activities and the particle size distribution of the material in the overflow and that remaining in the hopper or barge from the dredging of stiff clay and marl (DRL, 2005).

For the present study the model was used to simulate the dredging scenarios during a spring tide with low river flow. Reclamation runoff was also included. All the simulations were run for 3 tidal cycles with the dredgers releasing fine material (less than 60 microns) into the bottom 1 metre of the water column throughout the period.

The parameters used for the simulations were;

Sediment parameters

Critical shear stress for deposition	= 0.1 N/m ²
Critical shear stress for erosion	= 0.2 N/m ²
Erosion constant	= 0.001 m ⁻¹ s
Settling velocity (minimum)	= 1 mm/s
Diffusion coefficient	= 1.0 m ² /s
Dry density of settled material	= 500 kg/m ³

Cutter Suction Dredger

Filling time	= 27 mins
Overflow time	= 224 mins
Release rate	= 44 kg/s

Large Trailer Suction Hopper Dredger (6,000 m³ capacity)

Dredge cycle time	= 190 mins
Total dredge time	= 60 mins
Overflow time	= 60 mins
Release rate	= 173 kg/s
Transect length	= 1km
Speed of dredger when working	= 0.75 m/s (1.5 knots)

Figure 5.1 shows the four simulated cutter dredger positions and the two trailer dredger tracks. This figure also shows the positions of 7 'sensitive' receiver points at which time series of suspended concentration and depth of deposition were also extracted. The rationale for the points are as follows;

1. Power station intake,
2. Seaton Channel,
3. and 4. Seal Sands,
5. North Gare Sands,
6. Bran Sands and
7. Intertidal upstream of development (part of SSSI).

5.3.3 Simulation results

Cutter suction dredger

Figures 5.2 and 5.3 show the peak concentration and the net deposition achieved during the 3 tide simulation.

The use of the CSD in the area of the reclamation and Tees Dock turning circle is predicted to increase suspended sediment concentrations by 500mg/l in the immediate vicinity of the barge loading site but beyond this immediate zone, the increase in concentration is predicted to be of the order of 25mg/l or less.

Furthermore, peak deposition of material onto the seabed is also very localised to the barge loading site when dredging the Tees Dock turning circle. When dredging the area adjacent to the proposed reclamation, peak deposition of material onto the seabed is generally less than 5mm, with greater deposition in the immediate vicinity of the dredging activity. It should be noted that much of the material is predicted to deposit within the footprint of the dredging and/or reclamation and as such it would be re-dredged or would deposit within an area which has already been dredged.

The use of the CSD loading into barges on one or other side of the main channel limited the cross-channel dispersion of fines and a significant reduction in peak concentrations from one side of the channel to the other was predicted with the most dispersion along the main direction of flow. This would suggest that locations across the channel from the barge loading site would not receive as much sediment as those along the channel.

Trailer dredger

For spring tide conditions with low freshwater flow, the effect of dredging sandy material with a TSHD in the approach channel and pumping ashore at the reclamation site is shown in Figure 5.4. It can be seen that peak concentrations between 500mg/l and 1000mg/l occur along the dredger track and in the vicinity of the run-off from the reclamation. Increases in suspended sediment concentrations above those occurring with the CSD are predicted. Concentrations of up to 50mg/l are also predicted over parts of Seal Sands and up to 25mg/l in the Seaton Channel.

This scenario results in a fraction of a millimetre of deposition on Seal Sands per tide (up to 0.05mm for the three tides simulated; Figure 5.5). The effect of dredging in the approach channel on suspended sediment concentrations over Seal Sands and in the Seaton Channel is further illustrated by reference to Figure 5.6 and 5.7.

5.3.4 Conclusions

For all the dredger simulations the largest raising in peak concentrations and deposition were in the immediate vicinity of the dredger, centred either at the barge loading position (in the case of the cutter suction dredger) or along the trailer dredger track.

5.4 DISPERSION FROM DISPOSAL AREA(S)

5.4.1 Particle size distribution of material to be disposed

DRL (2005) have predicted the particle size distribution of the material arising in the barge or hopper from the dredging of the stiff clays and marl with CSD or TSHD. This material is likely to be placed offshore at the existing licensed maintenance or capital dredge disposal sites.

For the CSD loading into 4,000m³ barges and the 23,000m³ TSHD loading with twin pipes (the two scenarios simulated in Section 5.2) the predicted particle size distribution is as follows:

Particle size (micron)	4,000m ³ barges loaded by CSD Percentage composition	23,000m ³ TSHD Percentage composition
Less than 20	1.20	0.63
20 to 60	1.67	0.77
60 to 80	1.29	0.56
80 to 100	2.54	1.11
100 to 150	10.55	4.72
150 to 200	17.61	10.70
200 to 300	14.21	8.67
300 to 400	8.29	7.60
400 to 600	5.92	10.87
600 to 1000	5.92	10.87
1000 to 2000	5.92	10.87
2000 to 4000	5.93	10.87
4000 +	18.96	21.75

The dredgings arising from CSD are shown above to have proportionately greater amounts of fines (less than 60 microns) and fine sand (60 to 200 microns) than the dredgings arising from the TSHD.

5.4.2 Release of fine material at the offshore disposal sites

Both the existing licensed offshore disposal sites are being considered for placement of dredged material from the proposed works. There has been previous detailed investigation on behalf of what was then MAFF into the behaviour of maintenance dredged material at the inshore disposal site (HR Wallingford 1998b).

For the simulation of the release of fine material at the disposal sites the case of the CSD operating for the disposal of 2.9 million m³ was considered in this assessment because this scenario presents the largest disposal volume of fine material (hence this is a worse case scenario).

The simulation of the CSD barge disposal activities assumed a ten minute period for the disposal itself resulting in a release rate to the water column of 75kg/s over this period. Each placement from the CSD barge releases about 2977m³ material, 3% of which will be fine (clay or silt) with the remainder of the material being coarser, less dispersive, material. This compares to the hopper size of the small TSHD routinely undertaking the maintenance dredging in the Tees Estuary which is about 1,500m³, with the maintenance dredged material being fine. It can thus be seen that the capital dredging will result in far lower rates of introduction of fine material to the offshore disposal sites

than presently occurs during the course of routine (and near continuous) maintenance dredging. It can thus be concluded based on the detailed monitoring undertaken in 1996 and described in Section 28.3 that the physical effect of fines released at the offshore disposal sites as part of the proposed capital dredging will be significantly less than that associated with the disposal of maintenance dredged material.

To further illustrate the dispersion of fines from the capital dredging a flow field for the offshore area was developed from the near bed currents measured by the CEFAS bed frame during deployment 139 over the spring-neap-spring period 12 to 26 December 1996 (HR Wallingford 1998b). The flows were measured at a fixed height of 0.42m above the bed. The measured currents were scaled by a factor of about 1.6 to provide an estimate of the depth average current speed. The measured directions were assumed to be uniform through depth.

The measured flow field was used in this way to avoid establishing a high resolution offshore depth averaged flow model. This approach is justified because of the relatively weak currents and small distances over which offshore dispersion under currents alone will occur.

Simulations were undertaken for disposal activities over an entire spring-neap cycle at both the maintenance disposal site (inshore; Tees Bay A) and the capital disposal site (Tees Bay C). The results of the simulations are illustrated in Figures 5.8 to 5.11. The figures show the dispersion under calm (no wave) conditions and illustrate that under these conditions most of the fines deposit close to the point of disposal. Concentrations are increased by approximately 5 mg/l within an area 2km from the boundary of the disposal area.

No peak deposition depths greater than 1mm were predicted outside the boundary of the disposal areas during the simulation.

5.4.3 Dispersion of fine sand from the offshore disposal sites

Based on the DRL predictions (see Section 5.1) between 17% (TSHD) and 32% (barge loaded by CSD) of the material placed at the offshore disposal sites arising from the dredging of stiff clay and marls can be described as being fine sands (60 to 200 microns).

A series of calculations were undertaken to see if fine sandy material deposited at the offshore sites would tend to accumulate or if local hydrodynamic forces at the sites were enough to quickly disperse placed material.

The measured current data from CEFAS minipod deployment 139 in the Tees disposal site during the winter of 1996-1997 (HR Wallingford, 1998b) was used in order to investigate the dispersal of sediment in the disposal site.

Figure 5.12 shows a conceptual sediment transport diagram over the maintenance disposal site (the figure also shows the location of the minipods used for the analysis). The analysis concludes that the site is generally dispersive. The fine sandy sediment is transported both in the ebb and the flood directions so that it will disperse away from the site, with a slight preference over the flood.

The calculated gross rate of dispersal over the full width of the disposal site, using the measured currents and the full wave climate, is $100\text{m}^3/\text{tide}$ for a representative neap tide and $200\text{m}^3/\text{tide}$ for a representative spring tide.

One of the measurement periods included placement of maintenance dredging material covering a 6 week period during which a total of $92,500\text{ m}^3$ of dredged material were placed, 60% of which were sands. This gives a rate of sand placement of $1,100\text{ m}^3/\text{tide}$, i.e. 3-5 times the calculated dispersal rate due to tides alone. Short term accumulation would therefore be expected during disposal operations although once disposal operations are concluded the accumulated material would continue to be dispersed. However within the recorded period storm event were shown to increase the dispersal rate by an order of magnitude confirming the medium term dispersive nature of the disposal sites.

Assuming three placements of material from the large TSHD per day the total amount of fine sandy material placed will be about $12,000\text{m}^3/\text{day}$. This is at a significantly higher rate than that associated with the placement of maintenance material. Thus it would be expected that coarser material is retained in the vicinity of the disposal site and an observable change in bed conditions occurs, particularly over periods of low wave activity.

The analysis described above was carried out assuming a sediment size of 0.1mm. Sensitivity to the sediment size was investigated calculating the rate of dispersal for a 0.2mm sediment size. The calculated transport rate for the 0.2mm sediment size is halved when comparing it to the 0.1mm. Consequently, the timescale of dispersal will also be doubled with the coarser sediment size.

The conclusion of these calculations is that some short term build up of fine sandy sediment in the area would be expected during the dredging and disposal operations. However in the medium term material placed at the sites will be dispersed. This dispersal will be in flood and ebb directions but with a small bias towards the flood direction (southeast). This bias towards the south east is also evident in the dispersion of fines.

5.4.4 Behaviour of coarser material at offshore disposal sites

Approximately 30% to 40% of the material arising from the dredging of stiff clay and marl is predicted by DRL to be greater than 1mm in size. This material will be relatively immobile at the disposal sites and apart from the gradual weathering of the material and abrasion into smaller fragments this material can be expected to remain within the disposal sites.

5.5 DABHOLM GUT

5.5.1 Methodology

Dabholm Gut is a 1200m long canalised stretch of water at Teesport, with a gently sloping bed which dries out for a significant period during the tidal cycle. The area covered by the dispersion model's output mesh extended from North Gare Sands and Bran Sands to approximately 500m upstream of Tees Dock, with a mesh resolution of 20m.

For the model simulations, particles were released continuously near the head of Dabholm Gut (Figure 5.13). In reality, sediment may be released for just part of each

tidal cycle, but the approach was adopted in order for the results to indicate the envelope of deposition areas for releases at any time during the tidal cycle. During times when the particle source location was dry, particles were allowed to accumulate, so as to become available for transport as the water level rose subsequently. It is accepted that the model represents only approximately the rates at which particles pass from Dabholm Gut to the main Tees Estuary, but the approach is considered to be acceptable, given that the bathymetry of Dabholm Gut is not known accurately, and that any flow in the Gut is limited to a very narrow channel at times of low water level.

The sediment parameters were defined in the dispersion model as follows:-

Settling velocity	0.001m/s
Critical shear stress for deposition	0.10 N/m ²
Critical shear stress for erosion	0.11 N/m ²

Erosion was instantaneous whenever the bed shear stress exceeded the critical shear stress for erosion.

The particle discharge rate was equivalent to 174 tonnes per day which is the amount licensed although the present day discharge is thought to be less than half of this - 22,000 tonnes/year (about 60 tonnes/day; ABPmer, 2005).

The model was run, for both the existing layout and the proposed layout with dredged depths, to simulate the following conditions;

- mean spring tide, no freshwater input,
- mean spring tide, 60 cumecs freshwater input,
- mean neap tide, no freshwater input,
- mean neap tide, 60 cumecs freshwater input.

The existing and proposed bathymetries of the 3D flow model which provided flows for the plume dispersion modelling are shown in Figure 2.4.

For each test condition the model was run for a sufficient number of tidal cycles to establish a repeating pattern of the extents of suspended particle distributions.

For the last tide of each simulation, the results are shown as increases in deposits over the tidal cycle, as maximum deposits within the tidal cycle, and as depth-averaged suspended particle concentrations at four states of tide; peak flood, HW, peak ebb and LW.

5.5.2 Existing conditions

On the spring tide, low flow condition (Figure 5.14), the suspended solids plume leaves the Gut during the ebb tide and extends some 2km downstream at LW. At HW, the plume extends upstream of Dabholm Gut, beyond the landward limit of the model's output mesh. Figure 5.15 shows the increase in deposits over the tidal cycle. These are in the eastern part of the river, between Tees Dock and some 1500m north of Dabholm Gut, and also in the turning circle opposite Tees Dock. The maximum deposits over the tidal cycle are shown in Figure 5.16. Comparison of Figures 5.4c and 5.4d indicates that some deposition occurs in the western part of the river around slack water, but that these deposits are re-suspended at times of relatively high current speeds.

There are two principal differences between the low and high flow conditions which affect the simulated distributions of released particles. Firstly, in high flow conditions, the seaward net flow of low salinity water near the surface enhances ebb tide flows and reduces flood tide flows, whilst near the bed, the flood tide flows are enhanced in the winter and the ebb flows reduced; secondly, the absence of density variations in the water column under low flow conditions allows particles to mix over the depth relatively easily, whilst under high flow conditions, vertical mixing is inhibited by the vertical density gradients associated with salinity variations, so particles have a much reduced tendency to mix through the water depth. As a result of these differences, seaward movement of particles from Dabholm Gut is much less pronounced on the spring tide under high flow conditions (Figure 5.17) than on the equivalent tide in low flow conditions (Figure 5.14), and under high flow conditions particles are less widely distributed east-west across the River Tees. The pattern of increase in deposits and the distribution of maximum deposits (Figures 5.18 and 5.19 respectively) reflect the changes in suspended particle distributions between the two flow cases, with less deposition seaward of Dabholm Gut under high flow conditions, and a reduced spread of deposits across the River Tees.

Relative to the spring tides, the neap tide current speeds and tidal excursions in the River Tees are reduced. Furthermore, maximum water depths and flows in Dabholm Gut are lower on neap tides than on spring tides, so the tendency of particles to leave Dabholm Gut is reduced on neap tides. As a result of these differences, during the neap tide under low flow conditions (Figures 5.20 to 5.22), the extent of the plume of suspended particles is much reduced relative to the equivalent spring tide simulation (Figures 5.14 to 5.16). Similar differences are evident between the neap tide under high flow conditions (Figures 5.23 to 5.25) and the equivalent spring tide simulation (Figures 5.17 to 5.19).

5.5.3 *Proposed layout*

Qualitatively, the simulated suspended and deposited particle distributions for the spring tide under low flow conditions are generally similar for the proposed layout (Figures 5.26 to 5.28) to the existing conditions (Figures 5.14 to 5.16). The main differences are that the high suspended particle concentrations in the core of the plume are close to the shore to the north and south of Dabholm Gut for the proposed layout (compare Figure 5.26 with Figure 5.14), and that deposition near the shore immediately to the north of the Gut is enhanced in the proposed case (compare Figures 5.27 and 5.28 with Figures 5.15 and 5.16 respectively). Similar changes occur between the existing conditions and the proposed layout for the other tidal/flow conditions simulated (compare Figures 5.29 to 5.37 for the proposed layout with Figures 5.17 to 5.25 for the existing conditions). For spring tide conditions, deposition in the deepened turning circle at the mouth of Tees Dock is somewhat enhanced for the proposed layout, particularly under high flow conditions (compare Figures 5.30 and 5.31 for the proposed layout with Figures 5.18 and 5.19 respectively for existing conditions).

5.5.4 *Conclusions*

The HR Wallingford dispersion model SEDPLUME-RW(3D) was used to carry out plume simulations for suspended particles released into Dabholm Gut, within the area of Teesport. Four tide/freshwater flow combinations were modelled for both the existing and proposed port layouts and dredged depths. The plume model was driven by the results of tidal simulations carried out as described in Chapter 2 of this report.

On the whole, the model predictions indicate that the distributions of suspended and deposited particulates from Dabholm Gut will be similar for the proposed layout to existing conditions. The main differences are that for the proposed layout the core of the plume of suspended particles tends to be closer to the east bank of the River Tees than under existing conditions, so that deposition is enhanced near the shore to the north of Dabholm Gut. For spring tide conditions, deposition in the deepened turning circle at the mouth of Tees Dock is somewhat enhanced for the proposed layout, particularly under high flow conditions.

6. *In-combination effects for Northern Gateway and Seaton Channel deepening.*

6.1 INTRODUCTION

The effects of the proposed Northern Gateway development in-combination with the deepening of the Seaton Channel on the hydrodynamics and sediment transport regime of the area were studied using the suite of numerical models established for the EIA study for the Northern Gateway development as described above.

Det Norske Veritas have studied the Seaton Channel deepening on behalf of Able UK (DHV, (2004) and ABPmer have studied the deepening on behalf of PD Teesport (ABPmer, (2003)). Their predictions of the effect of the Seaton deepening were generally reduced currents with an associated increase in siltation rate in the channel, but with little effect on the adjacent intertidal areas of Seal Sands. Since these studies the proposed design of the deepened Seaton Channel has been refined resulting in a proposed channel deepened to -9m below Chart Datum (CD) but somewhat narrower than the present channel. This narrowing (to approximately 100m) acts to move the toe of the dredged channel further away from intertidal areas.

6.2 HYDRODYNAMICS

The deepening of the Seaton Channel to the proposed depth of -9.0m CD was added to the proposed channel deepening associated with the Northern Gateway Container Terminal. Details of the proposed layout were taken from drawing SC-01008 B drawn for Able UK. The two model bathymetries and the difference between them are plotted on Figure 6.1. The channel is deepened by a maximum of just over 5m. The proposed slight narrowing of the channel means that all the bed changes appear within the existing channel extents.

Figures 6.2 and 6.3 show the current magnitude before and after the Seaton deepening and the speed difference at times of peak ebb and flood current. The conditions illustrated are for depth averaged flows during a spring tide with high freshwater flow. At both stages of the tide a general reduction of current magnitude of 0.2–0.4 m/s is shown. The ebb tide results show a small area of speed increase to the north of the channel which does not appear at times of peak flood currents. Figures 6.4 and 6.5 show the changes in the near bed and near surface current pattern for the before and after deepening cases. Some changes in the current pattern in the eastern end of Seaton channel as it meets the Seaton Turning Circle are shown. Further detail of any changes to the 3D nature of the current is shown in Figures 6.6 and 6.7 where time histories of near surface, mid-depth and near bed currents are shown at two locations, one at the entrance to Seaton Channel (1) and one adjacent to the power station intake (2). The general reduction of the currents is confirmed by these plots with particular reductions in the near bed current shown at Position 2 during the flood tide. The balance of the near surface and near bed currents does not appear to be altered.

6.3 SEDIMENTATION

Presently Seaton Channel does not undergo regular maintenance, with dredging campaigns around major vessel movements. In the 3 year period following a recent dredging campaign siltation rates of approximately 90,000 m³ per year were observed,

mostly occurring at the eastern end of the channel (ABPmer, 2005), although longer term data is not available to see if this rate diminished for subsequent years. DNV (2004), estimated the infill rate in Seaton Channel from the overall volume removed from Chart area 9 scaled by plan area. This analysis produced an estimate of 36,000 m³ per year. Application of the 3D flow and fine sediment transport model suggested a rate of infill of 33,000m³ per year of fine material which would be added to by any sands.

The deepening of the Tees Approach Channel was predicted to increase the source of fine material at the entrance of the Seaton Channel which would enter the channel on the flood tide by approximately 10%. When the Seaton Channel deepening is included the predicted deposition rate was 34,000 m³ per year an increase of approximately 3% compared to baseline conditions. This increased deposition was a result of the generally reduced currents in Seaton Channel, which is also where the increase in deposition was predicted to occur mostly at the seaward end of the channel and decreasing towards the west. No increased import of sediment is predicted as the 3D nature of the currents is unaffected. However because the width of the channel is reduced compared to present conditions the increase in sedimentation in Seaton Channel accounts for only a third of the predicted increase in sediment supply to the Seaton Channel / Seal Sands area.

The implications of the in-combination test for Seal Sands are that the deepening of Seaton Channel will result in deposition of approximately a third of the increase of supply of fine sediment entering Seaton Channel resulting from the proposed Northern Gateway deepening.

This would also imply that a deepening of Seaton Channel alone would reduce the supply of fine material to Seal Sands.

7. *Sensitivity test for Tees Approach Channel and Seaton Turning Circle*

7.1 INTRODUCTION

A small variation to the scheme was proposed to remove the dredged areas further away from the embankments, reducing any risk of undermining them. The areas of concern were the half tide training wall on the southern side of the Channel adjacent to Bran Sands and the intertidal area immediately to the north of the entrance to Seaton Channel. The proposed changes were;

- moving the channel toe on the south channel edge 5m into the channel
- extending the deepened area of the Seaton turning circle to the south rather than the North
- leaving the section of the Seaton Turning area nearest to the intertidal foreshore at the existing declared depth of 11.8m CD.

The revised design change required modelling to compare it with the scheme reported on for the main study.

7.2 SIMULATIONS UNDERTAKEN

The established TELEMAC model of the area was amended to include the changed layout and run for spring tide conditions under high fluvial flow. These conditions were chosen to demonstrate the effect of the change on the highest typical currents in the area.

Figure 7.1 shows the model bathymetry for the initially proposed and amended cases alongside the difference between them. The changes to the Seaton Turning Area can be seen with shallower depths near to the foreshore and increases in depth on either side linked to the reshaping of the turning area. The changed alignment on the south side of the channel is too small to be displayed by the model resolution.

The model results are shown in Figures 7.2 and 7.3 which show the tidal current magnitudes at times of peak ebb and flood tide and the difference between the initially proposed and the amended layouts. The differences can be seen to be localised to the areas of bed change with the only consistent change being speed reductions in the small deepened areas. Figure 7.4 shows the pattern of depth averaged tidal currents at the times of peak ebb and flood tide. This figure confirms the small and localised effect of the revised scheme compared to that reported on for the main studies.

It can be concluded that the impacts of the proposed deepening reported on for the main studies above would not be significantly altered by the revised scheme except to reduce the potential adverse effect on the slag embankments adjacent to the dredged area.

8. *Summary and conclusions*

Numerical models of the Tees Estuary have been established for the modelling of tidal and density driven flow, waves and sediment transport. Where available these have been calibrated against the best available data.

The models have been applied to study the impacts of the proposed Northern Gateway Container Terminal in terms of changes to the hydrodynamic and sediment transport regimes.

Plume models have been applied to study the fate of material released by the capital dredging and disposal operations and the impact of the scheme on the dispersion of solids discharged into Dabholm Gut.

The findings of the study in terms of the predicted impacts of the development were;

During the construction phase

The sediment plumes resultant from the operation of cutter suction and trailer suction hopper dredgers at the main dredging locations were simulated. For all the dredger simulations the largest rise in peak concentrations and deposition were in the immediate vicinity of the dredger, centred either at the location of the barge loading pontoon or along the line of the trailer dredger track.

Disposal operations during the construction phase were not predicted to lead to enhanced deposition of fine material greater outside the boundary of the disposal areas. The suspended fine sediment concentrations increases were predicted to be less than 5mg/l further than 2km from the boundary of the disposal areas. A short term accumulation of the sand sized fraction within the disposed material at the disposal sites was predicted. However in the medium term the deposited material is predicted to be dispersed from the offshore disposal sites by the tidal currents, a process which would be strongly enhanced by wave effects.

During the operational phase

The scheme is predicted to have a very small effect on water levels with tidal range increased by less than 2mm at the proposed Container Terminal and less than 4mm at the Barrage.

Currents were predicted to decrease in the deepened areas and some increase in the near bed net landward flow associated with the density driven, gravitational circulation present in the area.

The wind waves generated in the estuary are affected by the proposed changes in reflective properties of the Teesport Container Terminal, but are unaffected by the changes to dredging at depth, as they are short period waves.

The modelling of incoming swell waves showed that the deepened channel reflects more wave energy from these long period waves increasing the significant wave height on the eastern side of the Norse Oil Terminal. This increased reflection within the channel leads to a slight decrease in significant wave height on North Gare Sands and Bran Sands. The pattern of change was similar for all return periods modelled and showed only a slight dependence on the direction of incoming swell. The swell waves do not

reach as far up the estuary as the Teesport Container Terminal, and so are unaffected by the reclamation itself.

The predicted volumes of infill to maintained areas for sandy material in the existing and the proposed scenario do not change by a great amount. These results highlight that channel infill is only very slightly modified by the dredging and therefore unlikely to rise to any adjustment in the maintenance figures for sandy material.

Sand transport processes in the outer estuary over the intertidal areas at the mouth are unchanged for representative conditions. For storm wave conditions a small reduction in wave energy over the intertidal areas, particularly over North Gare, is predicted which would suggest an increase in the potential for deposition or a reduction in the rate of erosion. These small changes are unlikely to be significant in terms of the overall morphology of the intertidal areas within the variability of the number of storm events in any given year. A further potential effect is a reduction in sand transport from North Gare towards Seaton Channel and from there onto Seal Sands.

Deposition in the Estuary system from fine material (clay and silt) was predicted to increase by about 60,000 m³/year. This could vary considerably from year to year considering the variation in the number of storm event bringing material into suspension and the variation in the freshwater flow changing the rate of near bed import by the gravitational circulation. Suitable lower and upper estimates of the change of deposition rate from the development were between a 5% and 25% increase compared to present conditions.

The general increase in sediment import in the area of the Seaton Channel turning circle is predicted to result in some slight increases in Seaton Channel itself (order 10%). Since Seaton Channel is the main route for fine material supply onto Seal Sands this would indicate a potential for a slightly increased supply of fine material to Seal Sands. Within the material deposited on Seal Sands the proportion of fines is predicted to slightly increase.

The dispersion of suspended solids released into Dabholm Gut at Teesport is predicted to be of the whole similar after the development. The core of the plume of suspended particles is predicted to be closer to the east bank of the River Tees than under existing conditions, so that deposition is enhanced near the shore to the north of Dabholm Gut. Some enhancement of deposition in the upstream turning circle is predicted for larger tide ranges particularly under high freshwater flow conditions.

The tested scheme was further simulated in combination with the proposed deepening of the Seaton Channel to -9m CD. The in combination simulation showed the speed decrease in Seaton Channel would result in deposition of approximately a third of the extra sediment imported due to the Approach Channel deepening.

The sensitivity of the simulation results to a change to the detail of the Approach channel and Seaton Turning circle was tested. This sensitivity test demonstrated no significant difference in the hydrodynamic effects compared to the original scheme

The overall conclusion of the study was that the proposed development once operational would not significantly change the hydrodynamic or sedimentological regimes or morphology in the Estuary.

9. *References*

ABPmer (2002) Tees Entrance Channel Study. Conceptual Model of Estuary Processes. Report R.972.

ABPmer, (2003). Tees Entrance Channel Study Part 2. Numerical modelling of deepening of Seaton Channel. Report R.991.

ABPmer (2005) Tees Maintenance Dredging Baseline Document. Report R.1149.

Allsop N W H (1990), "Reflection Performance of Rock Armoured Slopes in Random Waves", Proc Int Conf Coastal Engineering, Delft.

Babtie (1998). Shoreline Management Plan – Seaham Harbour to Saltburn (Sub-Cell 1c) & Consultation Document

Bsi (1984). Code of Practice For Maritime Structures – Part 1: General Criteria. Bs6349-1:1984.

Chesher, T.J., and Miles, G.V. (1992). The concept of a single representative wave for use in numerical models of long term sediment transport predictions. In Hydraulic and Environmental Modelling: Coastal Waters. Proceedings of the Second International Conference on Hydraulic and Environmental Modelling of Coastal, Estuarine and River Waters, Volume 1. Falconer, Chandler-Wilde and Liu (Eds). Ashgate.

Det Norske Veritas, (2004). Environmental assessment of dredging operations, changes in hydrodynamics and sediment transport, TERRC facility. Report 2004-1387.

Dredging Research Limited (2005) PD Teesport – Northern Gateway EIA, Dredging Aspects, Report to PD Teesport prepared by R N Bray, 8th December 2005 - CONFIDENTIAL

Goda, Y. (1985). Random Seas and Design Of Maritime Structures. University Of Tokyo Press, 1985.

Halcrow (1991) Tees Estuary Dredging Review. Report for Tees and Hartlepool Port Authority.

Haskoning UK (2005). Northern Gateway Container Terminal. Environmental scoping report.

HR Wallingford (1977). Hartlepool Power Station – Flooding Hazard Assessment. Report EX 3711.

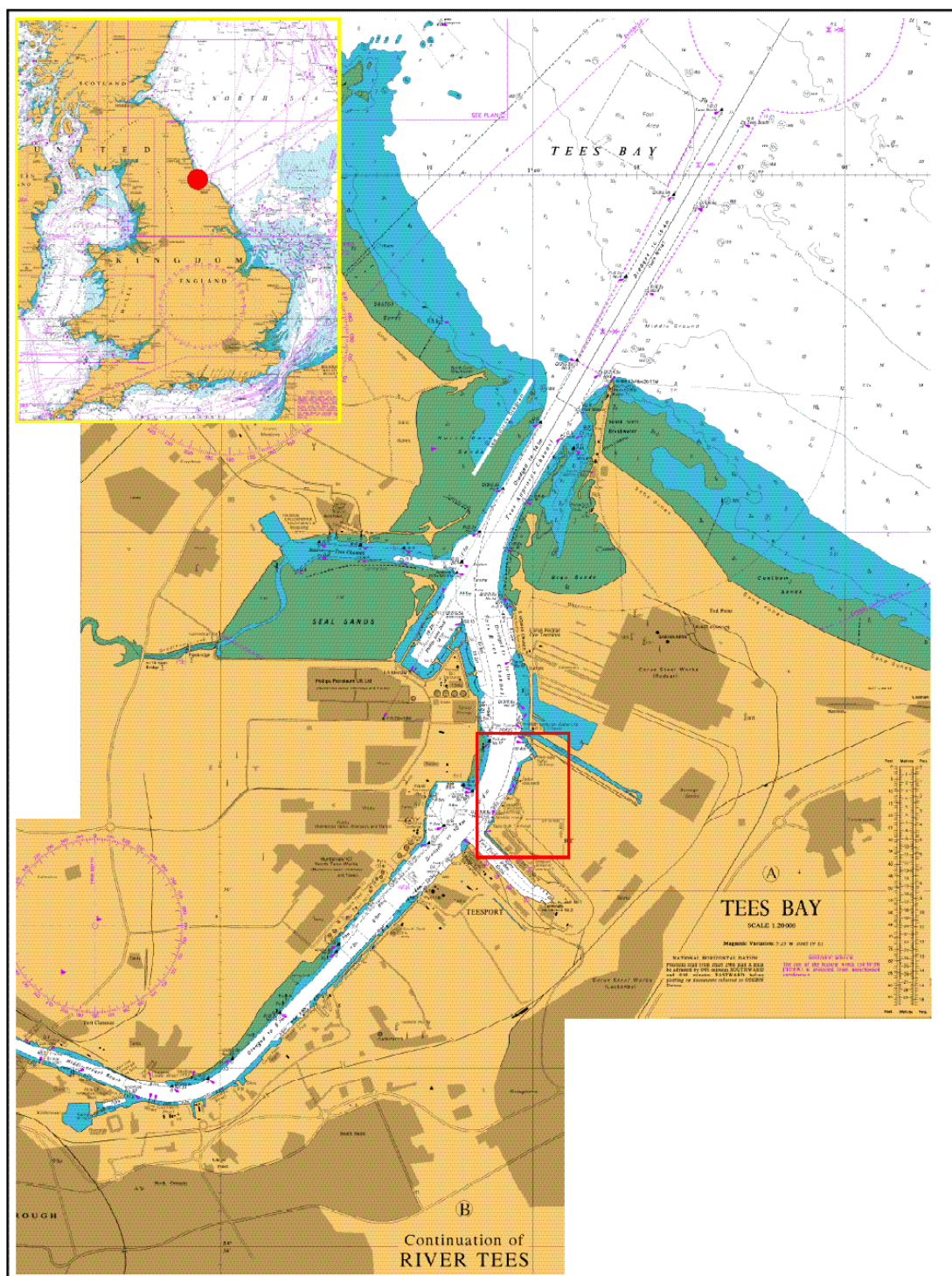
HR Wallingford (1989a). Tees Barrage. Effect of the barrage on marine mud siltation. EX 1975.

HR Wallingford (1989b). Tees Weir feasibility study Phase 2. Correlation between waves, tides and suspended mud concentrations in Tees Bay. EX 1938.

HR Wallingford (1992). Tees and Hartlepool Port Authority. Review of Dredging. EX 2580.

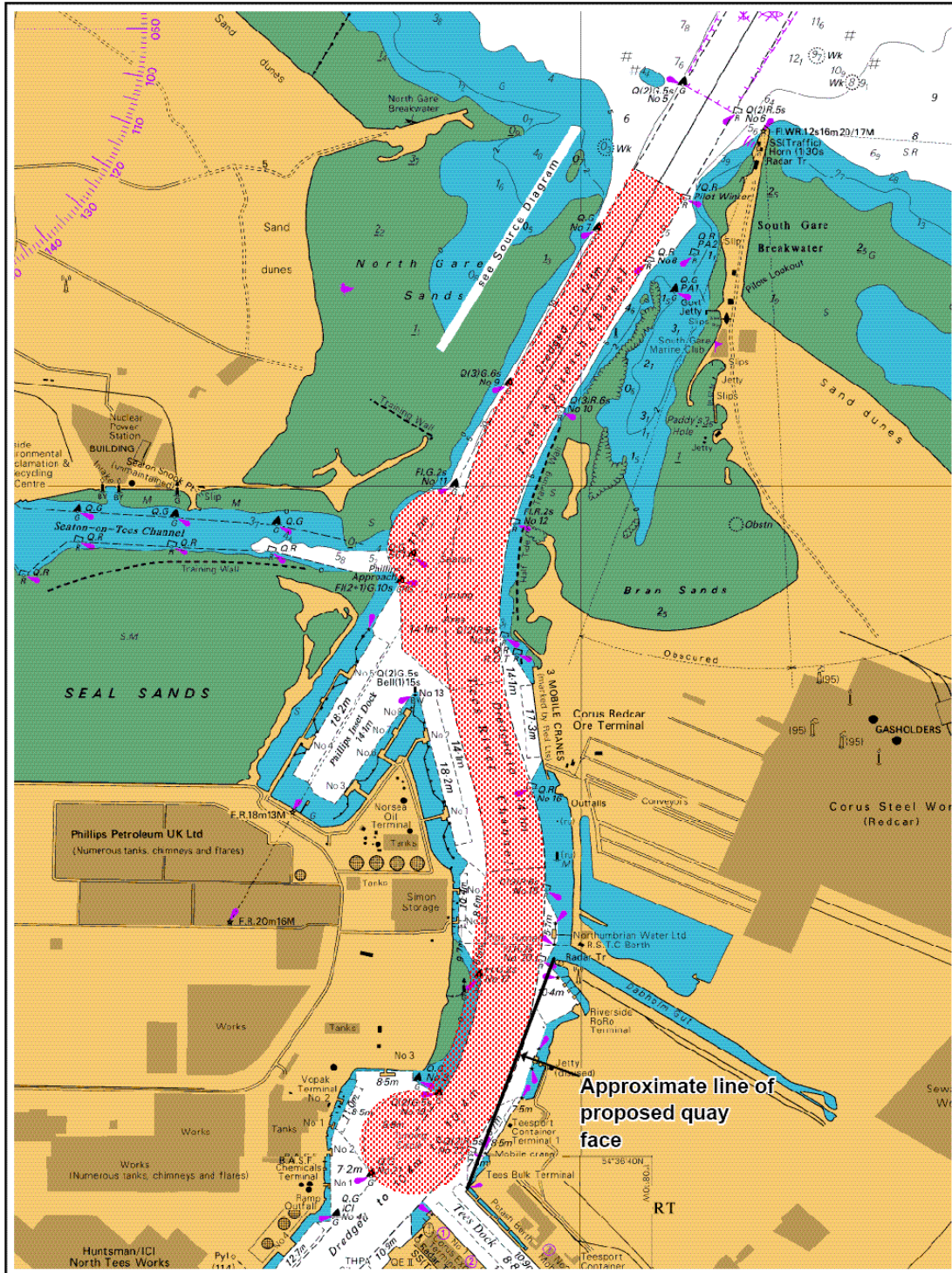
- HR Wallingford (1995) Hydraulic Studies for Teesport 2000. EX 3284.
- HR Wallingford (1998a) Measurement of sediment properties of dredged material from the Tees estuary, Report TR 54.
- HR Wallingford (1998b) Minipod deployments at the Tees disposal site, Report TR 61.
- HR Wallingford (2000) Properties of Dredged Material, Final Report, Report SR 517.
- HR Wallingford (2002). Teesmouth Sediment Study. EX 4514.
- Luck M. and Guesmia M., (2002). SUBIEF-3D Version 5.3. Manuel d'utilisation. HP 75/02/086/A.
- Malcherek A., Markofsky M., Kielce W., Peltier E., Le Normant C., Teisson C., Cornelisse J., Molinaro P., Corti S., Grego G., (1996), Three dimensional numerical modelling of cohesive sediment transport processes in estuarine environments. Final report to the EC contract MAST2-CT92-0013.
- Manning, A. (2004). Estuary Research Project Phase 2 (EstProc). The development of new algorithms to parameterise the mass settling flux for Estuarine sediments. HR Wallingford Report TR 145.
- Plater, A.J., Ridgeway, J., Appleby, P.G., Berry, A., and Wright, M.R. (1998). Historical contaminant fluxes in the Tees Estuary, UK: Geochemical, Magnetic and Radionuclide
- Winterwerp, J.C. (2003) On the Deposition flux of cohesive sediment. Proceedings of 7th International Conference on Nearshore and Estuarine Cohesive Sediment Transport Processes. In press.
- Soulsby, R.L. (1997). Dynamics of Marine Sands. Thomas Telford Publications.

Figures



<p>Key:</p> <p>Source: ARCS Charts under license from the UKHO</p>	<p>General location of proposed container terminal</p> <p>Northern Gateway Container Terminal EIA</p> <p>PD Teesport</p> <p>JUNE 2005</p> <p>Approx scale: 1cm - 0.5km</p>	<p>Figure 1.1</p> <p>ROYAL HASKONING</p>
-----------------------------------------------------------------------------------	----------------------------------------------------------------------------------------------------------------------------------------------------------------------------	-------------------------------------------------

Figure 1.1 Study area




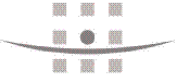
<p>Key:</p> <p> Proposed dredge area</p>	<p>Footprint of proposed capital dredging</p> <p>Northern Gateway Container Terminal EIA</p> <p>PD Teesport</p>	<p>Figure 2.3</p>
<p>Source: ARCS Charts under license from the UKHO</p>	<p>JUNE 2005</p> <p>Approx scale: 1cm - 0.16km</p>	 <p>ROYAL HASKONING</p>

Figure 1.2 Proposed development

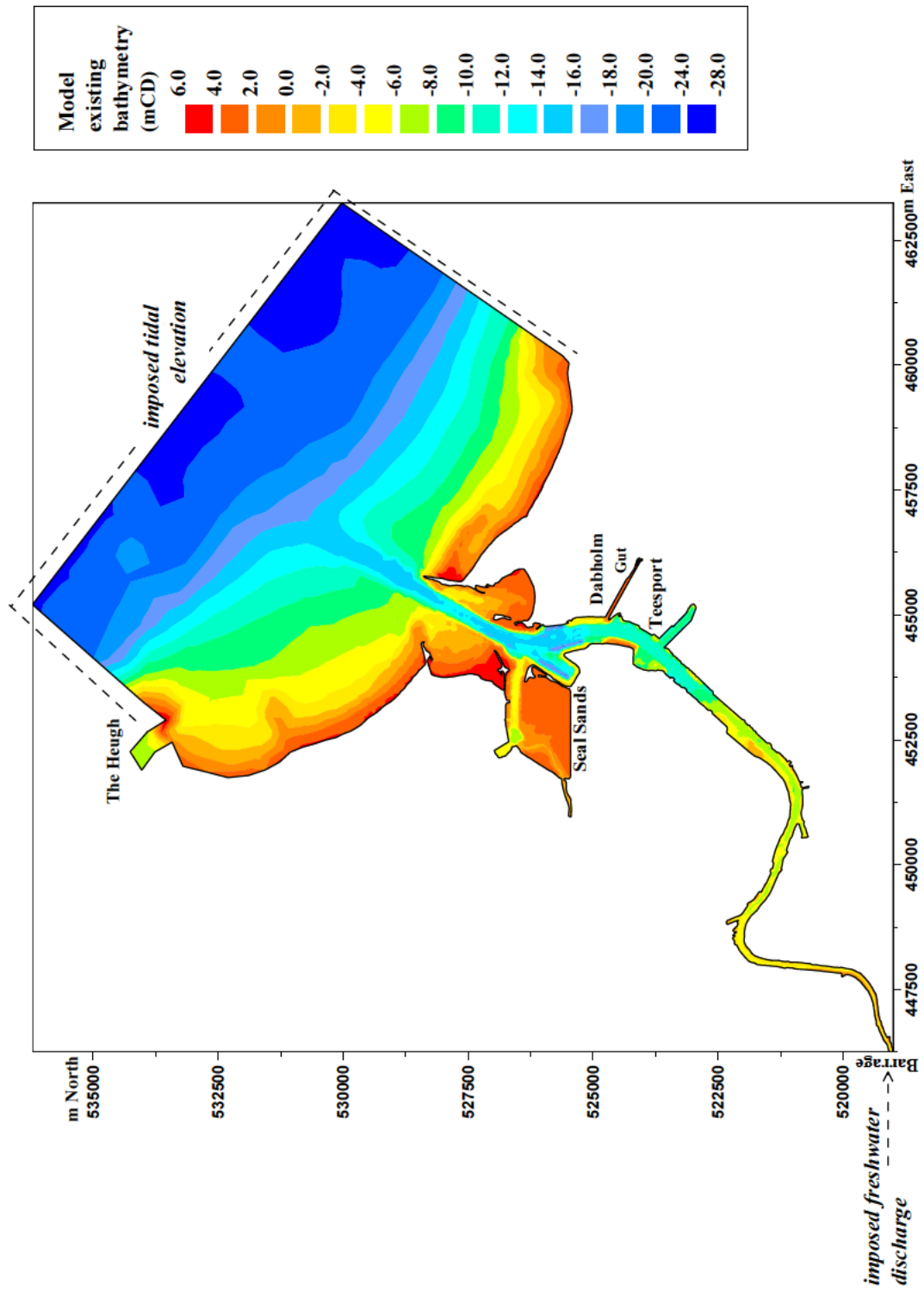


Figure 2.1 Model domain and bathymetry

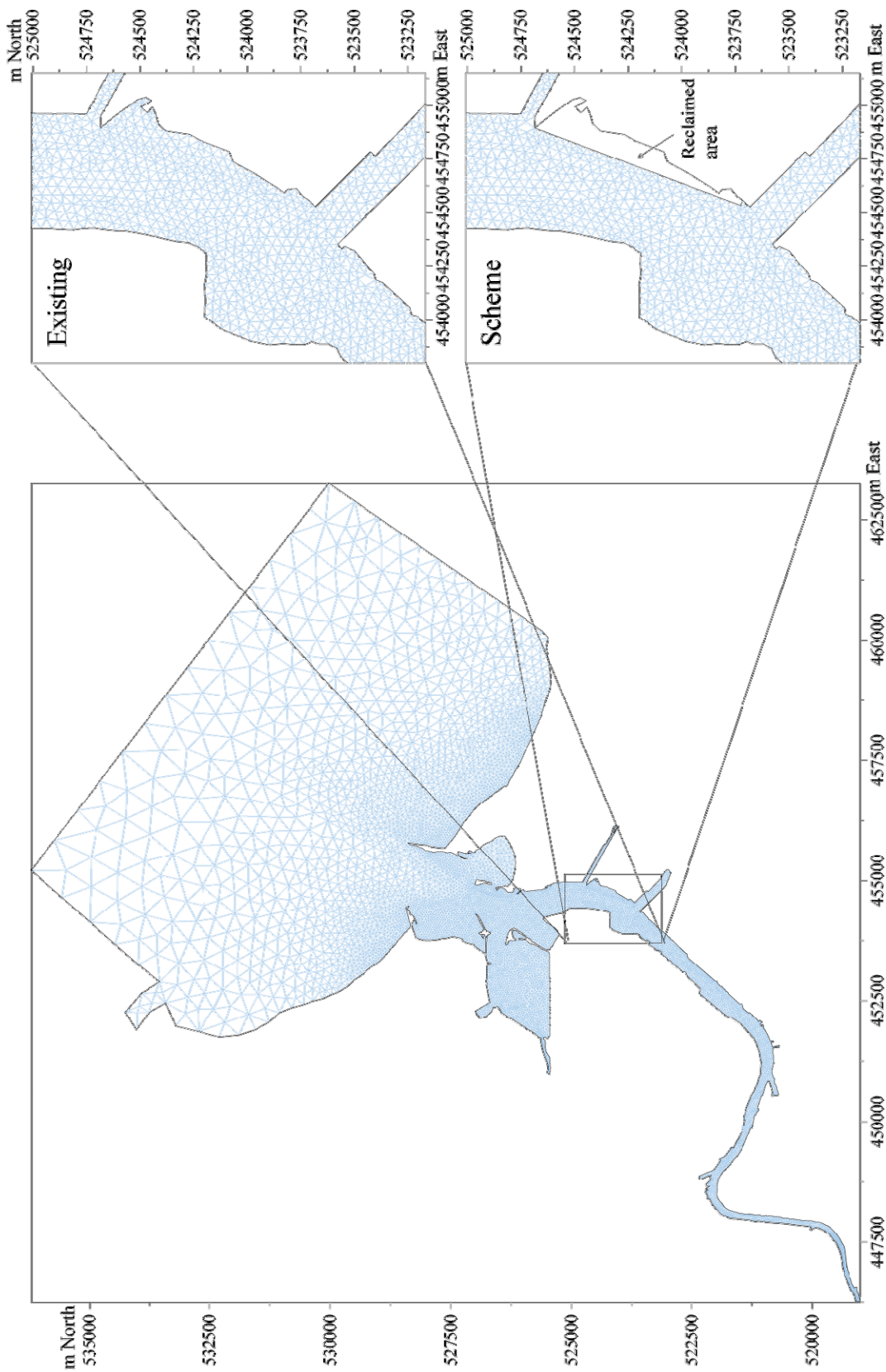


Figure 2.2 Model mesh (existing and scheme)

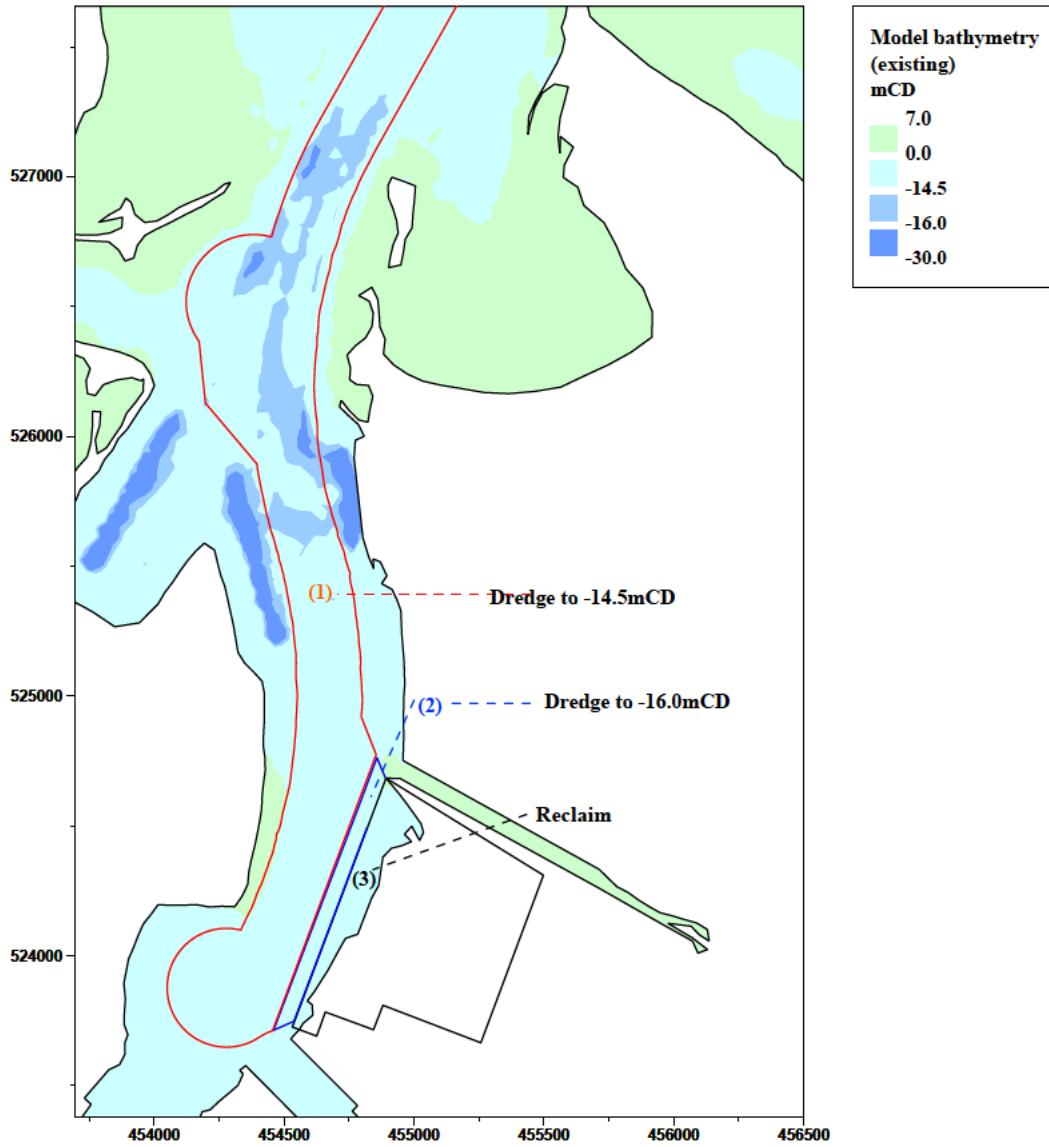


Figure 2.3 Details of proposed scheme

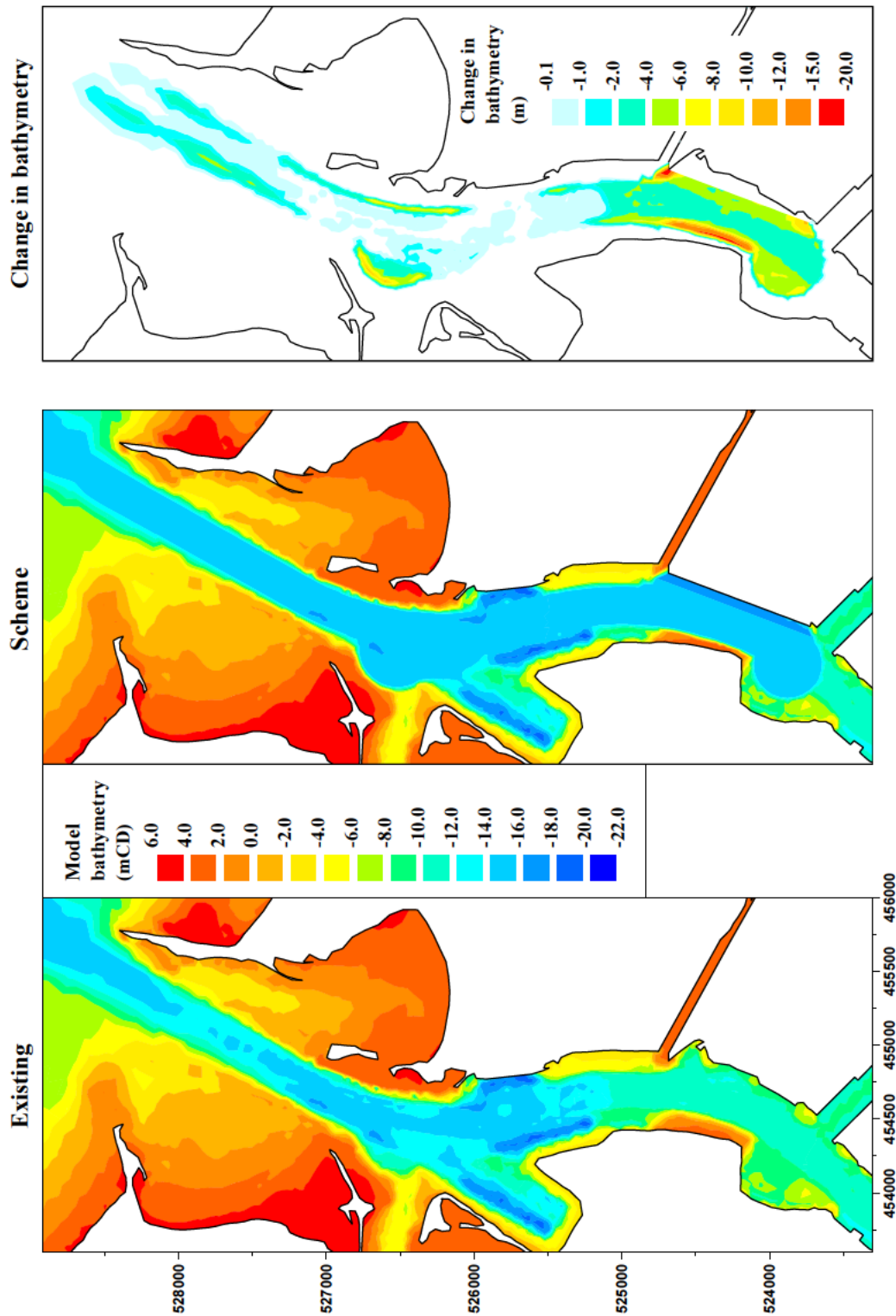


Figure 2.4 Existing and scheme model bathymetry, and change in bathymetry

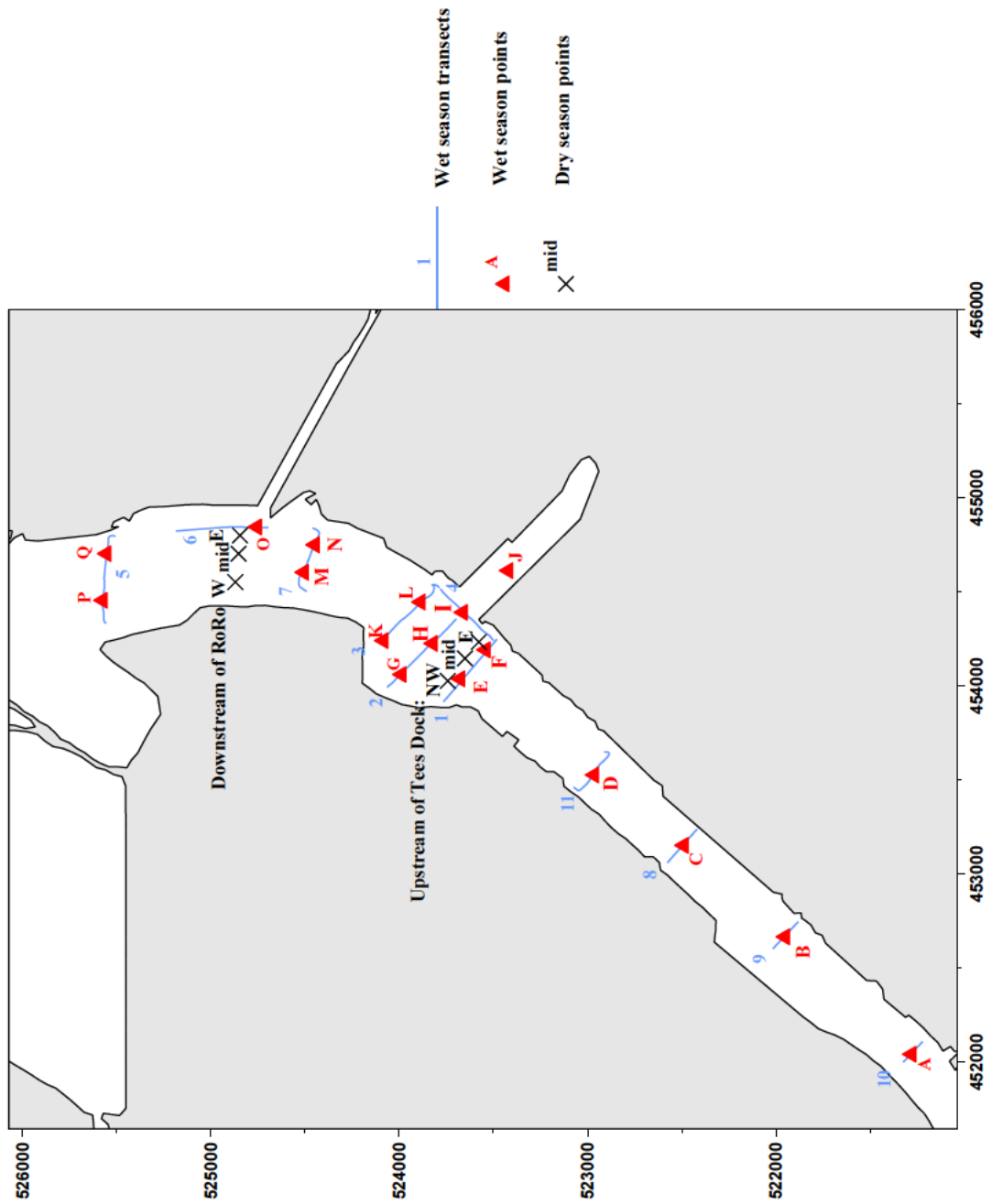


Figure 2.5 Locations of observations

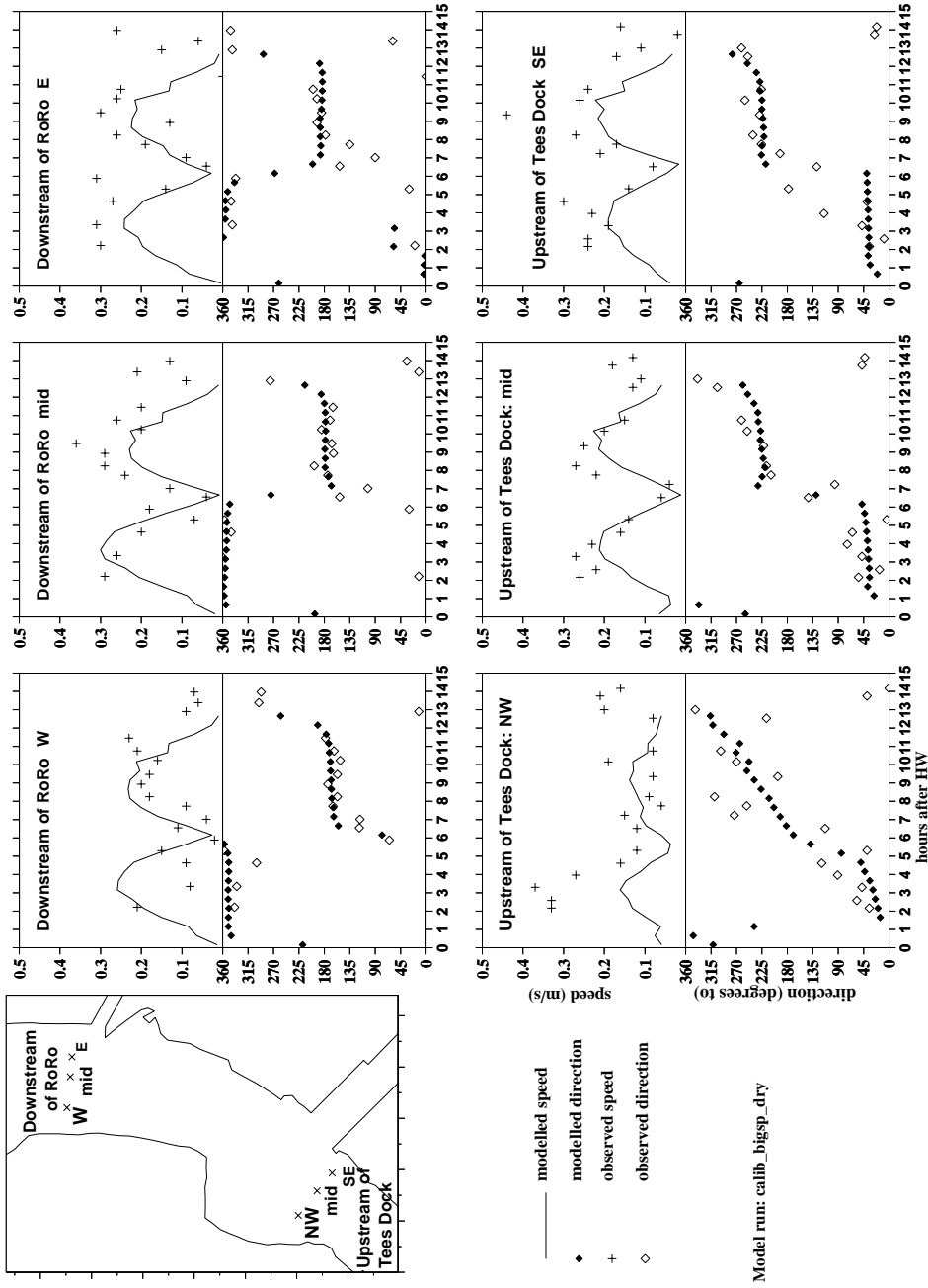


Figure 2.6 Calibration: dry season

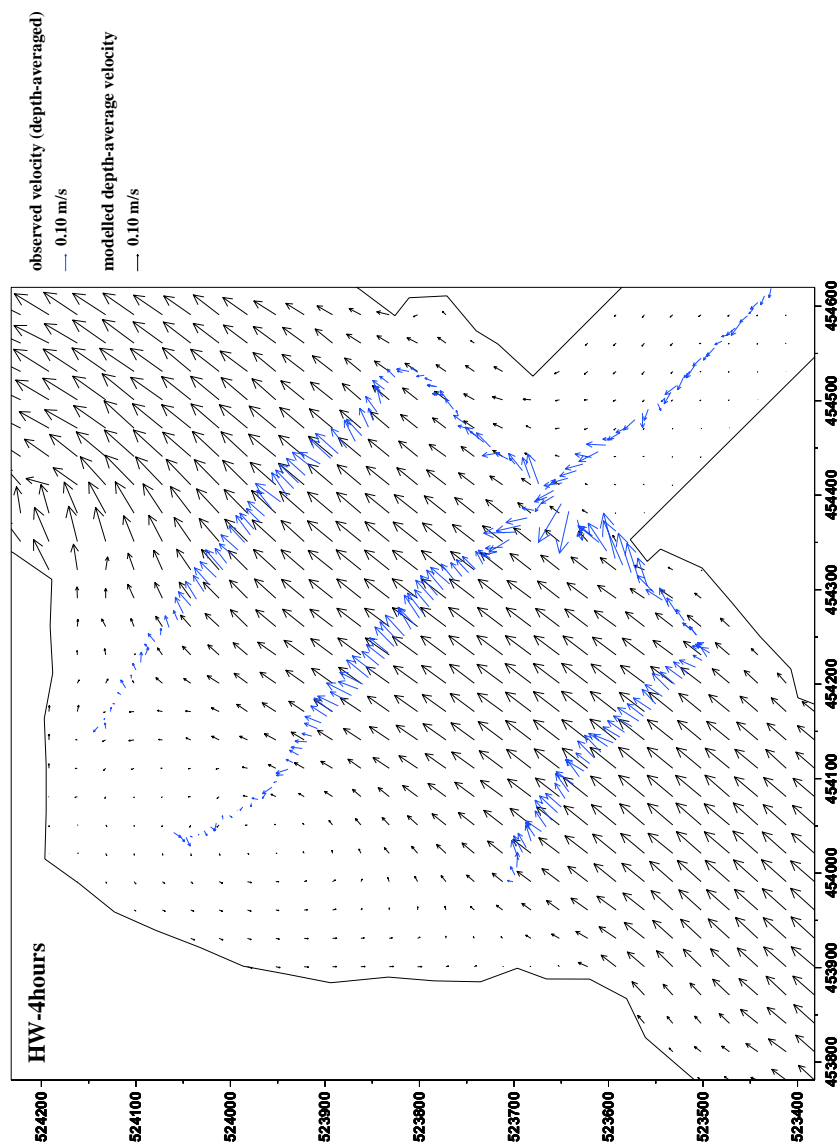


Figure 2.7 Calibration: observation wet season ebb velocity

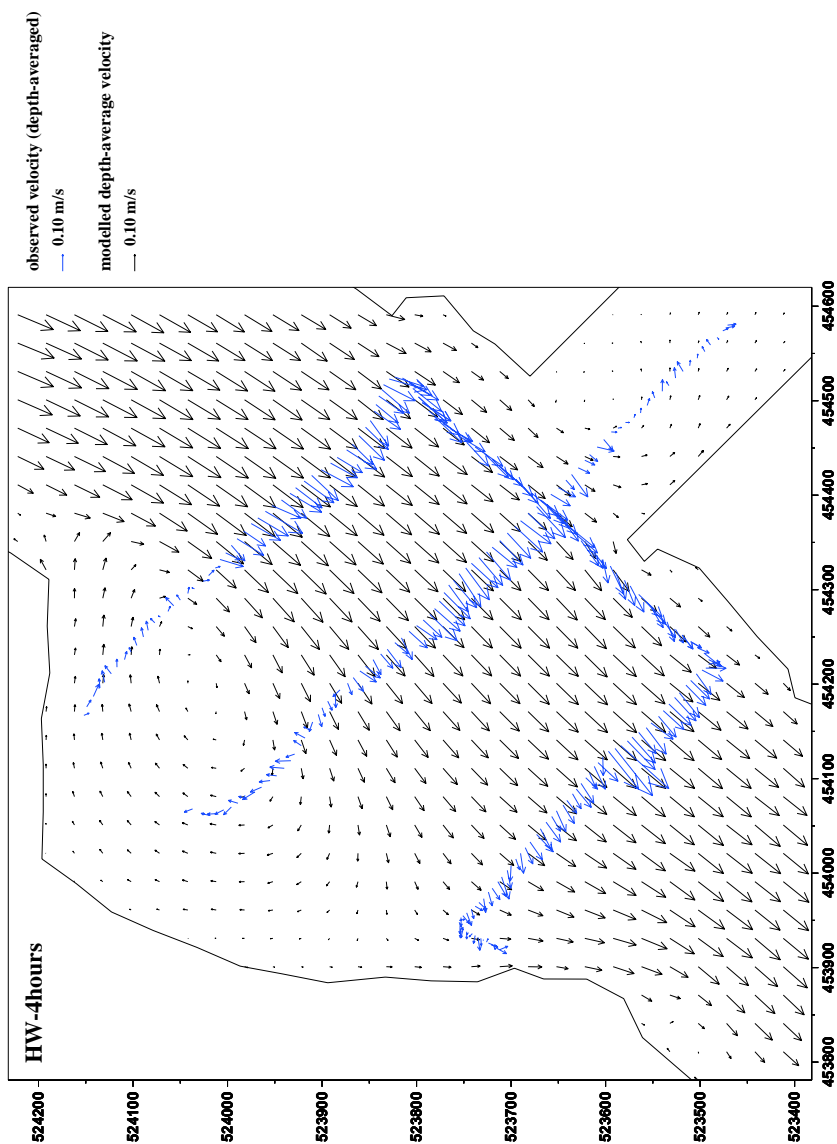


Figure 2.8 Calibration: observation wet season flood velocity

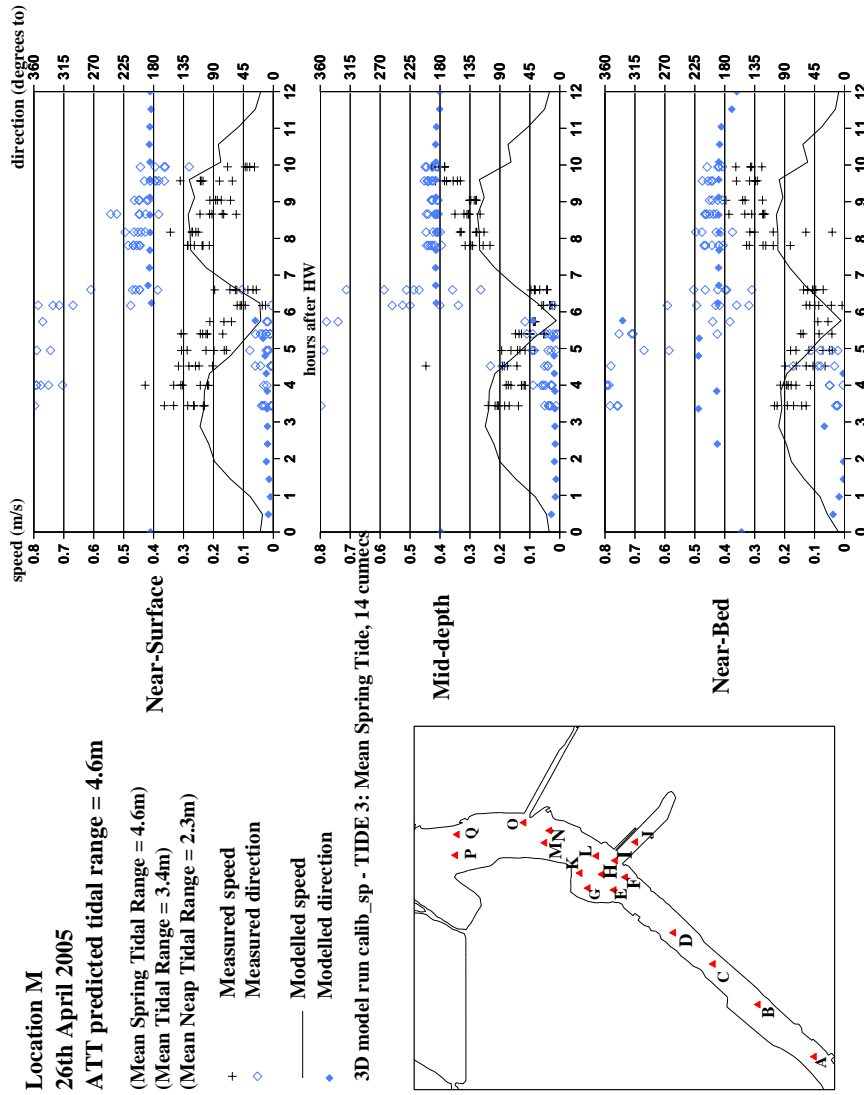


Figure 2.9 Calibration: observation wet season, mean spring tide at Location M

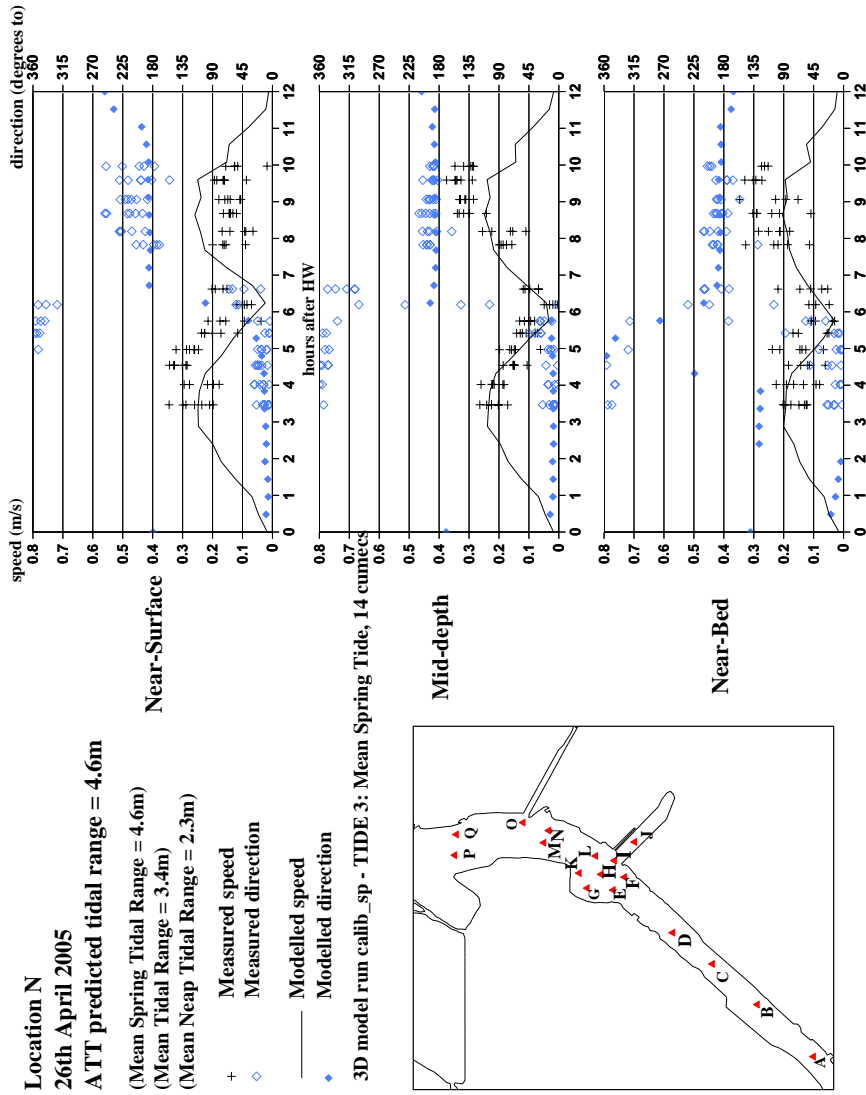


Figure 2.10 Calibration: observation wet season, mean spring tide at Location N

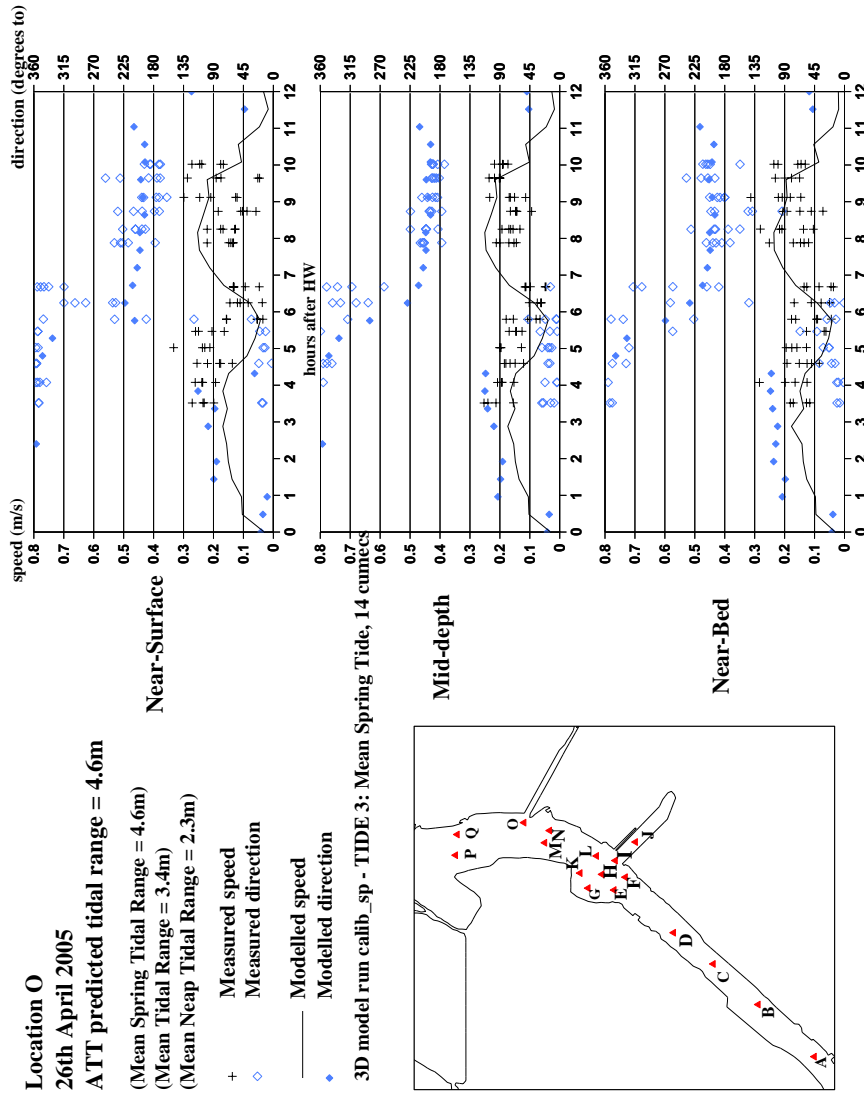


Figure 2.11 Calibration: observation wet season, mean spring tide at Location O

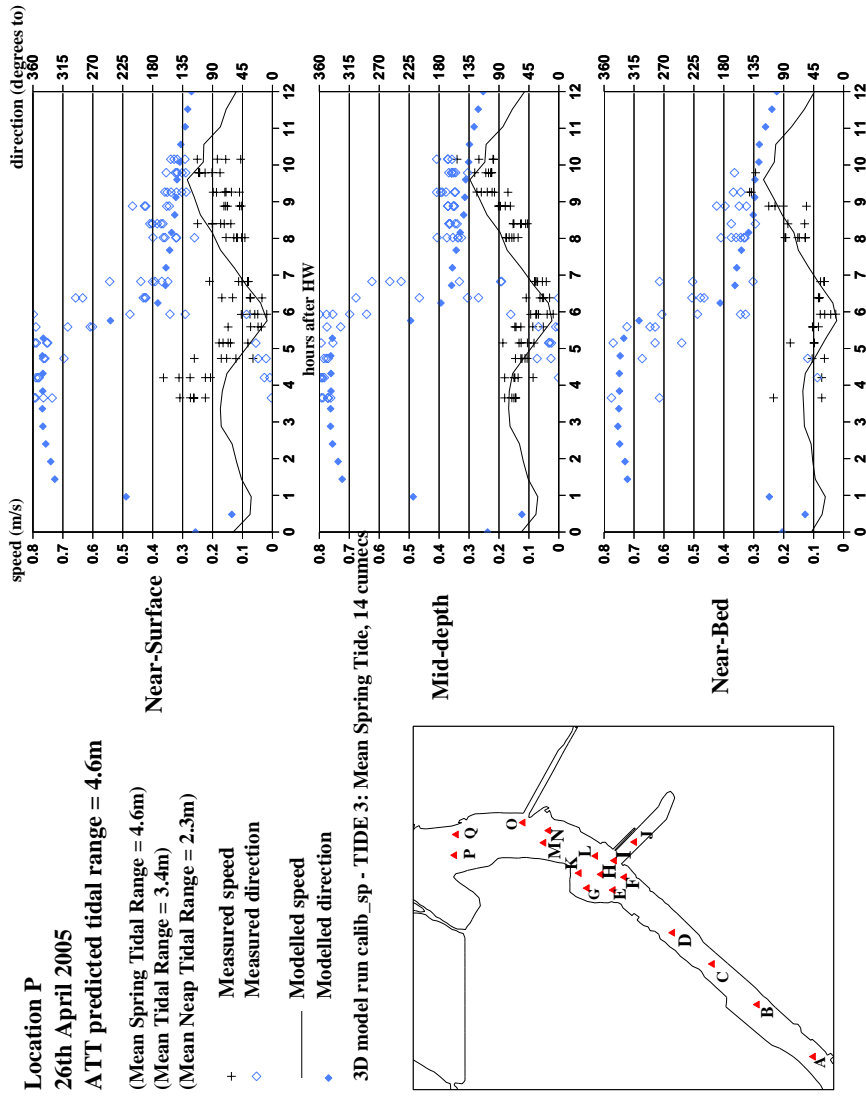


Figure 2.12 Calibration: observation wet season, mean spring tide at Location P

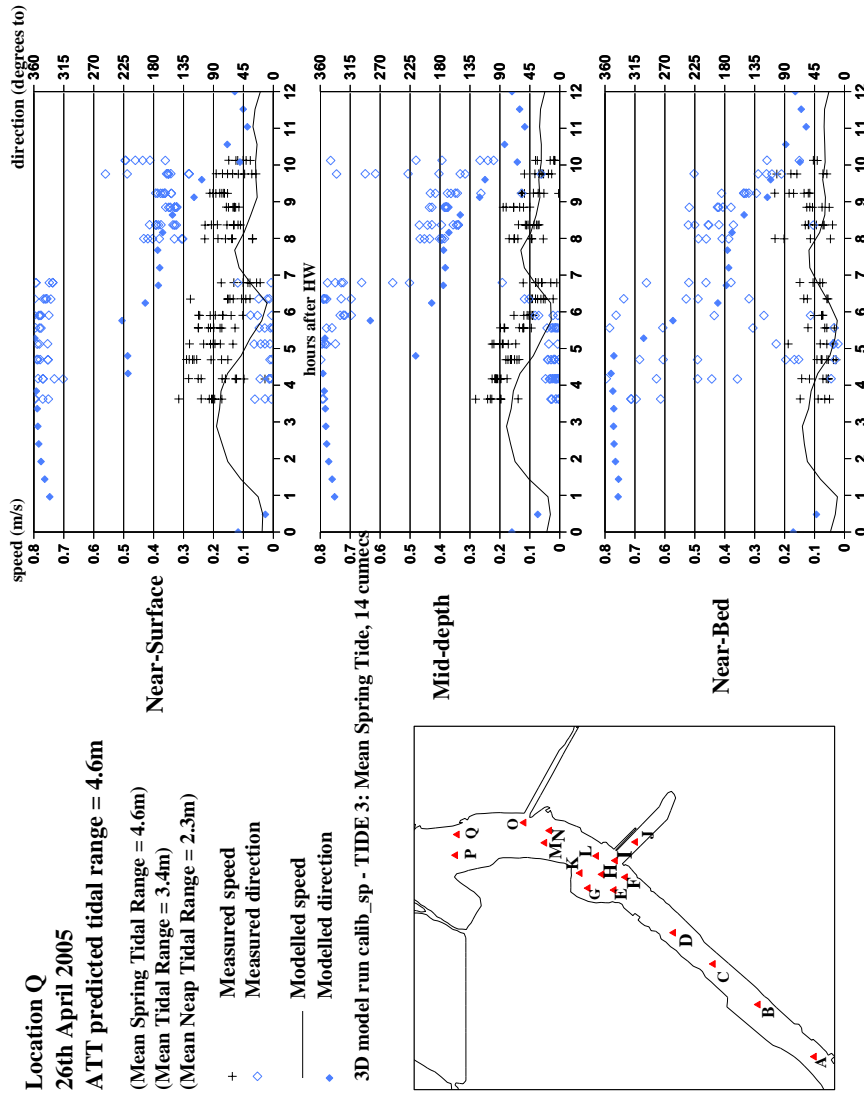


Figure 2.13 Calibration: observation wet season, mean spring tide at Location Q

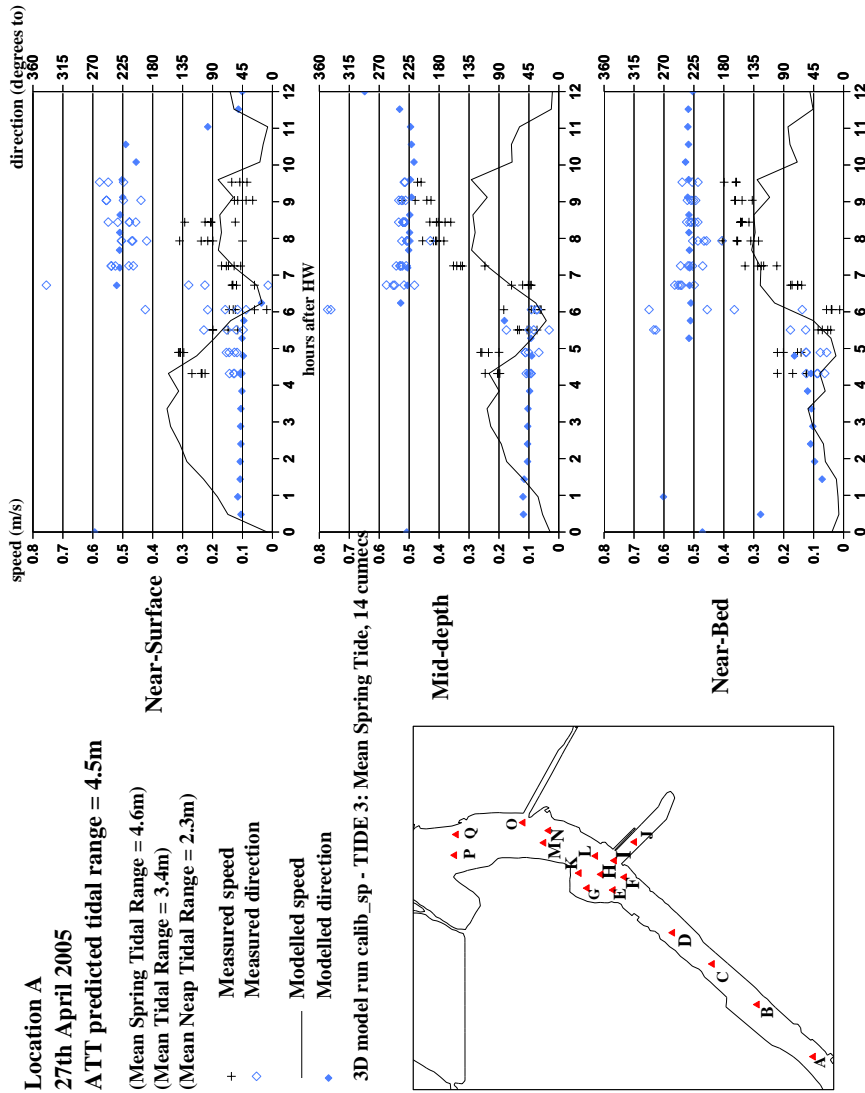


Figure 2.14 Calibration: observation wet season, mean spring tide at Location A

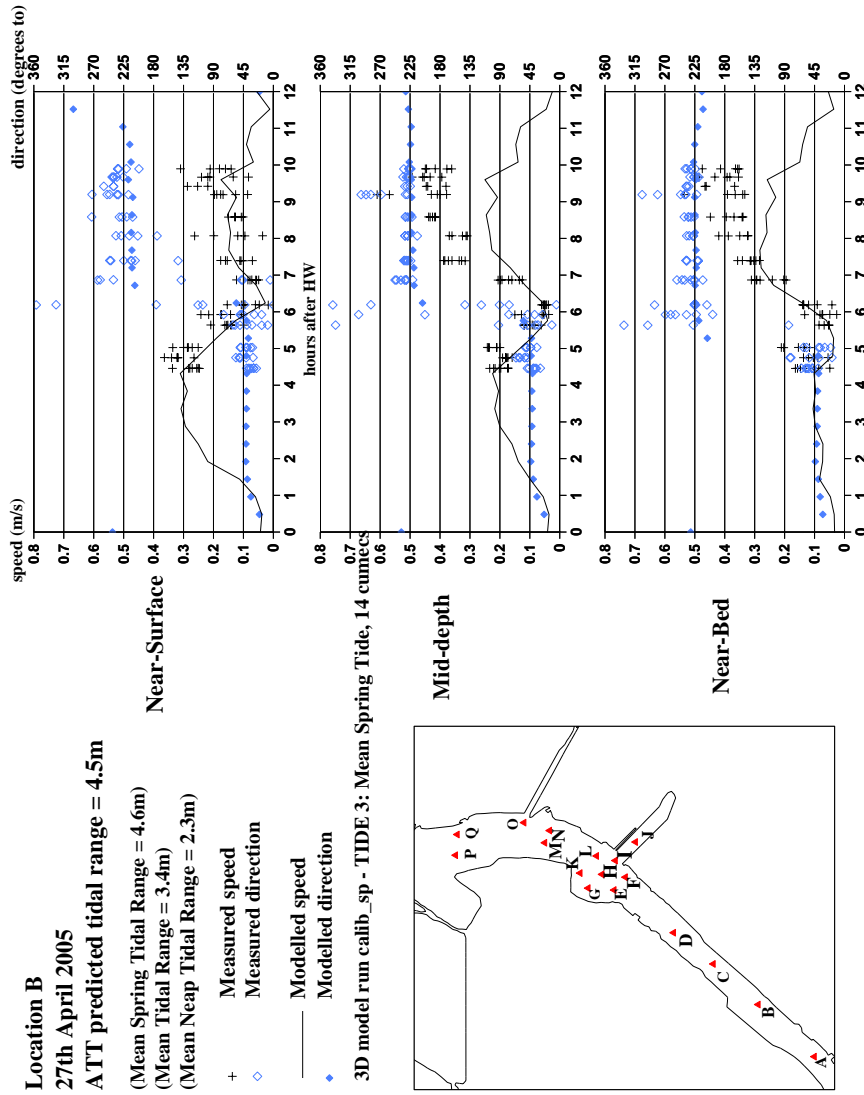


Figure 2.15 Calibration: observation wet season, mean spring tide at Location B

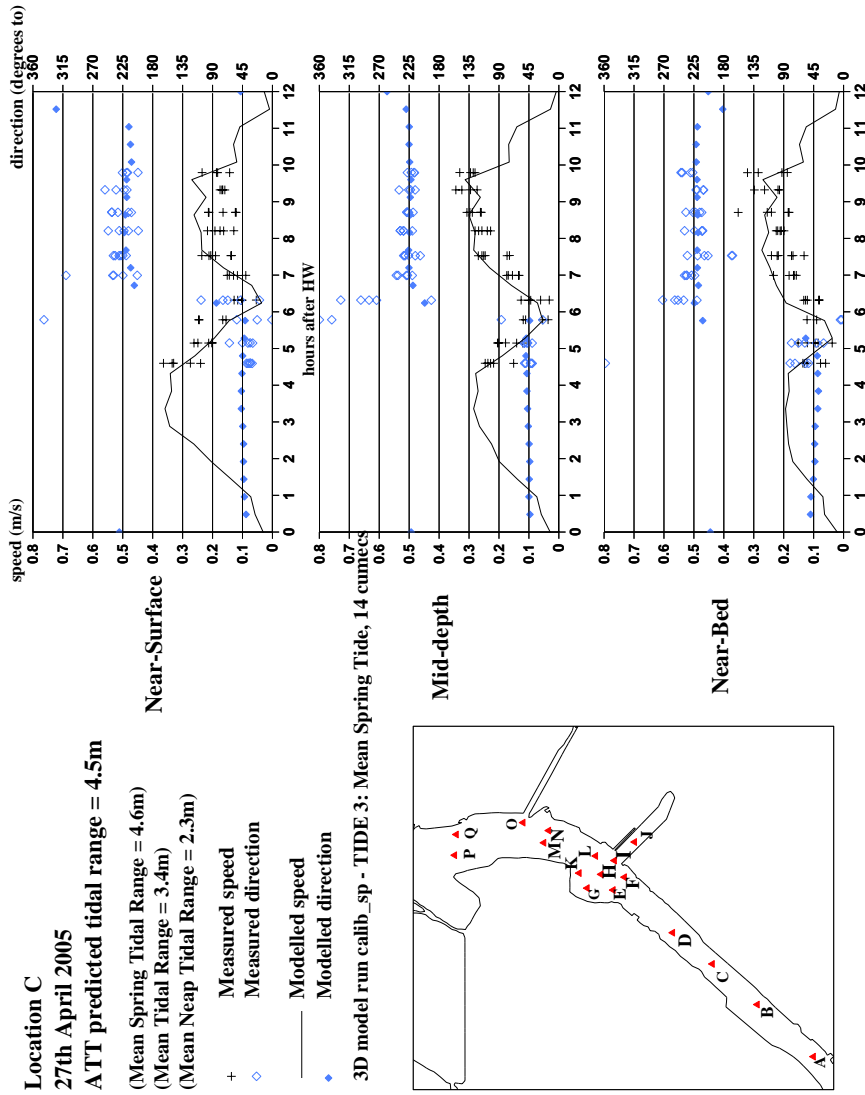


Figure 2.16 Calibration: observation wet season, mean spring tide at Location C

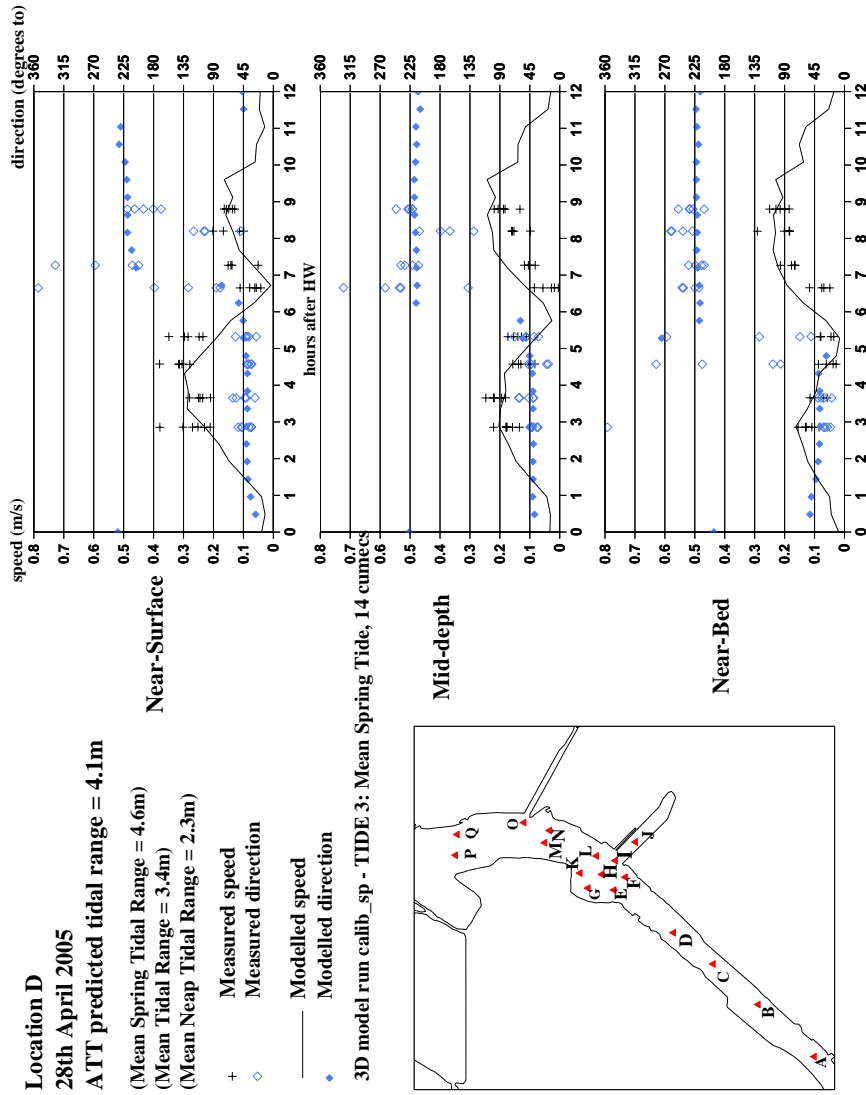


Figure 2.17 Calibration: observation wet season, mean spring tide at Location D

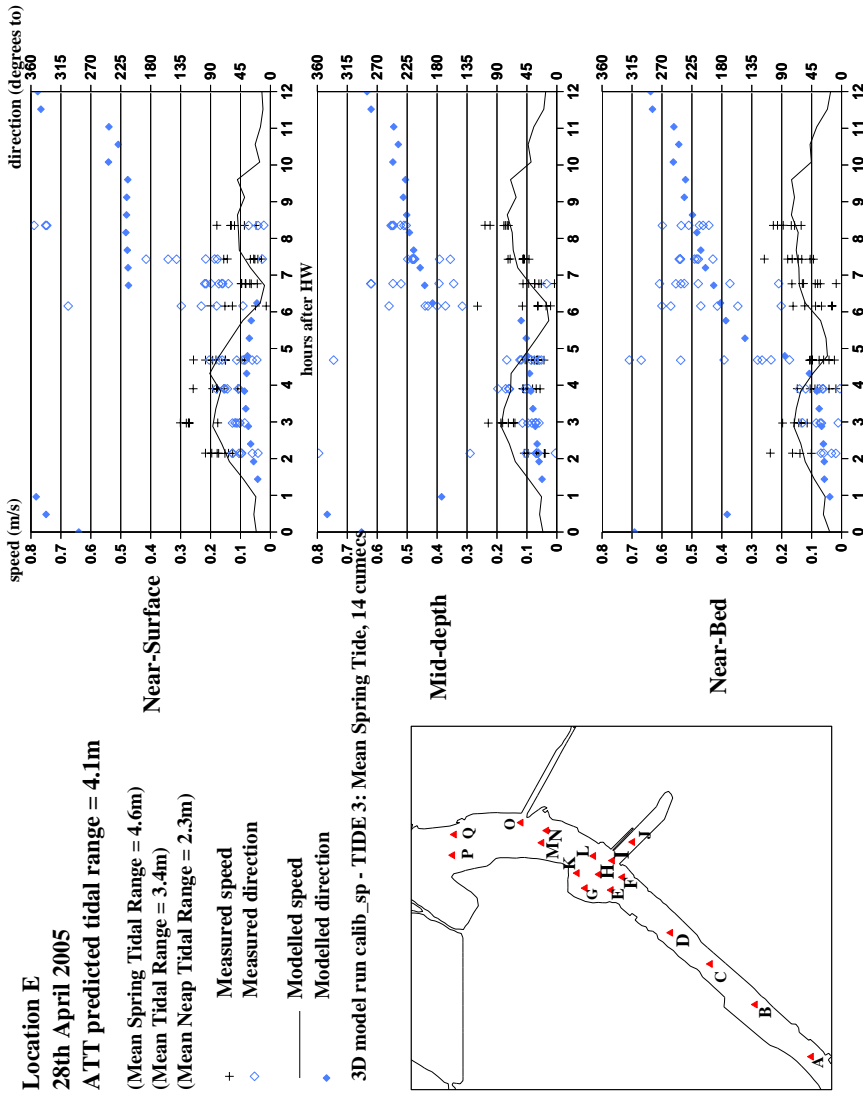


Figure 2.18 Calibration: observation wet season, mean spring tide at Location E

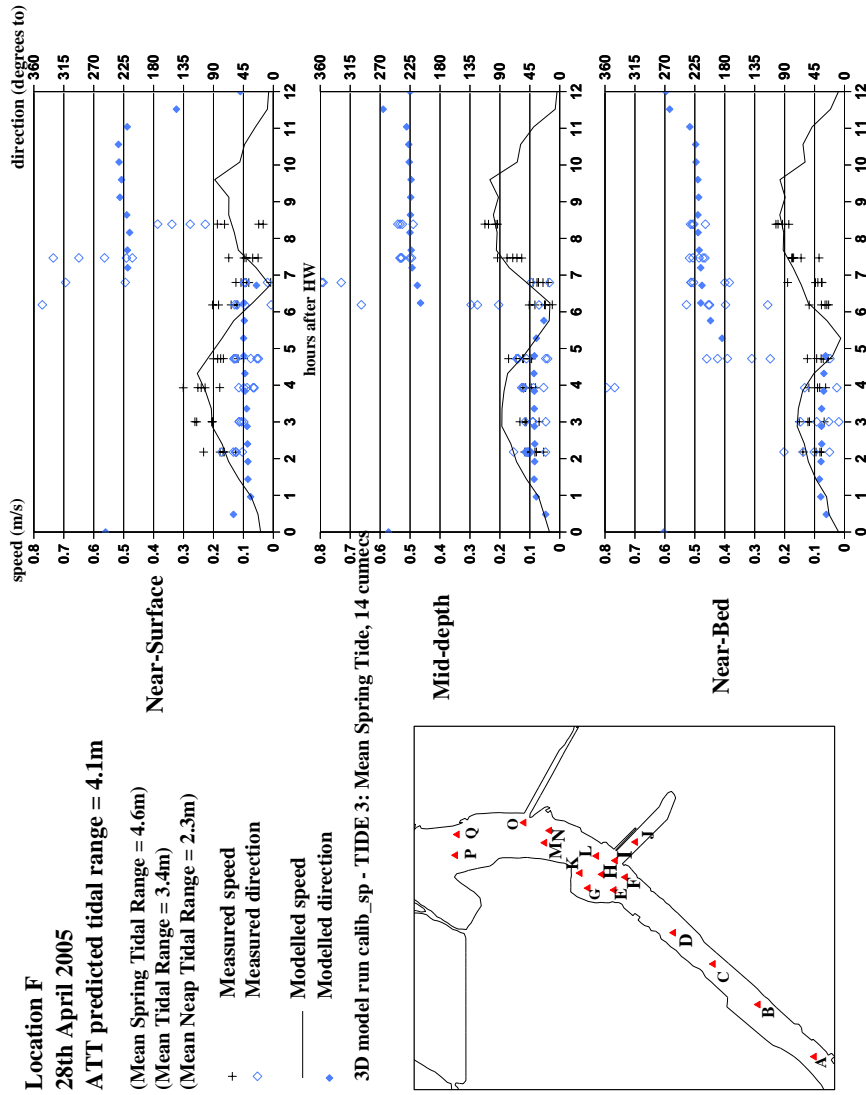


Figure 2.19 Calibration: observation wet season, mean spring tide at Location F

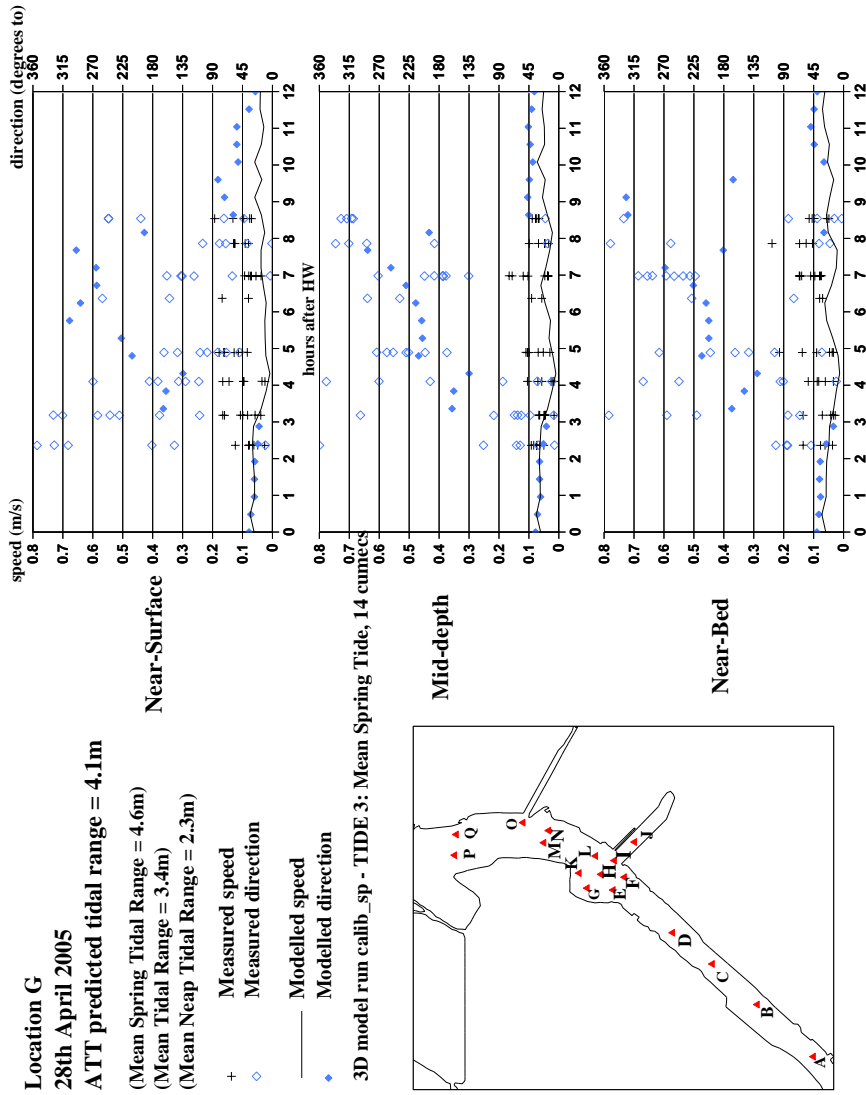


Figure 2.20 Calibration: observation wet season, mean spring tide at Location G

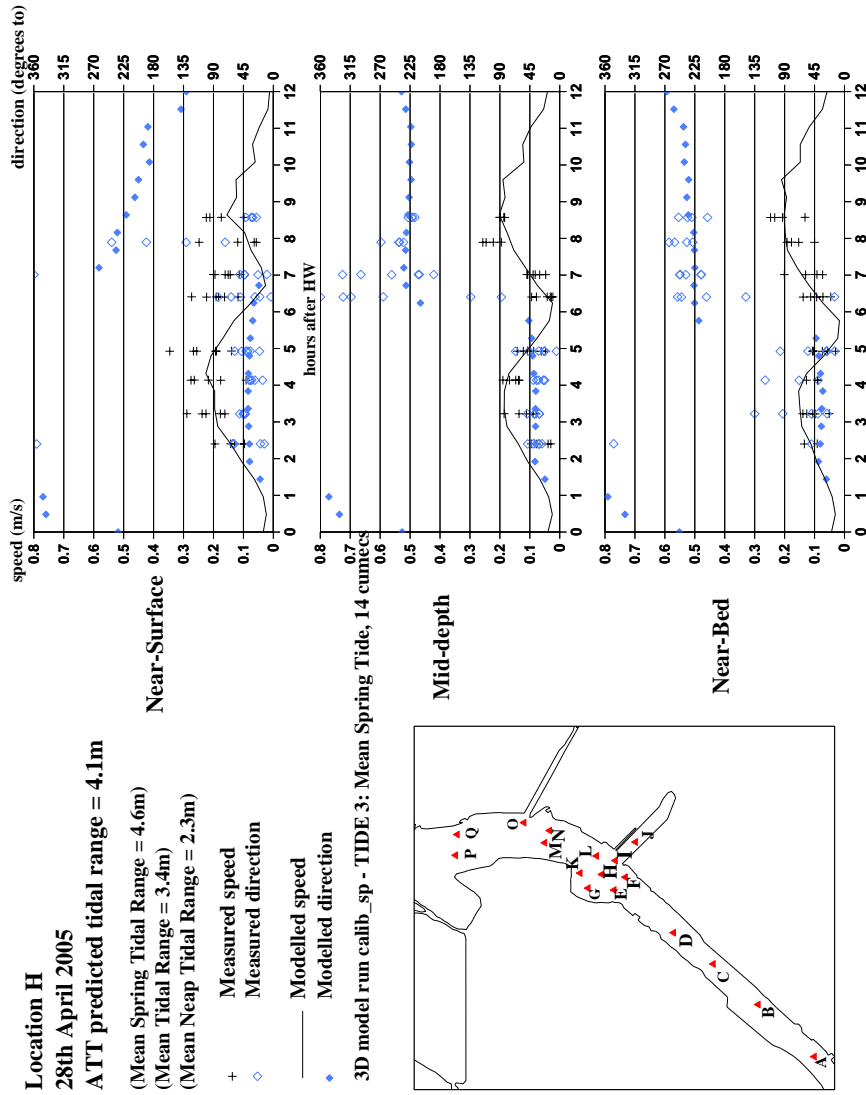


Figure 2.21 Calibration: observation wet season, mean spring tide at Location H

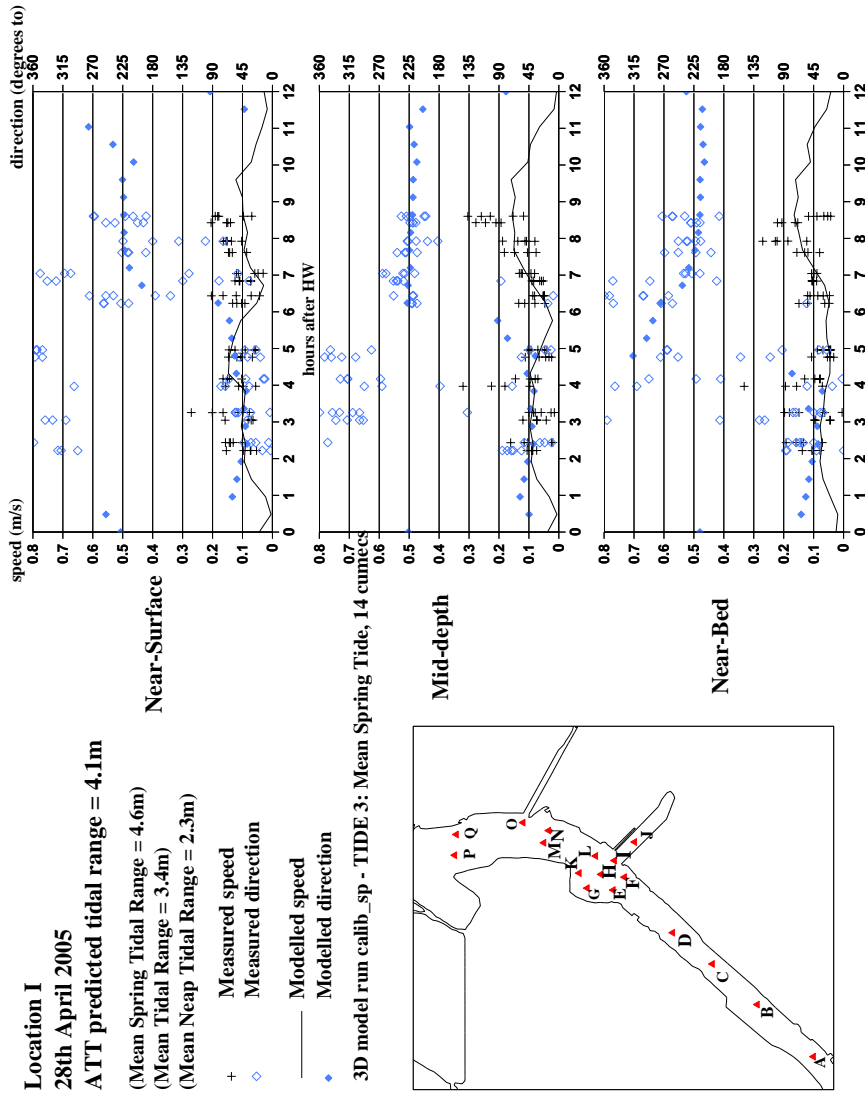


Figure 2.22 Calibration: observation wet season, mean spring tide at Location I

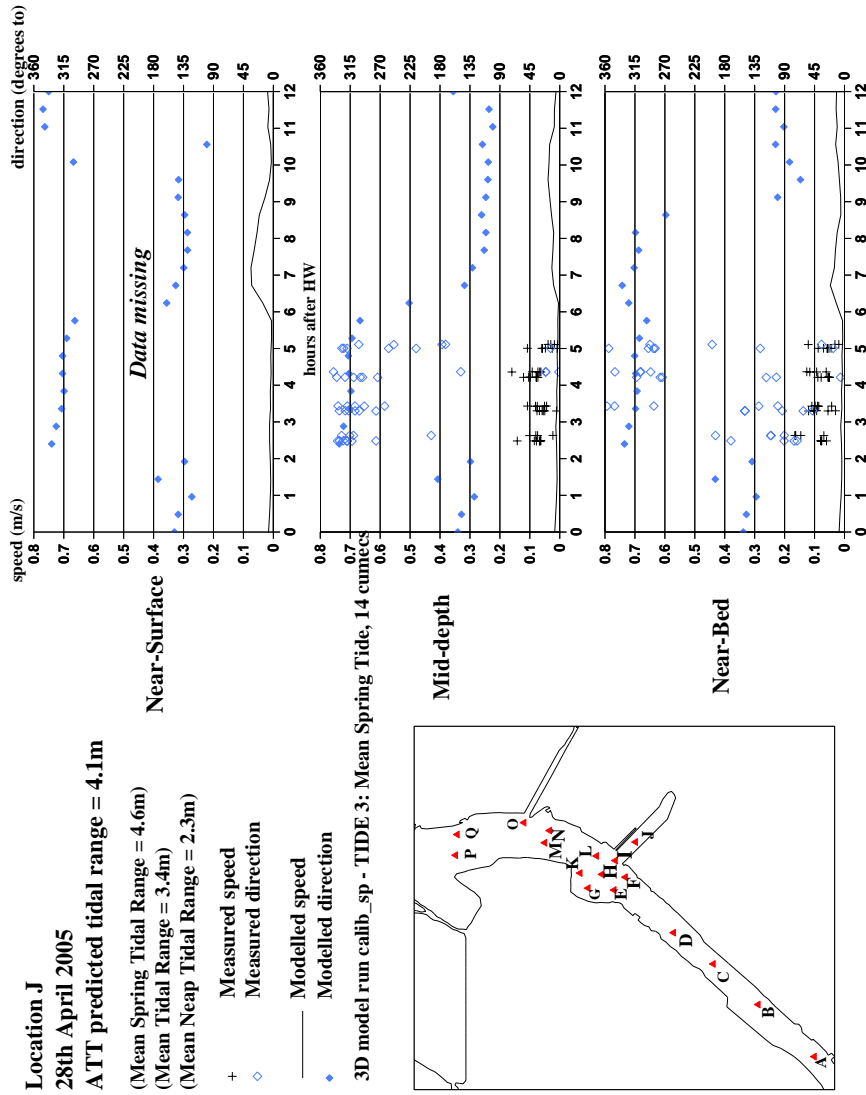


Figure 2.23 Calibration: observation wet season, mean spring tide at Location J

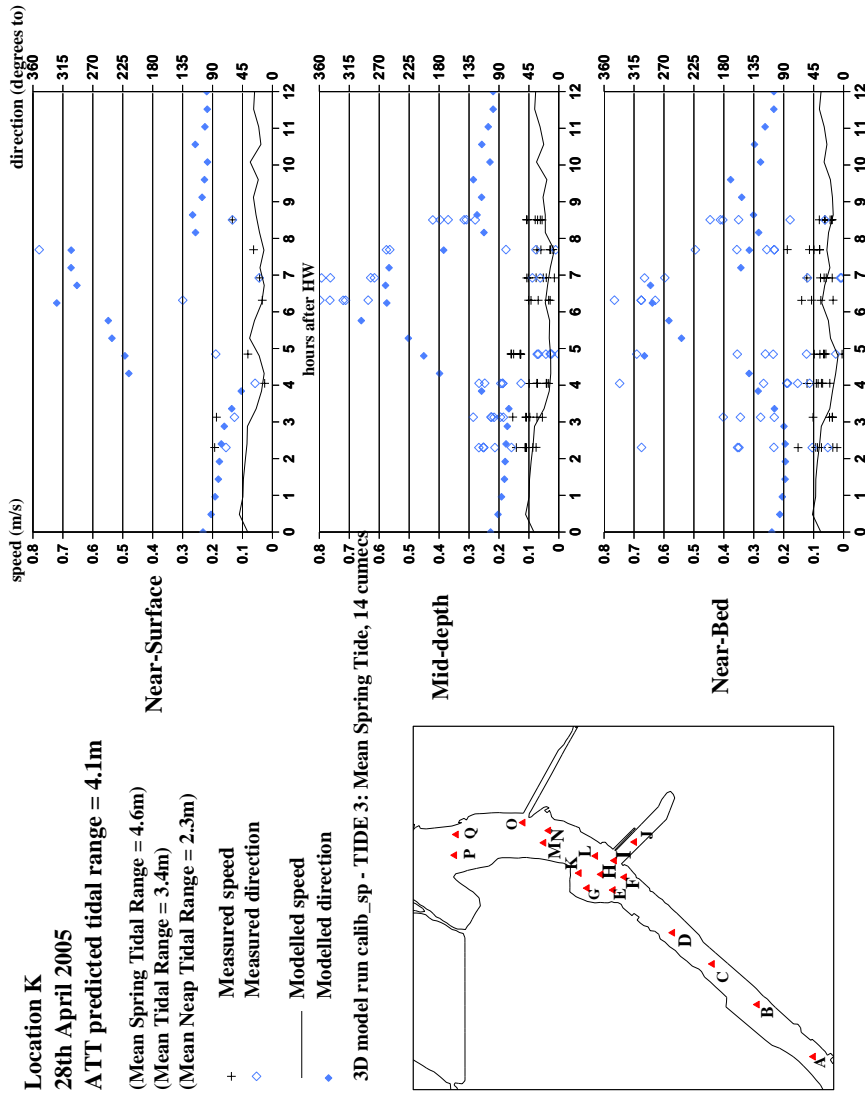


Figure 2.24 Calibration: observation wet season, mean spring tide at Location K

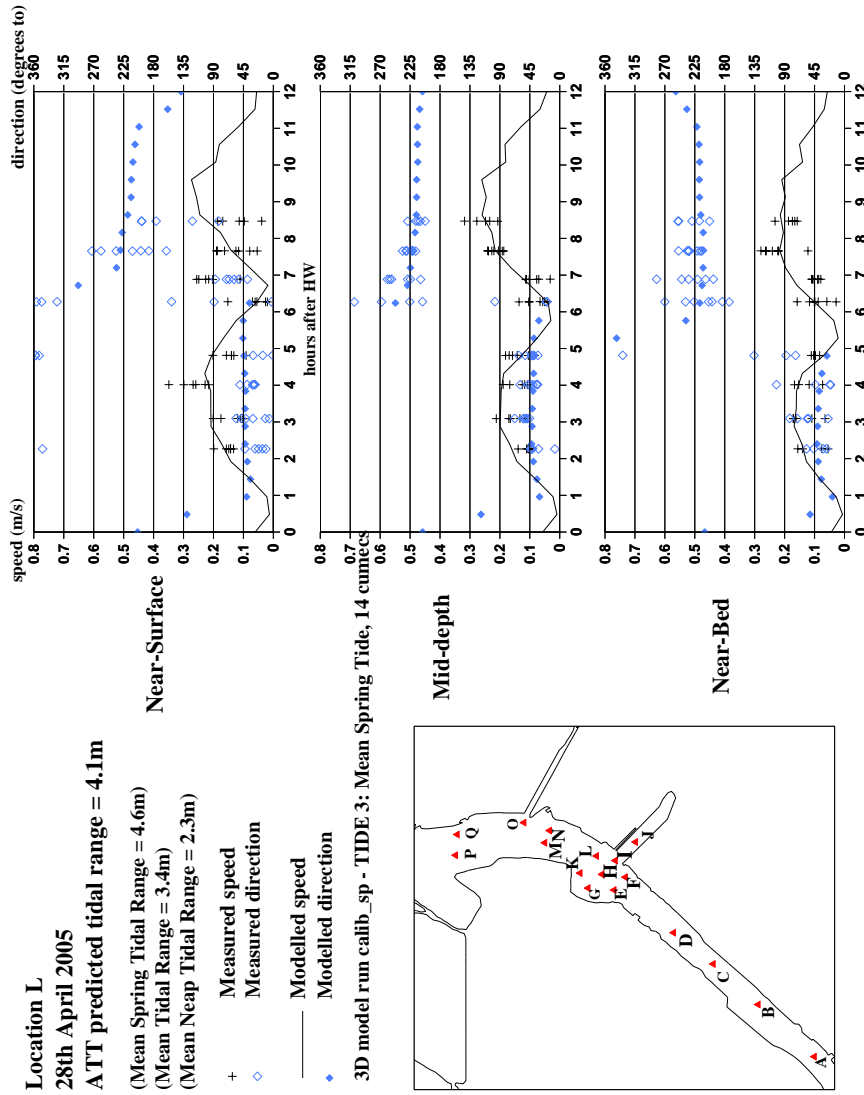


Figure 2.25 Calibration: observation wet season, mean spring tide at Location L

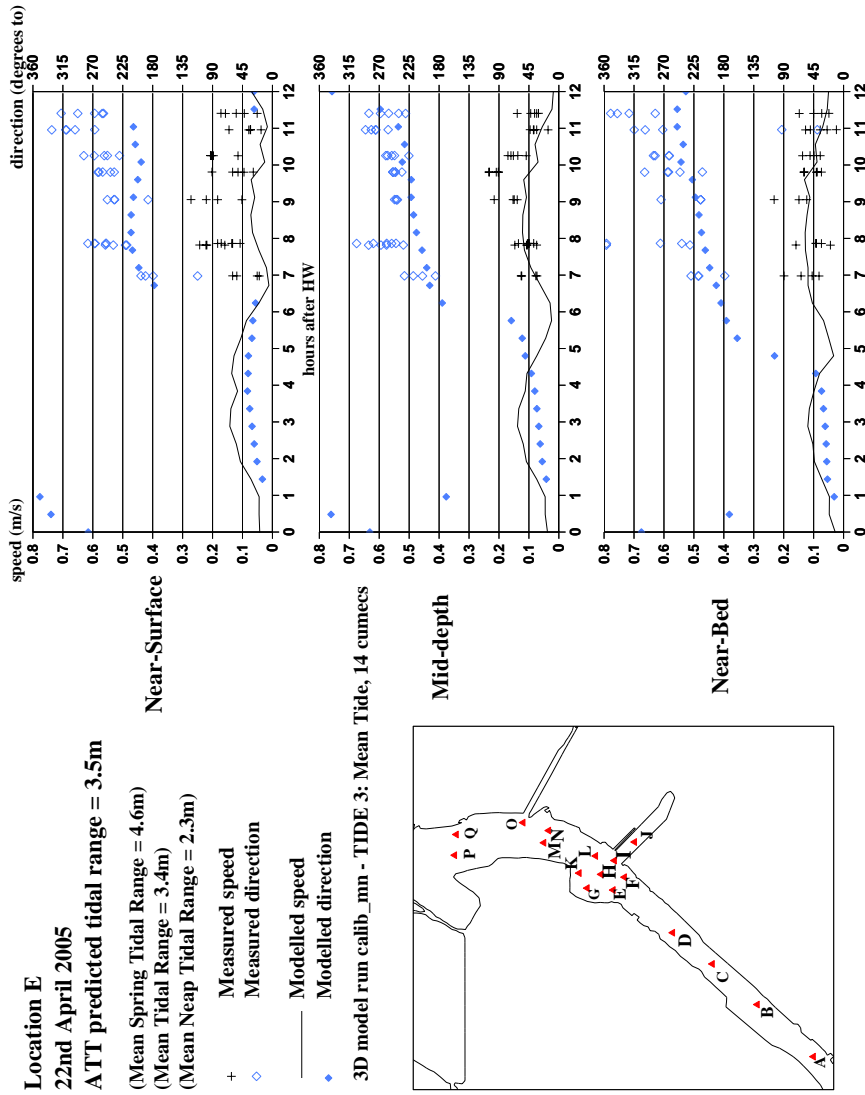


Figure 2.26 Calibration: observation wet season, mean tide at Location E

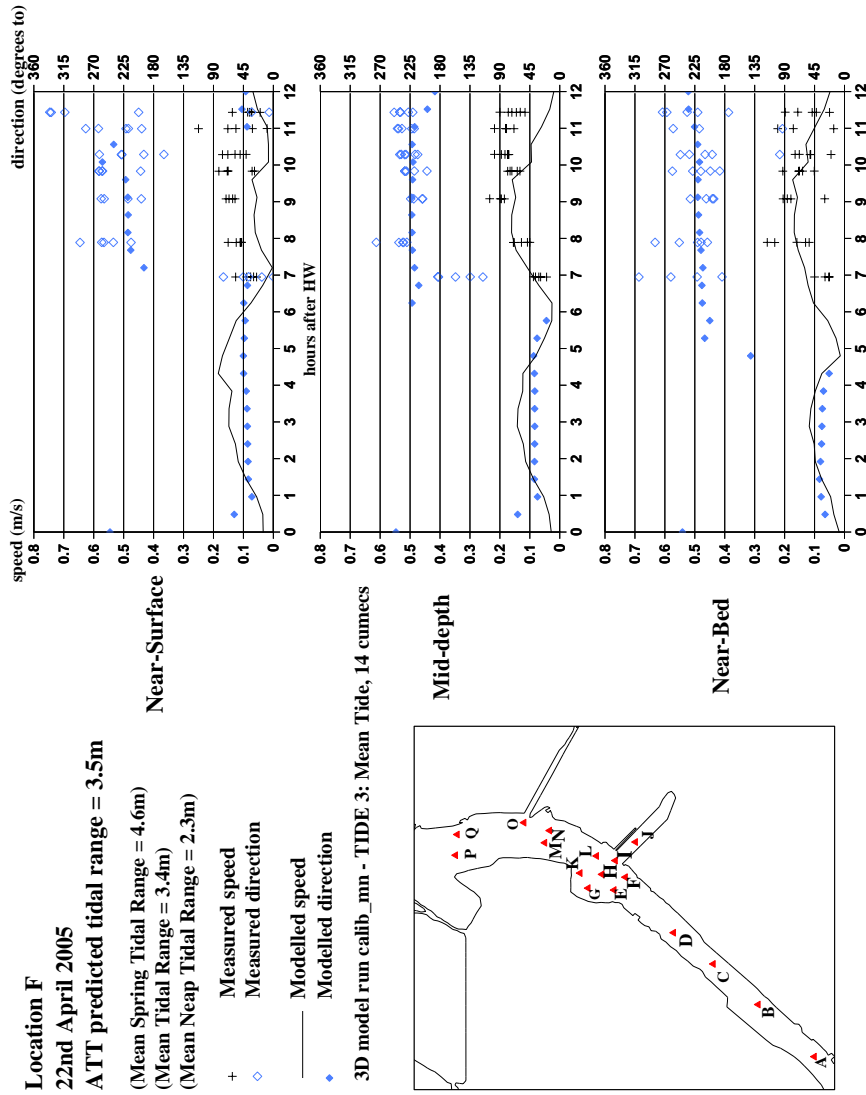


Figure 2.27 Calibration: observation wet season, mean tide at Location F

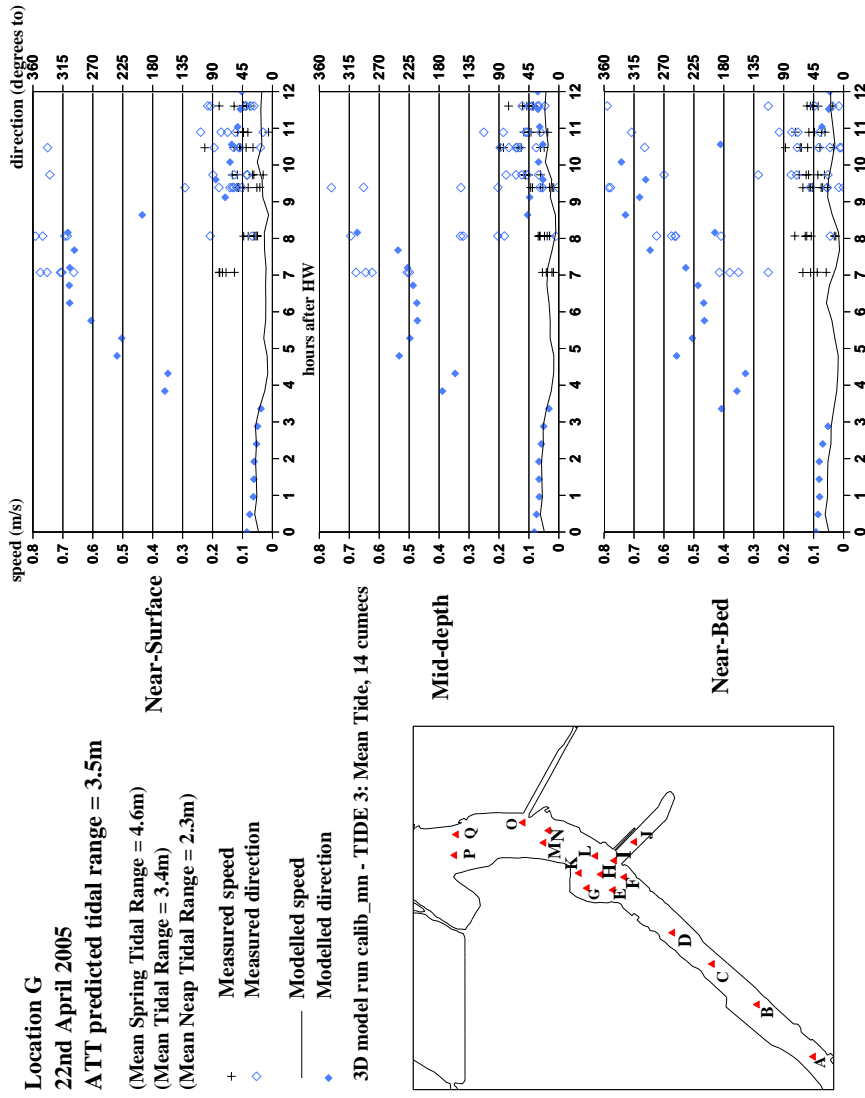


Figure 2.28 Calibration: observation wet season, mean tide at Location G

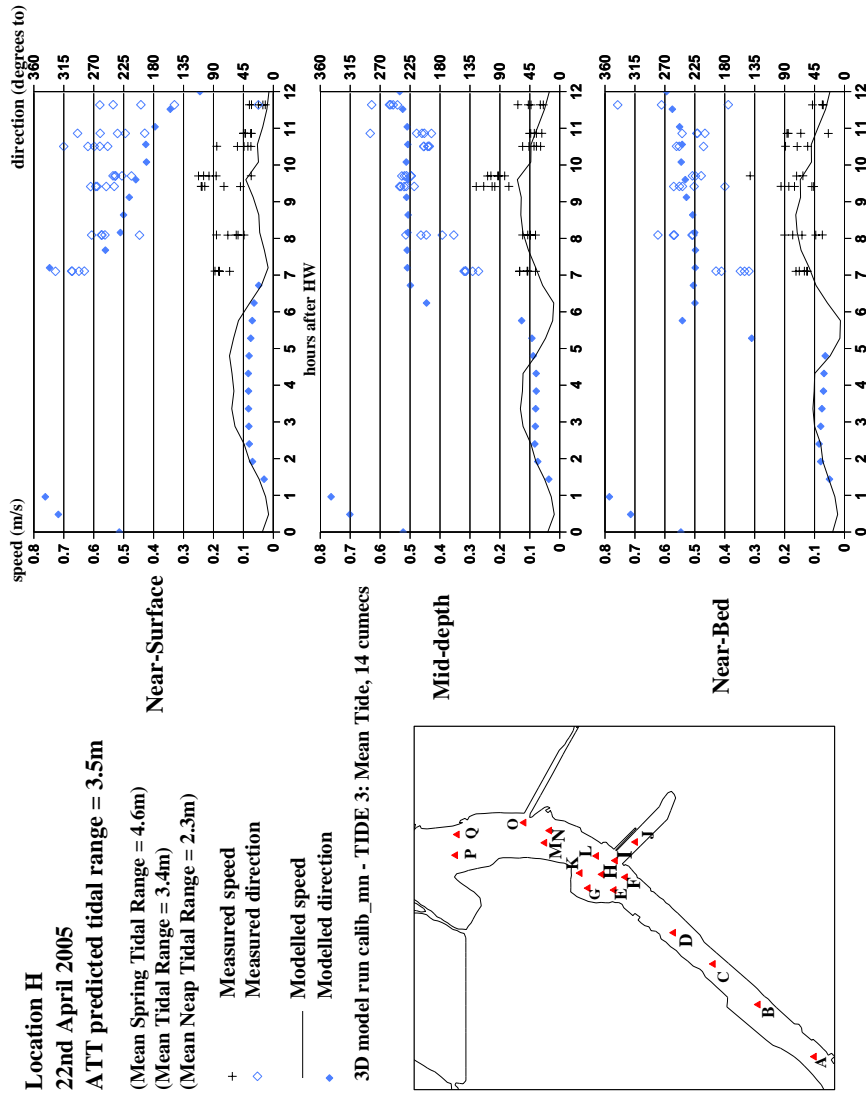


Figure 2.29 Calibration: observation wet season, mean tide at Location H

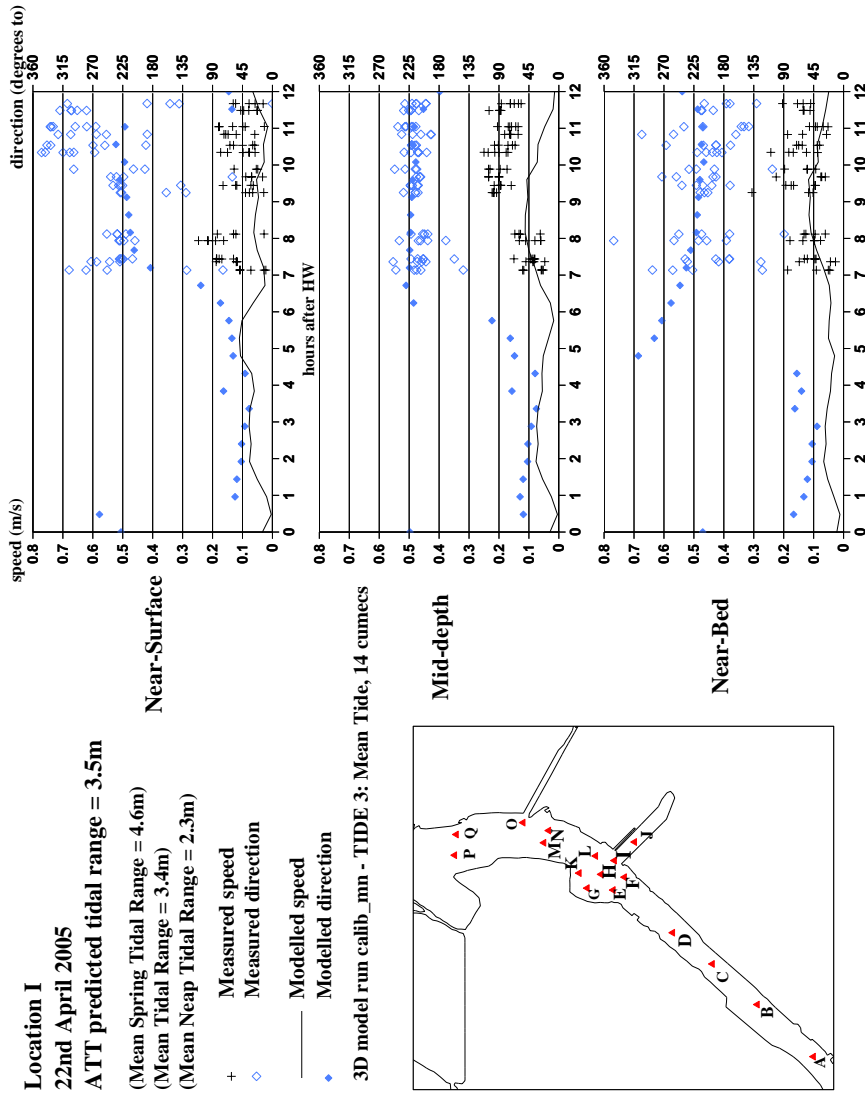


Figure 2.30 Calibration: observation wet season, mean tide at Location I

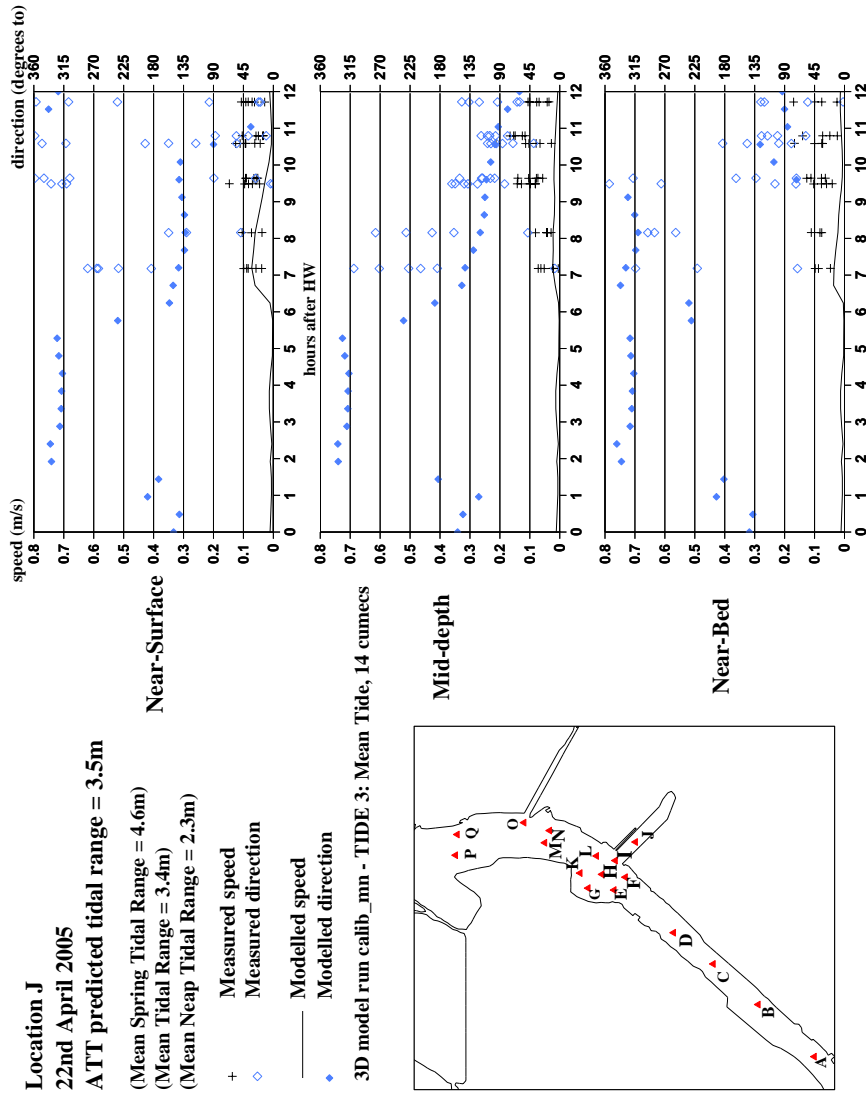


Figure 2.31 Calibration: observation wet season, mean tide at Location J

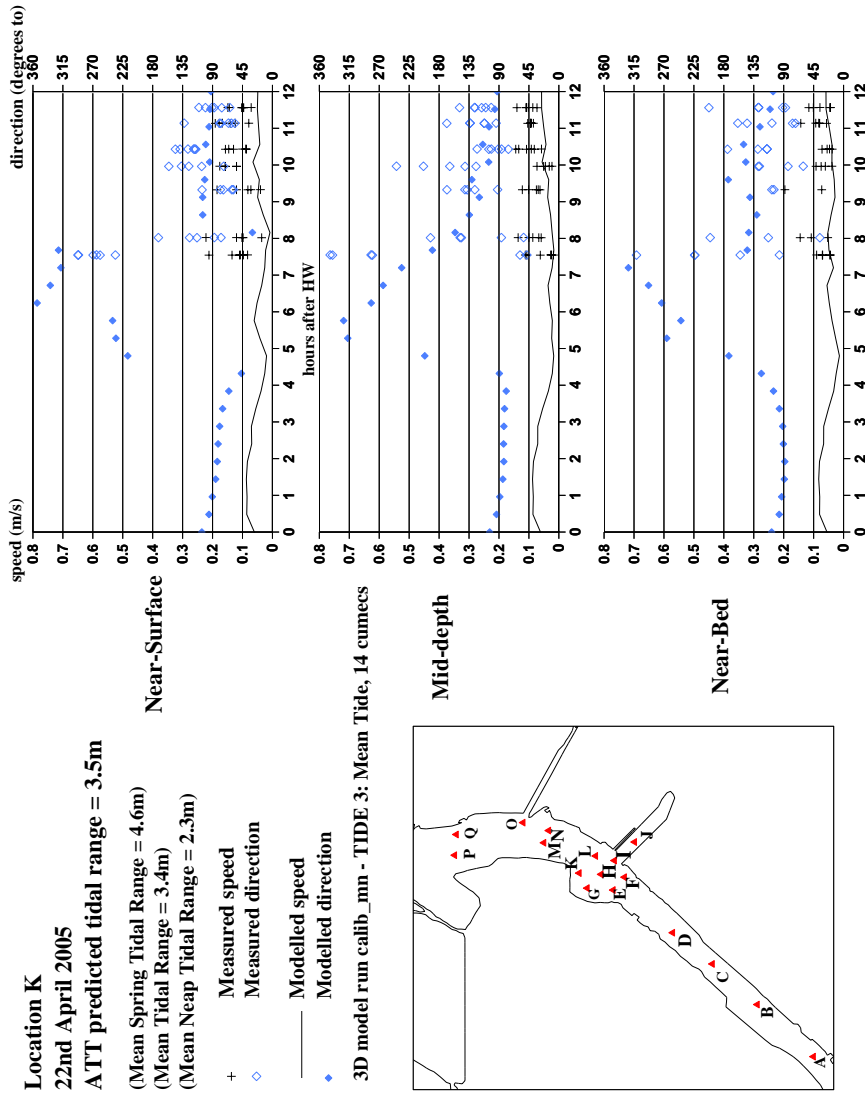


Figure 2.32 Calibration: observation wet season, mean tide at Location K

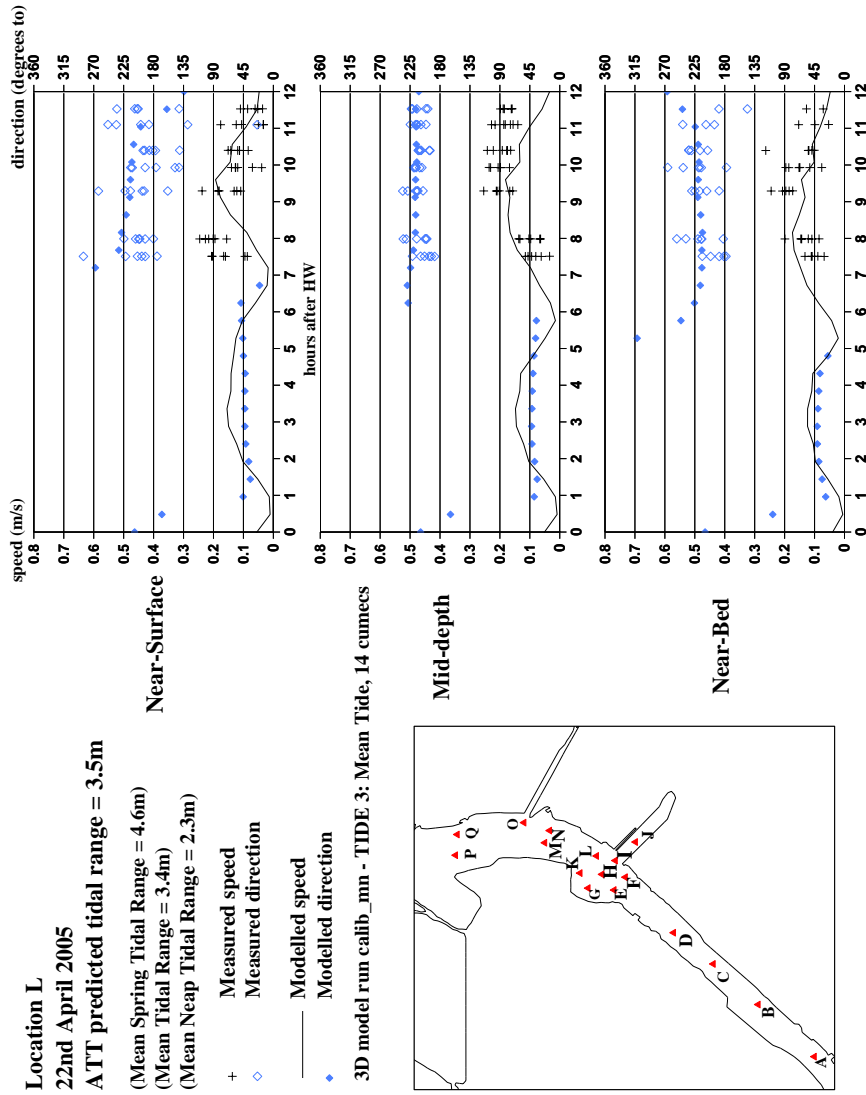


Figure 2.33 Calibration: observation wet season, mean tide at Location L

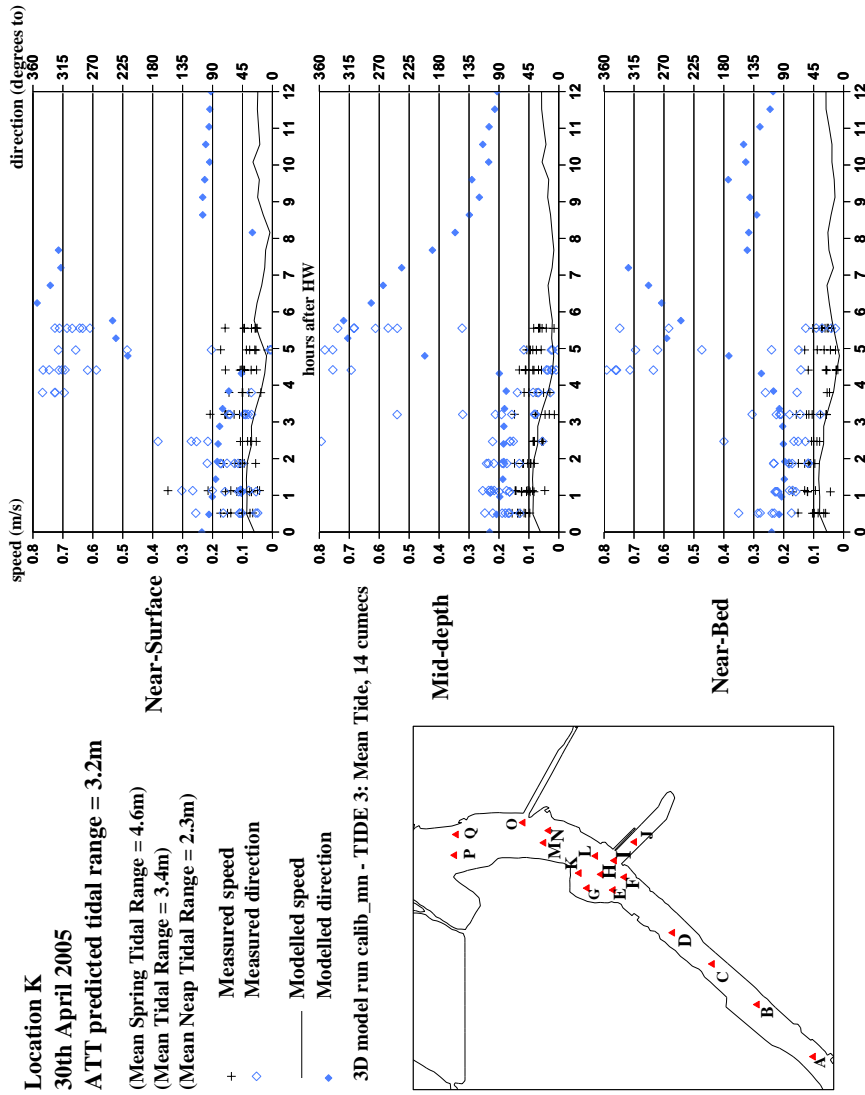


Figure 2.34 Calibration: observation wet season, mean tide at Location K

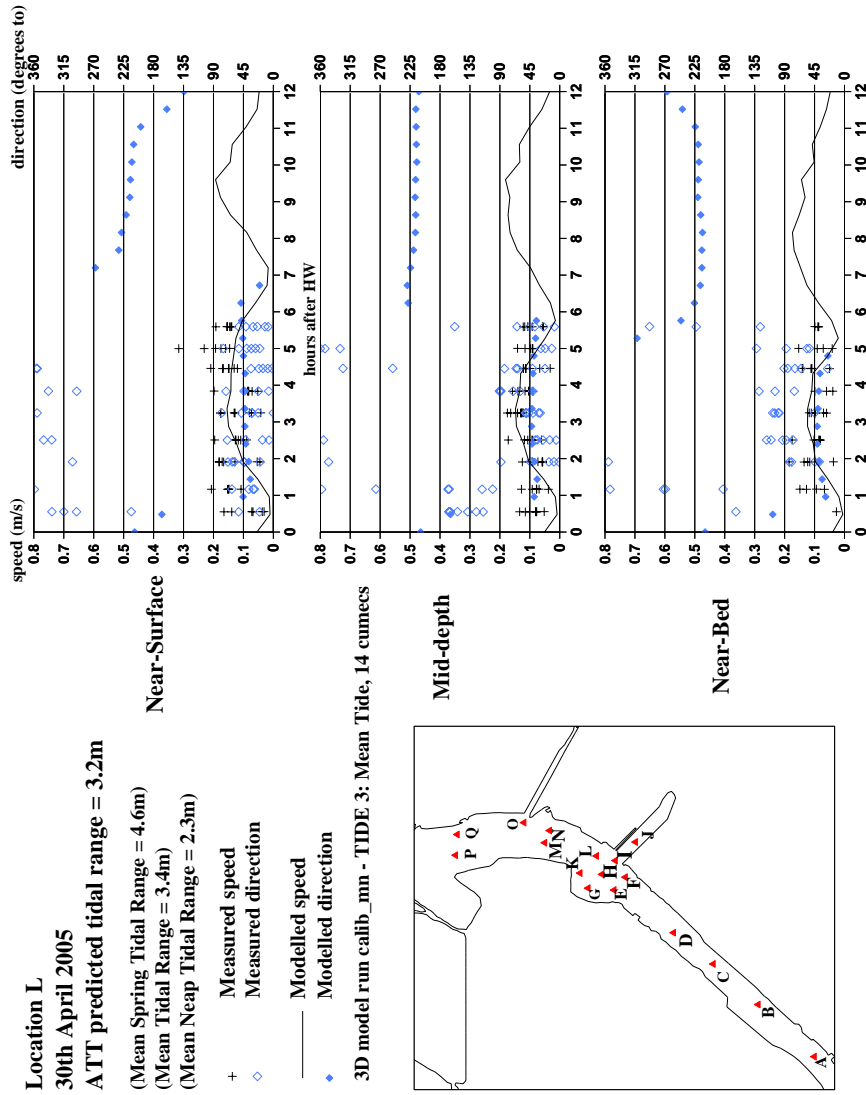


Figure 2.35 Calibration: observation wet season, mean tide at Location L

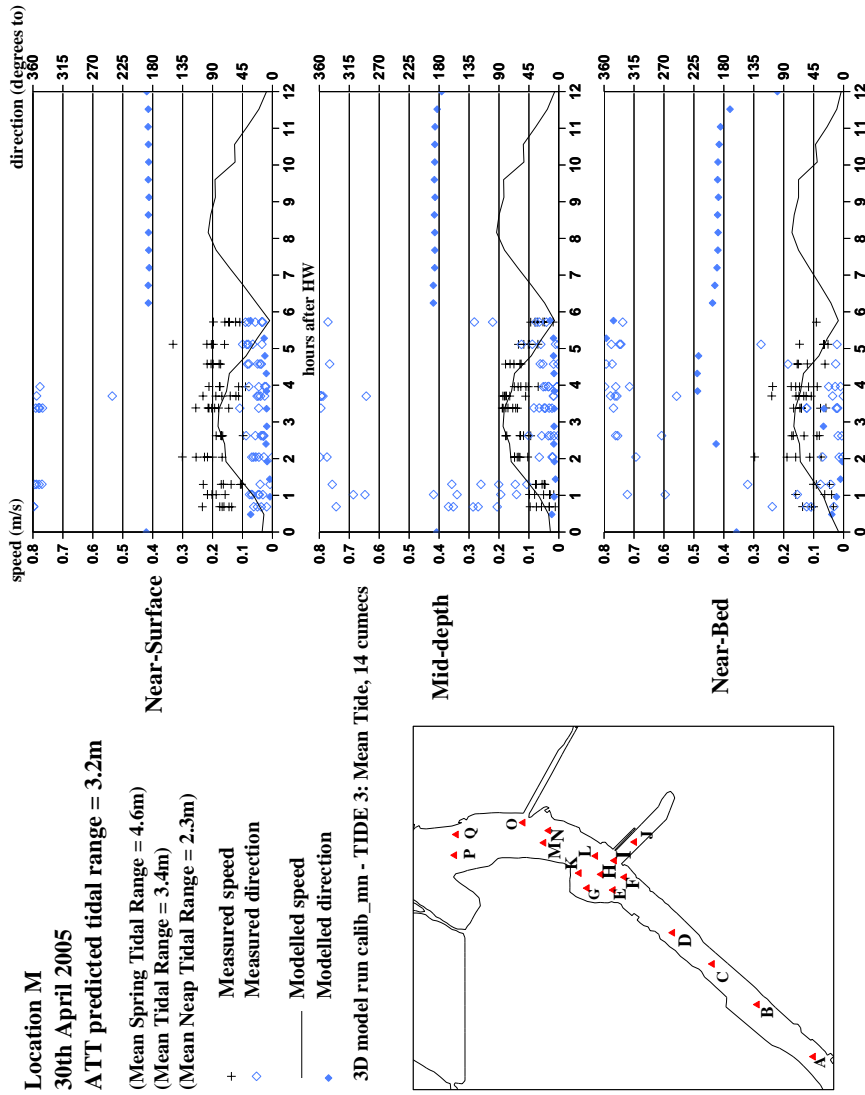


Figure 2.36 Calibration: observation wet season, mean tide at Location M

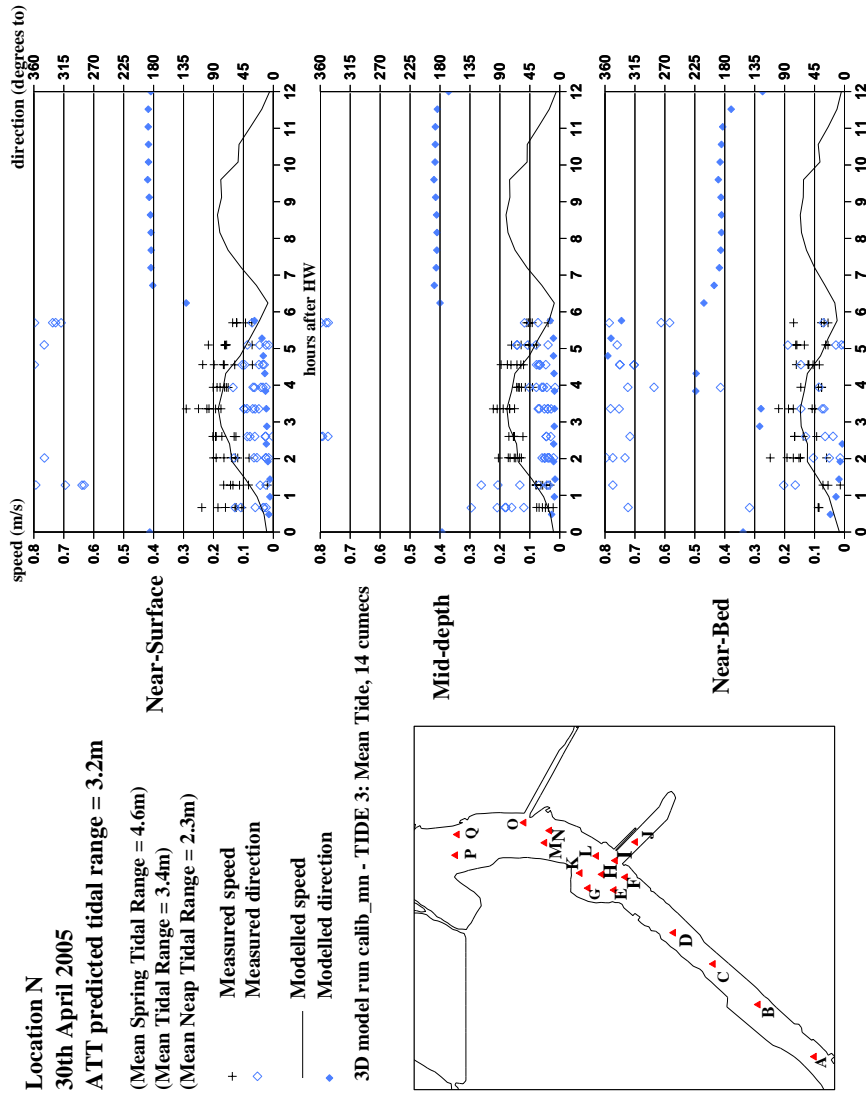


Figure 2.37 Calibration: observation wet season, mean tide at Location N

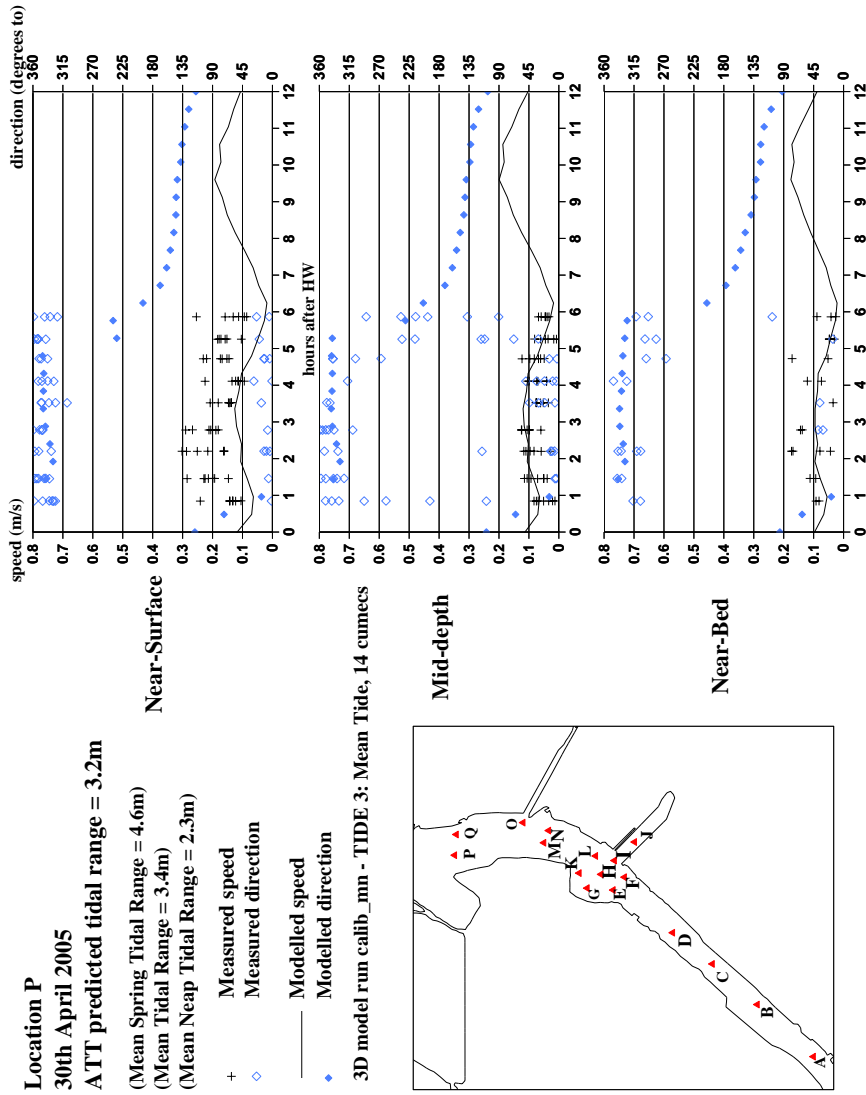


Figure 2.38 Calibration: observation wet season, mean tide at Location P

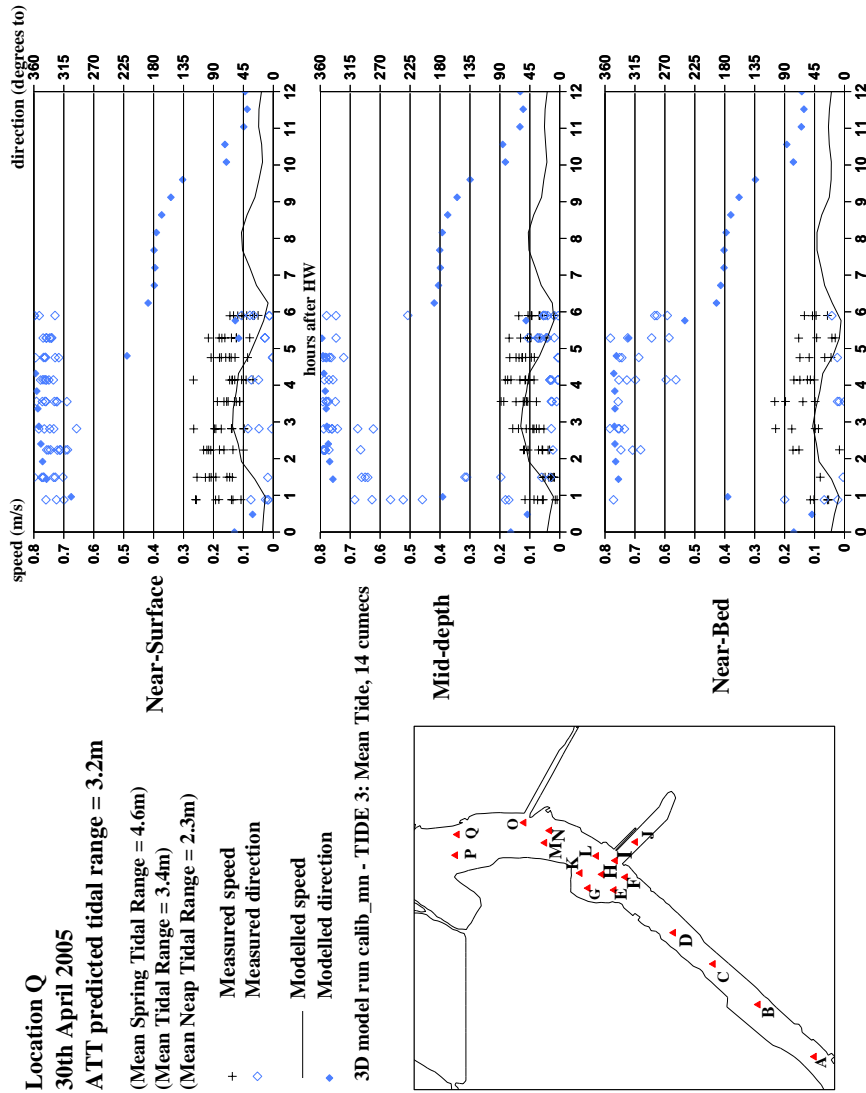


Figure 2.39 Calibration: observation wet season, mean tide at Location Q

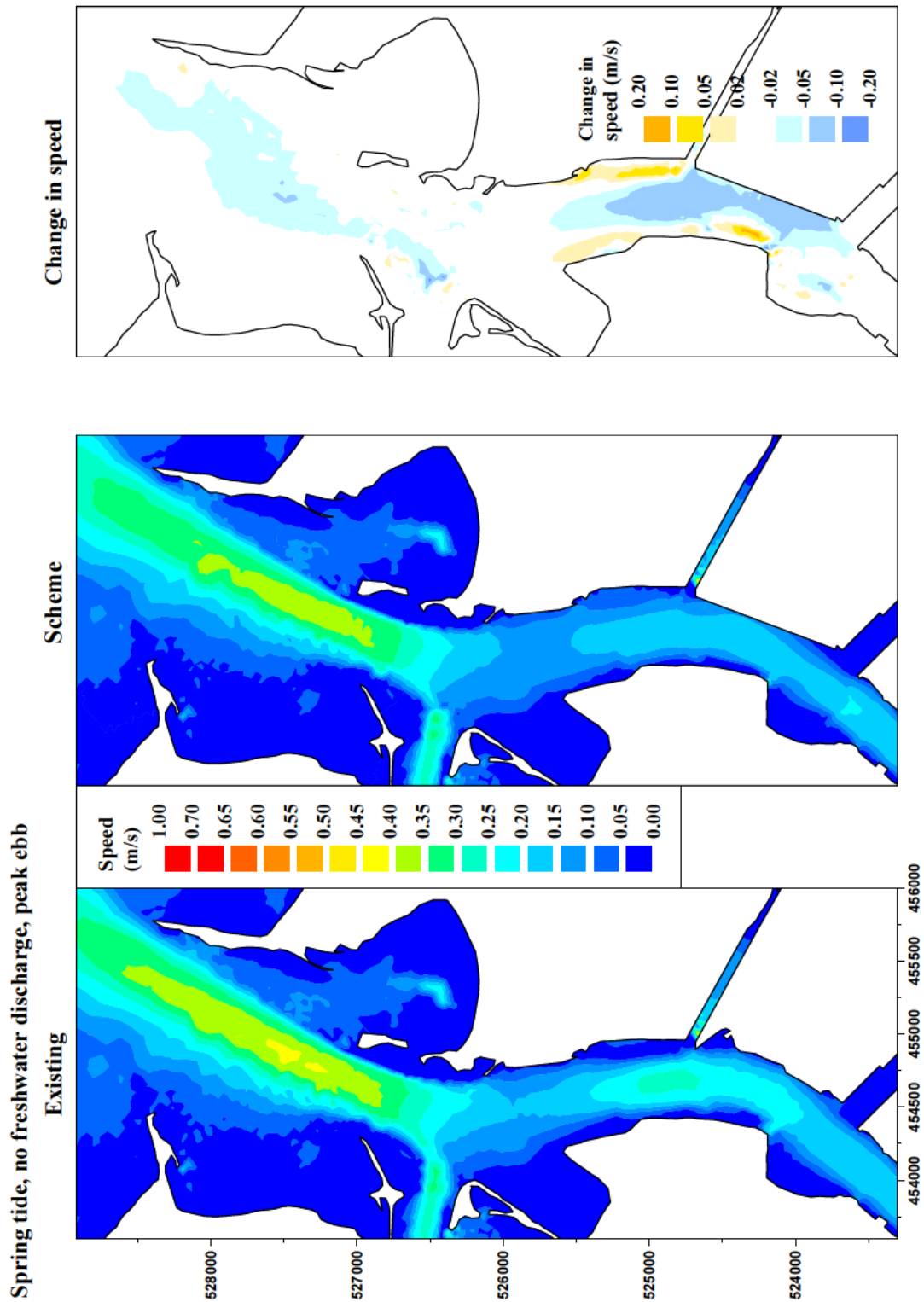


Figure 2.40 Dry spring conditions: depth-mean ebb speed – existing, scheme, difference

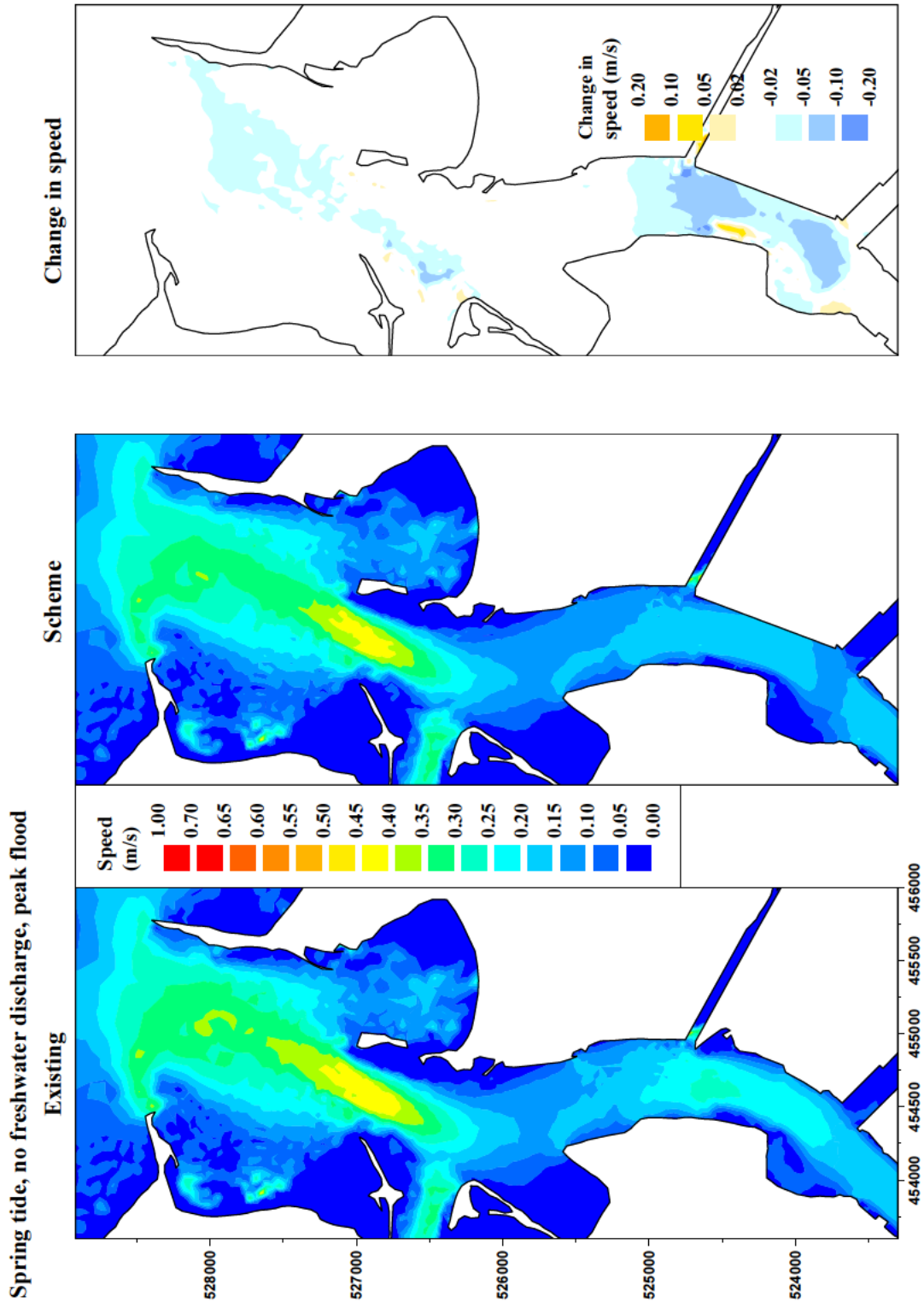


Figure 2.41 Dry spring conditions: depth-mean flood speed – existing, scheme, difference

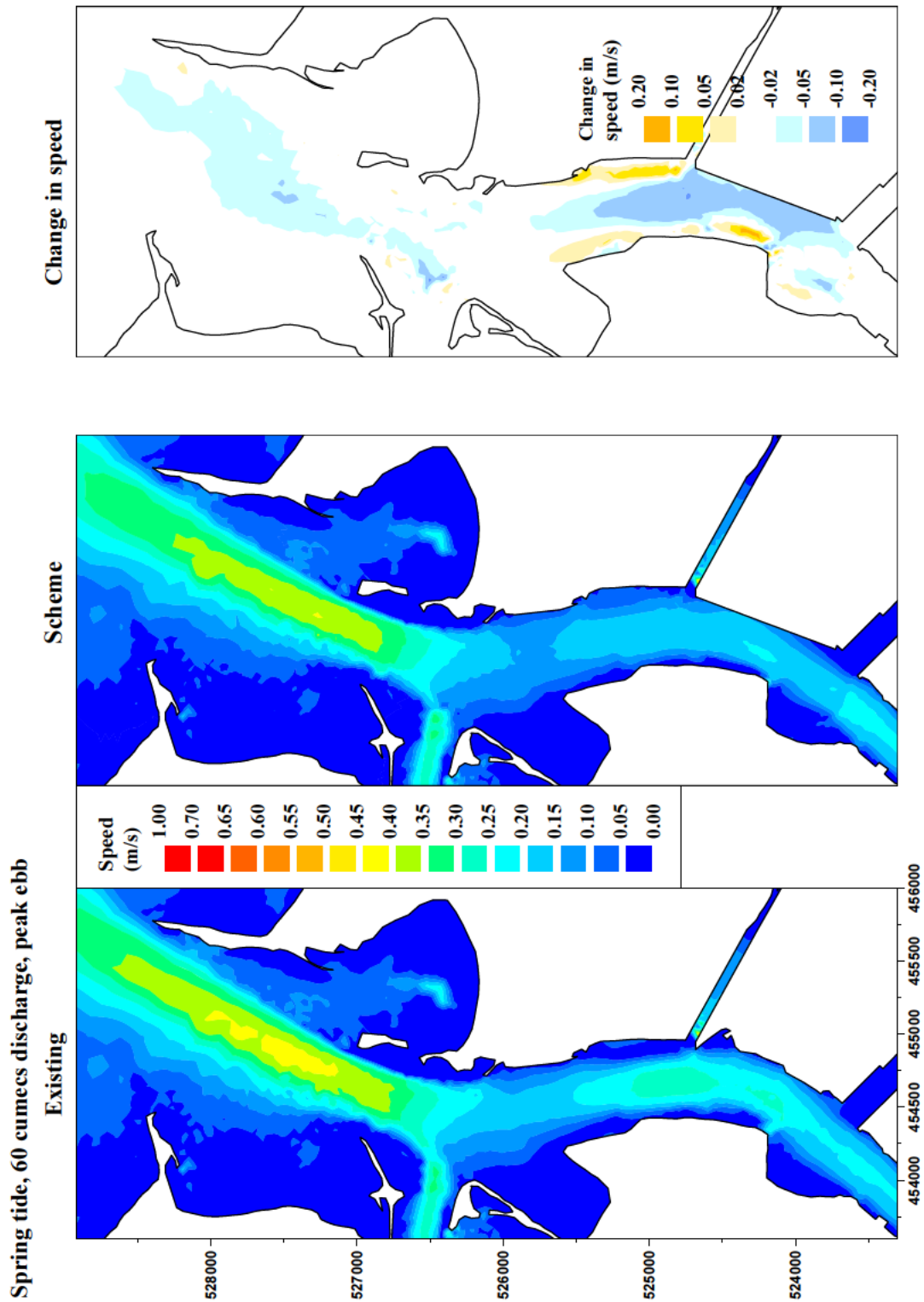


Figure 2.42 Wet spring conditions: depth-mean ebb speed – existing, scheme, difference

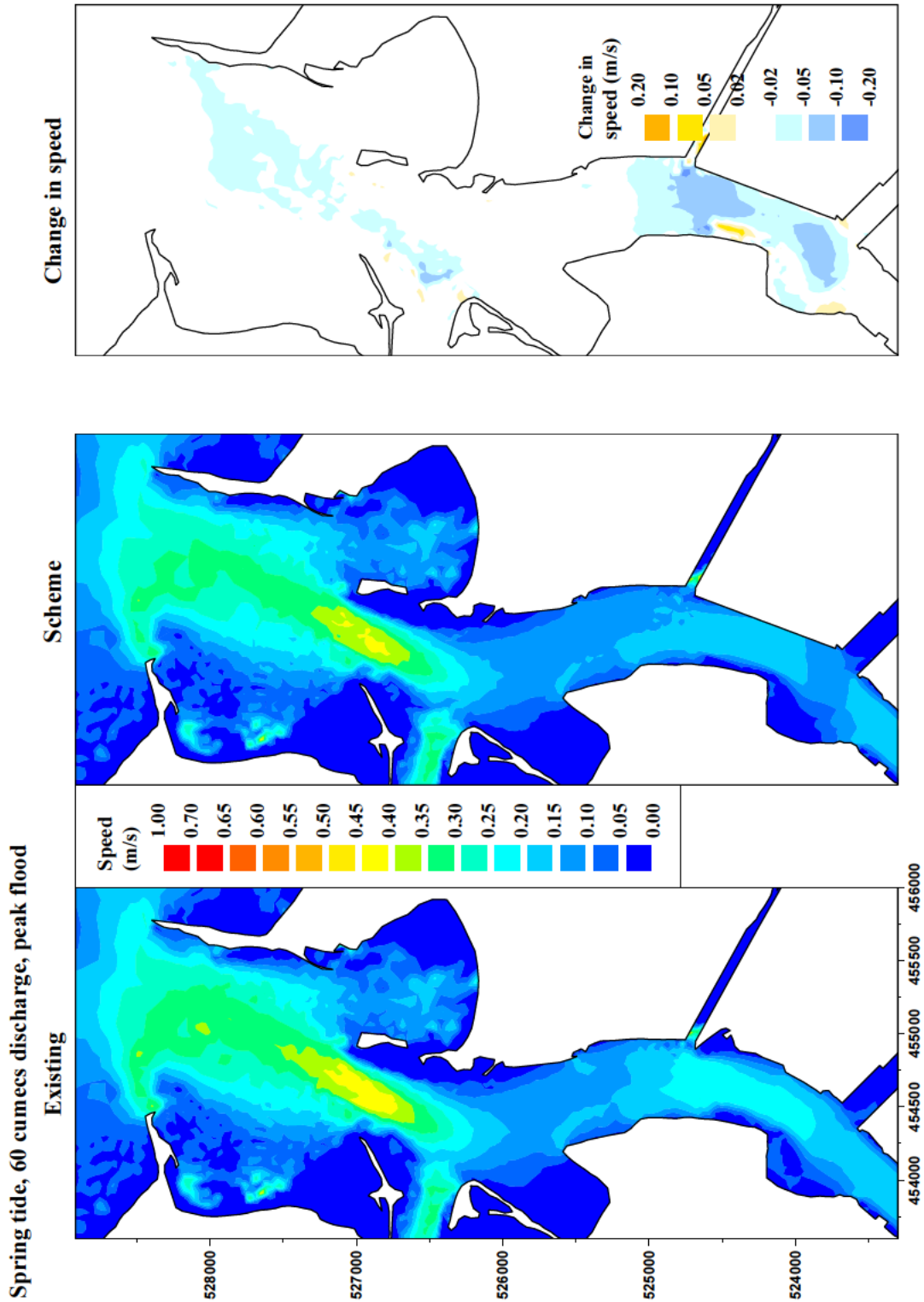


Figure 2.43 Wet spring conditions: depth-mean flood speed – existing, scheme, difference

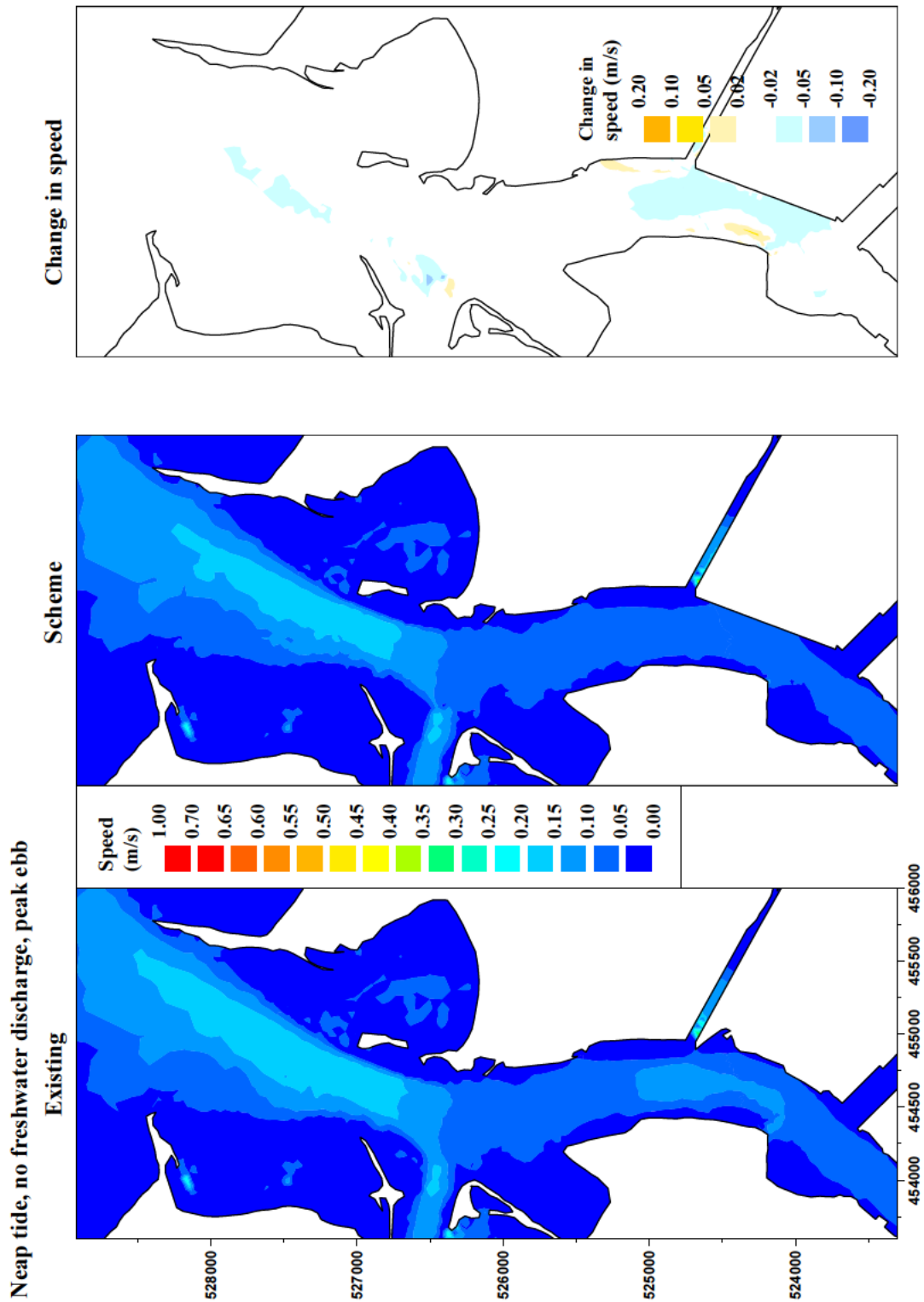


Figure 2.44 Dry neap conditions: depth-mean ebb speed – existing, scheme, difference

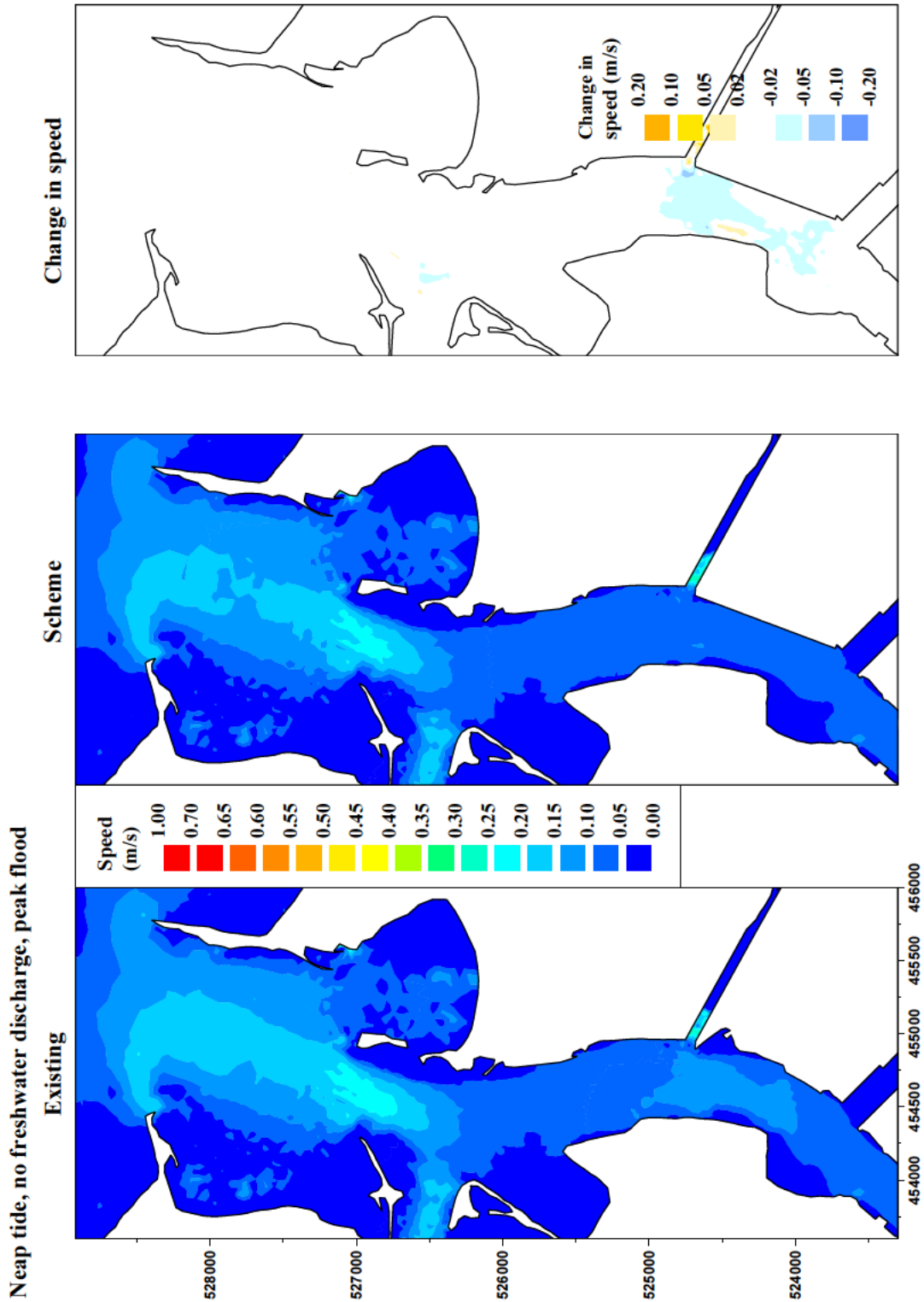


Figure 2.45 Dry neap conditions: depth-mean flood speed – existing, scheme, difference

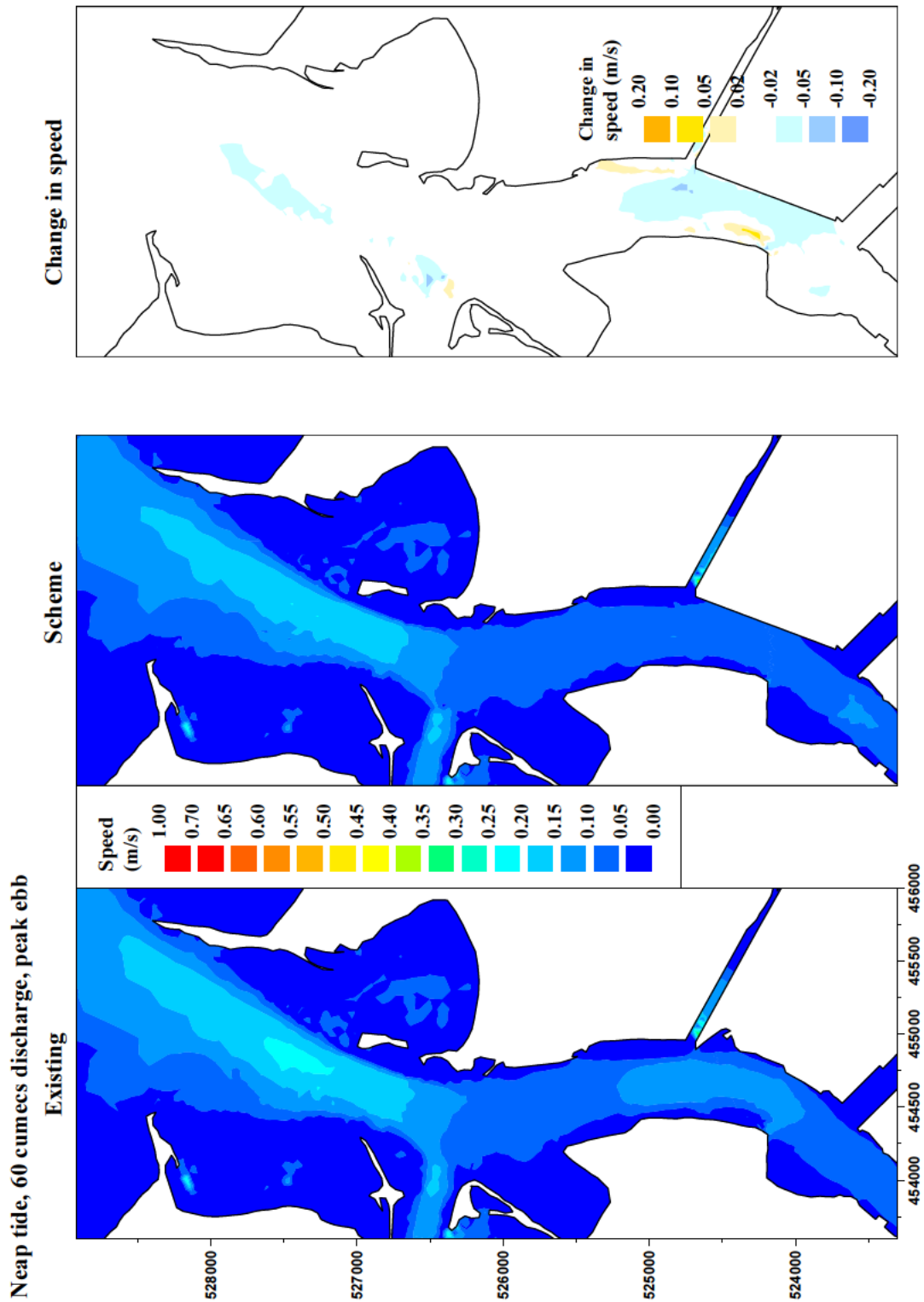


Figure 2.46 Wet neap conditions: depth-mean ebb speed – existing, scheme, difference

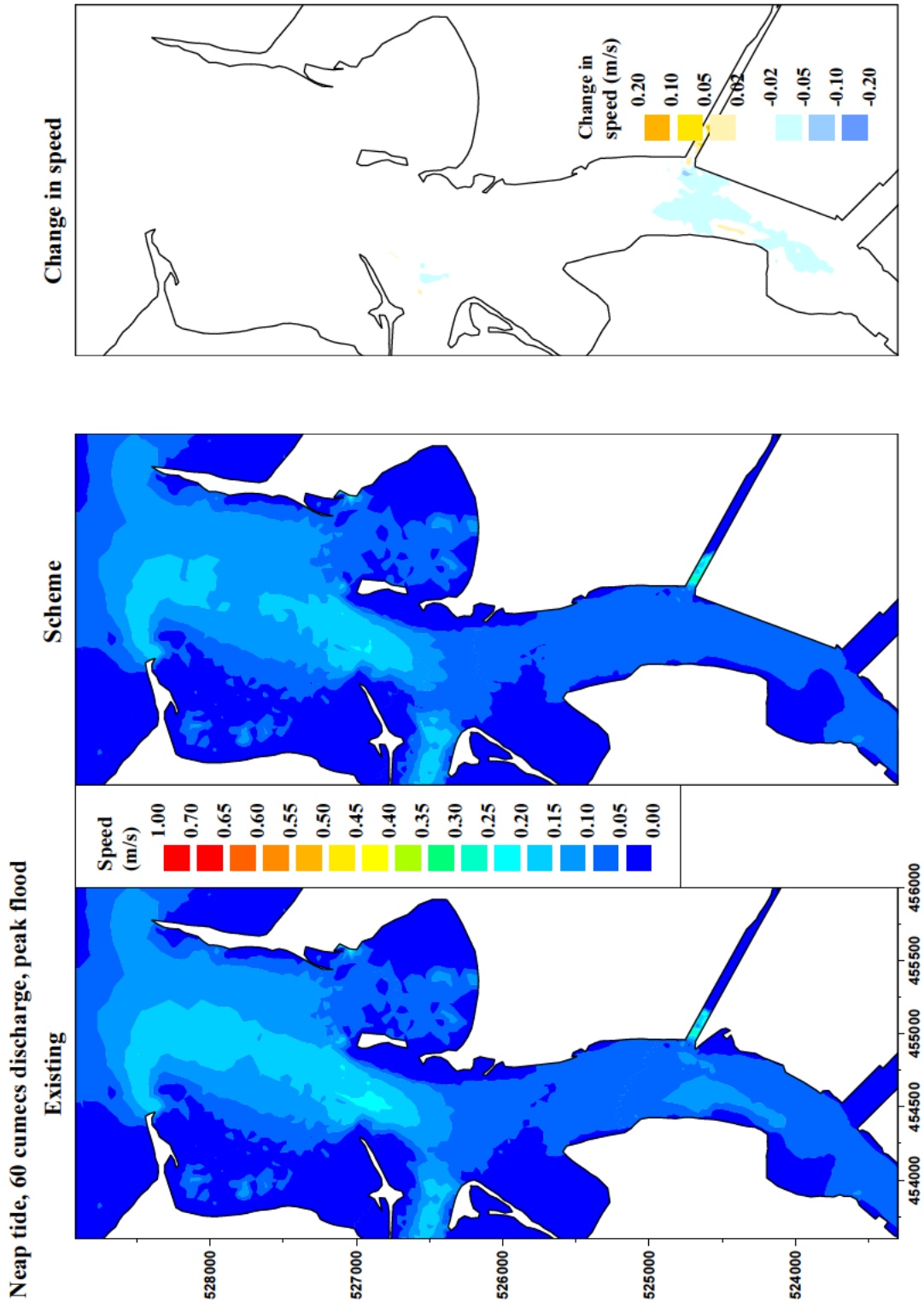


Figure 2.47 Wet neap conditions: depth-mean flood speed – existing, scheme, difference

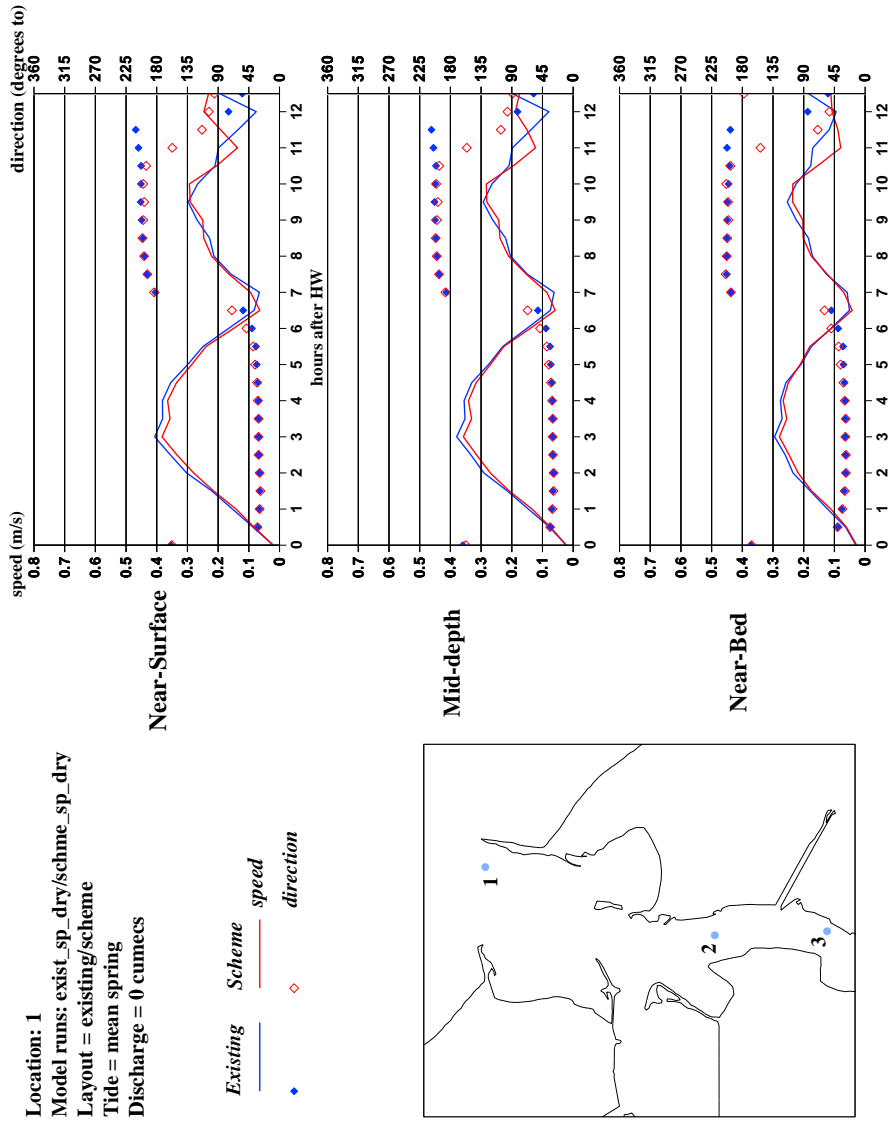


Figure 2.48 Dry spring conditions at Location 1: existing and scheme

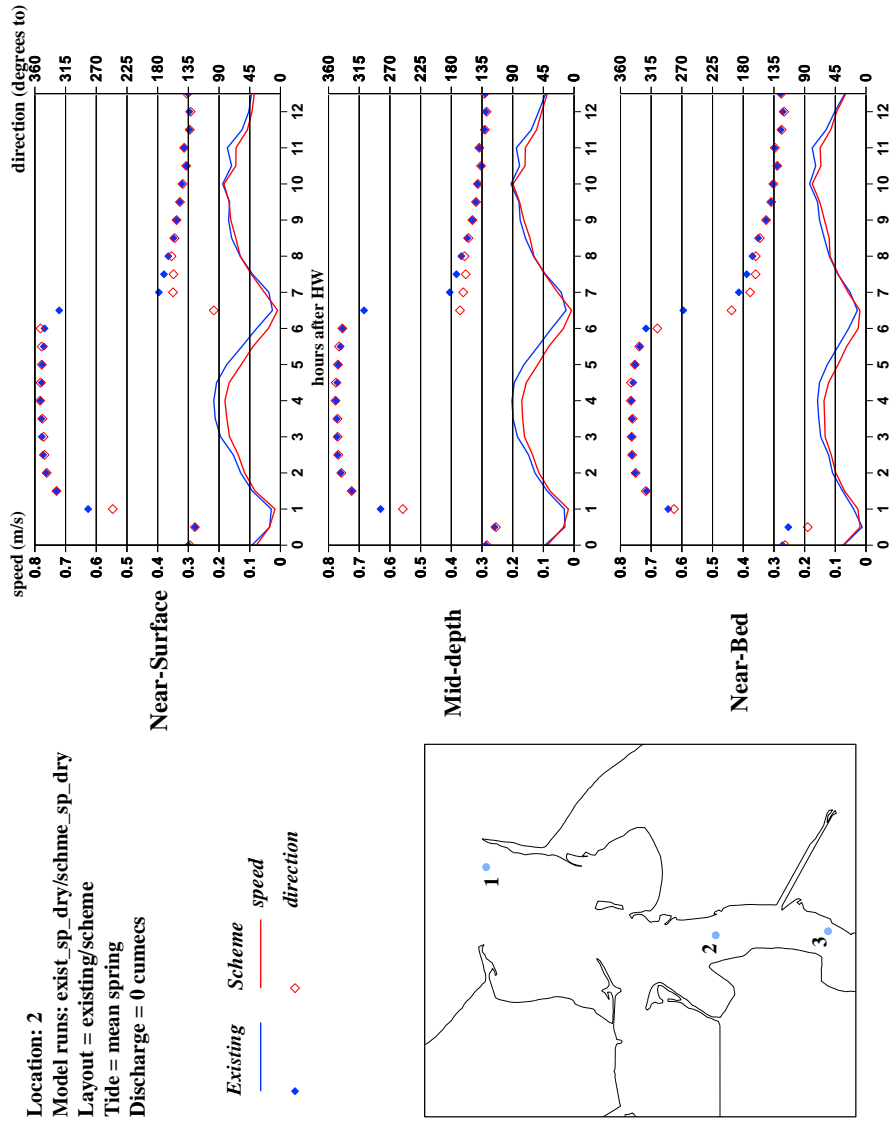


Figure 2.49 Dry spring conditions at Location 2: existing and scheme

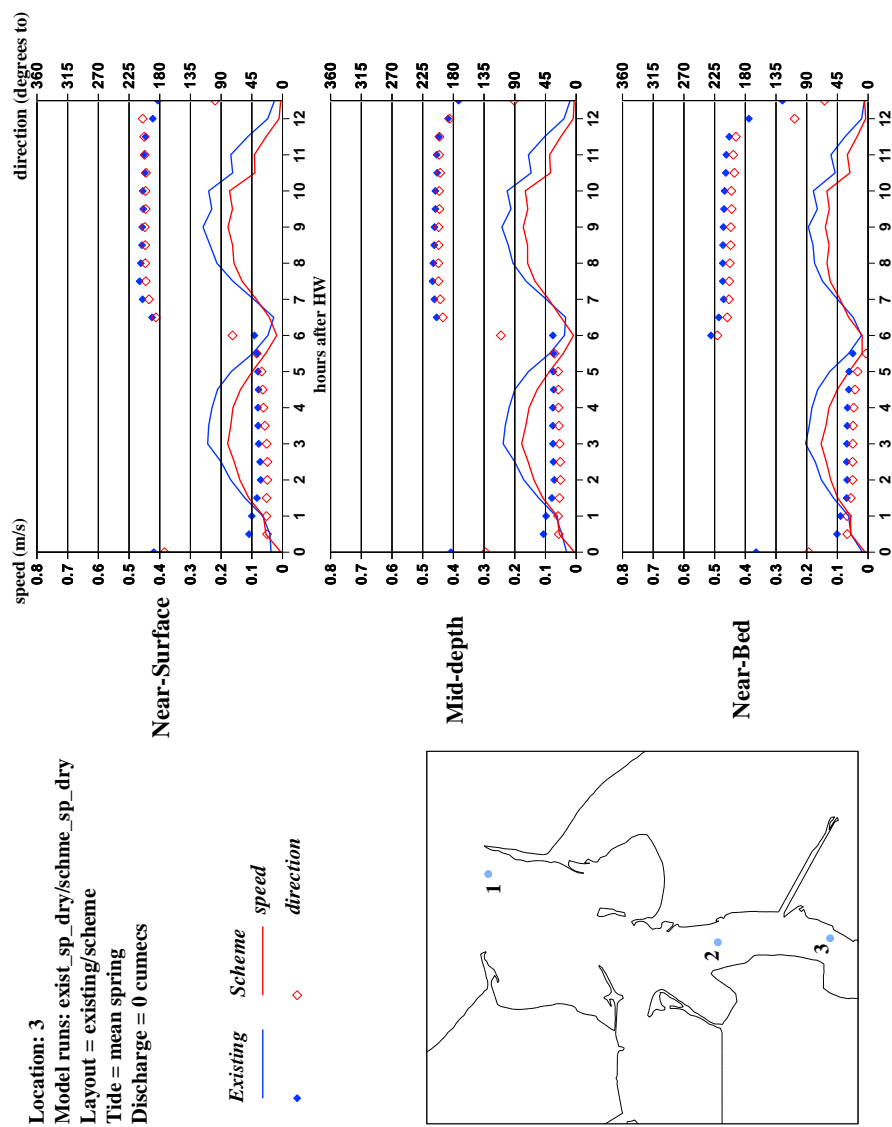


Figure 2.50 Dry spring conditions at Location 3: existing and scheme

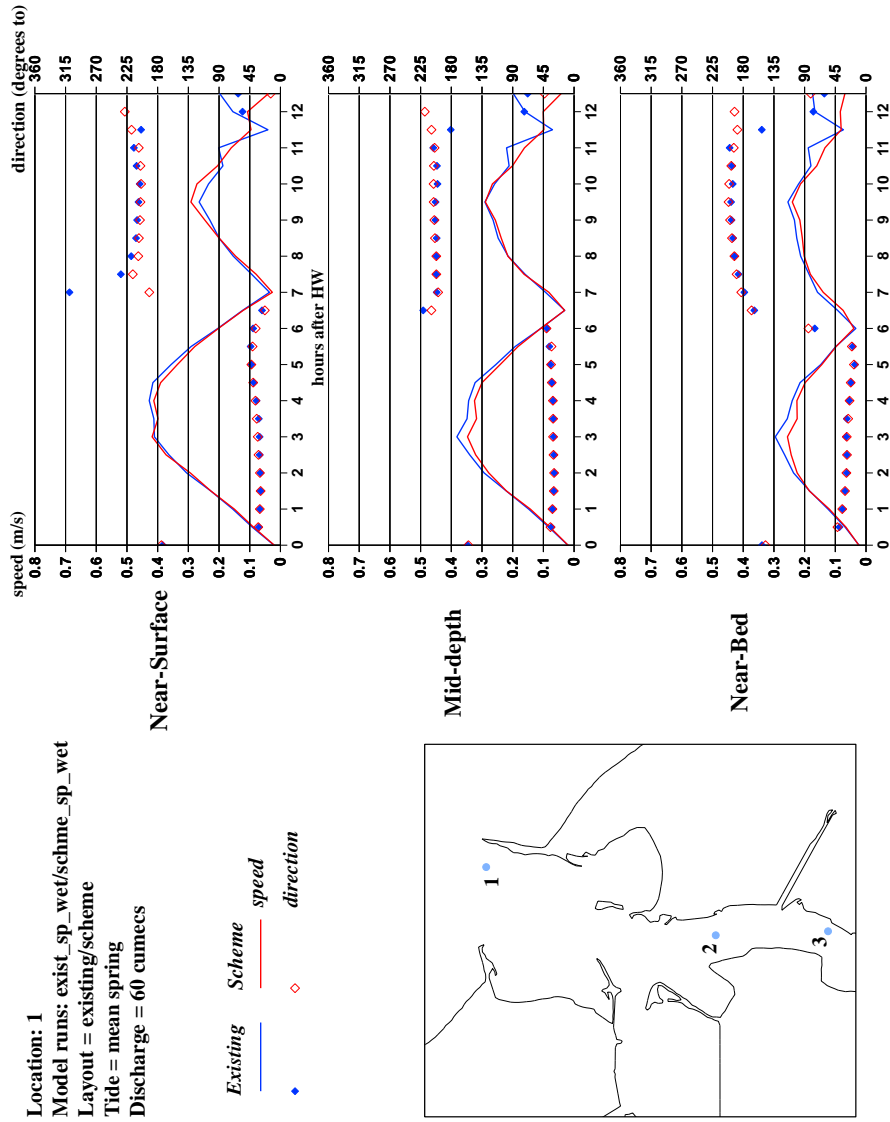


Figure 2.51 Wet spring conditions at Location 1: existing and scheme

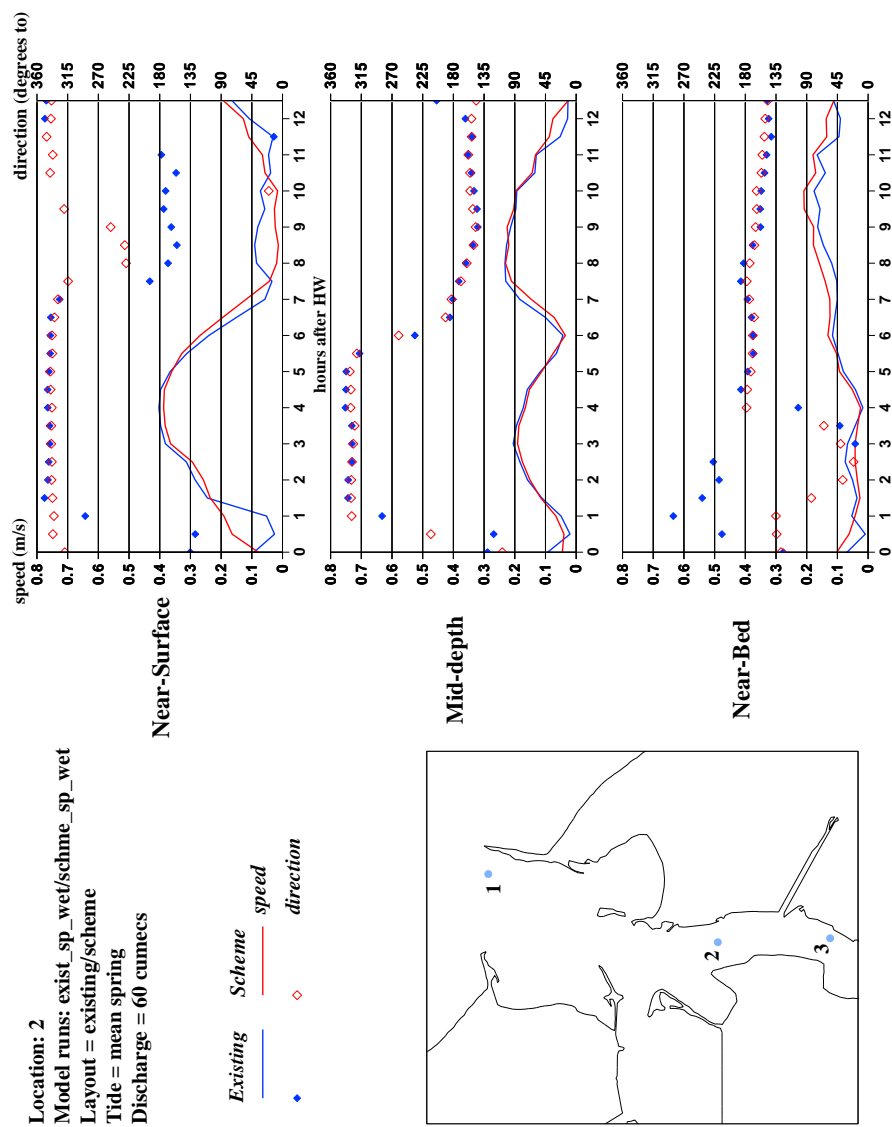


Figure 2.52 Wet spring conditions at Location 2: existing and scheme

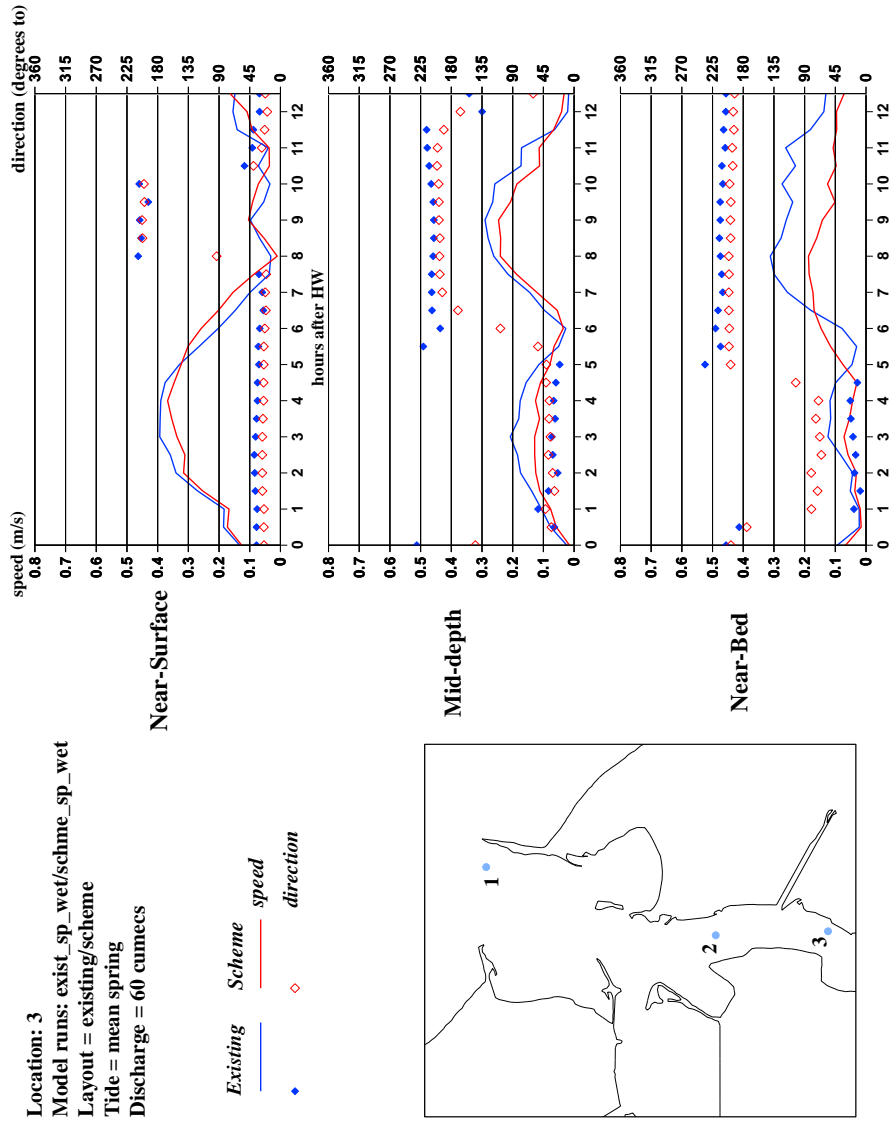


Figure 2.53 Wet spring conditions at Location 3: existing and scheme

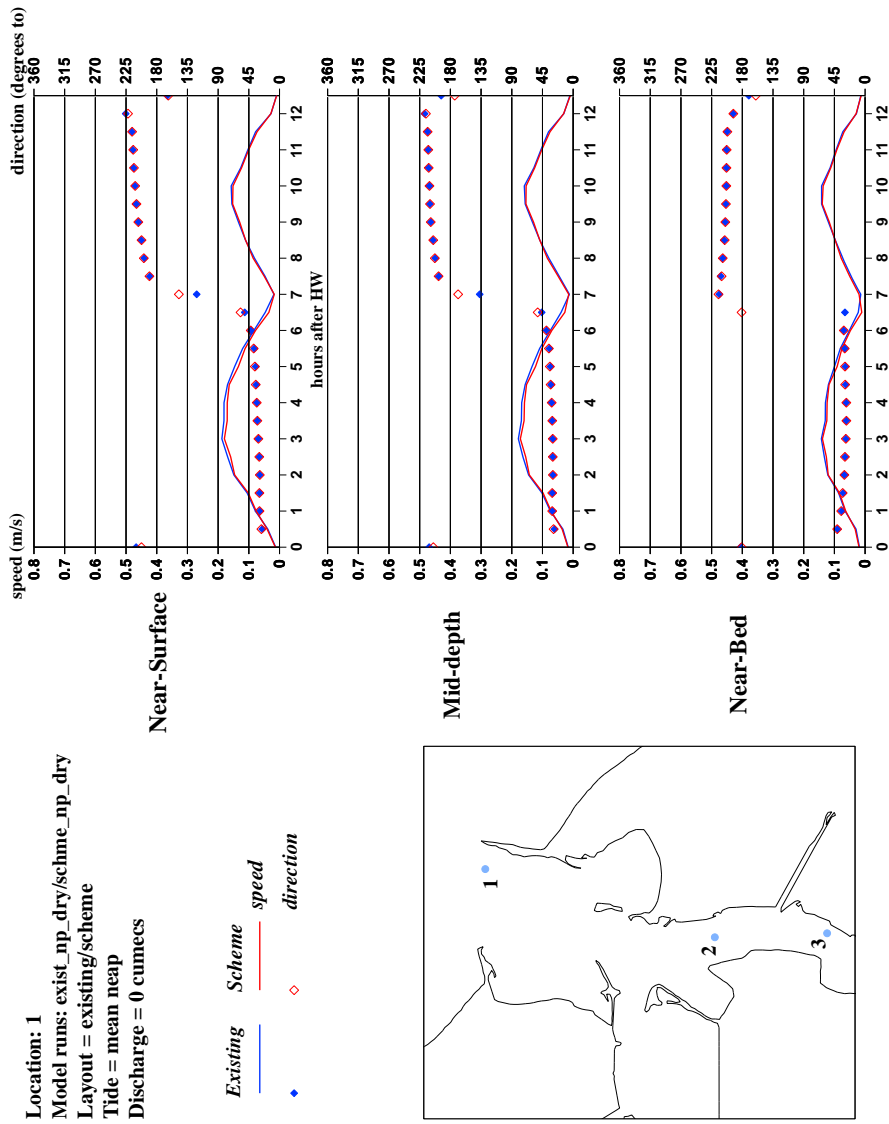


Figure 2.54 Dry neap conditions at Location 1: existing and scheme

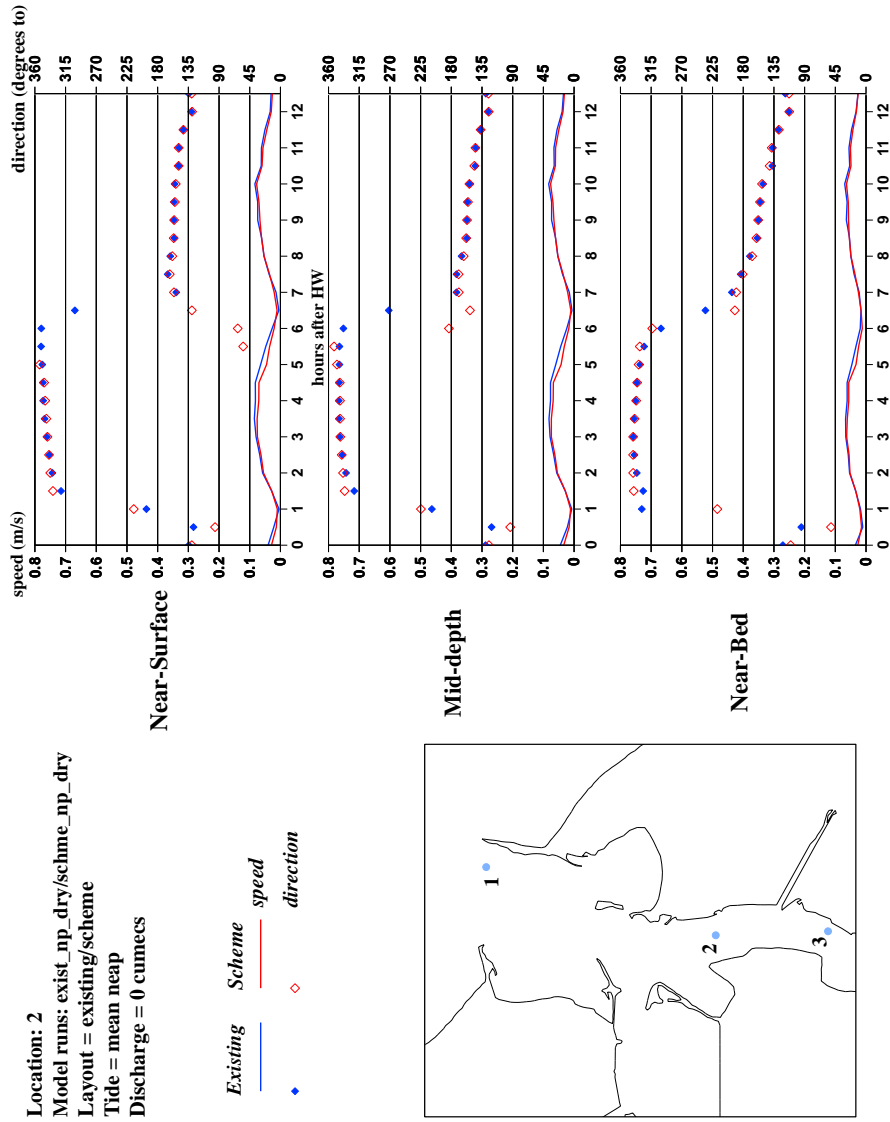


Figure 2.55 Dry neap conditions at Location 2: existing and scheme

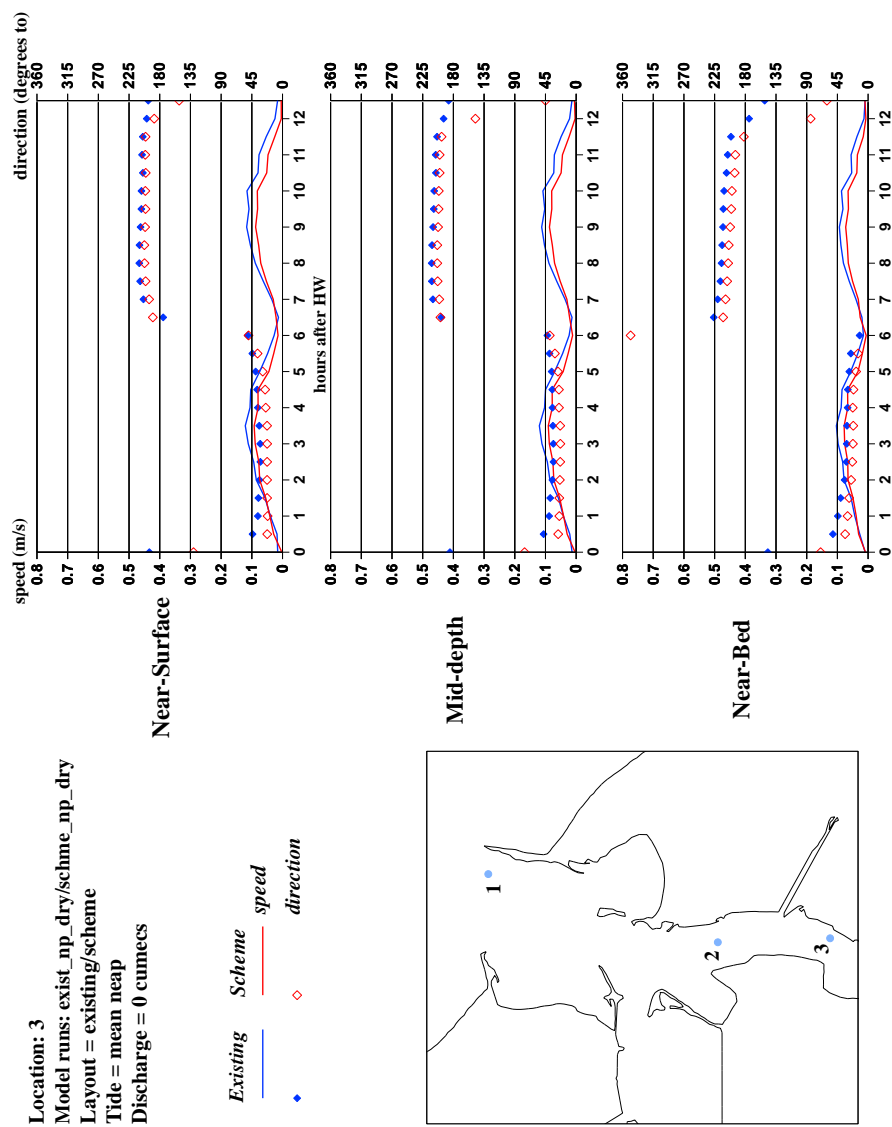


Figure 2.56 Dry neap conditions at Location 3: existing and scheme

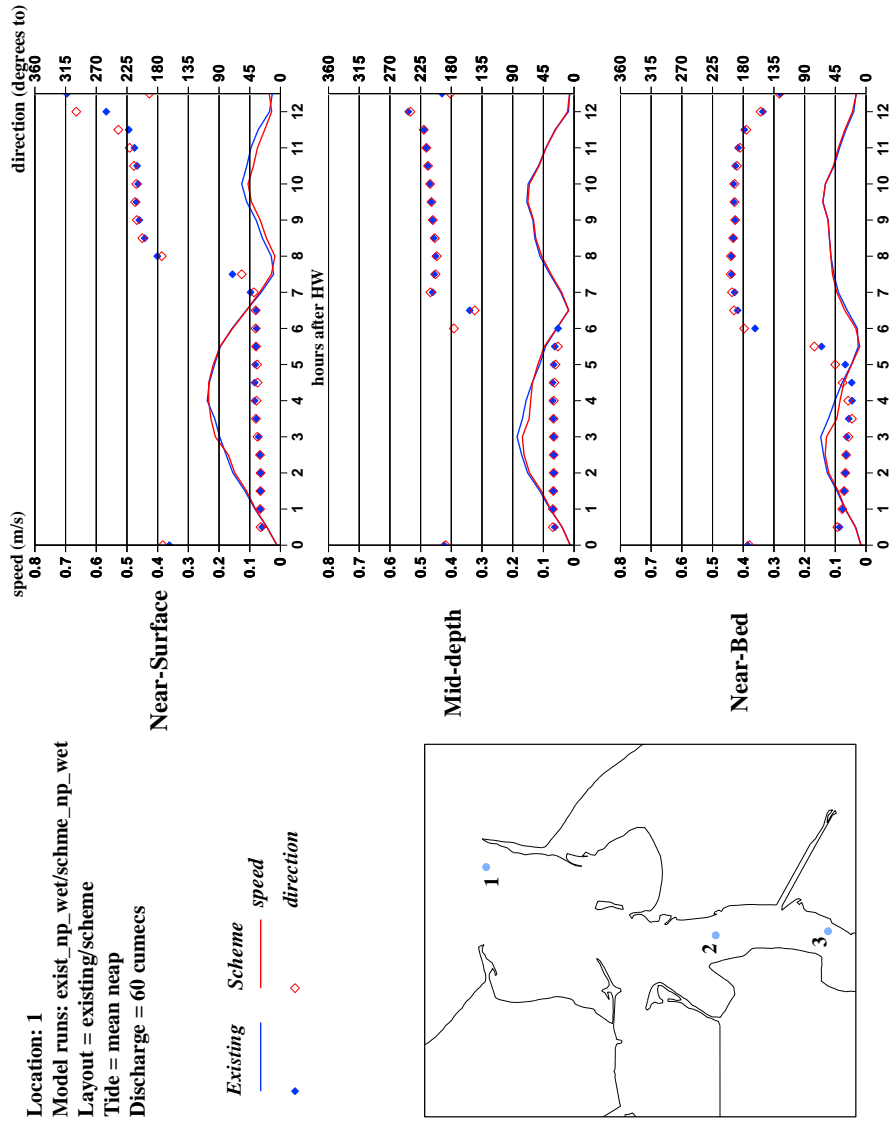


Figure 2.57 Wet neap conditions at Location 1: existing and scheme

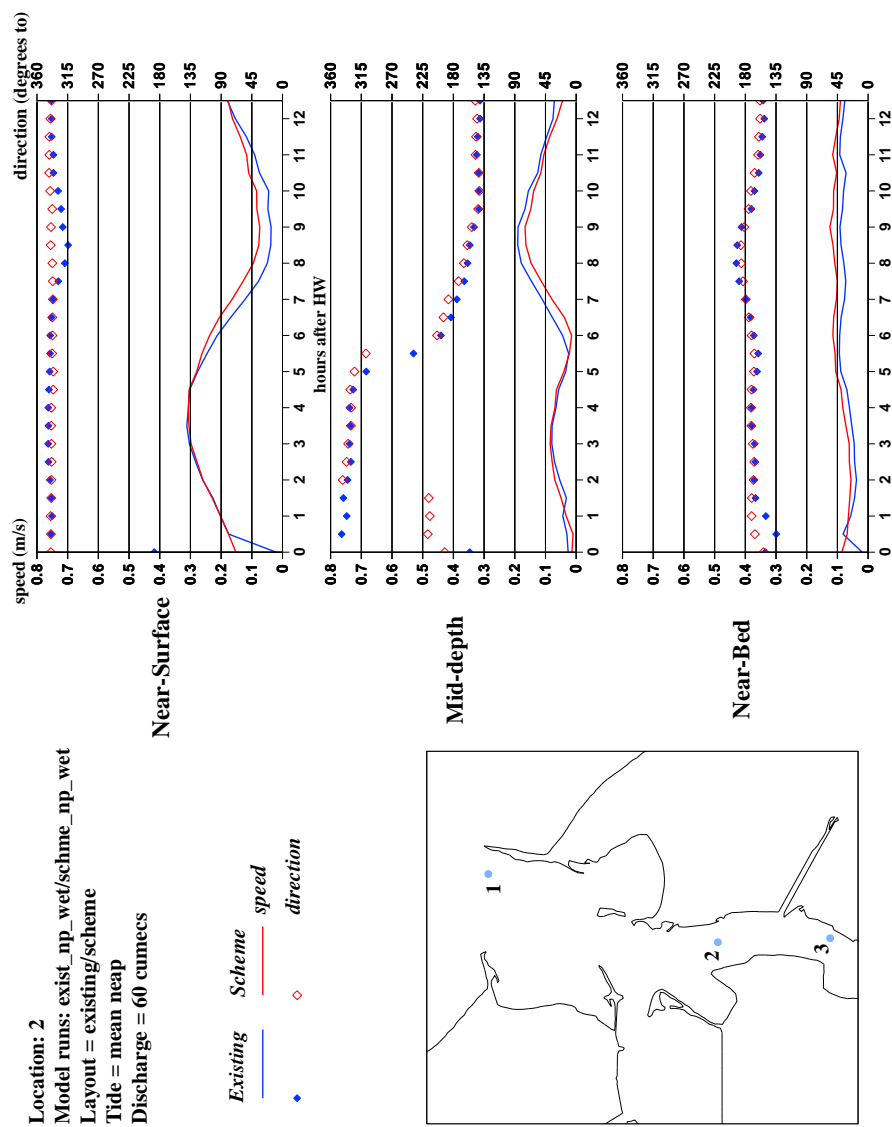


Figure 2.58 Wet neap conditions at Location 2: existing and scheme

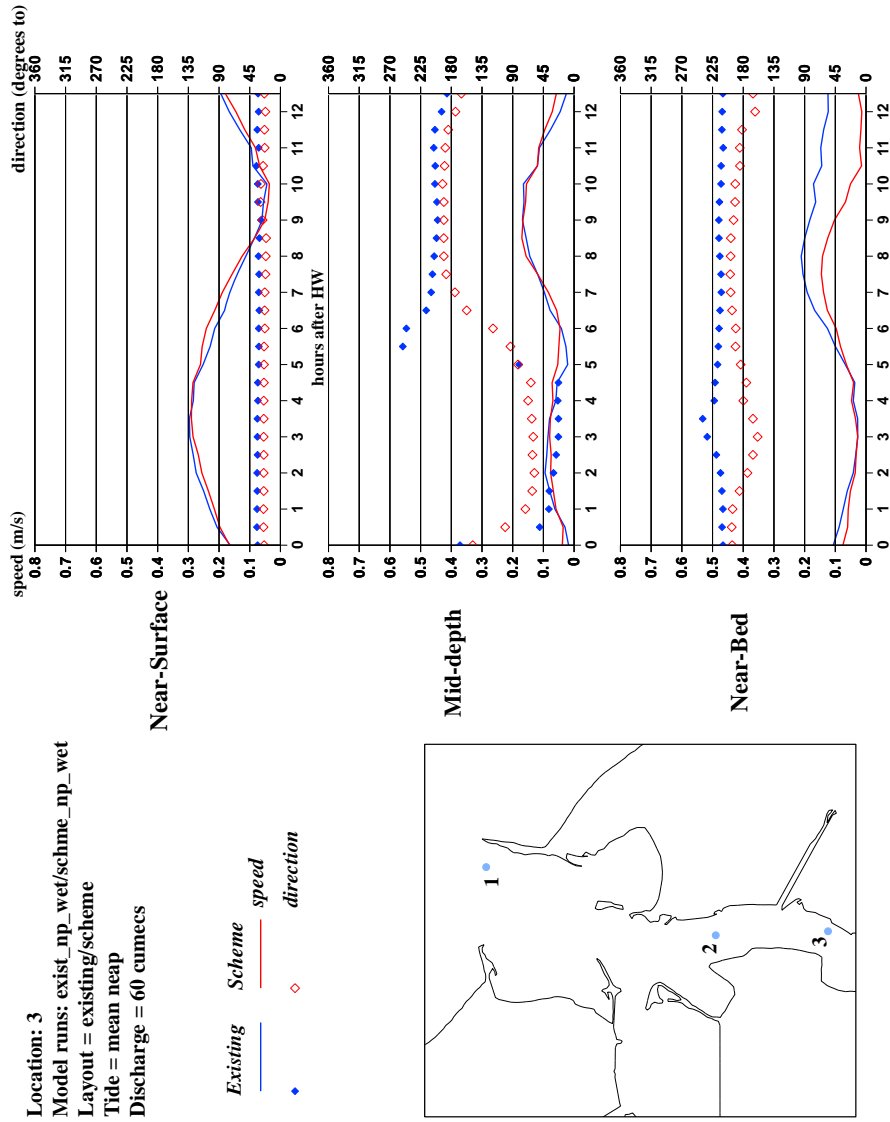


Figure 2.59 Wet neap conditions at Location 3: existing and scheme

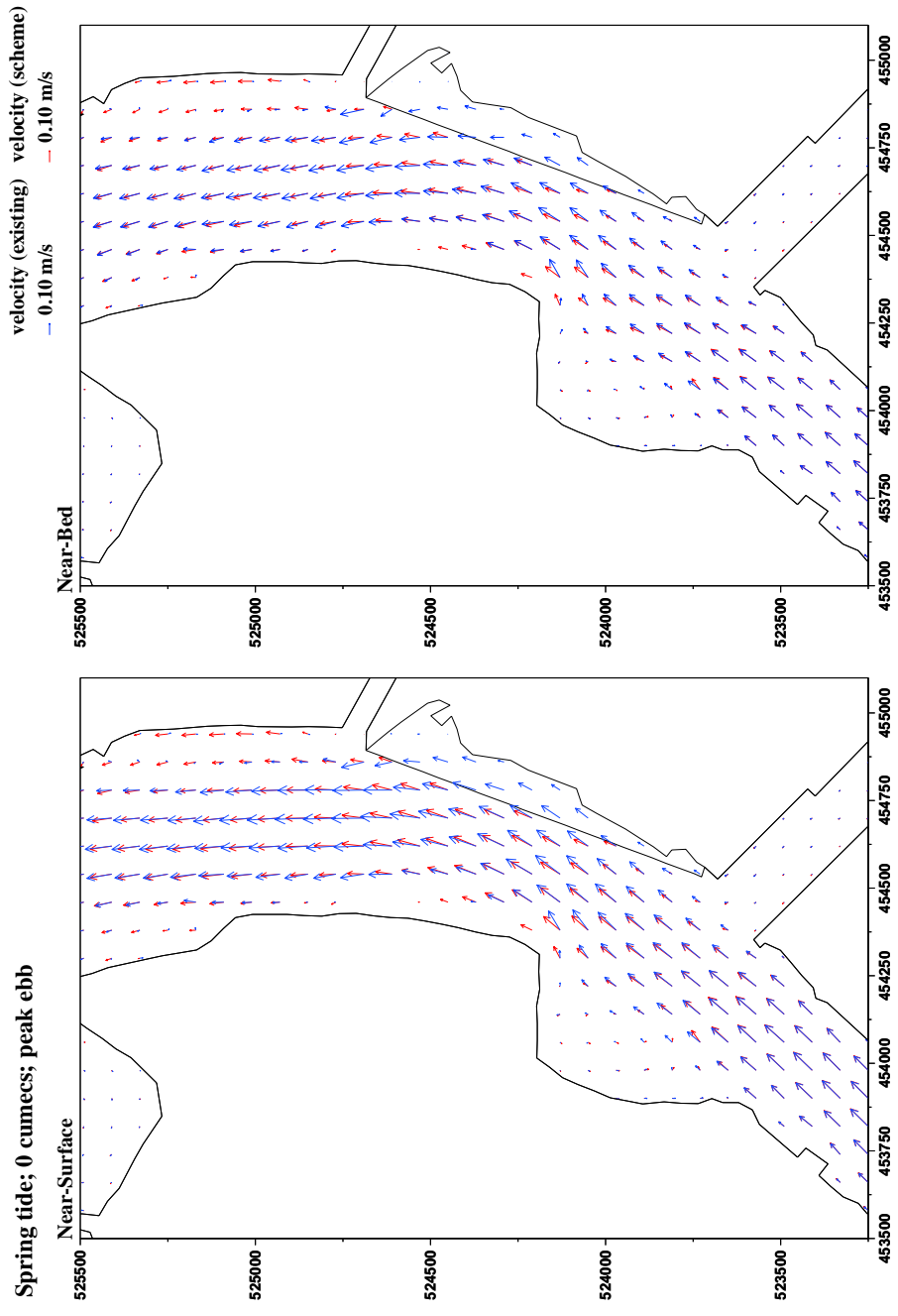


Figure 2.60 Dry spring conditions: ebb velocity near surface and bed – existing, scheme

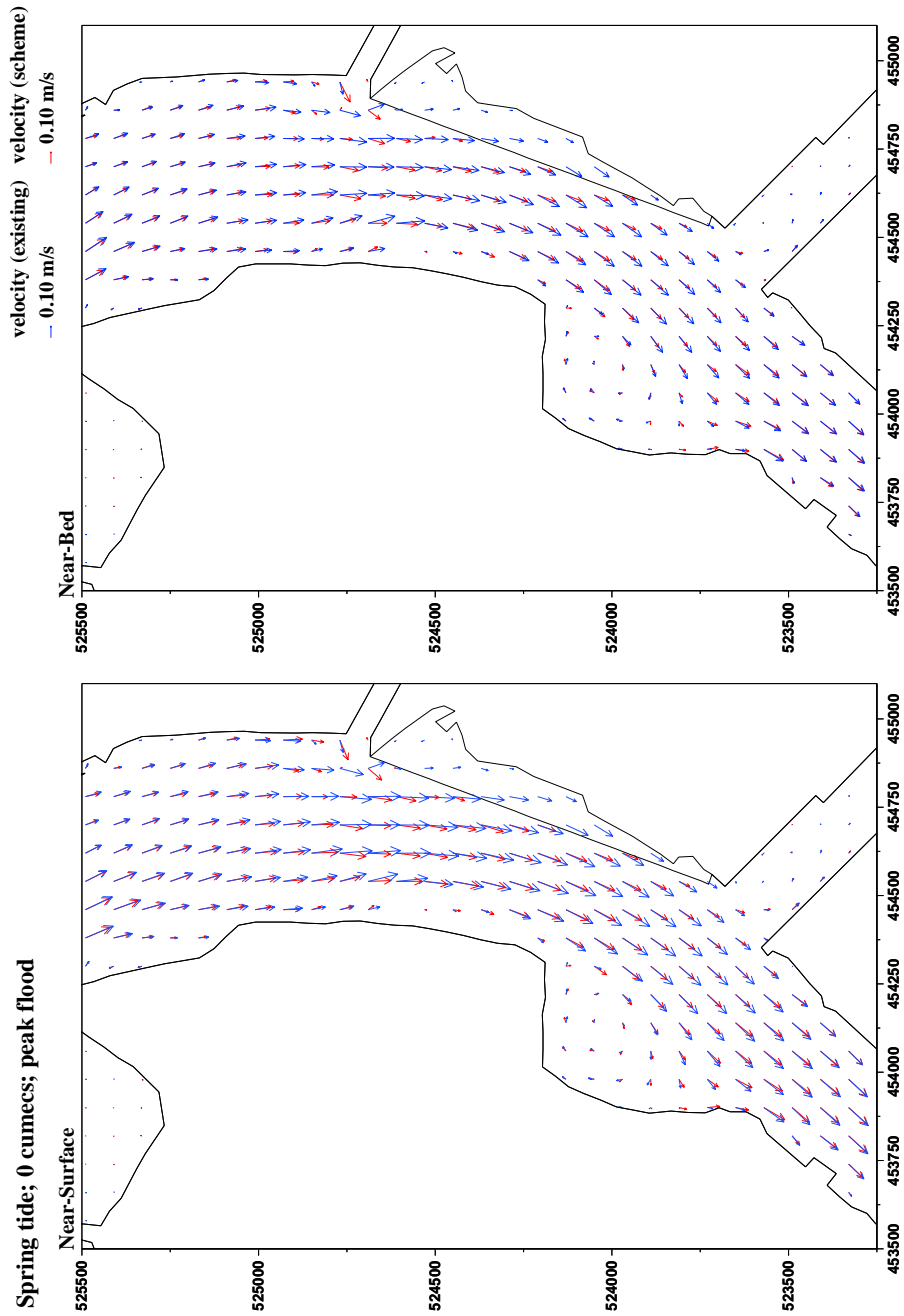


Figure 2.61 Dry spring conditions: flood velocity near surface and bed – existing, scheme

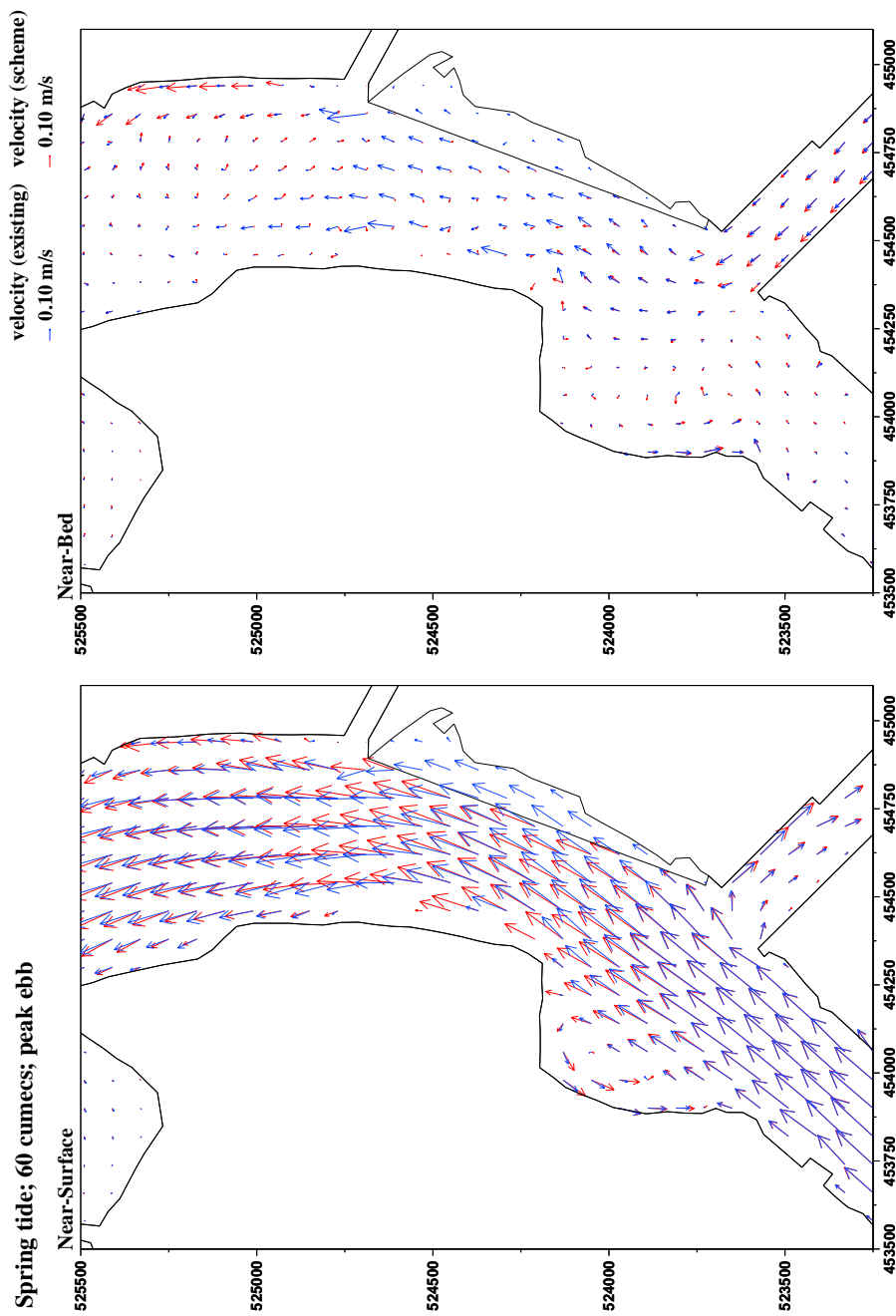


Figure 2.62 Wet spring conditions: ebb velocity near surface and bed – existing, scheme

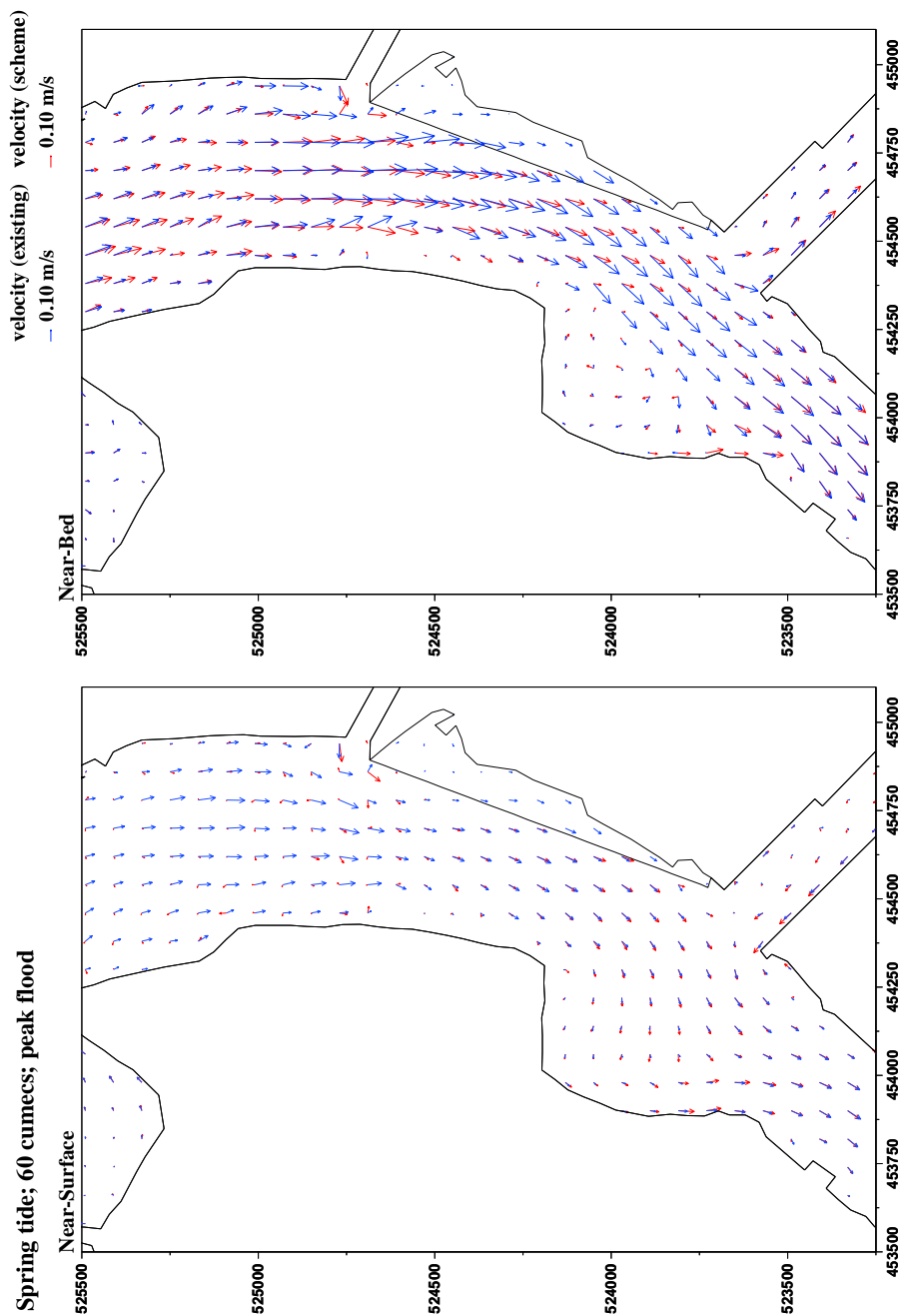


Figure 2.63 Wet spring conditions: flood velocity near surface and bed – existing, scheme

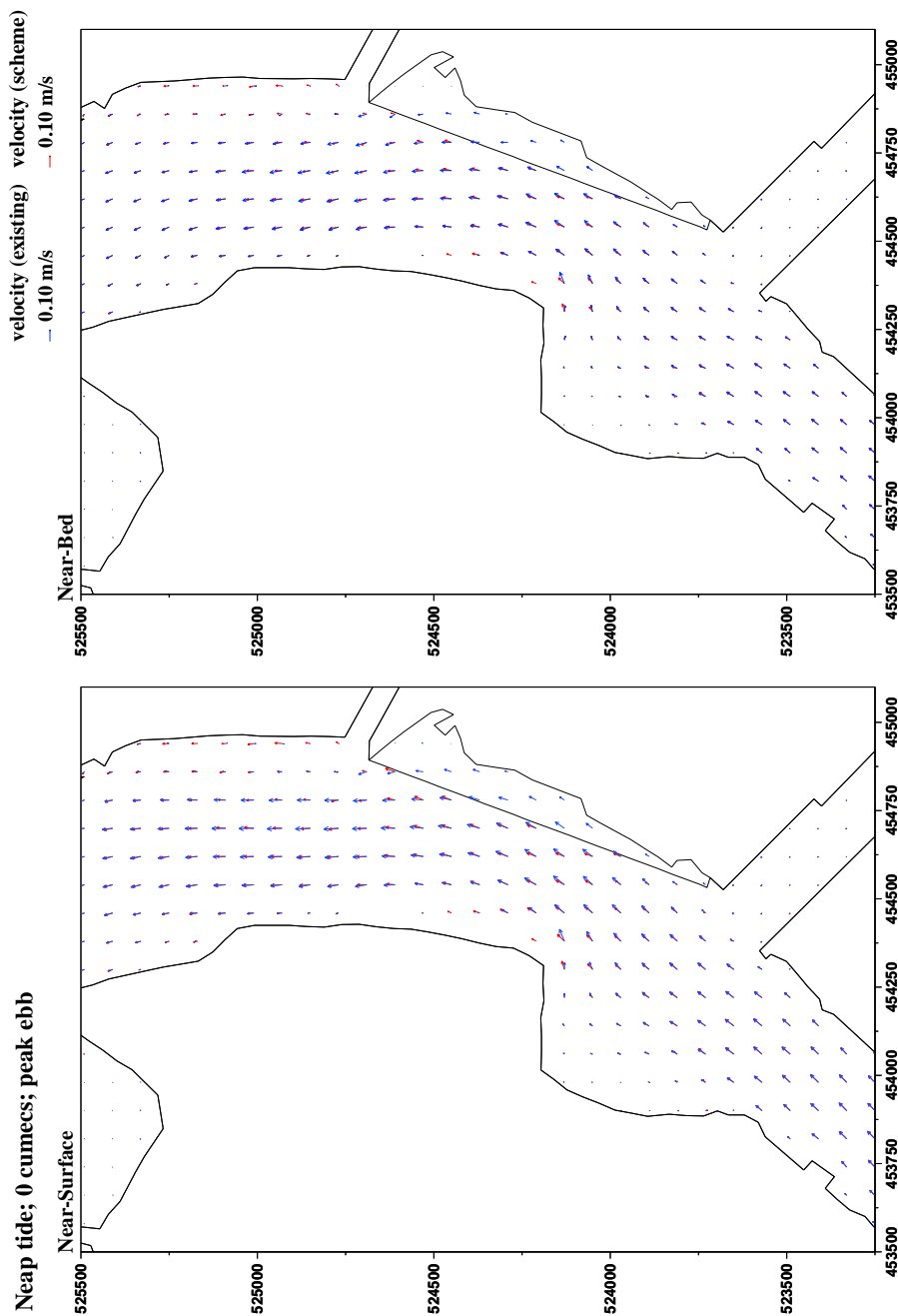


Figure 2.64 Dry neap conditions: ebb velocity near surface and bed – existing, scheme

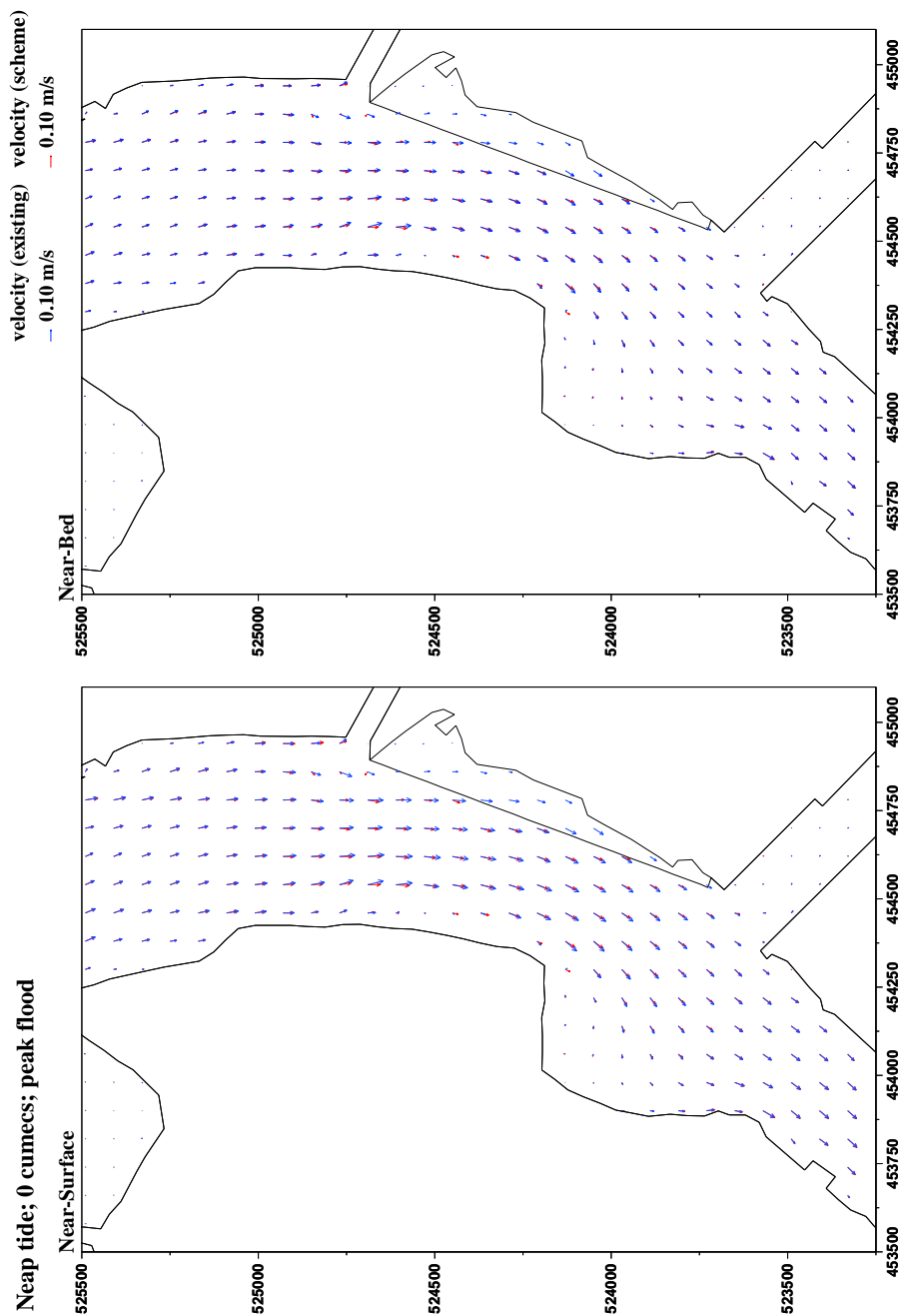


Figure 2.65 Dry neap conditions: flood velocity near surface and bed – existing, scheme

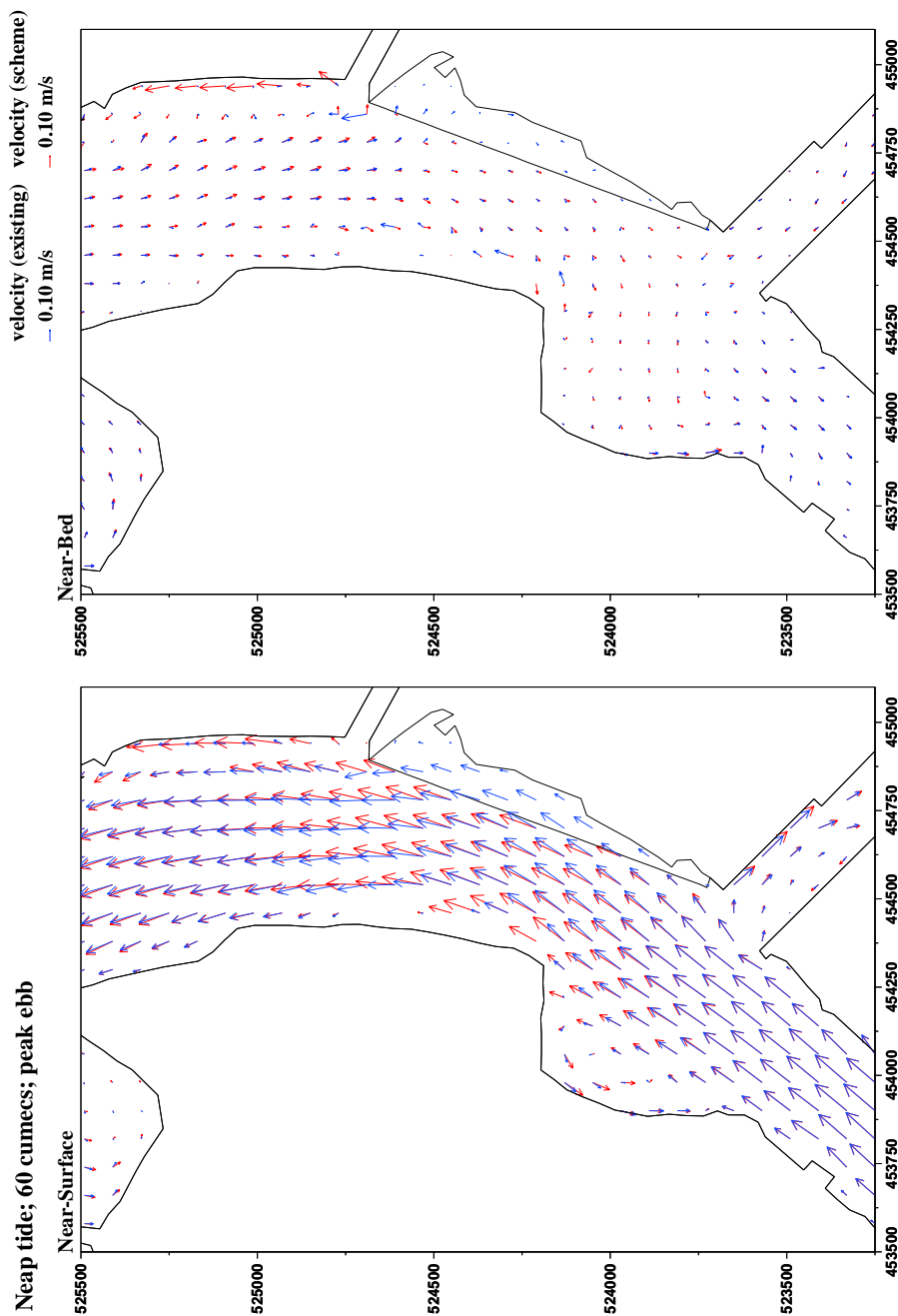


Figure 2.66 Wet neap conditions: ebb velocity near surface and bed – existing, scheme

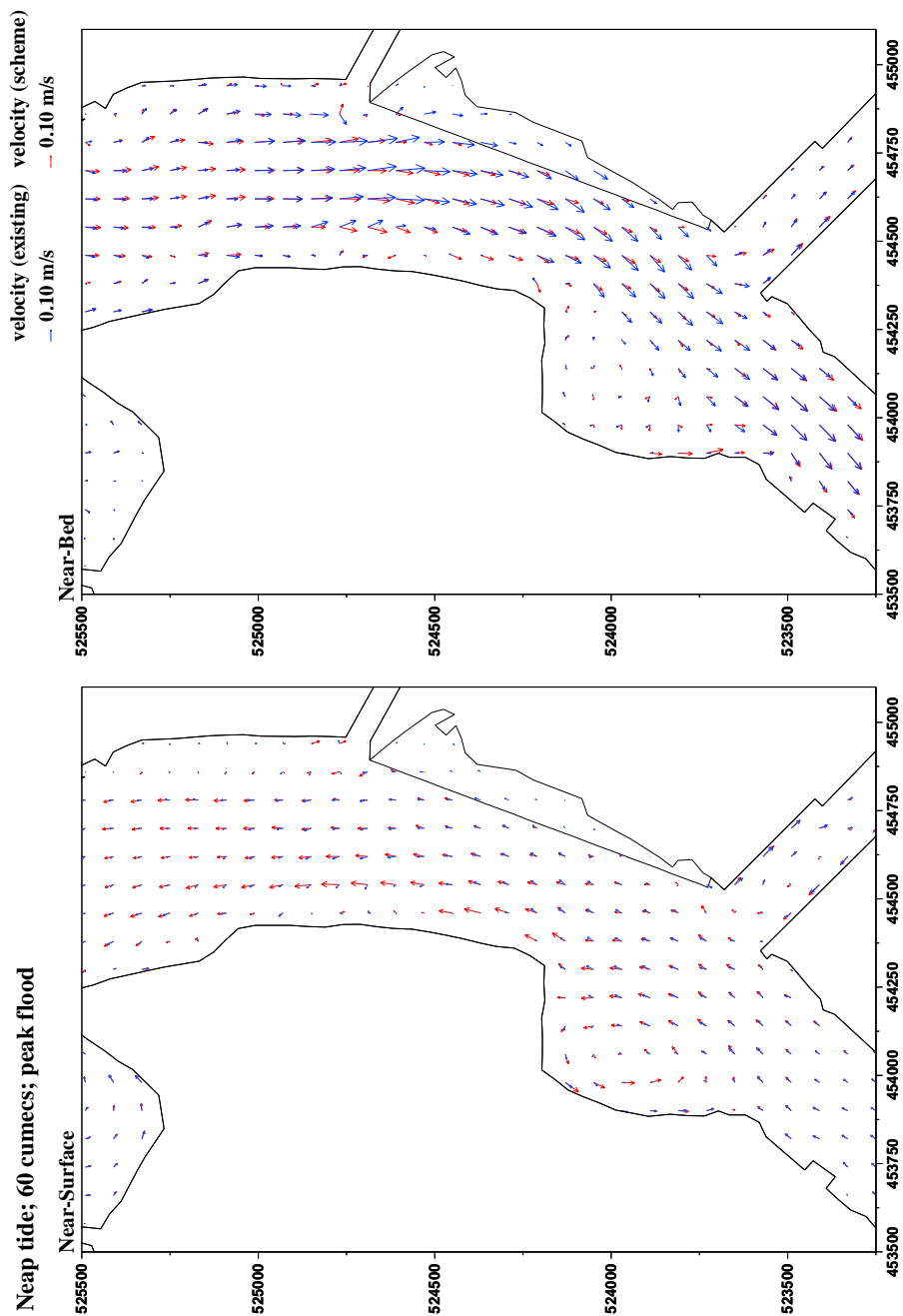


Figure 2.67 Wet neap conditions: flood velocity near surface and bed – existing, scheme

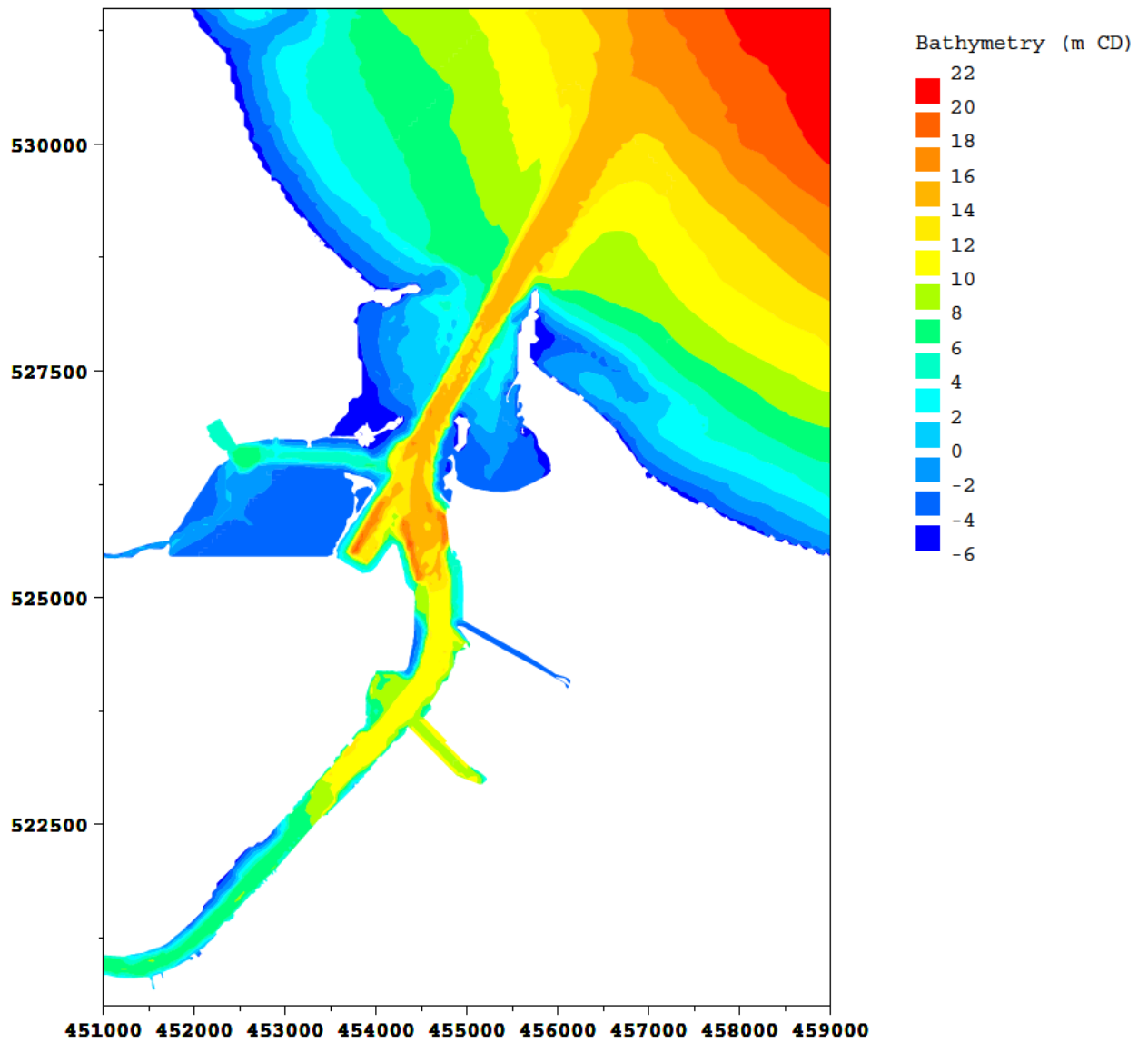


Figure 3.1 Model bathymetry – existing layout

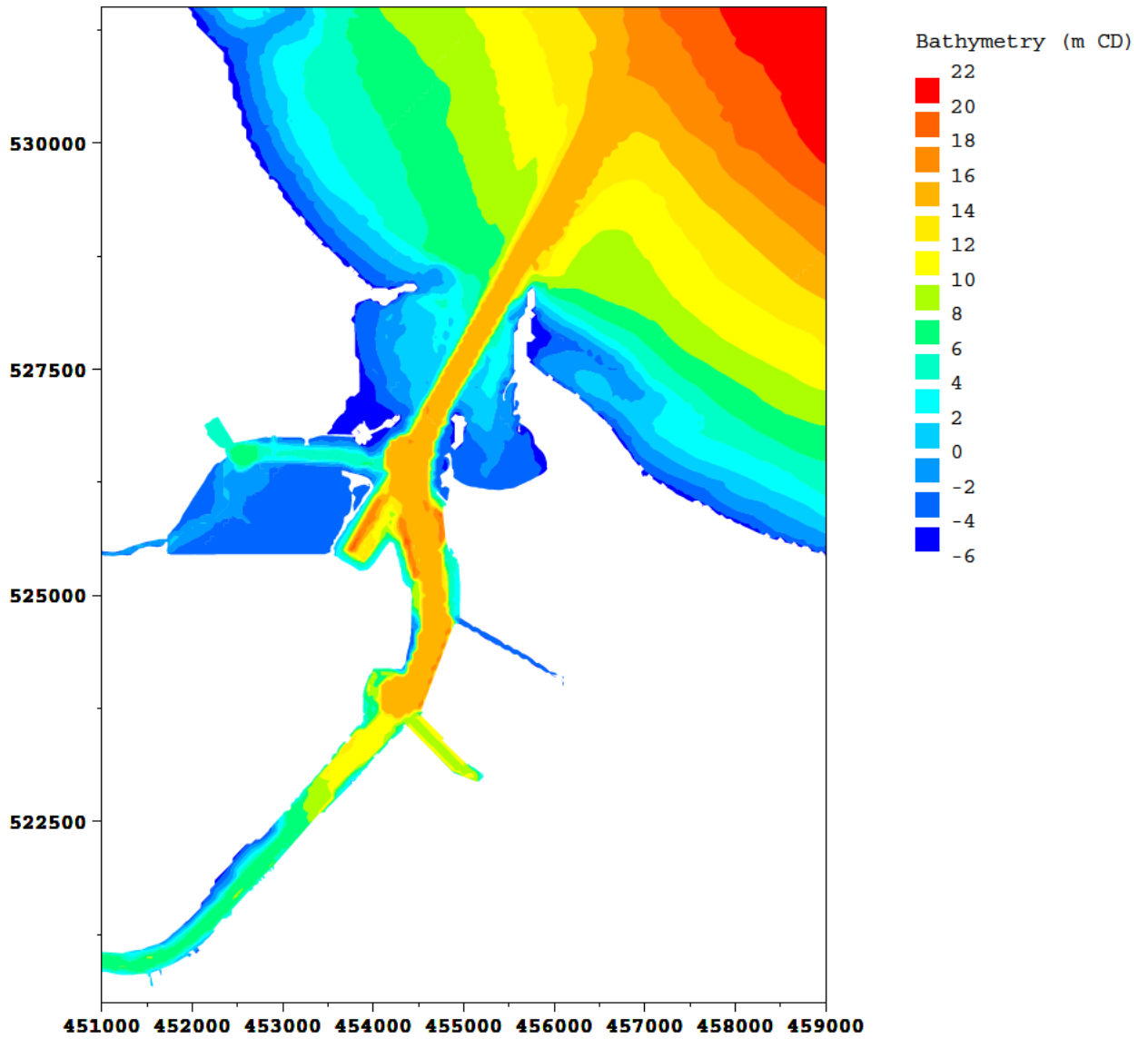


Figure 3.2 Model Bathymetry – proposed layout (mark on waverider buoy)

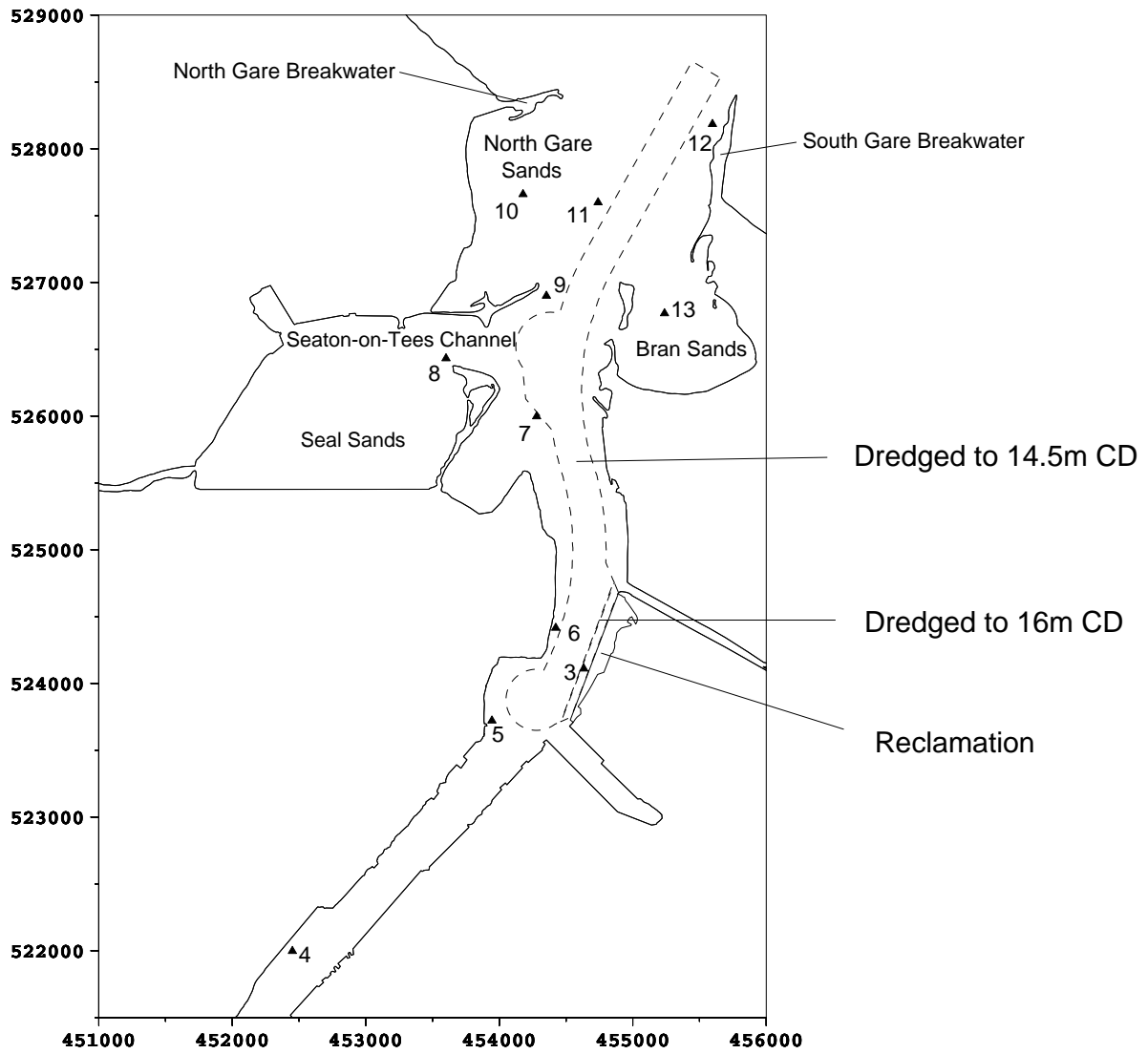


Figure 3.3 Model Layout – existing and proposed, map of output points

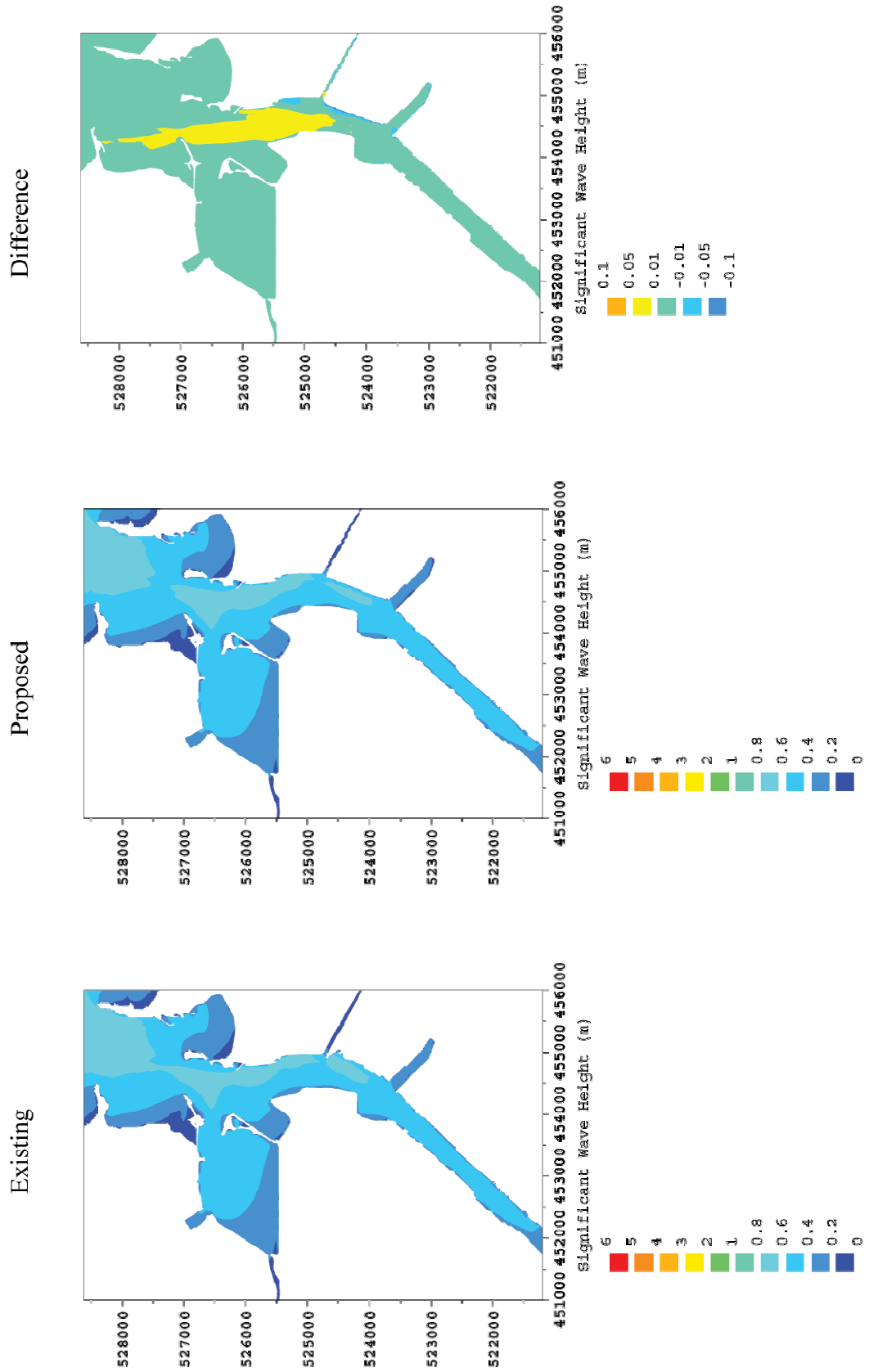


Figure 3.4 Model results: Significant wave height for 20 m/s winds from 225°N

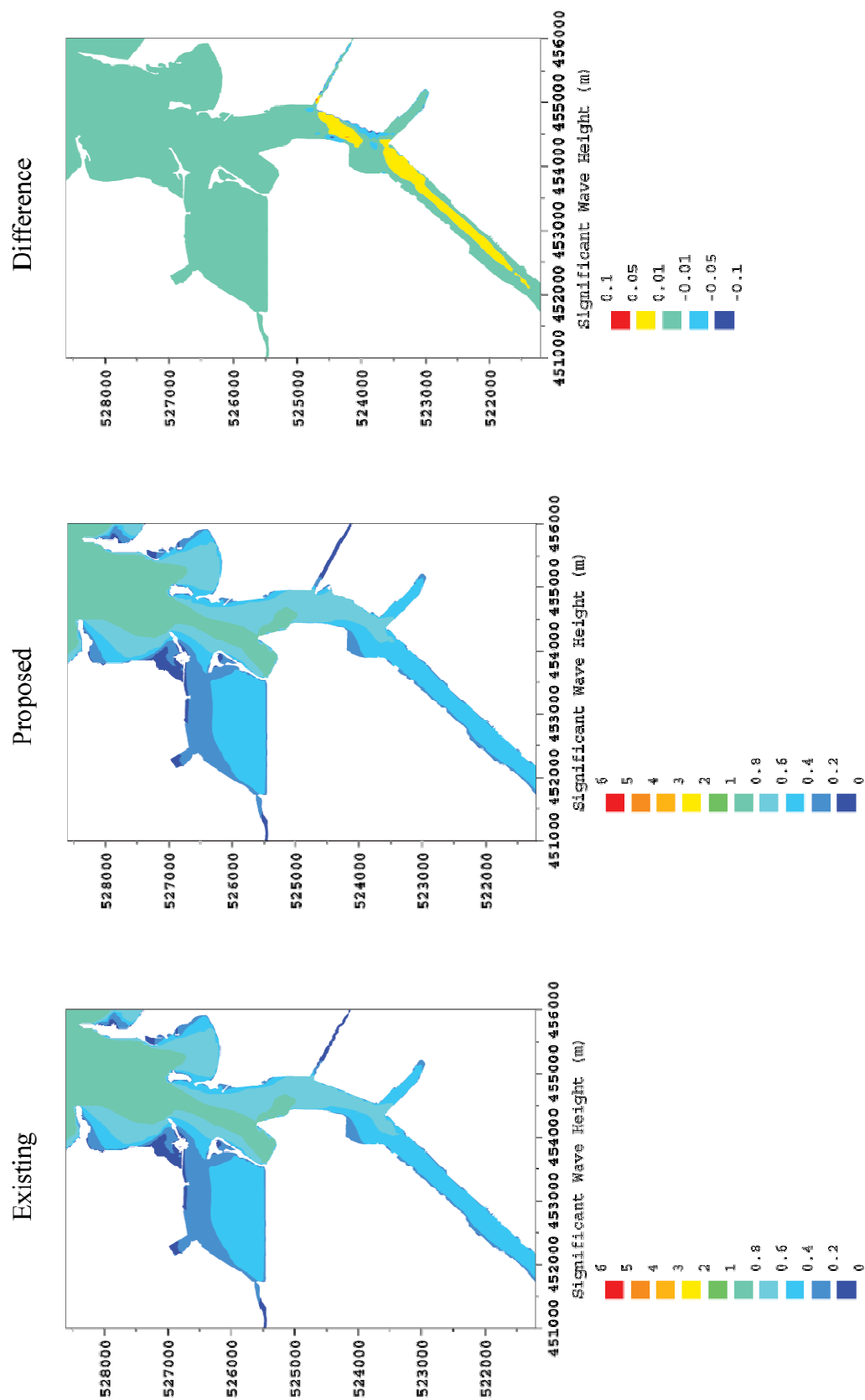


Figure 3.5 Model results: Significant wave height for 20 m/s winds from 0°N

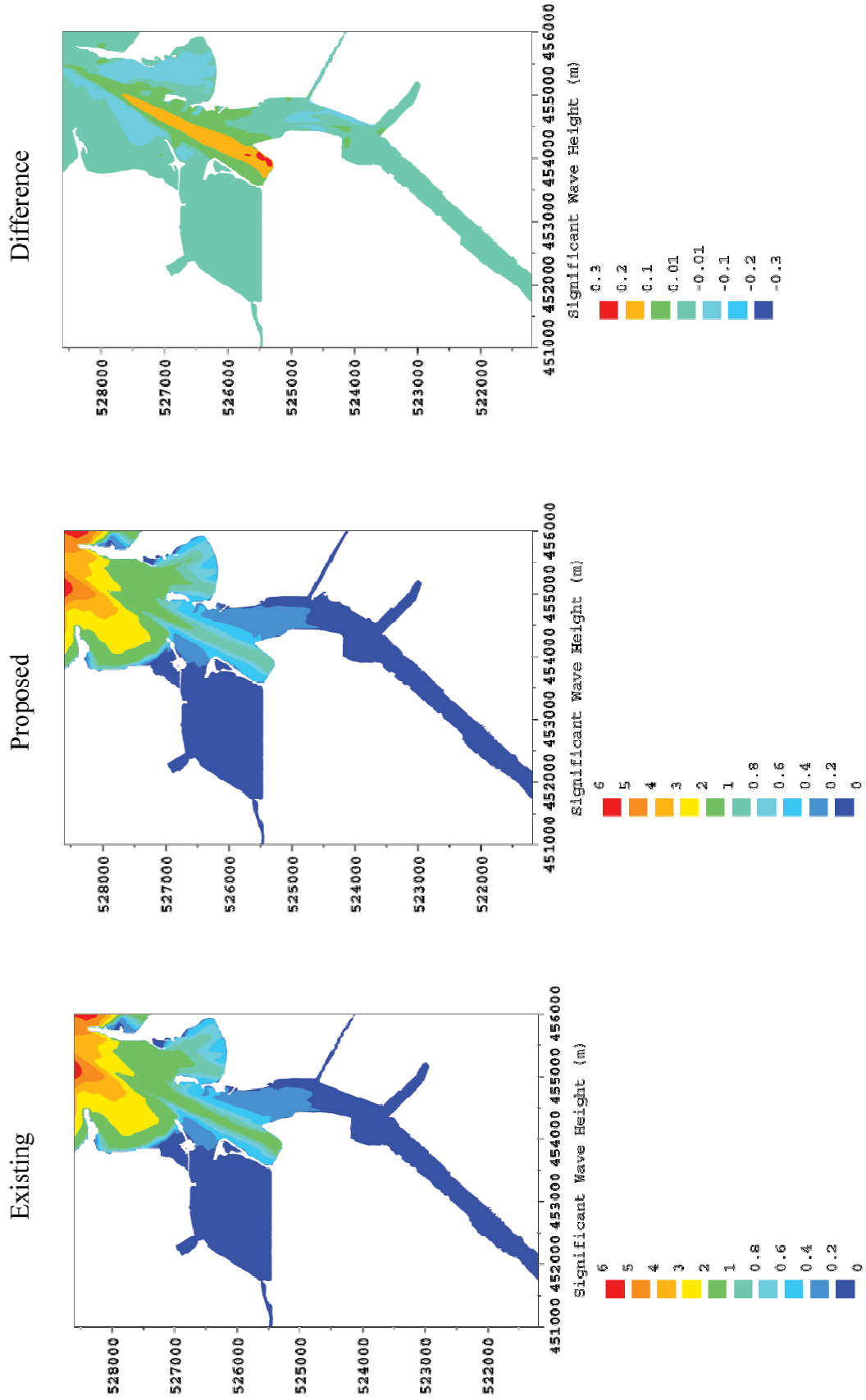


Figure 3.6 Model results: Significant wave height for 6m swell from 15°N

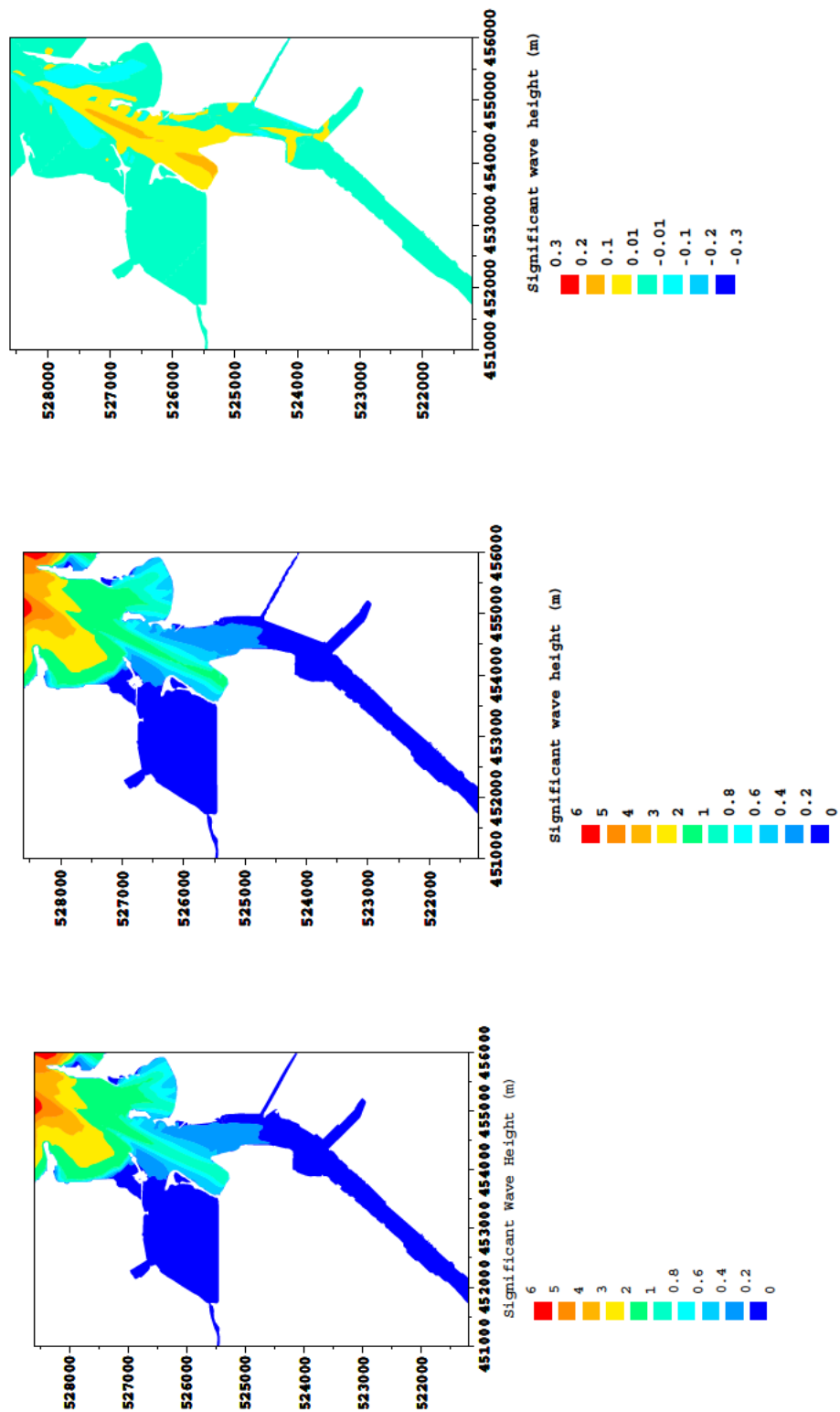


Figure 3.7 Model results: Significant wave height for 6m swell from 15°N with channel dredged to declared depth of -14.1m CD

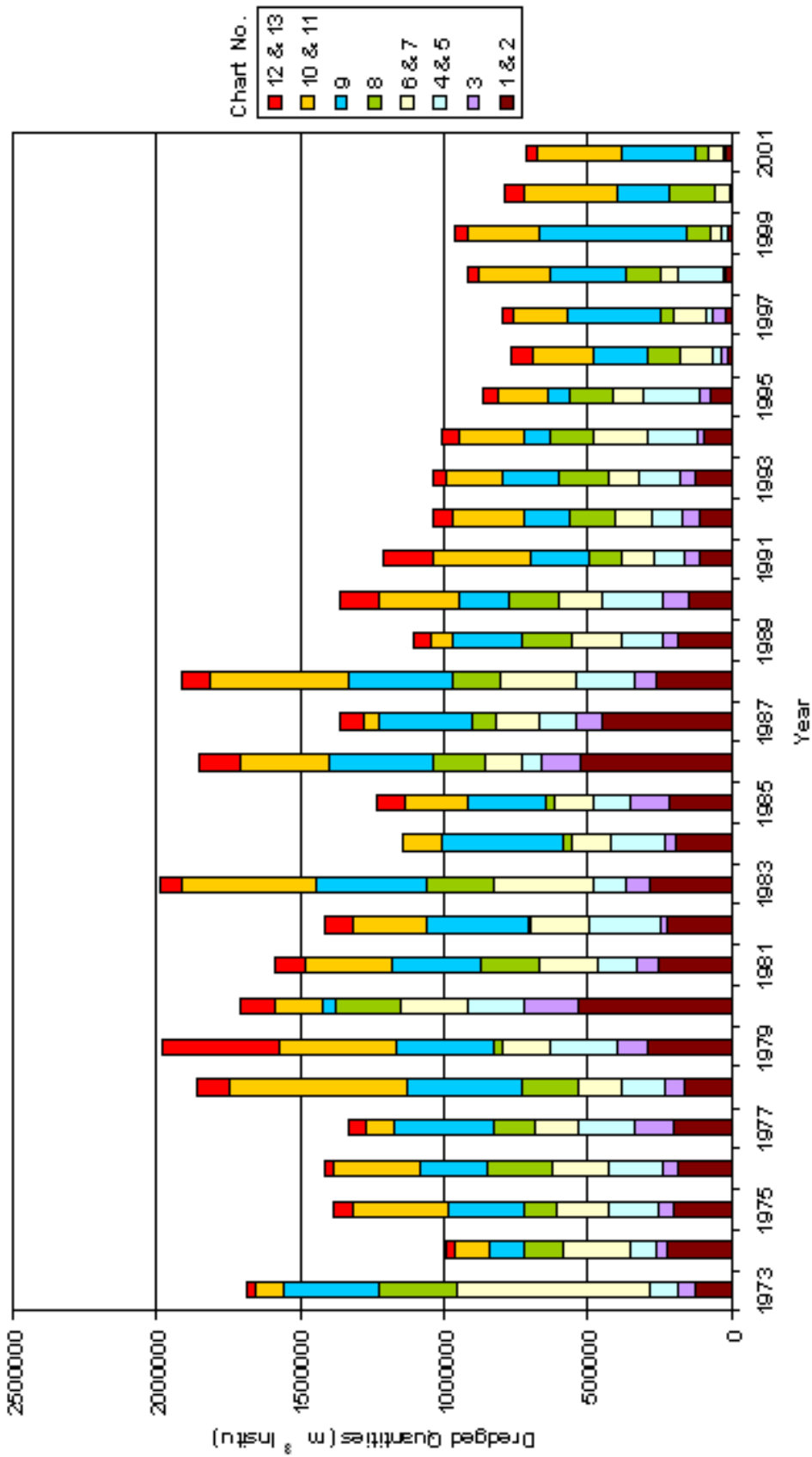


Figure 4.1 Dredged volumes for the period 1973 to 2001

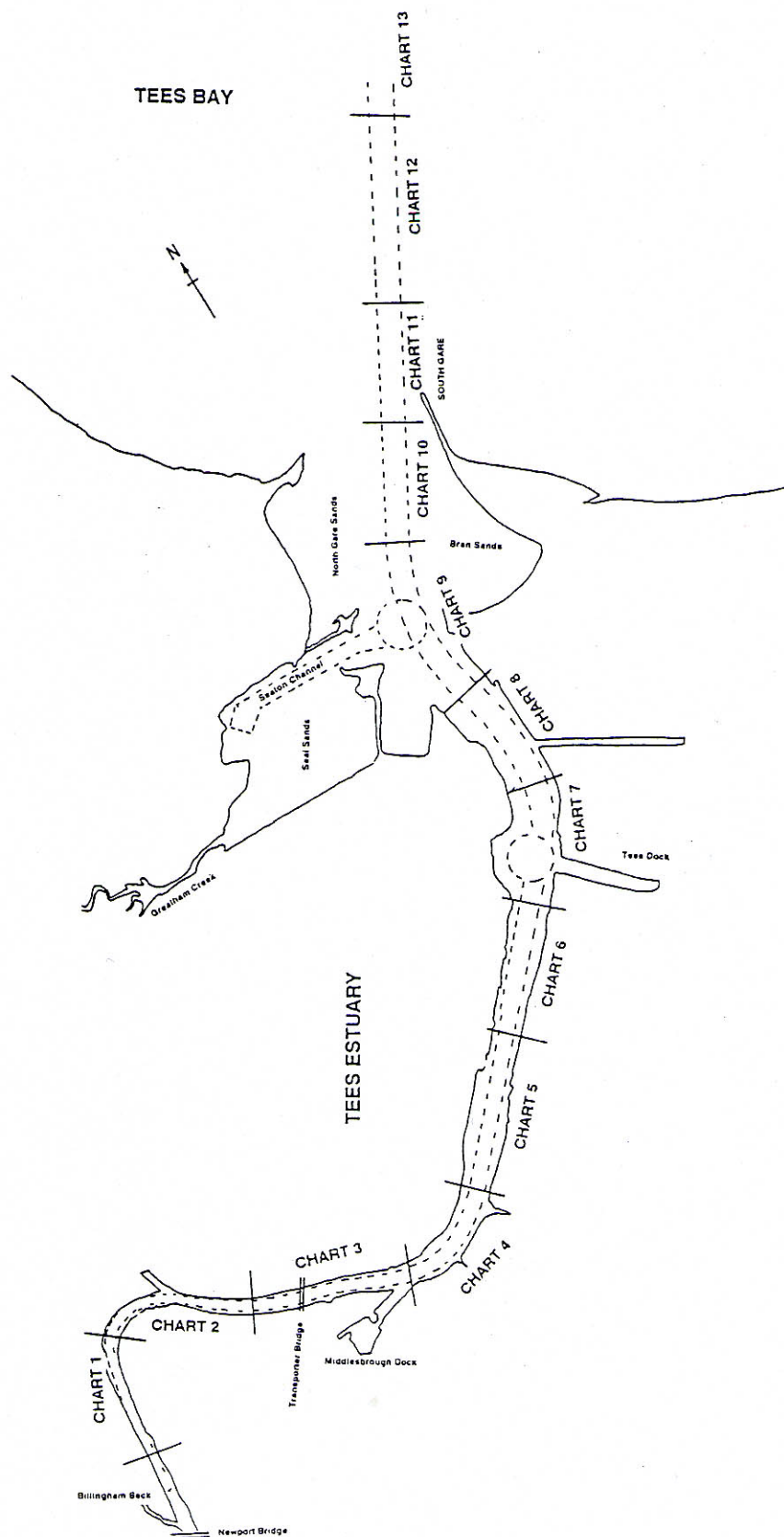


Figure 4.2 Chart areas

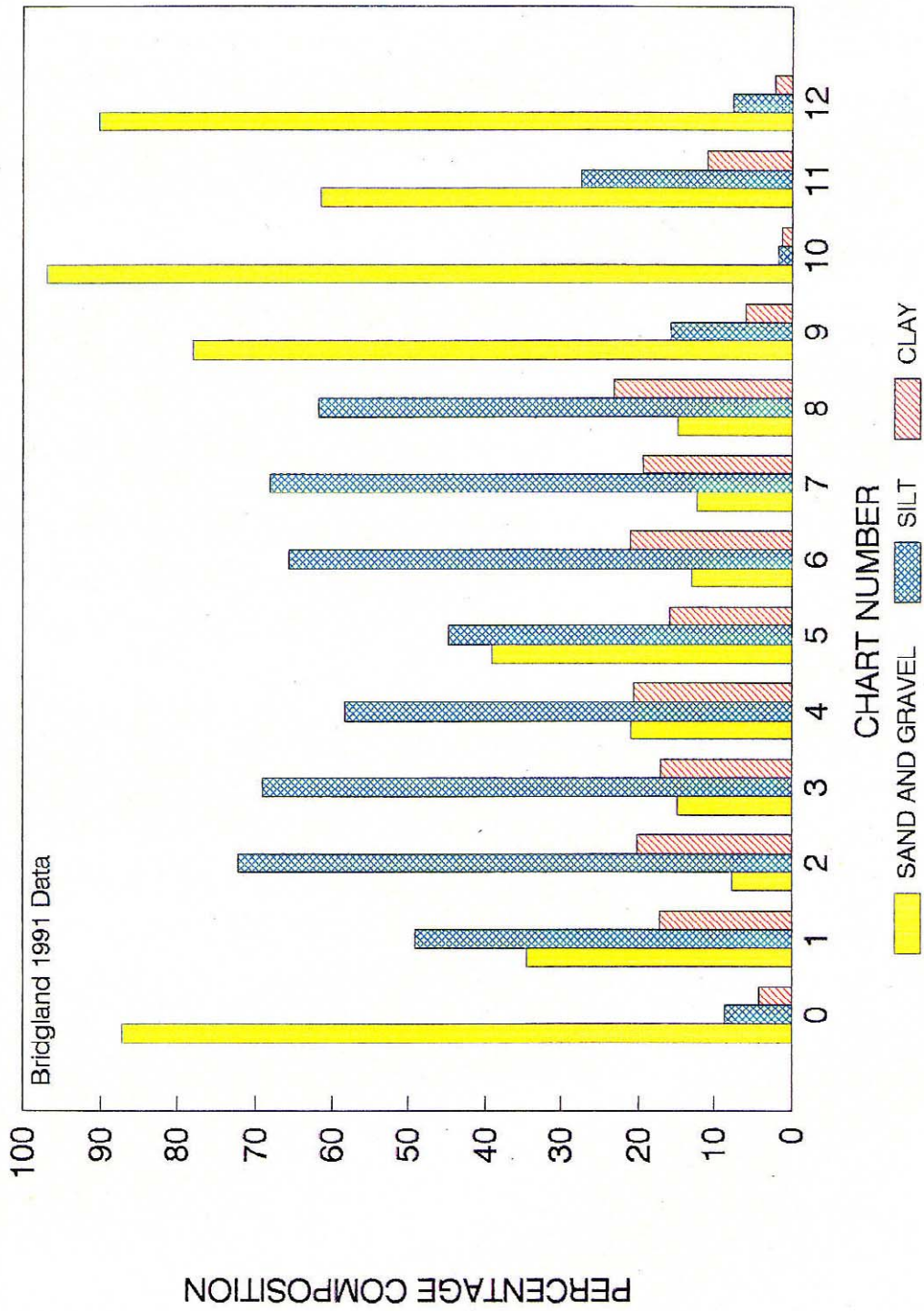


Figure 4.3 Particle size distribution, 1991 data (after Bridgland (1991))

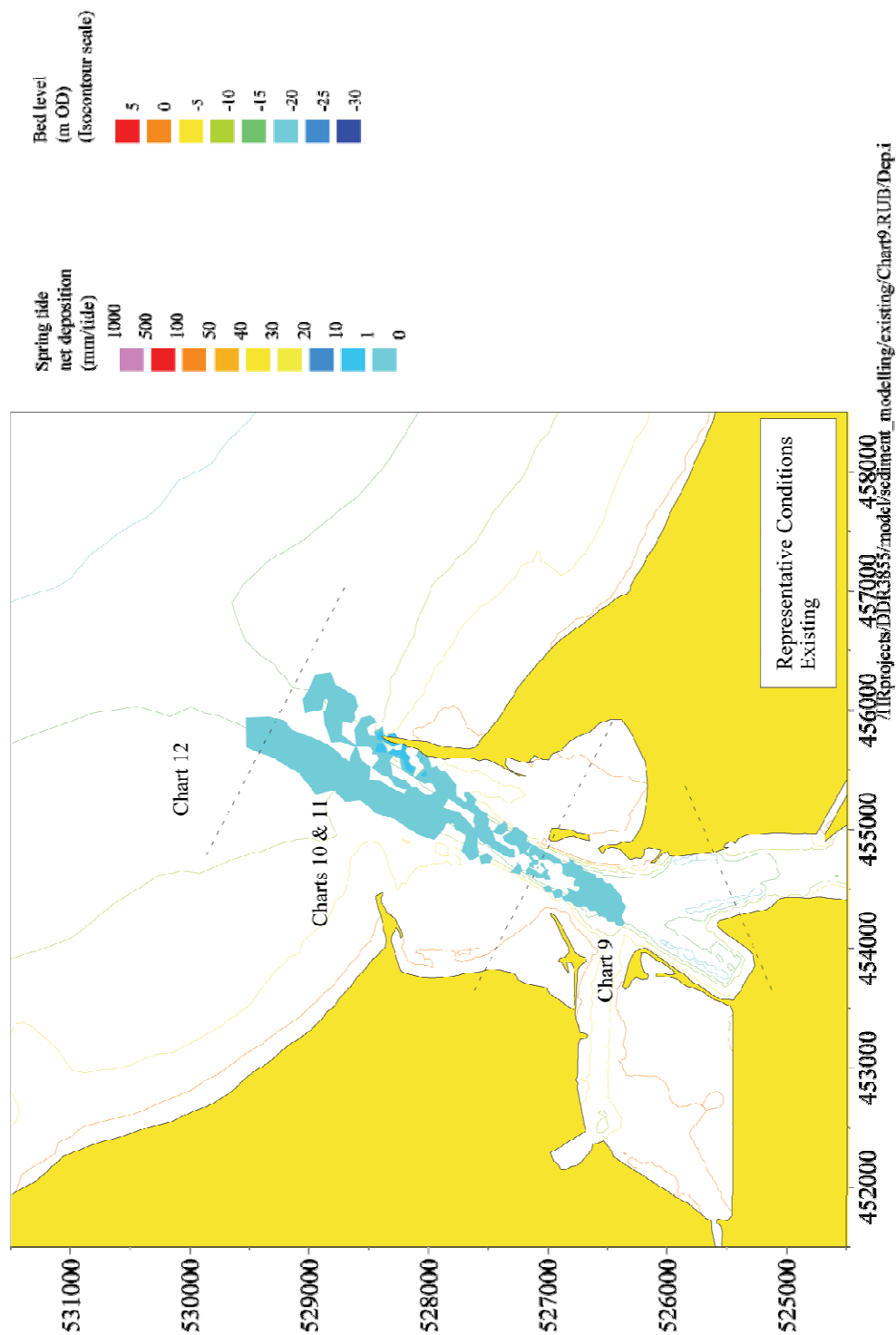


Figure 4.4 Net tidal deposition for existing condition under representative wave conditions

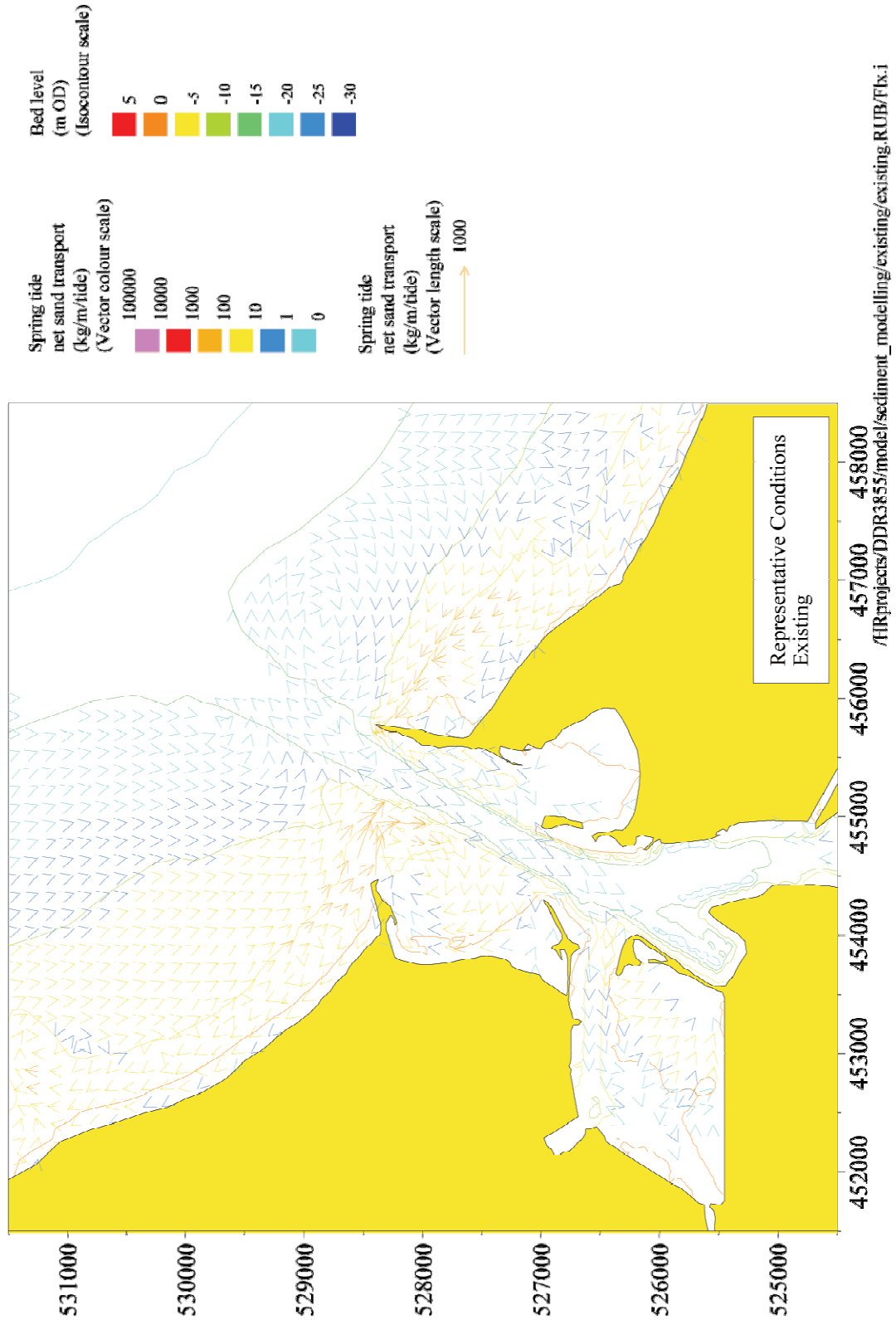


Figure 4.5 Net tidal sediment transport for existing condition under representative wave conditions

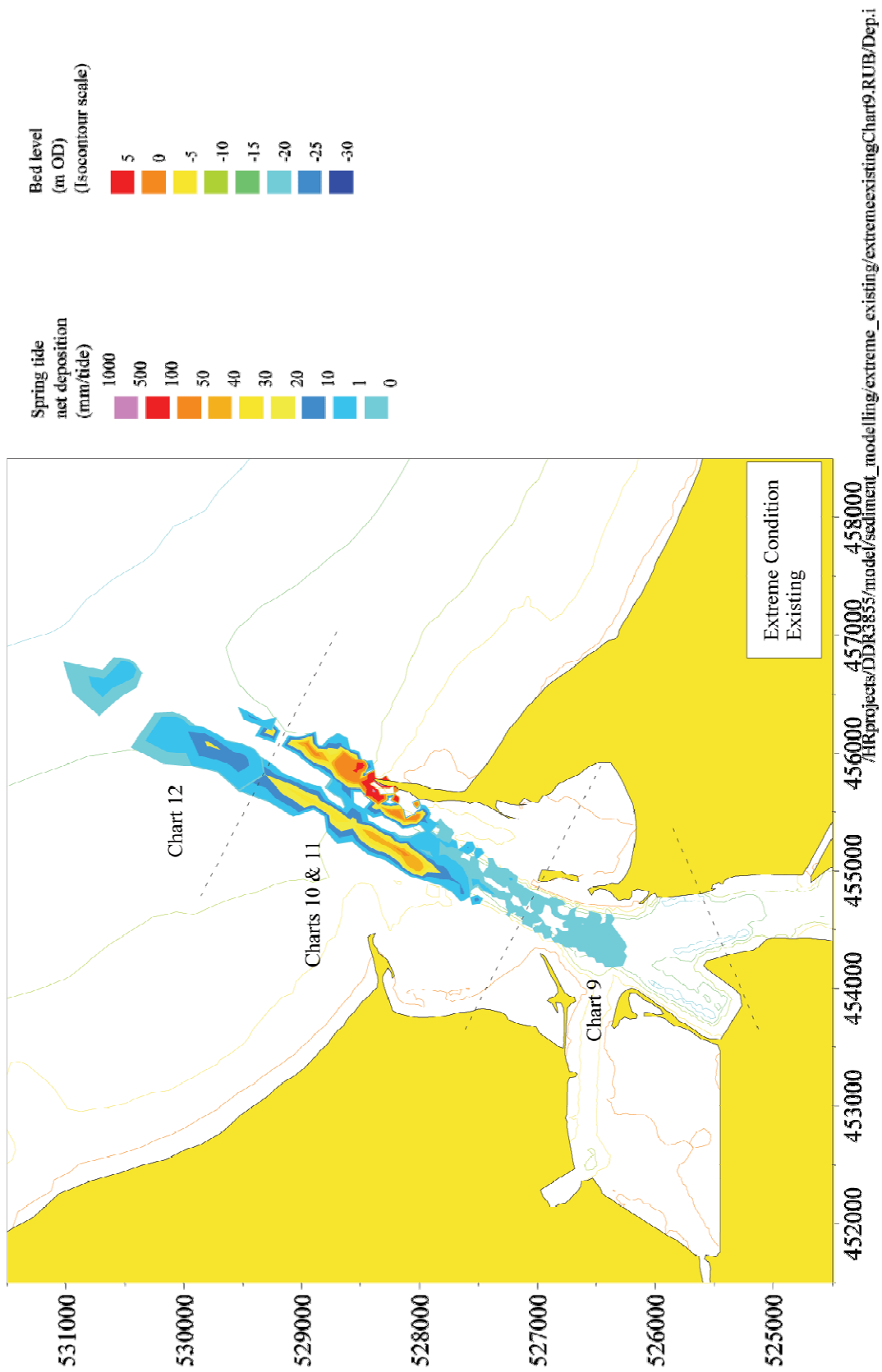


Figure 4.6 Net tidal deposition for existing condition under an extreme wave condition

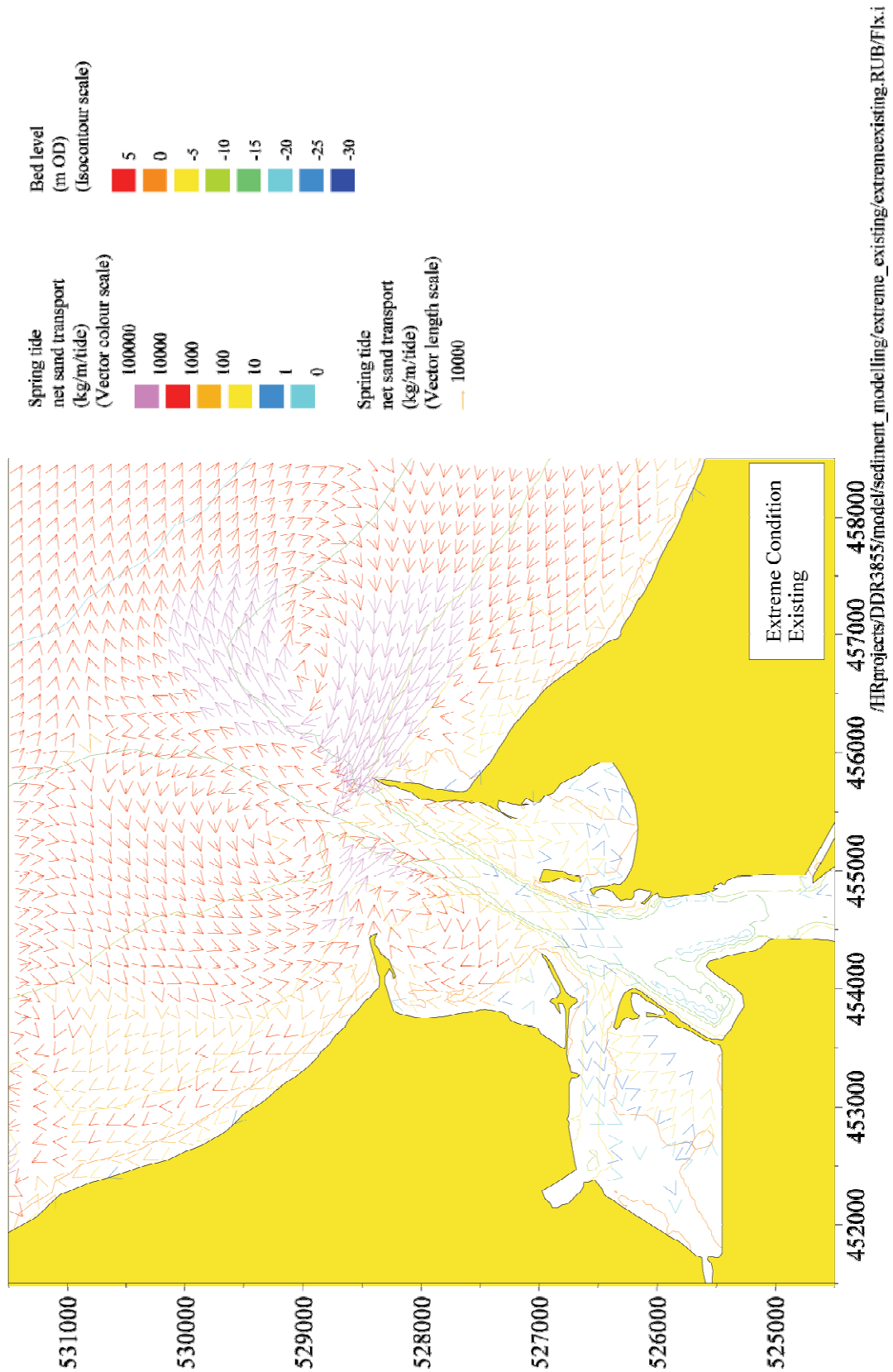


Figure 4.7 Net tidal sediment transport for existing condition under an extreme wave condition

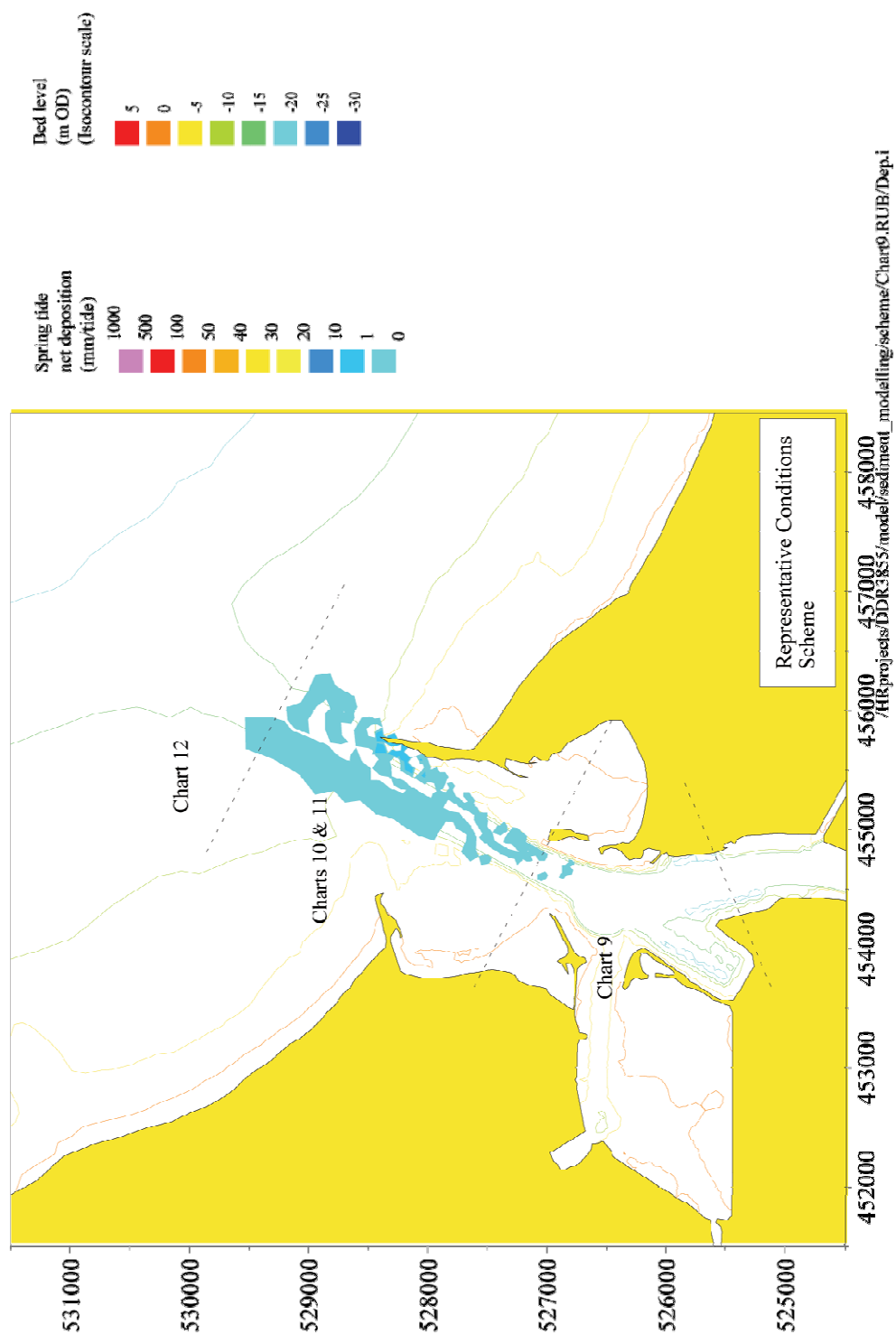


Figure 4.8 Net tidal deposition for proposed scheme under representative wave conditions

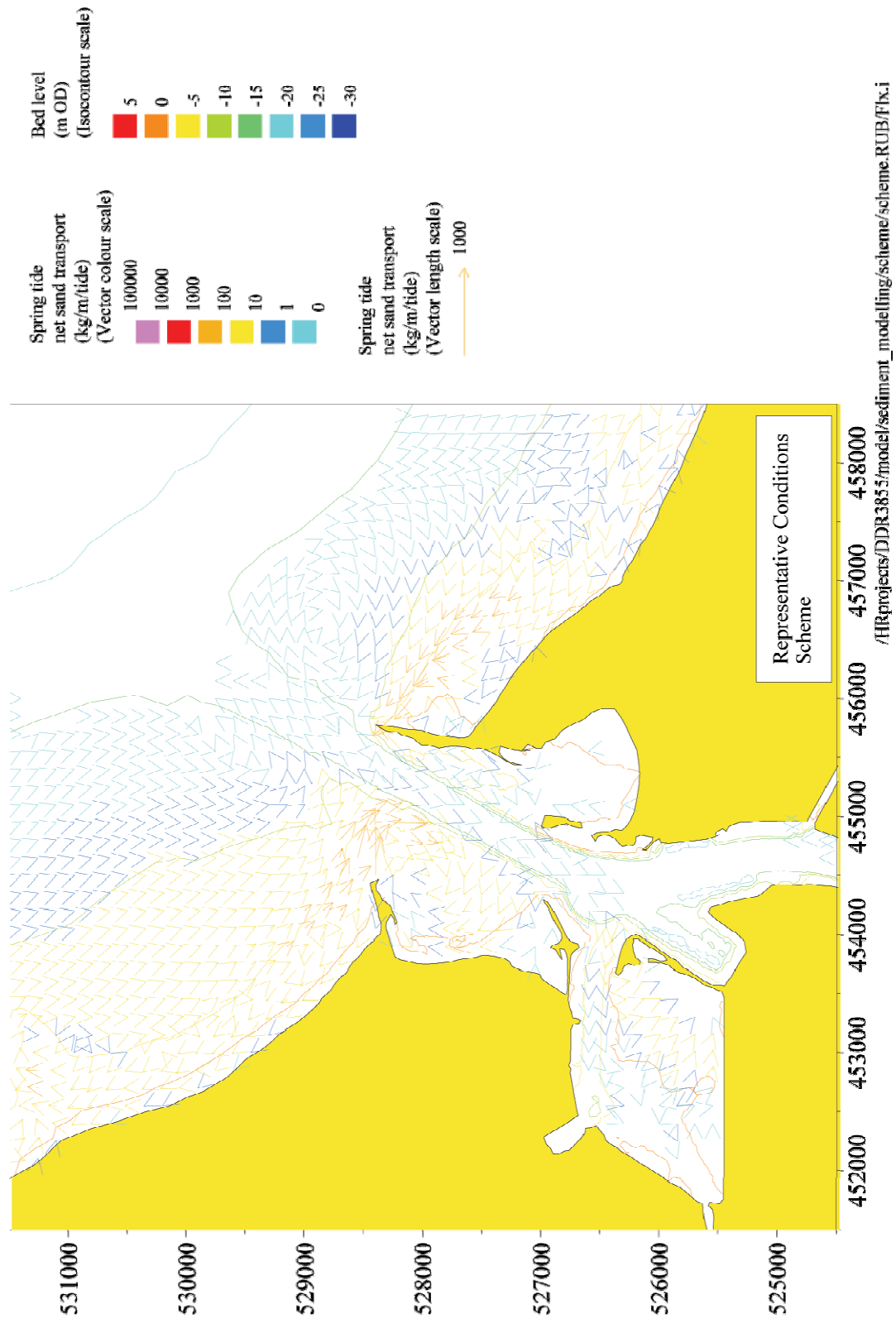


Figure 4.9 Net tidal sediment transport for proposed scheme under representative wave conditions

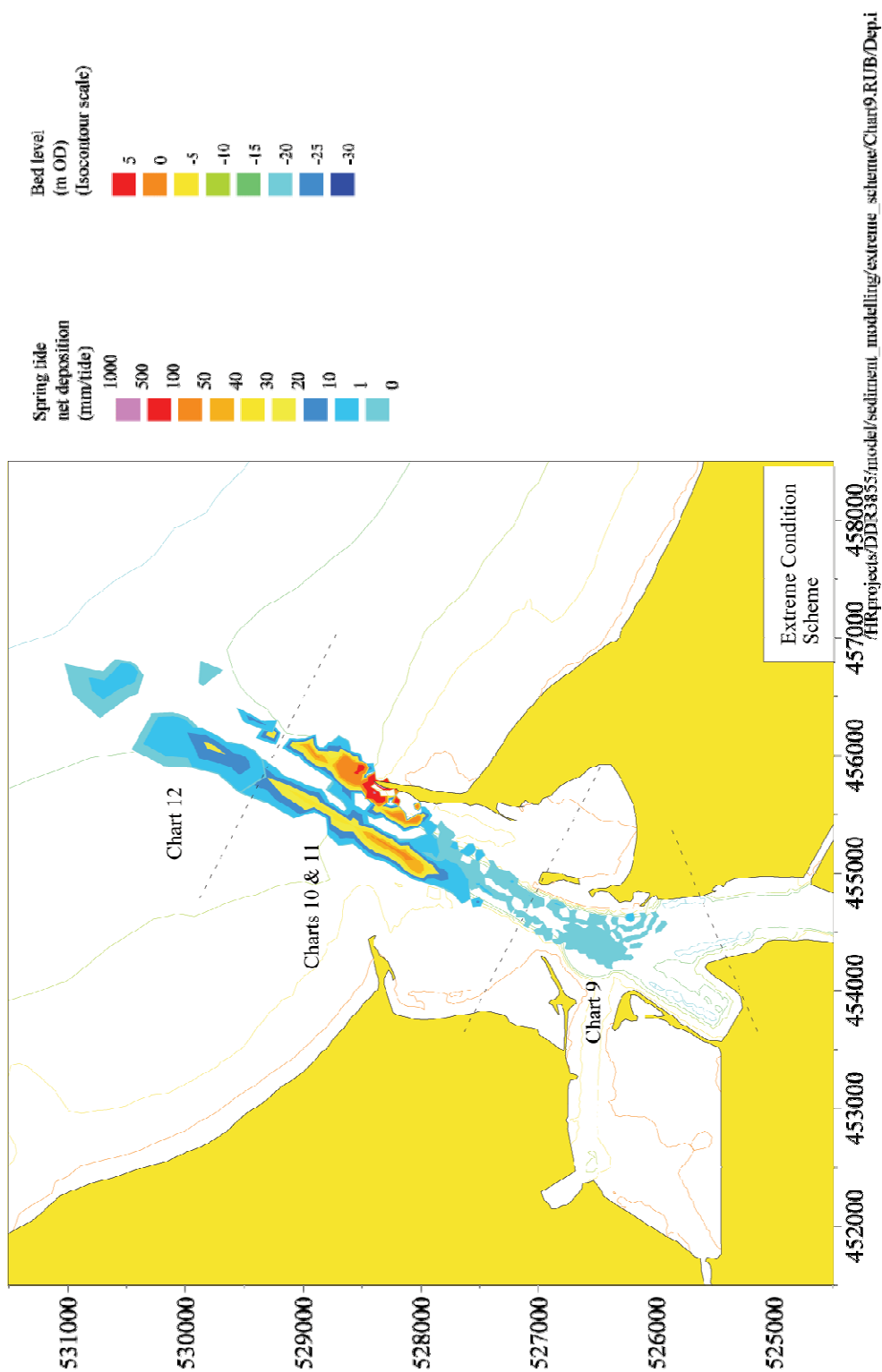


Figure 4.10 Net tidal deposition for proposed scheme under an extreme wave condition

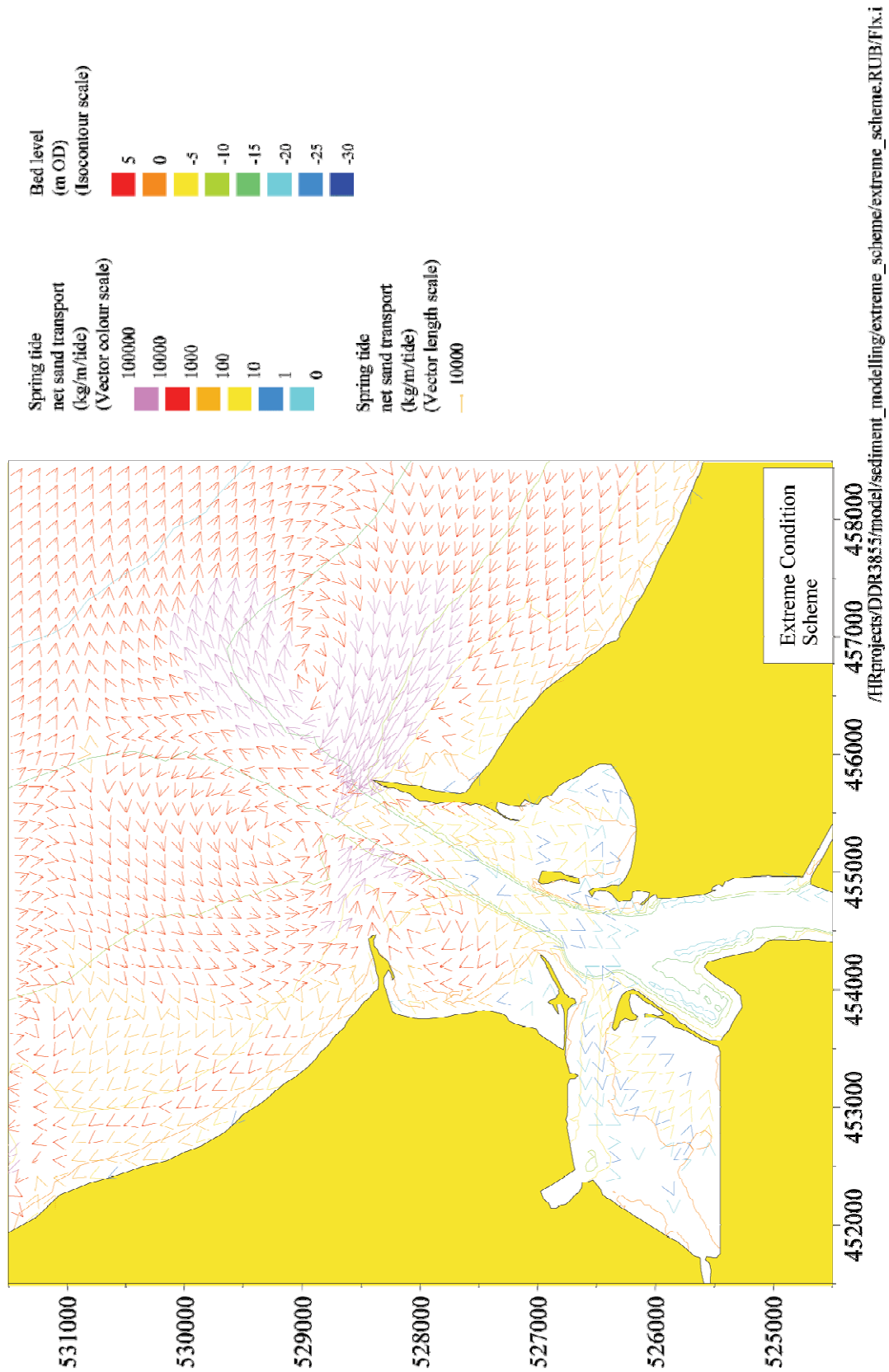


Figure 4.11 Net tidal sediment transport for proposed scheme under an extreme wave condition

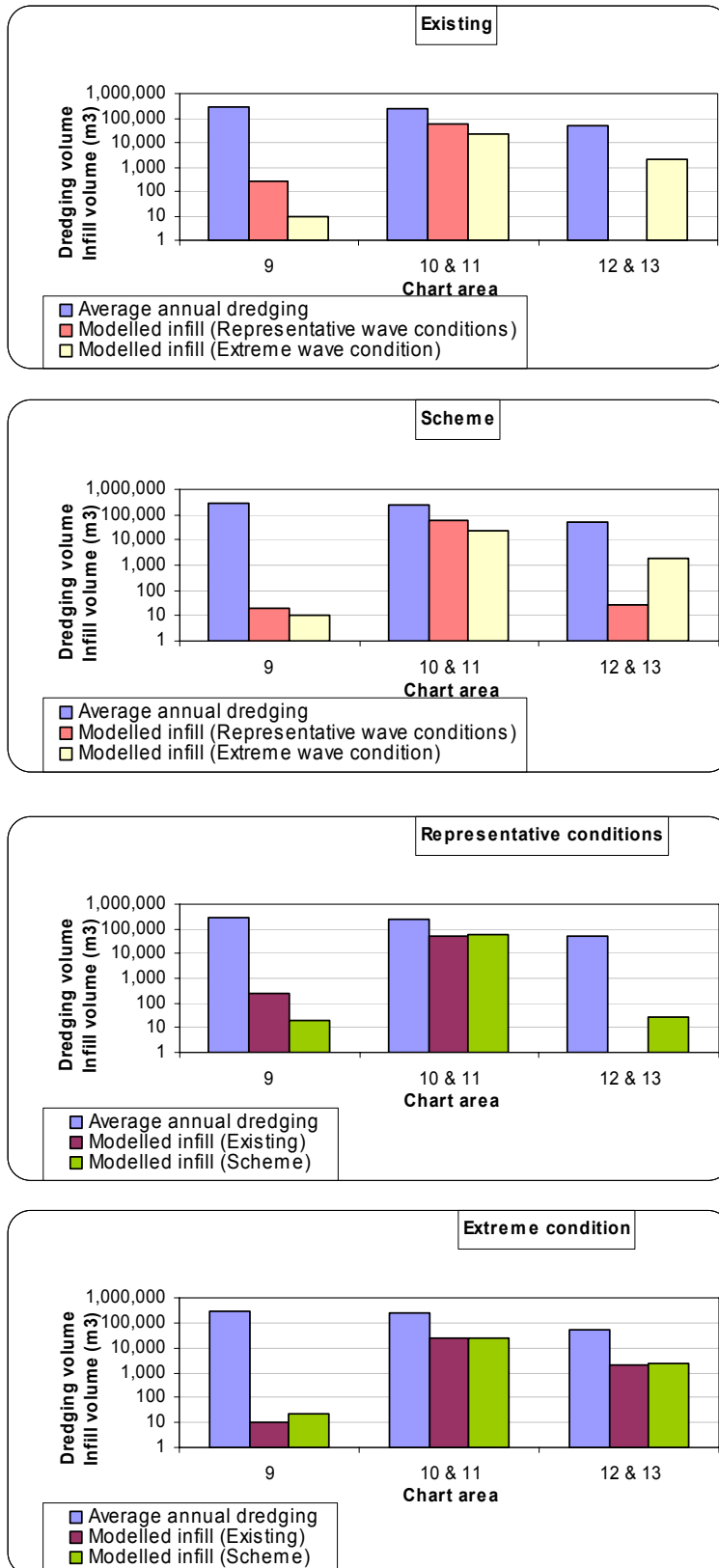


Figure 4.12 Modelled channel infill volumes comparison

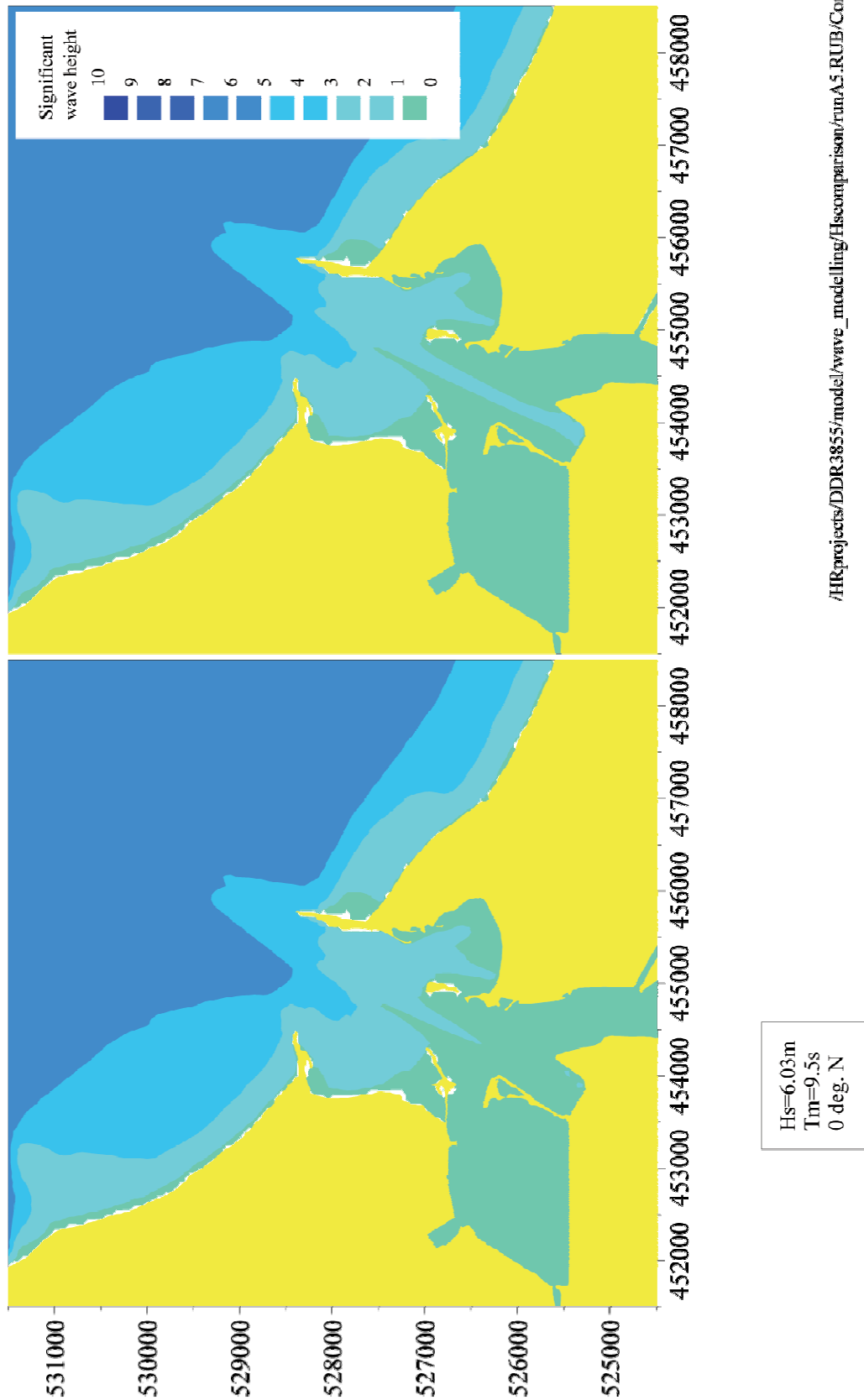


Figure 4.13 Significant wave height for existing and scheme. Offshore wave conditions $H_s=6.03$, $T_m=9.5s$, 0° N

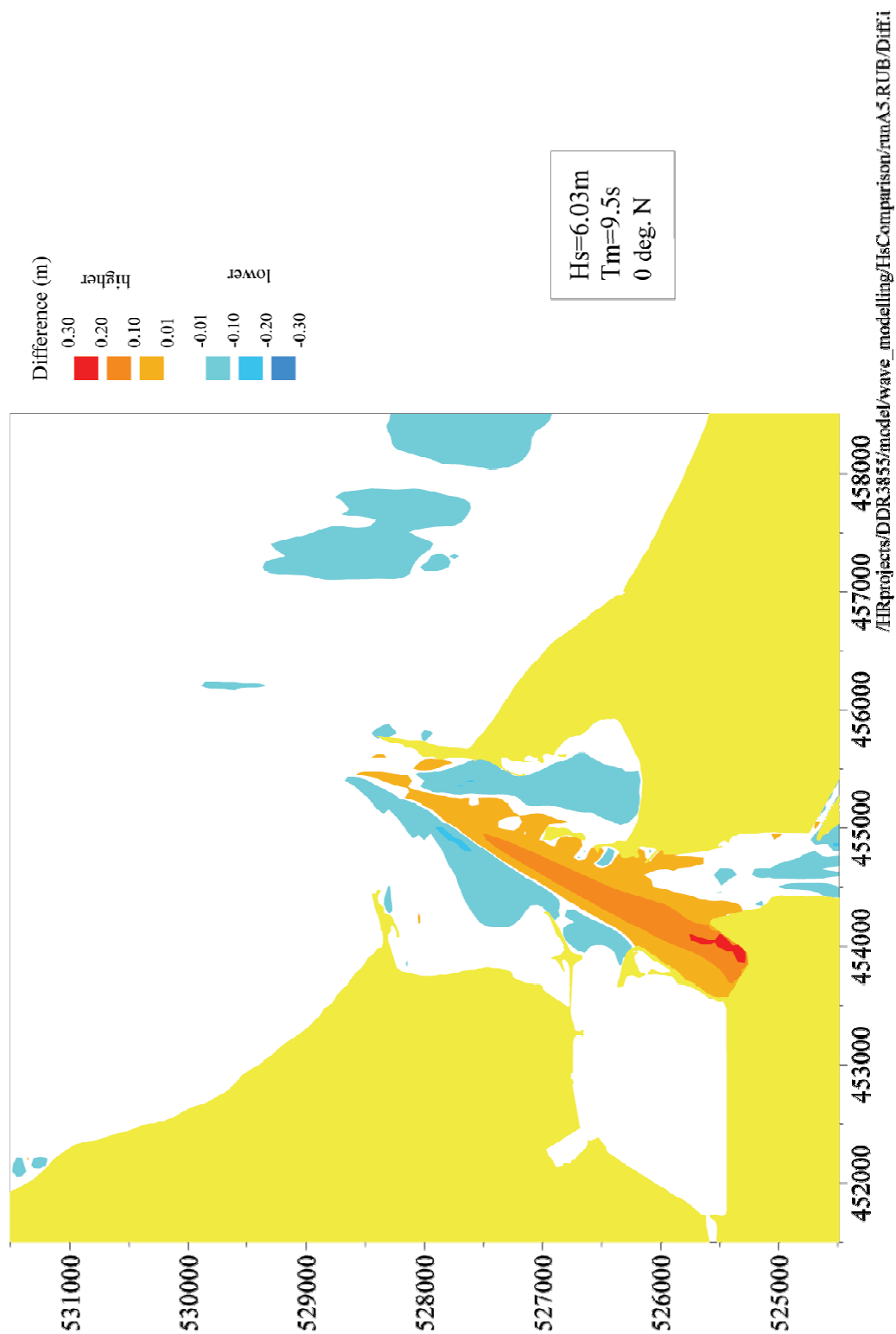


Figure 4.14 Significant wave height differences. Offshore wave conditions $H_s=6.03$, $T_m=9.5s$, $0^\circ N$

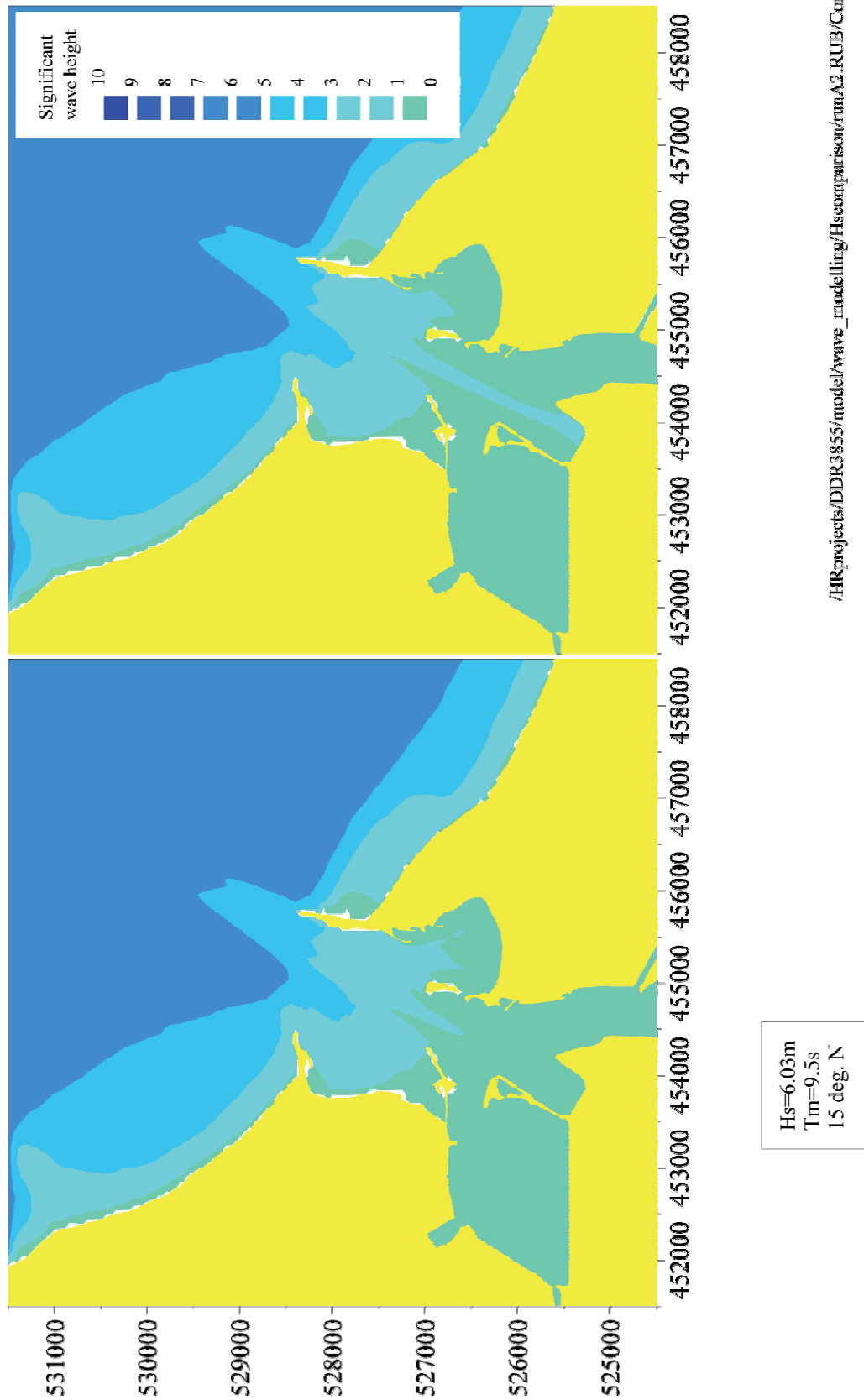


Figure 4.15 Significant wave height for existing and scheme. Offshore wave conditions $H_s=6.03$, $T_m=9.5\text{s}$, 15°N

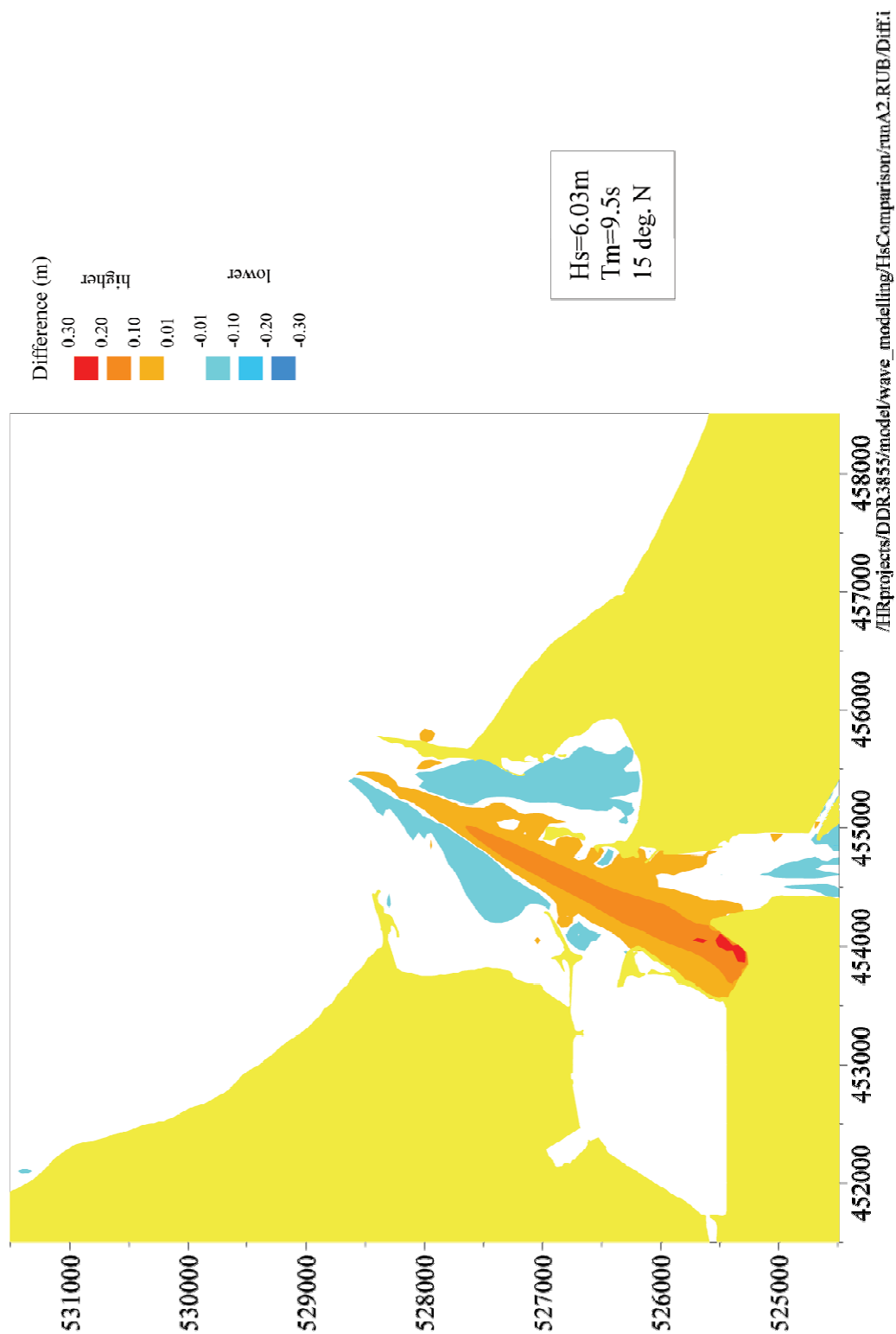


Figure 4.16 Significant wave height differences. Offshore wave conditions $H_s=6.03$, $T_m=9.5s$, $15^\circ N$

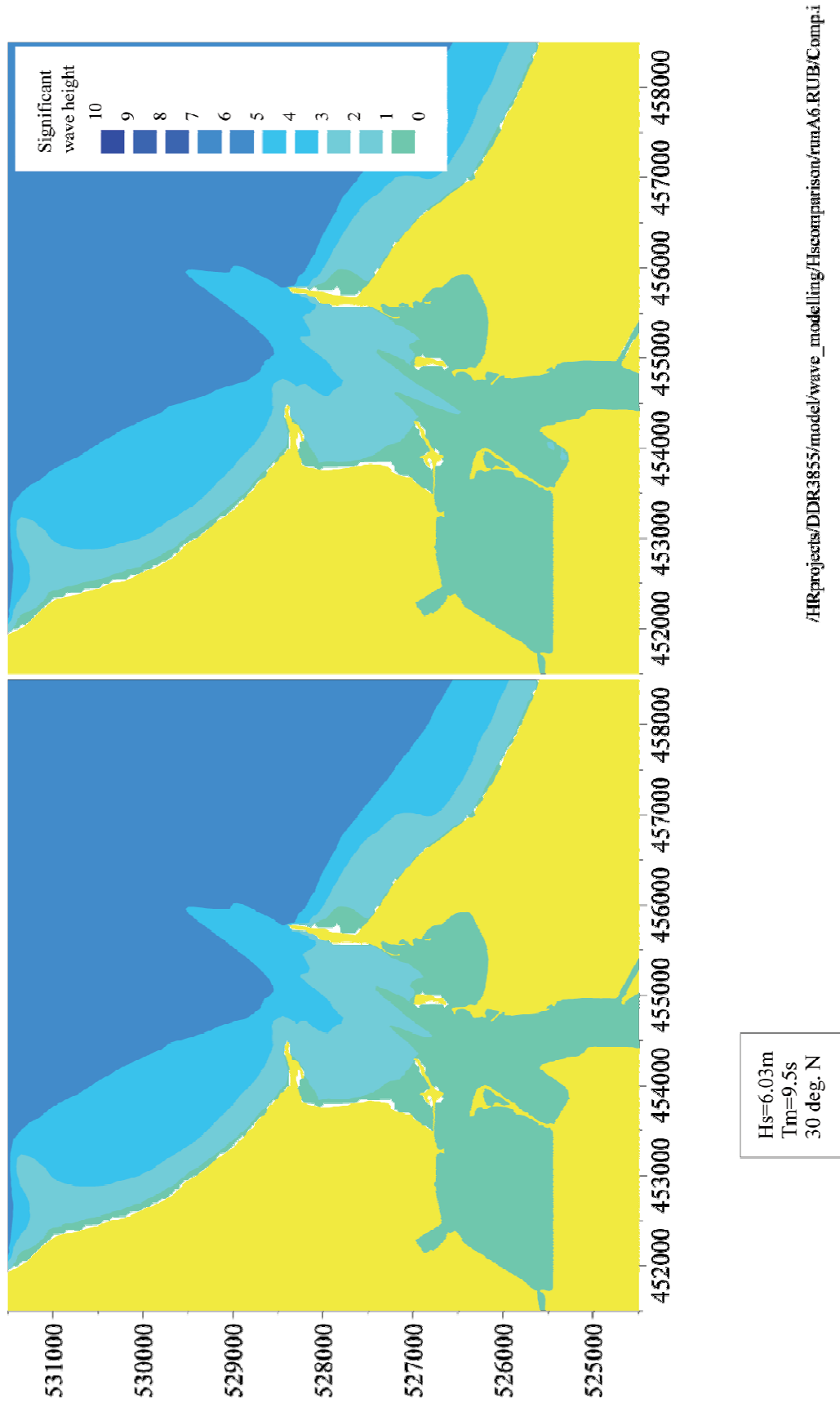


Figure 4.17 Significant wave height for existing and scheme. Offshore wave conditions $H_s=6.03$, $T_m=9.5s$, $30^\circ N$

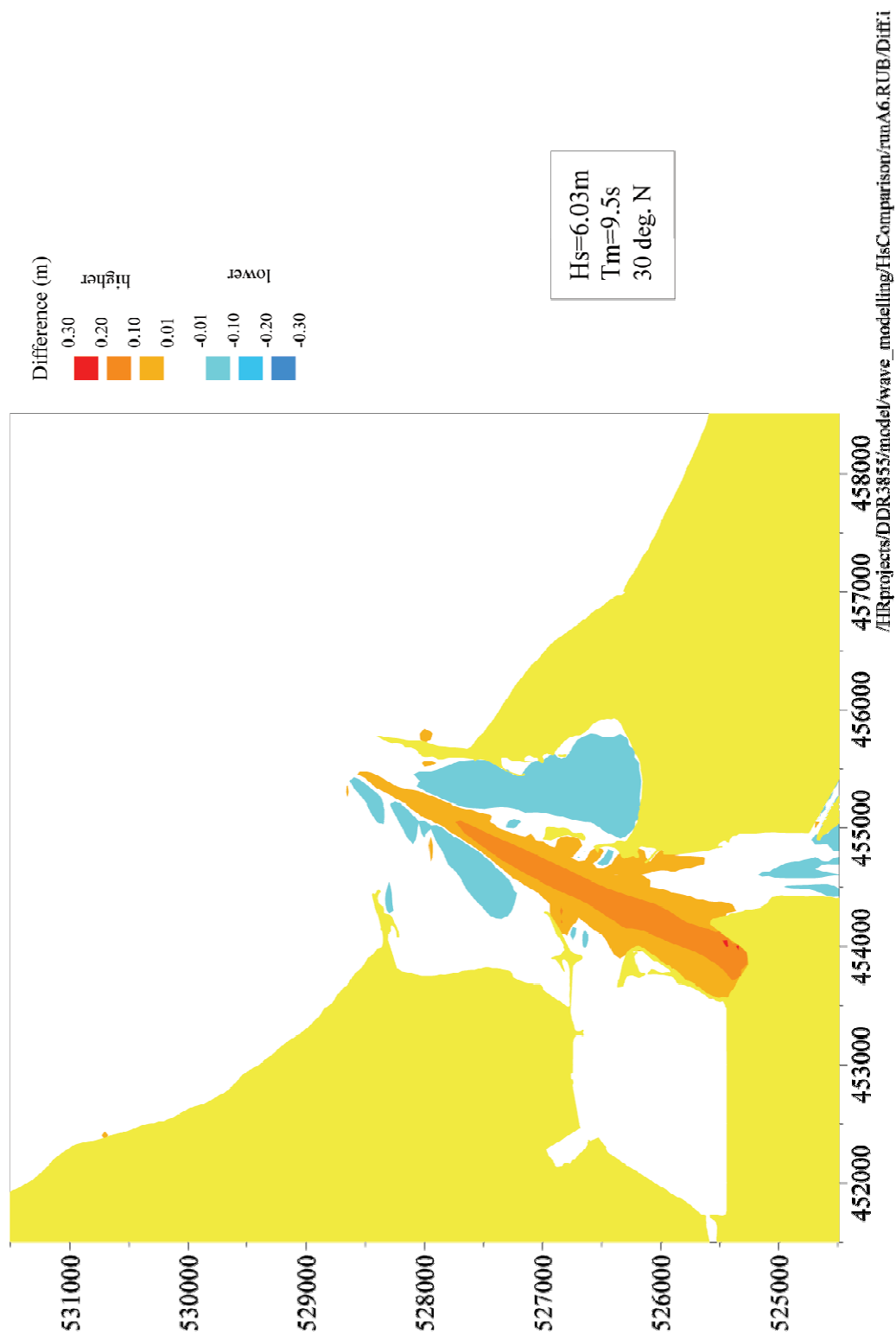


Figure 4.18 Significant wave height differences. Offshore wave conditions $H_s=6.03$, $T_m=9.5s$, $30^\circ N$

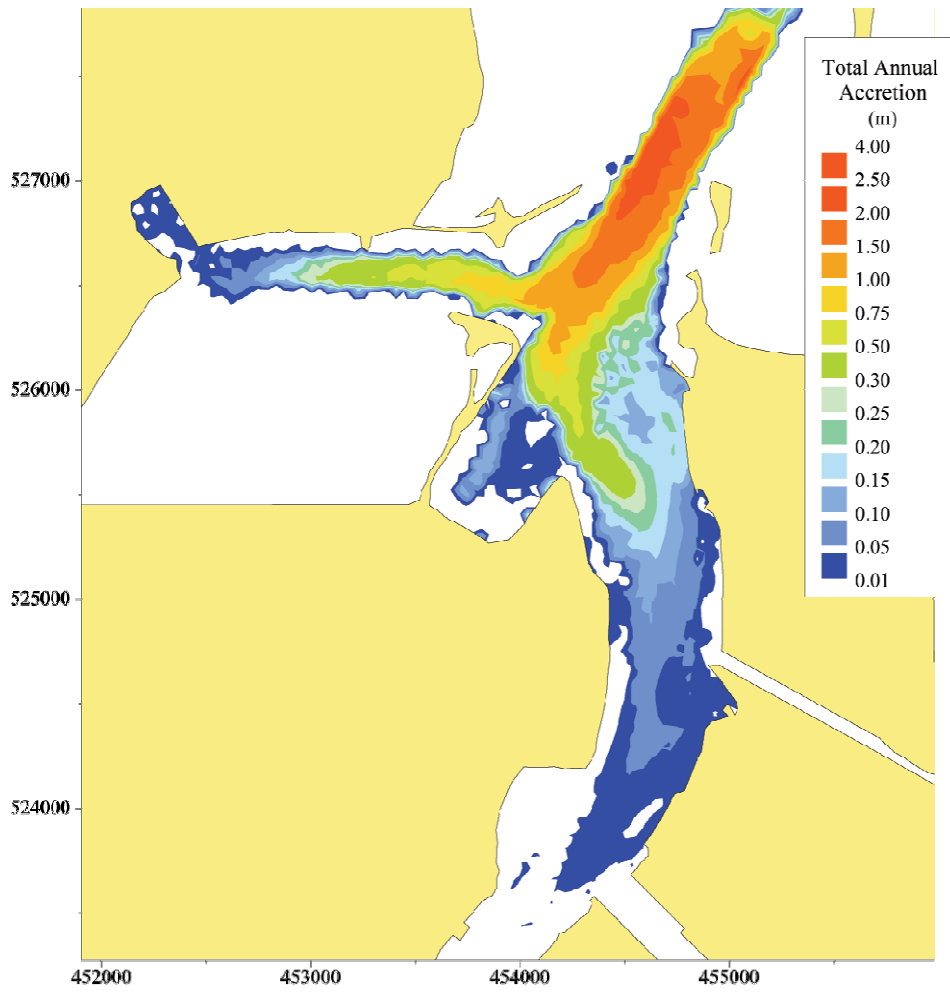


Figure 4.19 Simulated total annual accretion depths for existing conditions

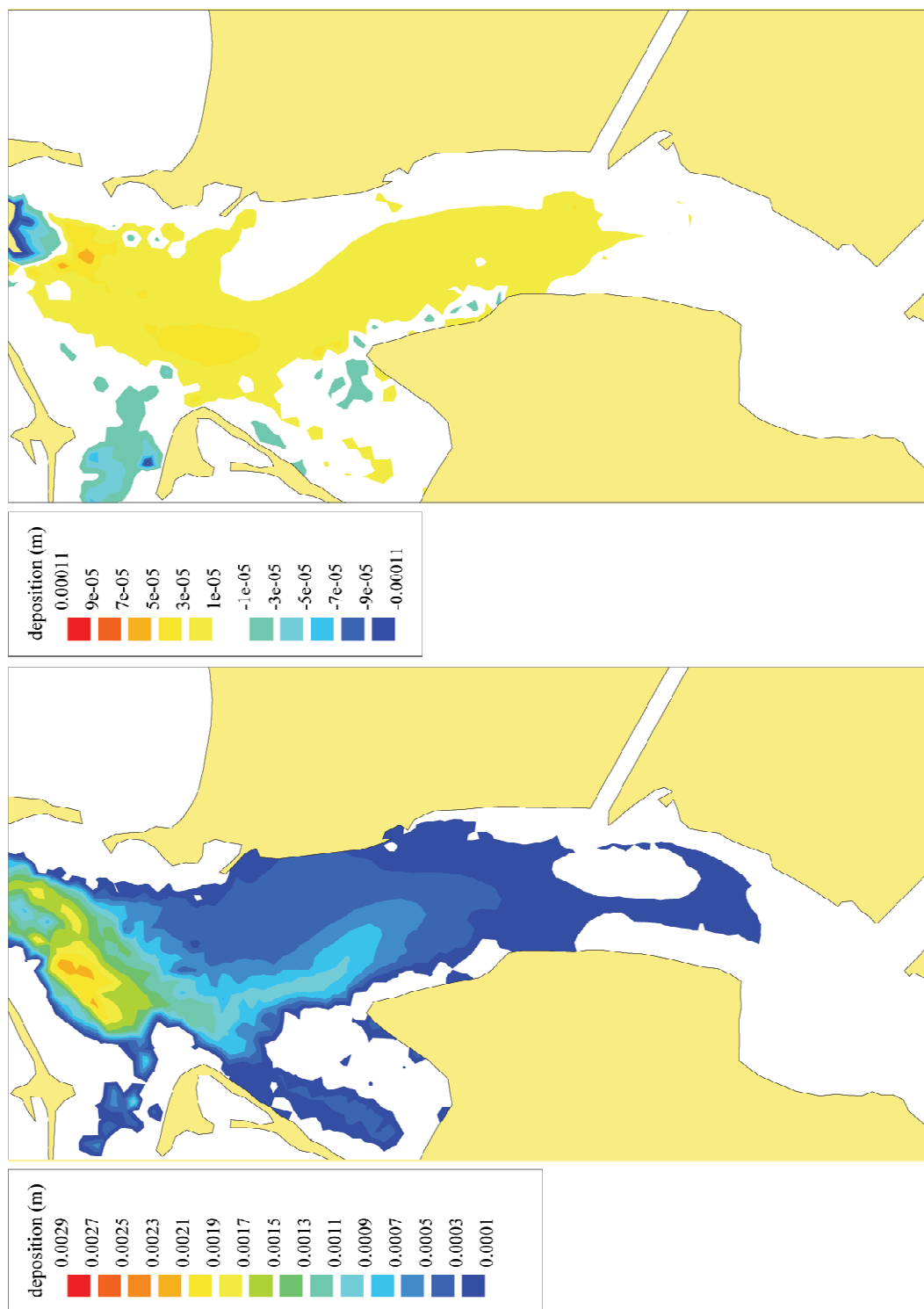


Figure 4.20 Sensitivity of accretion predictions to resuspension processes in the Estuary

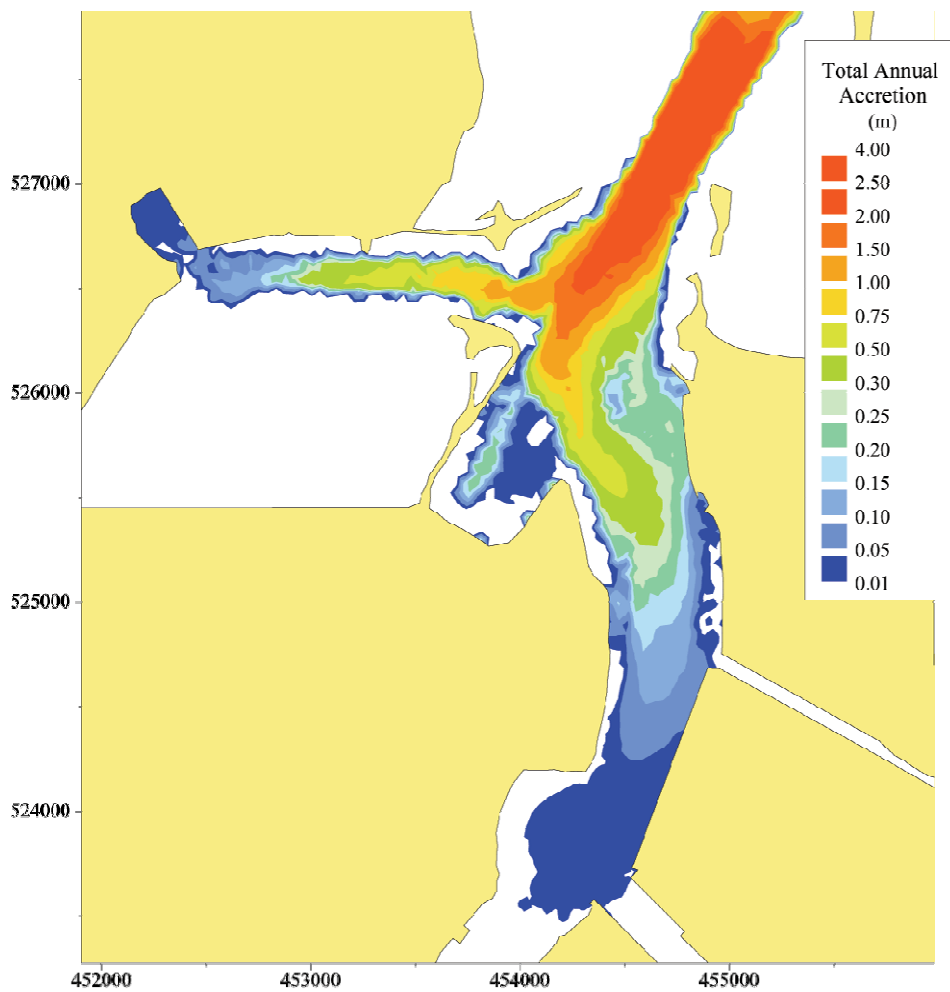


Figure 4.21 Simulated total annual accretion depths after development

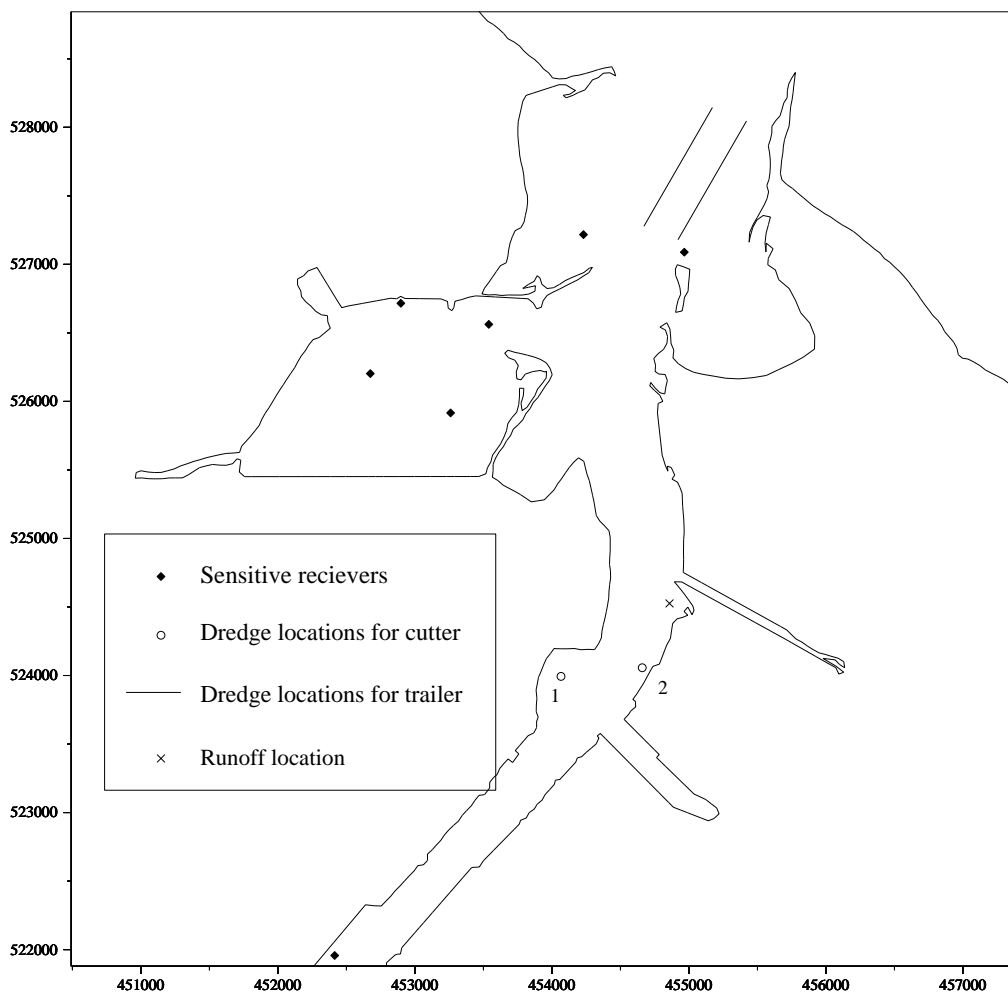


Figure 5.1 Simulated dredge locations and sensitive receiver points

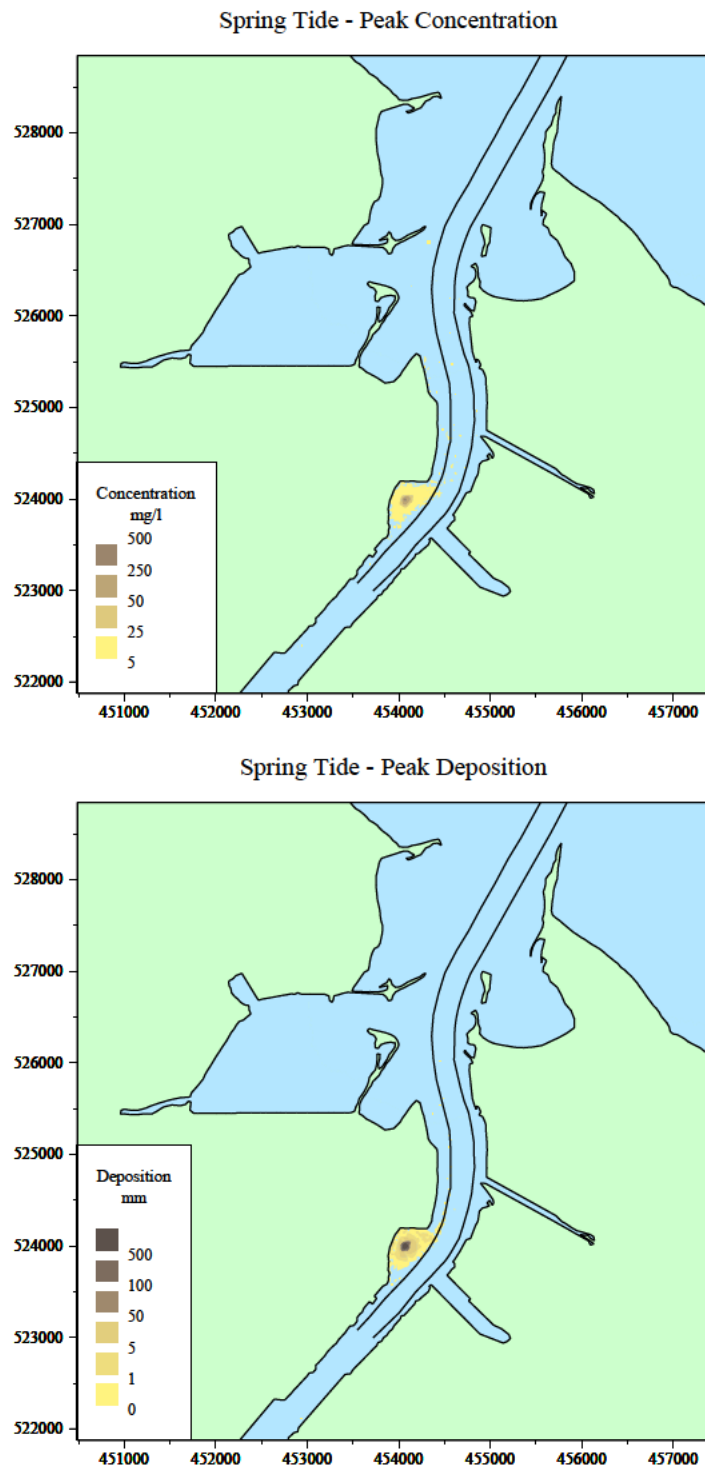


Figure 5.2 Peak concentration and peak deposition for cutter dredger at location 1, spring tide, low flow

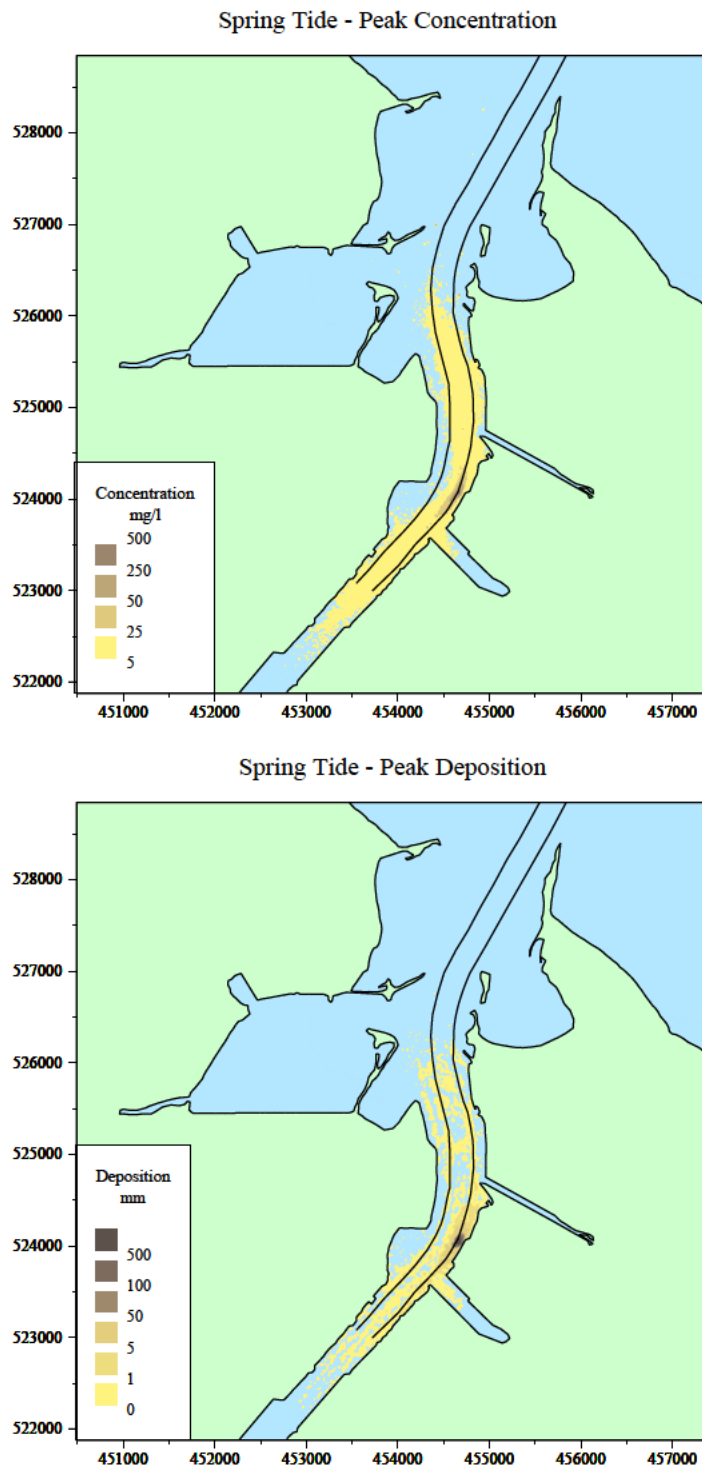


Figure 5.3 Peak concentration and peak deposition for cutter dredger at location 2, spring tide, low flow

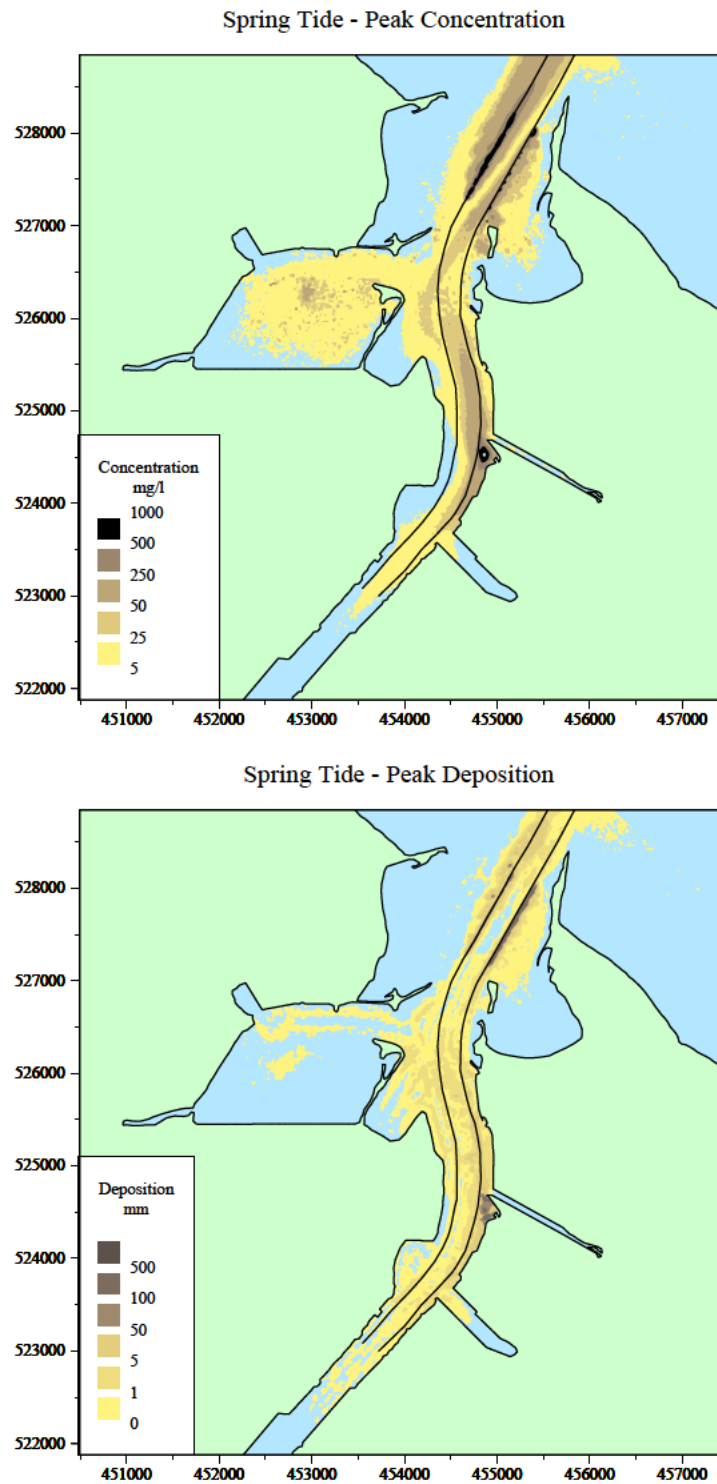


Figure 5.4 Peak concentration and deposition for trailer in approach channel, spring tide, low flow conditions

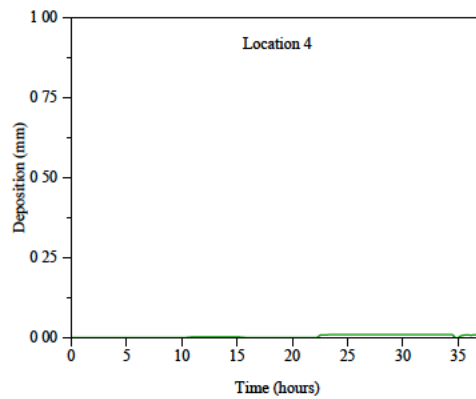
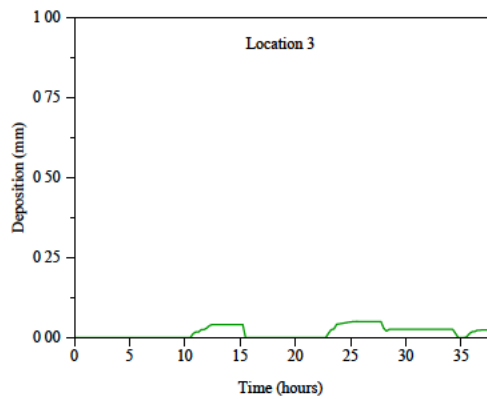
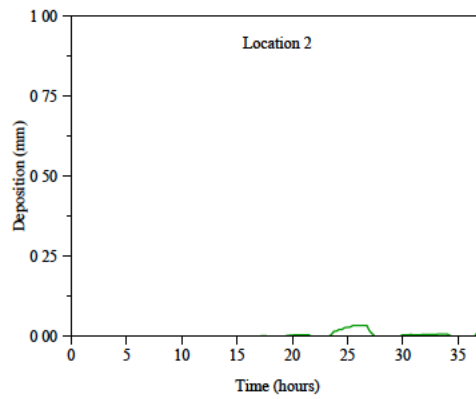
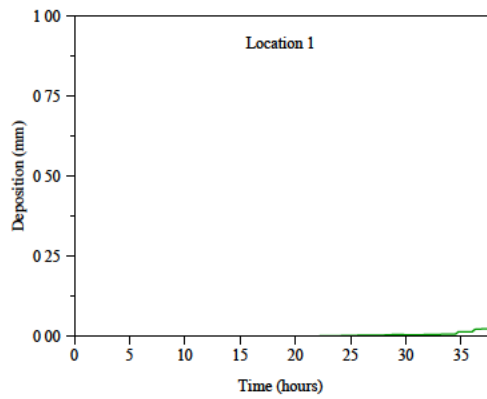
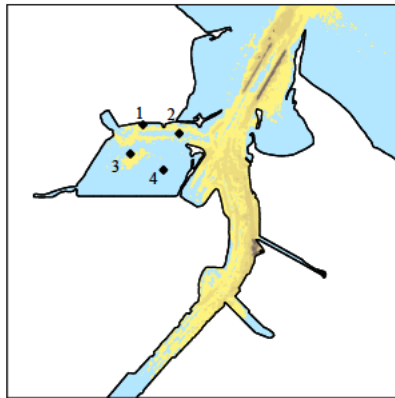


Figure 5.5 Time histories of deposition in Seaton Channel (Locations 1 and 2) and Seal Sands (Locations 3 and 4) for TSHD dredging sand in the approach channel, spring tide, low flow conditions

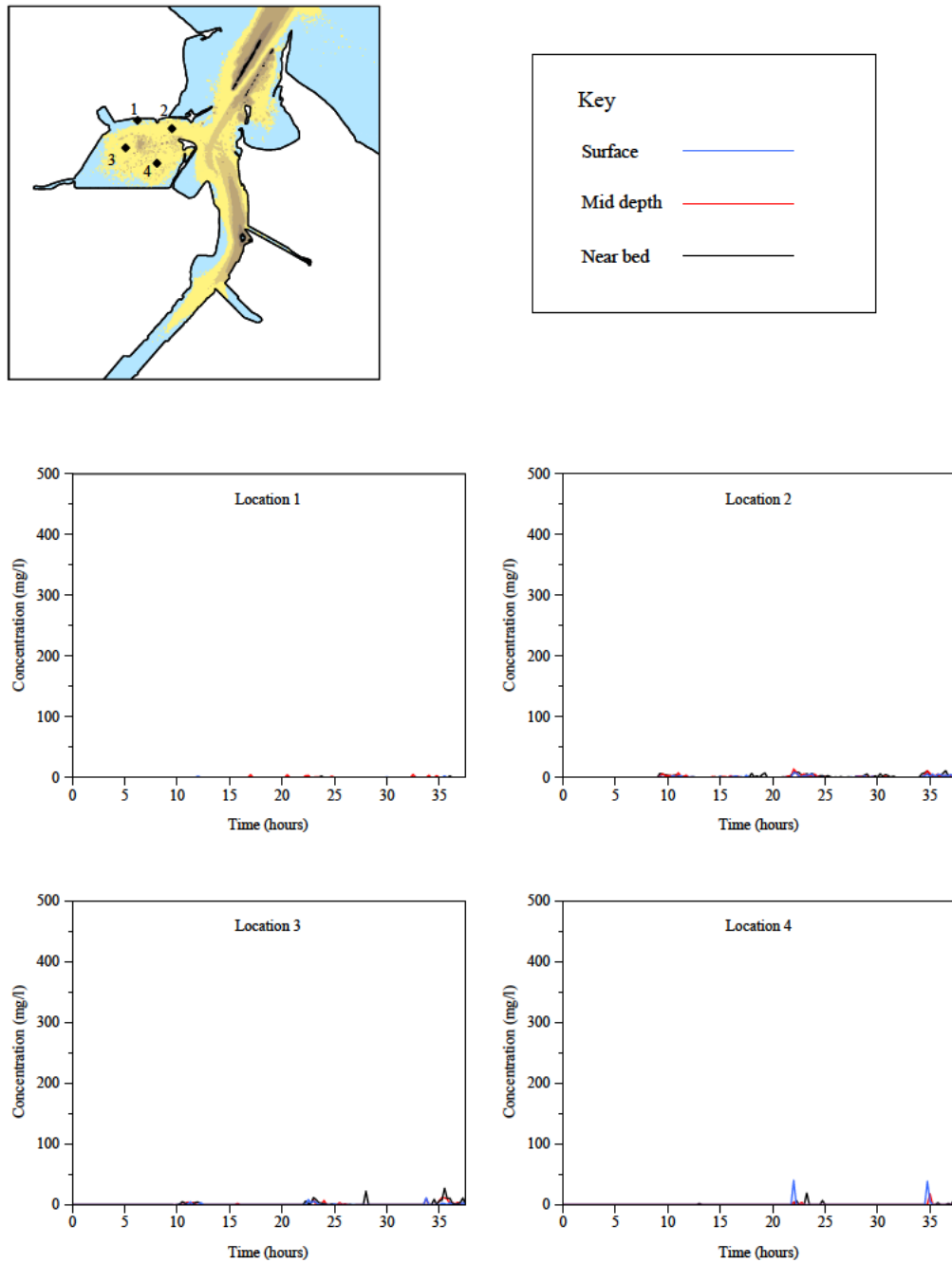


Figure 5.6 Time histories of concentration in Seaton Channel (Locations 1 and 2) and Seal Sands (Locations 3 and 4) for TSHD dredging sand in the approach channel, spring tide, low flow conditions

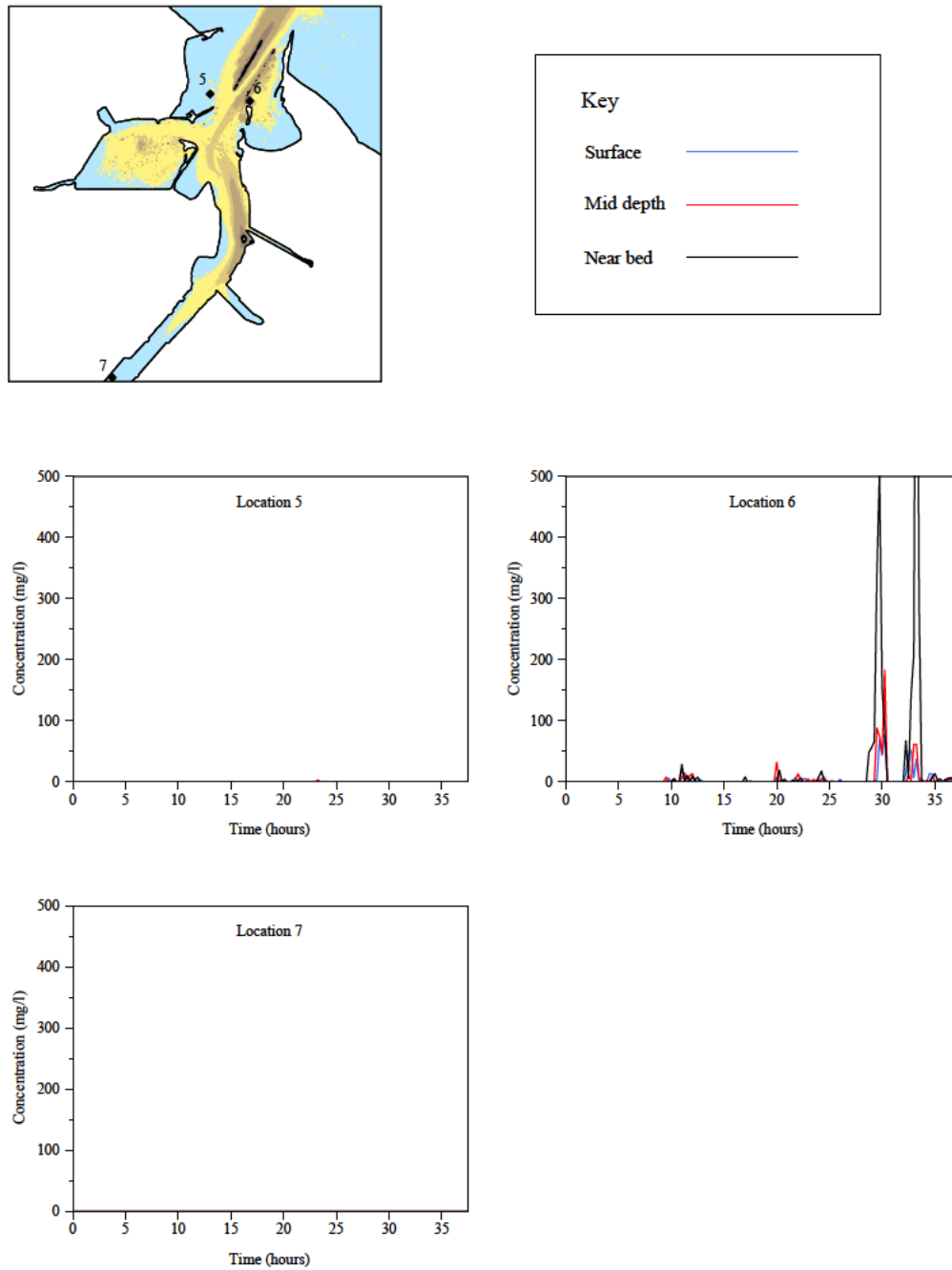


Figure 5.7 Time histories of concentration at Bran and North Gare Sands for TSHD dredging sand in approach channel, spring tide low flow conditions

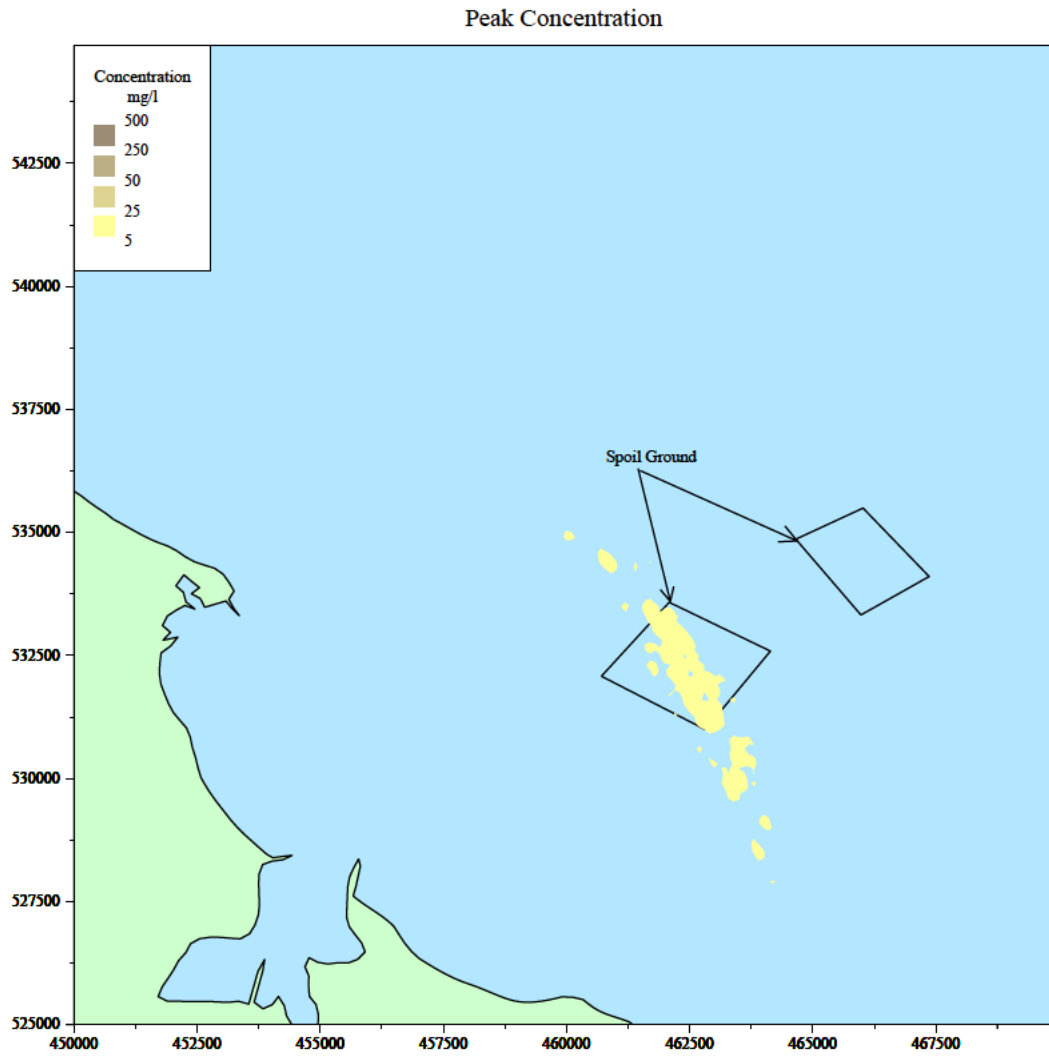


Figure 5.8 Simulated peak concentration for disposal operations at present maintenance disposal site

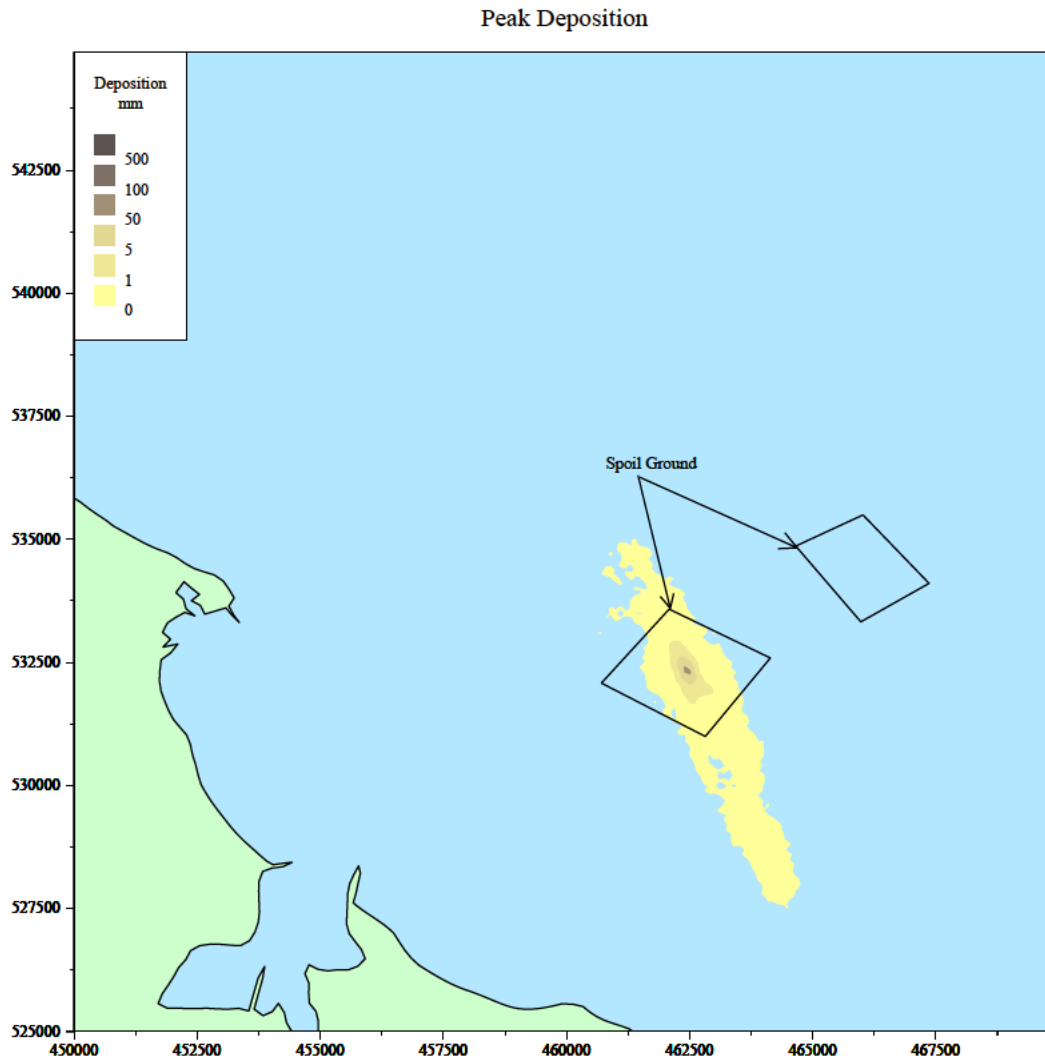


Figure 5.9 Simulated peak deposition for disposal operations at present maintenance disposal site

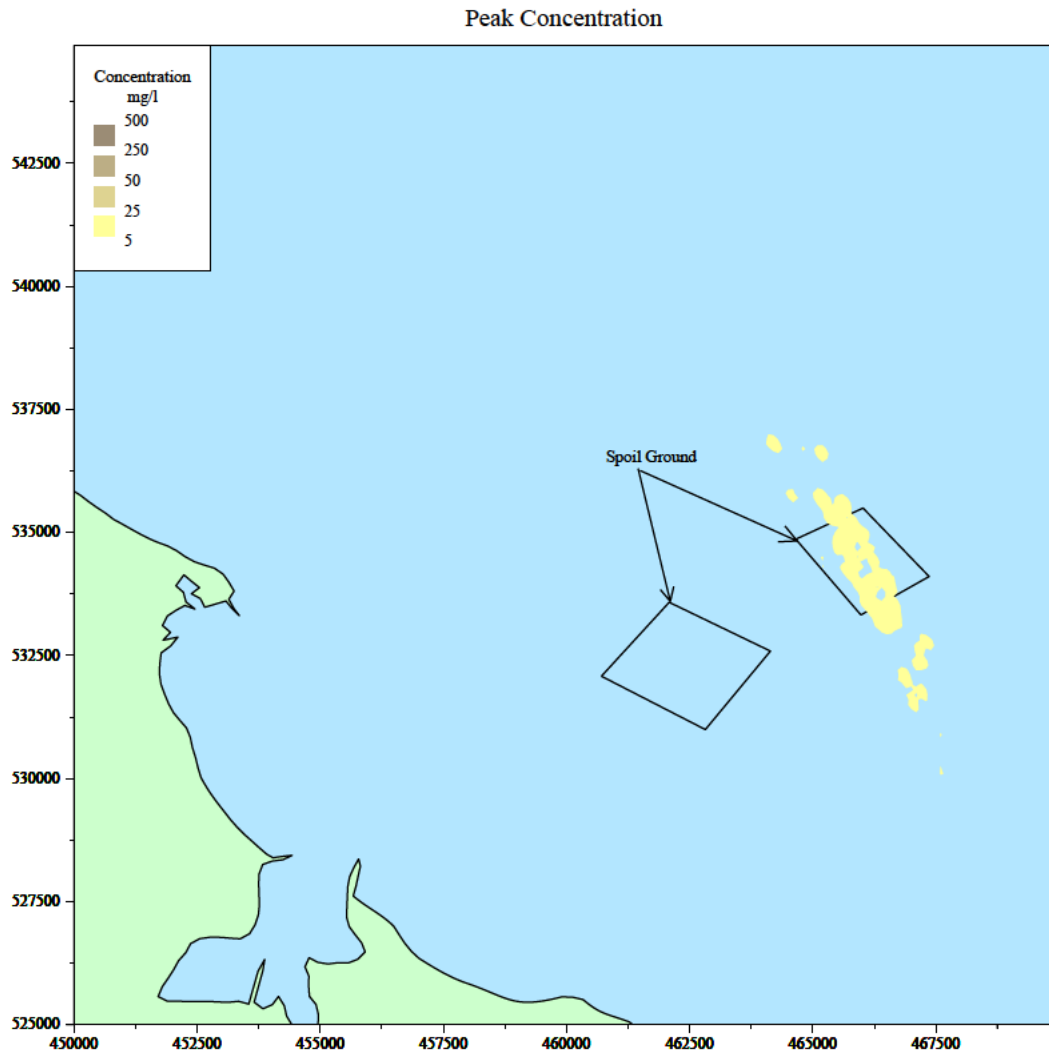


Figure 5.10 Simulated peak concentration for disposal operations at present capital disposal site

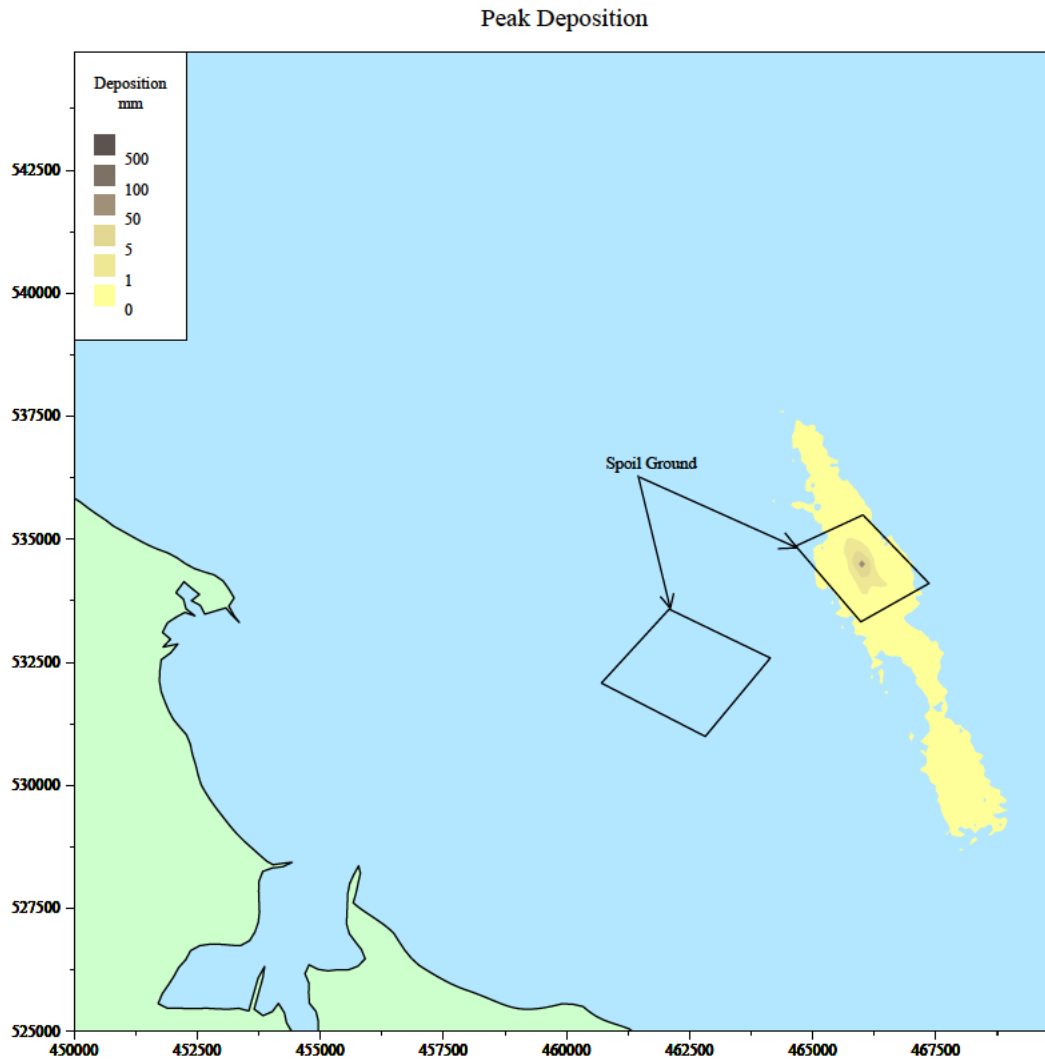


Figure 5.11 Simulated peak deposition for disposal operations at present capitol disposal site

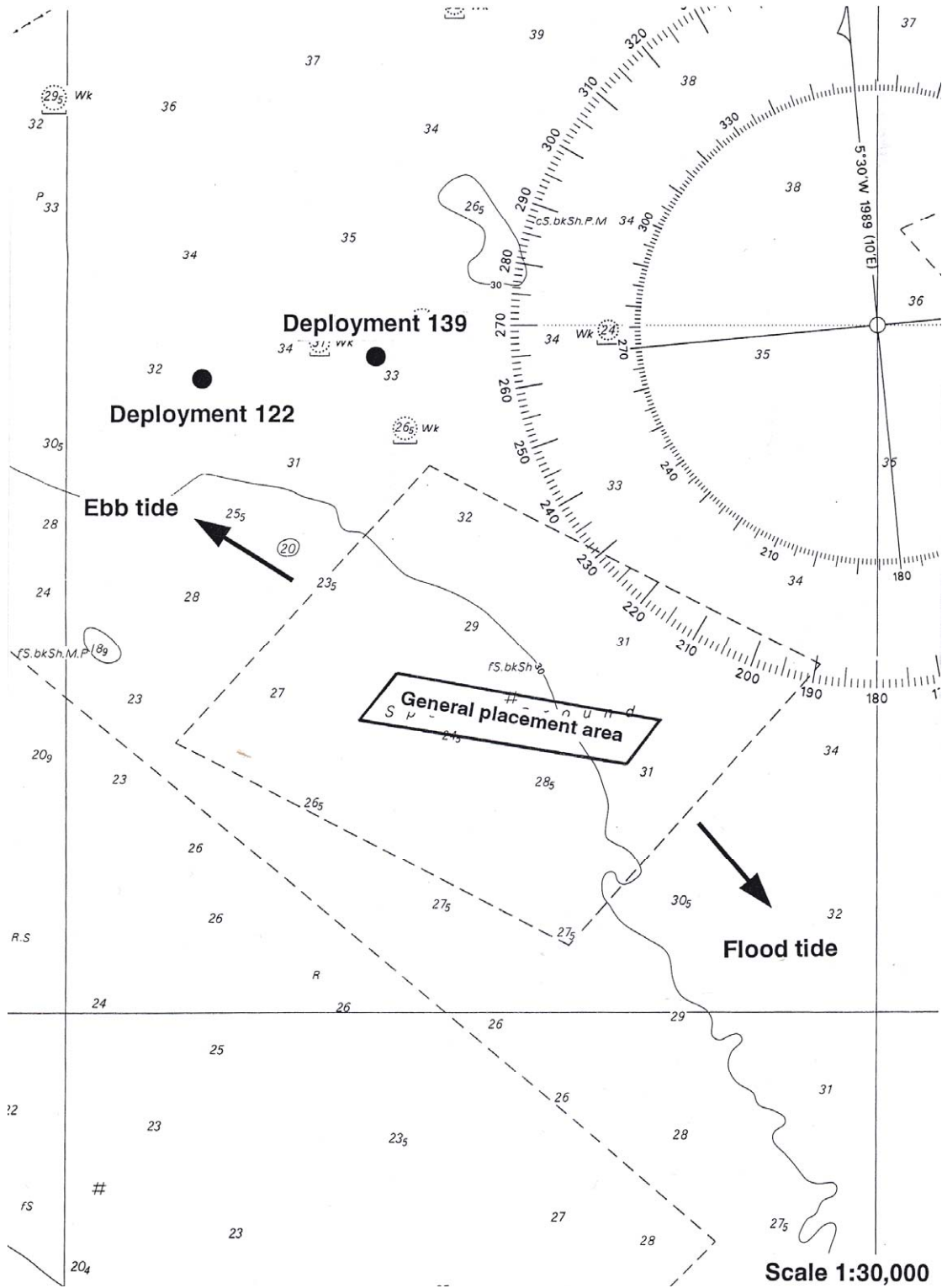


Figure 5.12 Conceptual sediment transport diagram at disposal sites

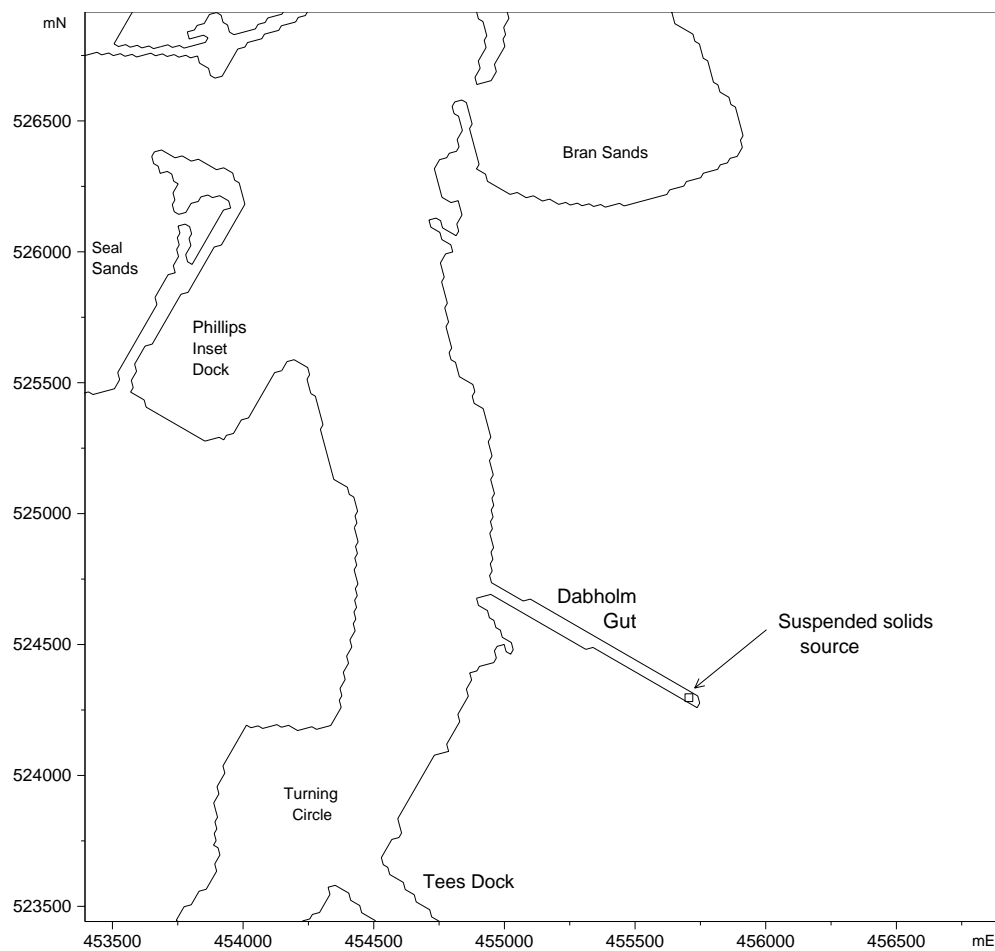


Figure 5.13 Location of Dabholm Gut

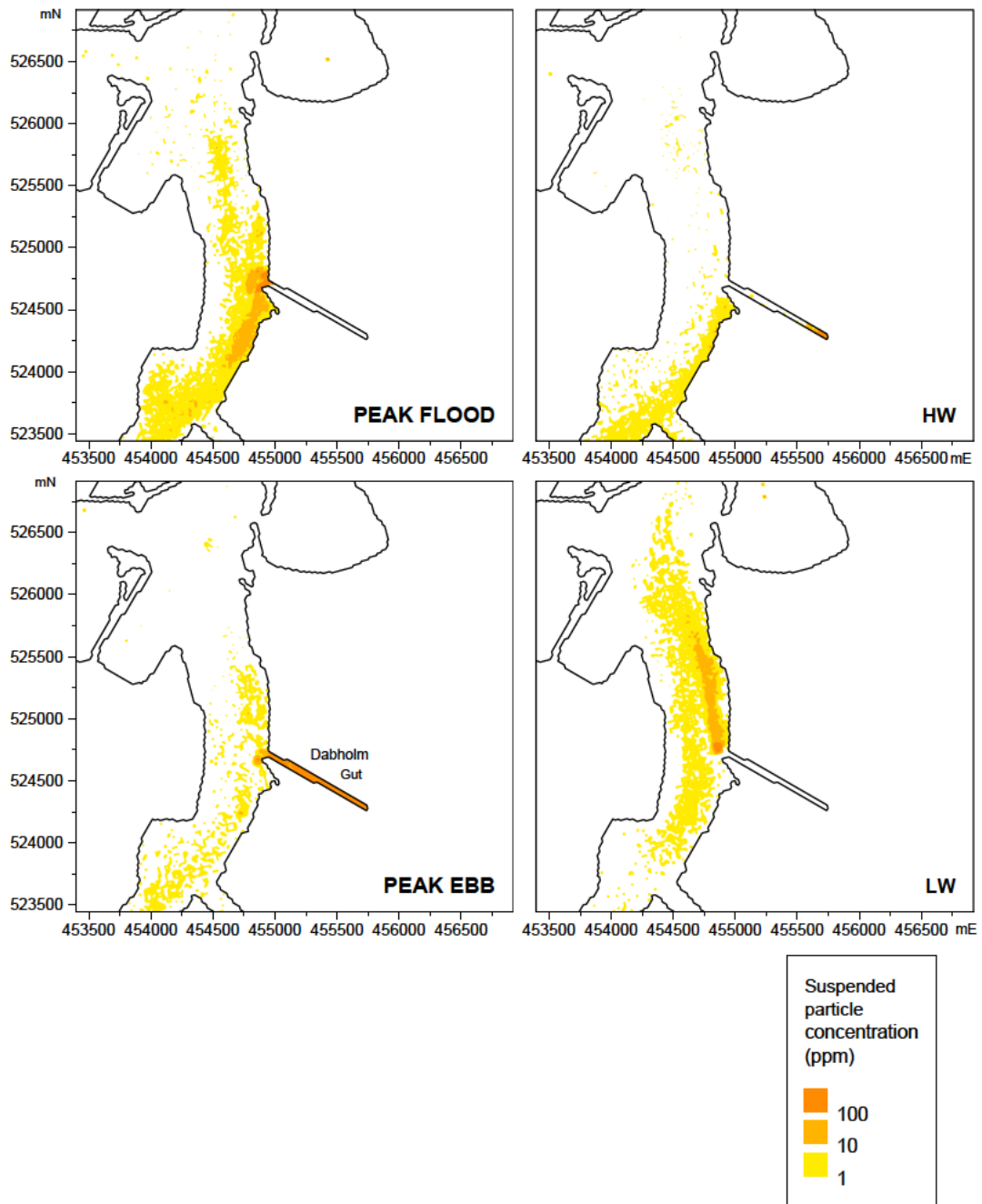


Figure 5.14 Depth-averaged suspended particle concentrations. Existing layout, spring tide, summer condition

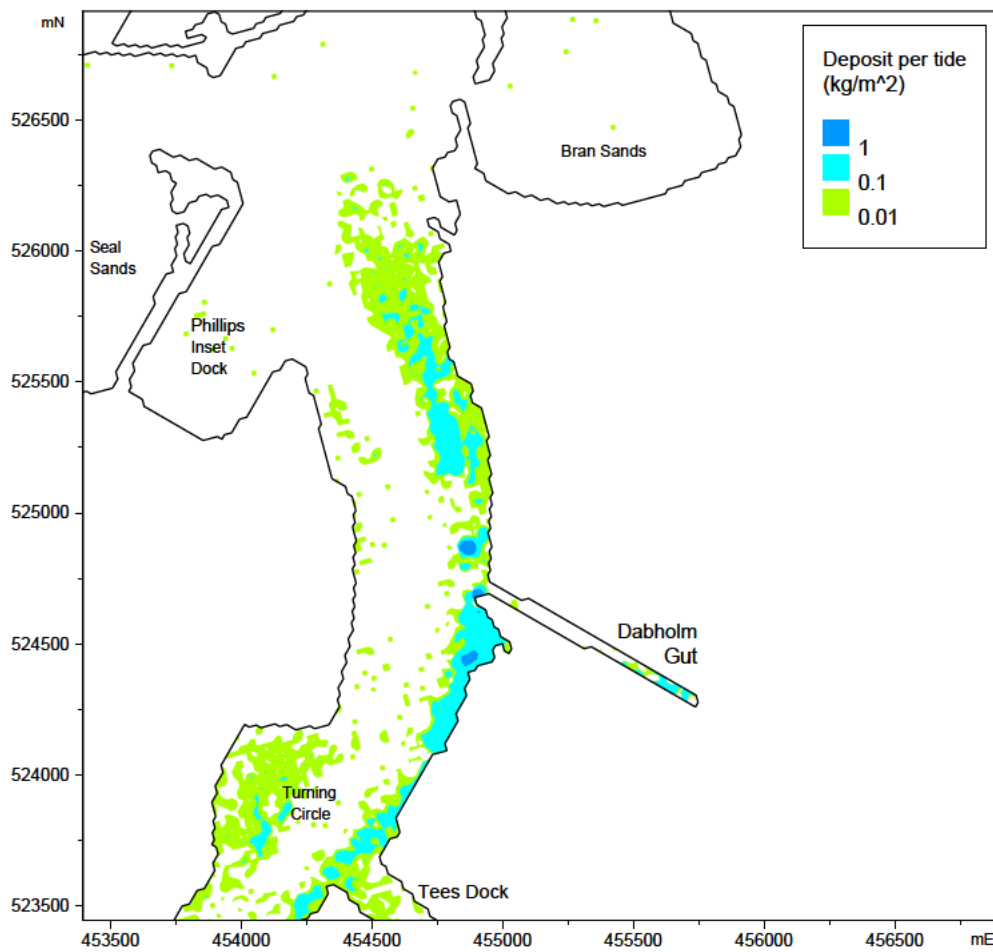


Figure 5.15 Increase in deposits over a tidal cycle – Existing layout, spring tide, summer conditions

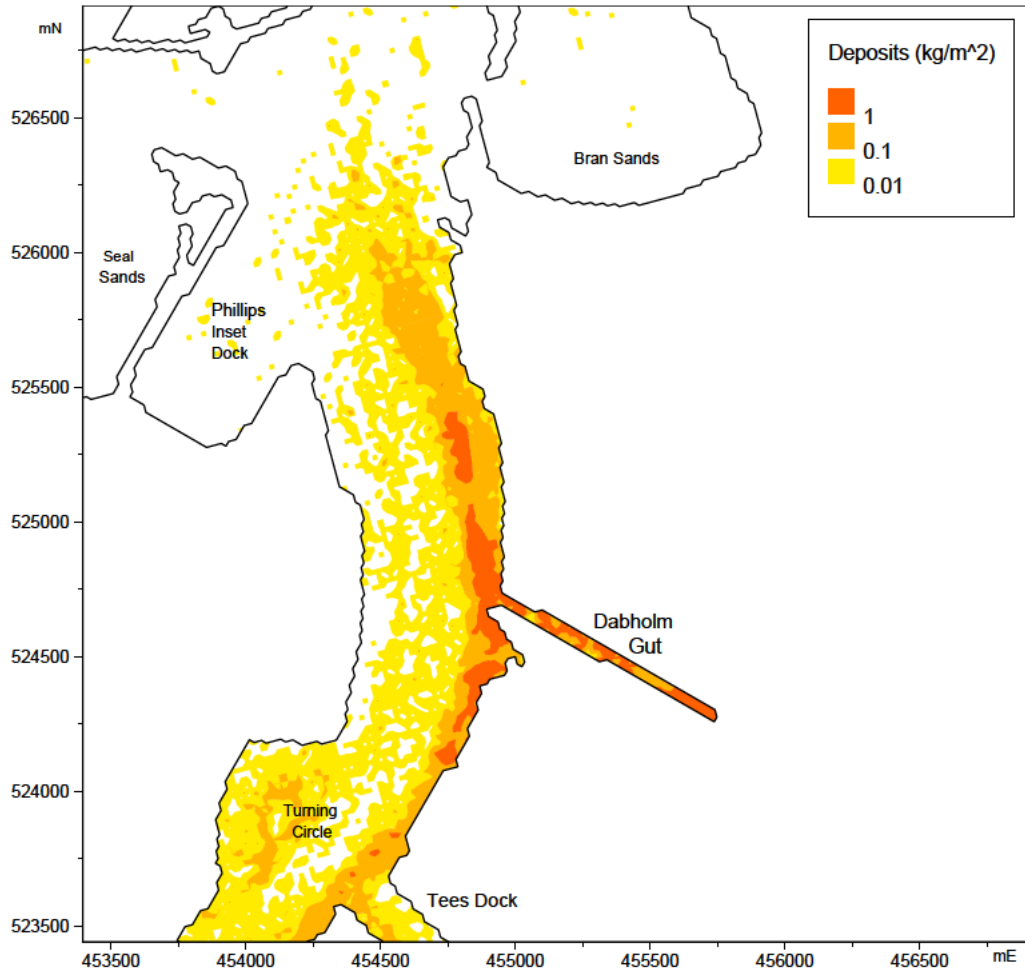


Figure 5.16 Distribution of maximum deposits over the tidal cycle. Existing layout, spring tide, summer conditions

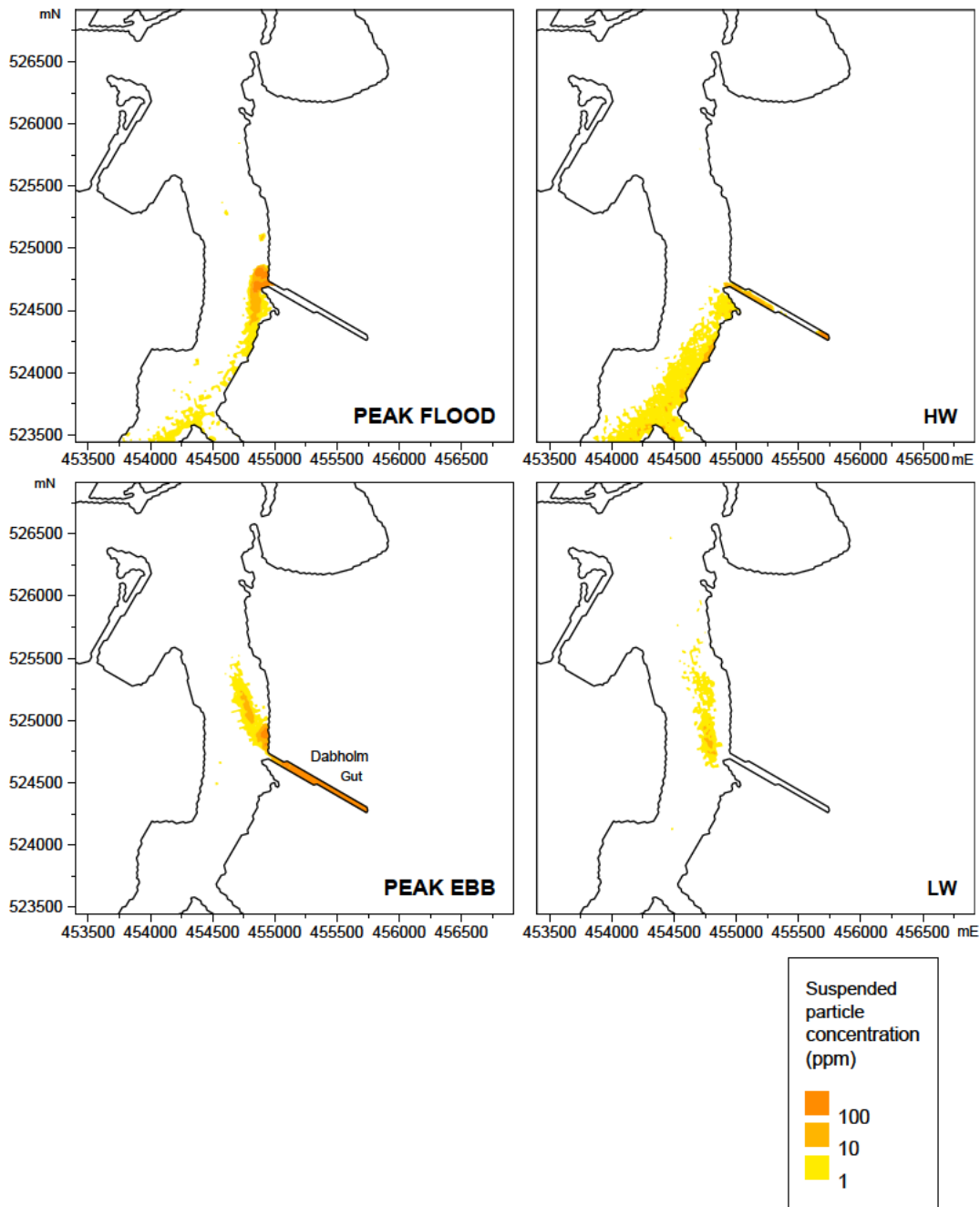


Figure 5.17 Depth-averaged suspended particle concentrations. Existing layout, spring tide, winter condition

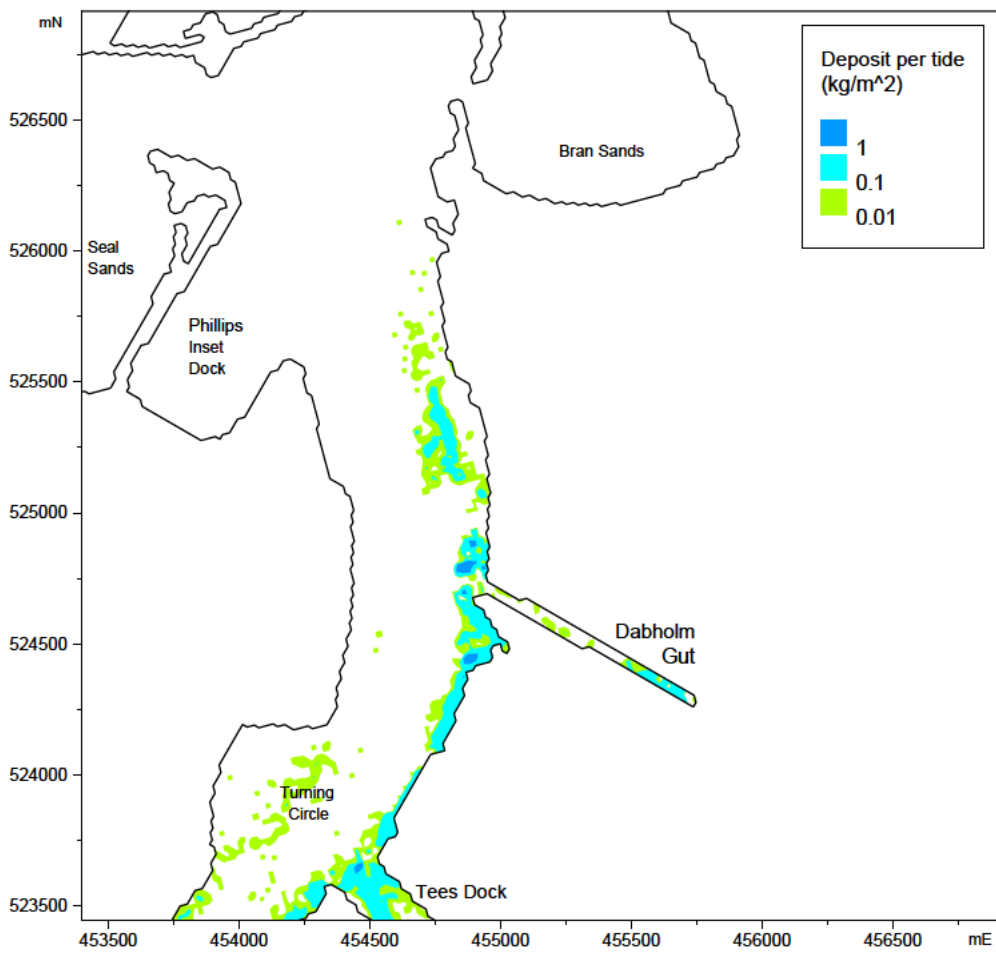


Figure 5.18 Increase in deposits over a tidal cycle – Existing layout, spring tide, winter conditions

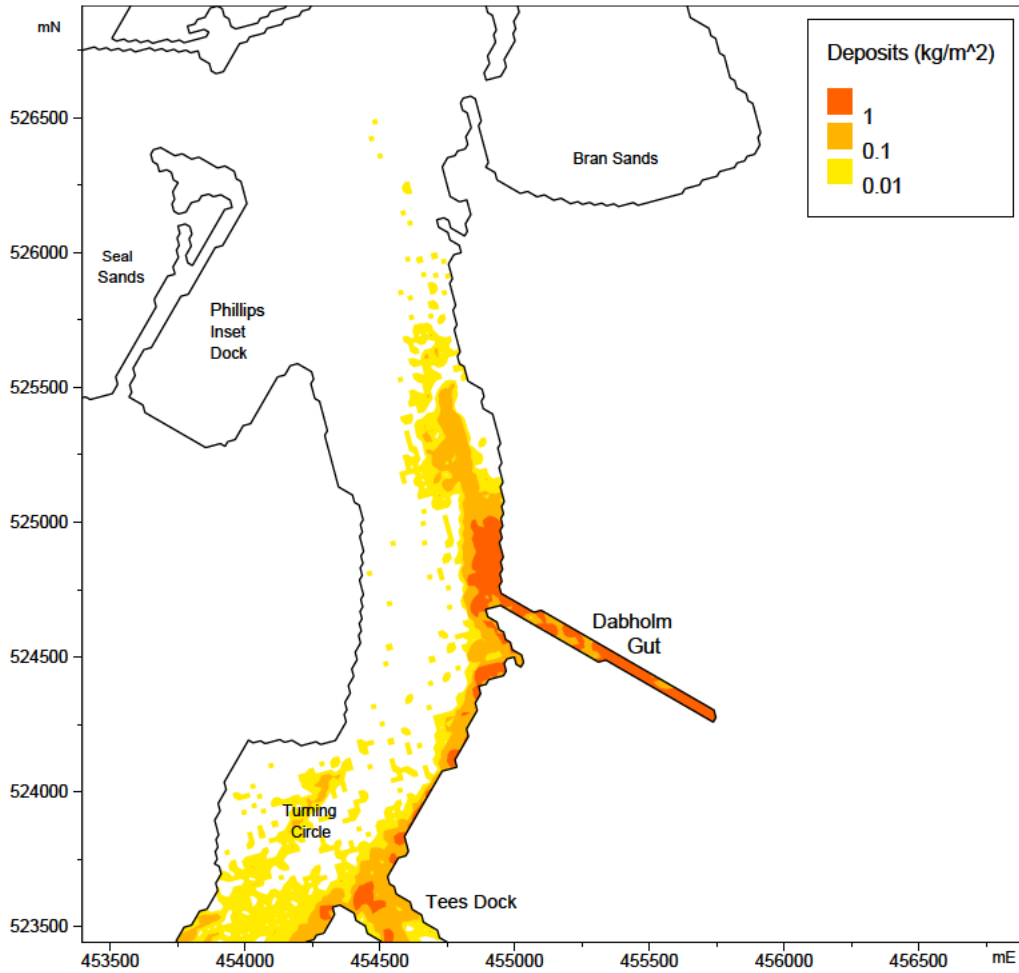


Figure 5.19 Distribution of maximum deposits over the tidal cycle. Existing layout, spring tide, winter conditions



Figure 5.20 Depth-averaged suspended particle concentrations. Existing layout, neap tide, summer condition

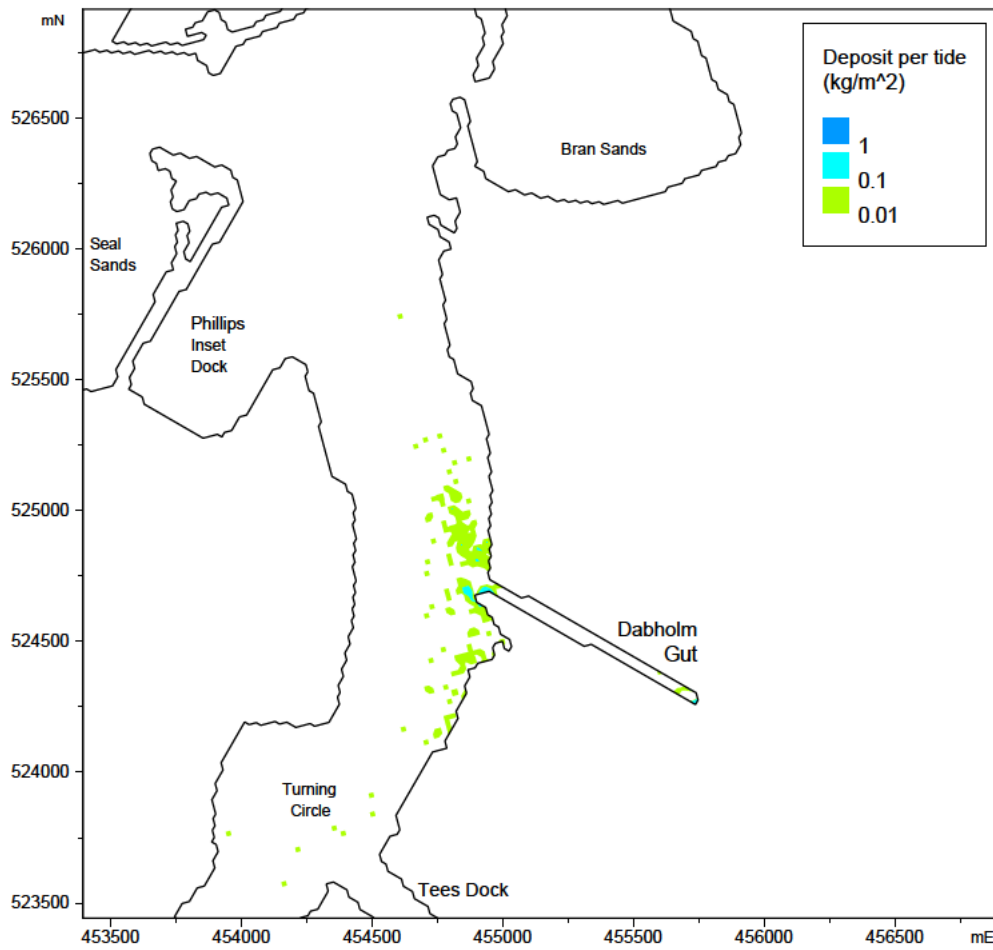
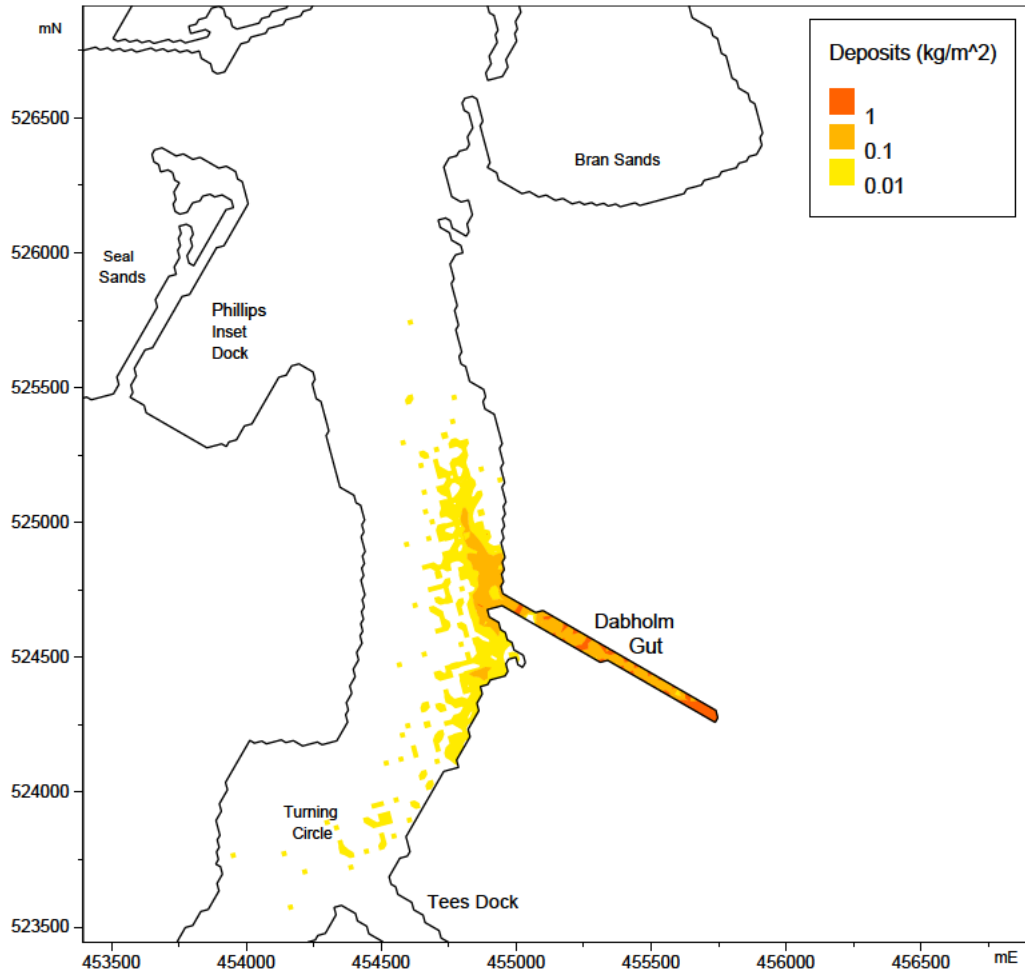


Figure 5.21 Increase in deposits over a tidal cycle – Existing layout, neap tide, summer condition



**Distribution of maximum deposits over the tidal cycle.
Existing layout, neap tide, summer conditions.**

Figure 5.22 Distribution of maximum deposits over the tidal cycle. Existing layout, neap tide, summer conditions

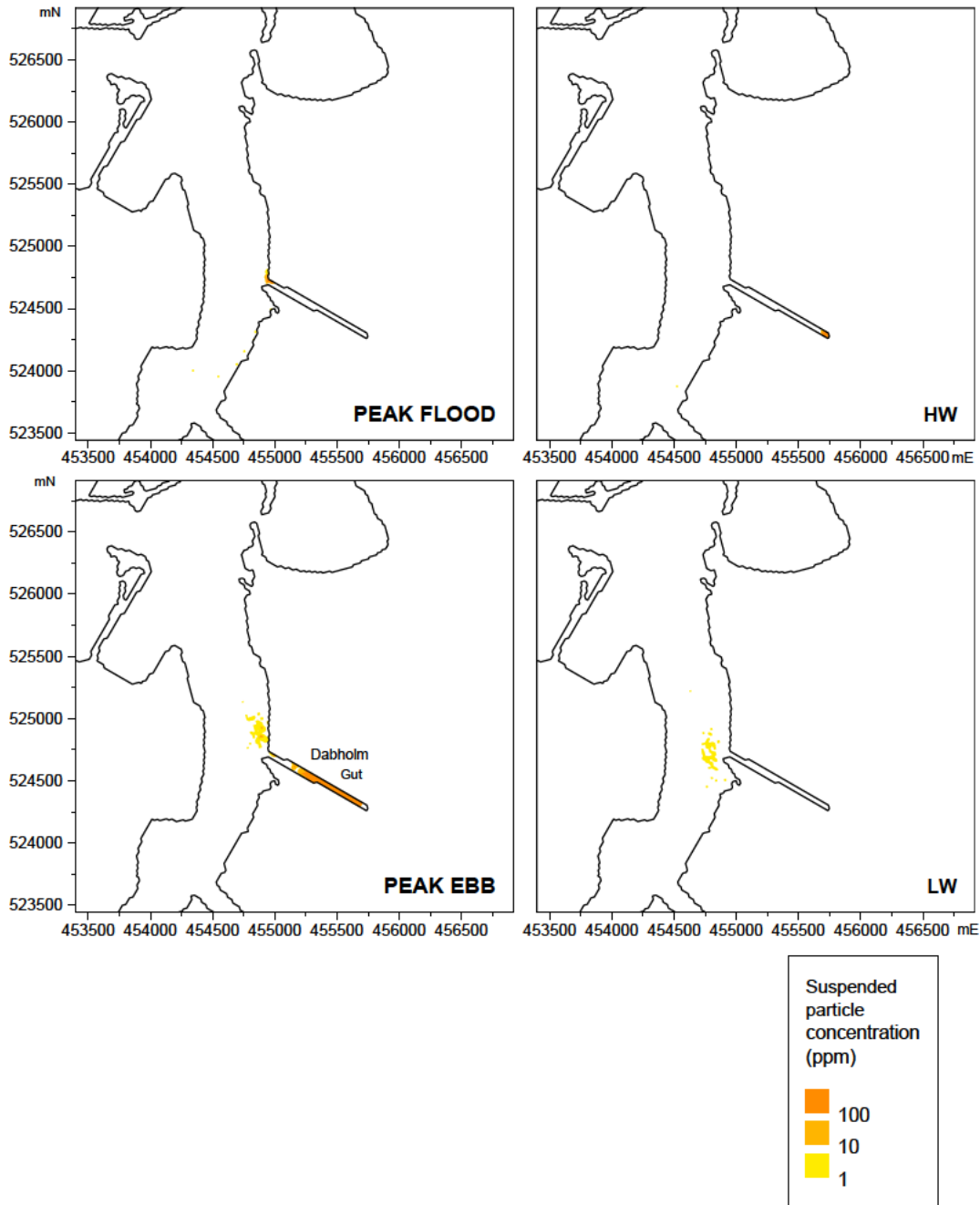


Figure 5.23 Depth-averaged suspended particle concentrations. Existing layout, neap tide, winter condition

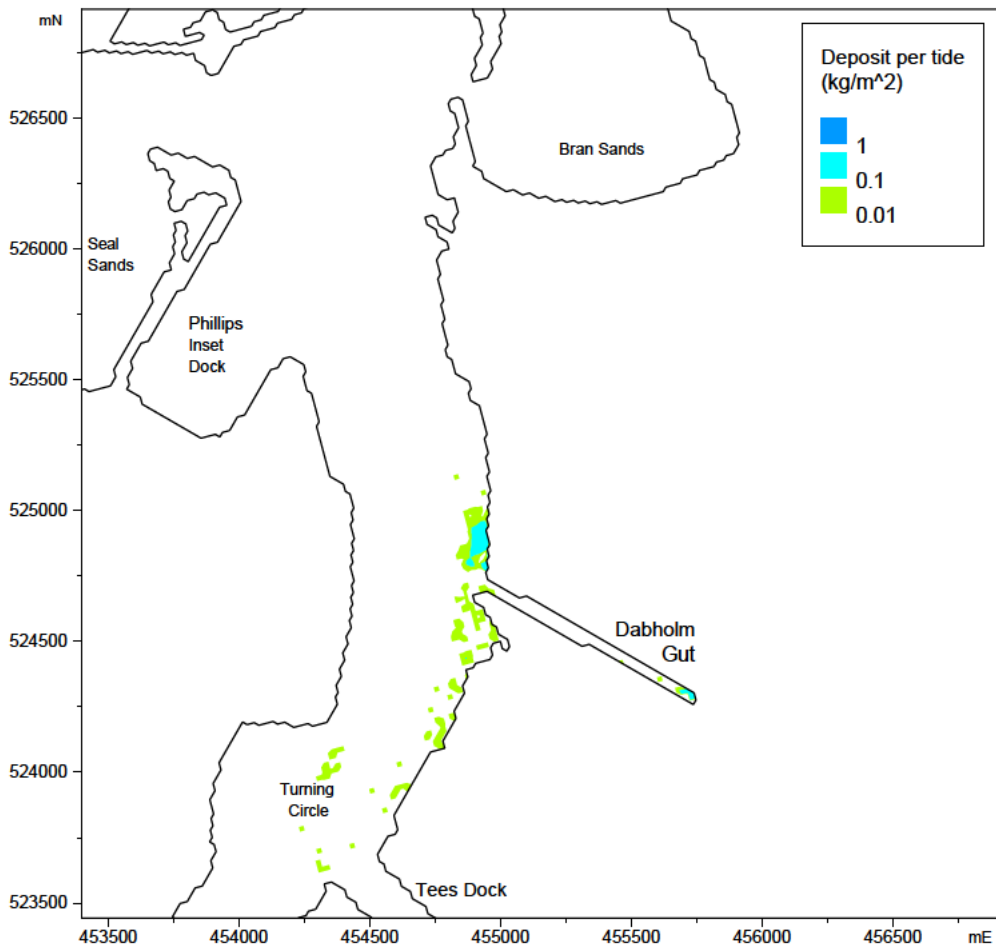


Figure 5.24 Increase in deposits over a tidal cycle – Existing layout, neap tide, winter conditions

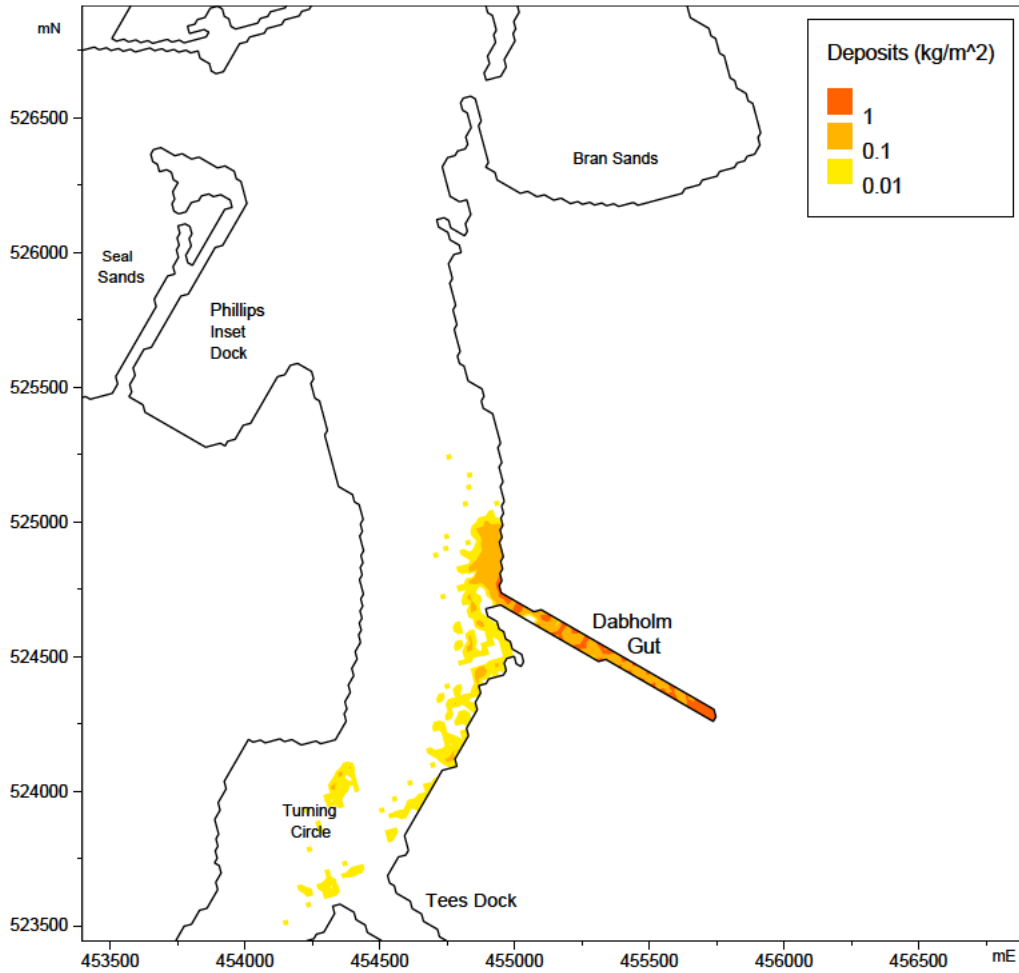


Figure 5.25 Distribution of maximum deposits over the tidal cycle. Existing layout, neap tide, winter conditions

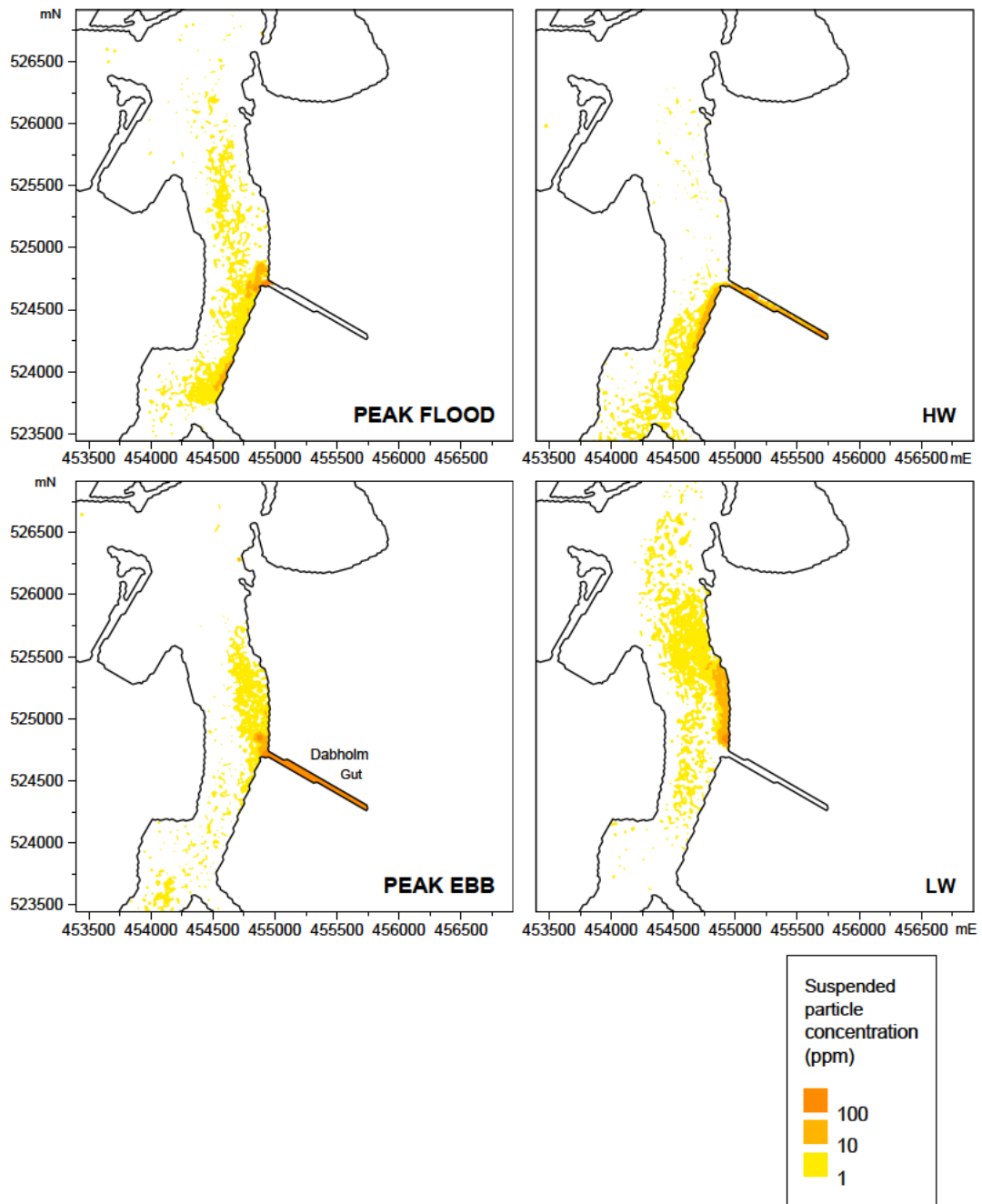


Figure 5.26 Depth-averaged suspended particle concentrations. Proposed layout, spring tide, summer condition

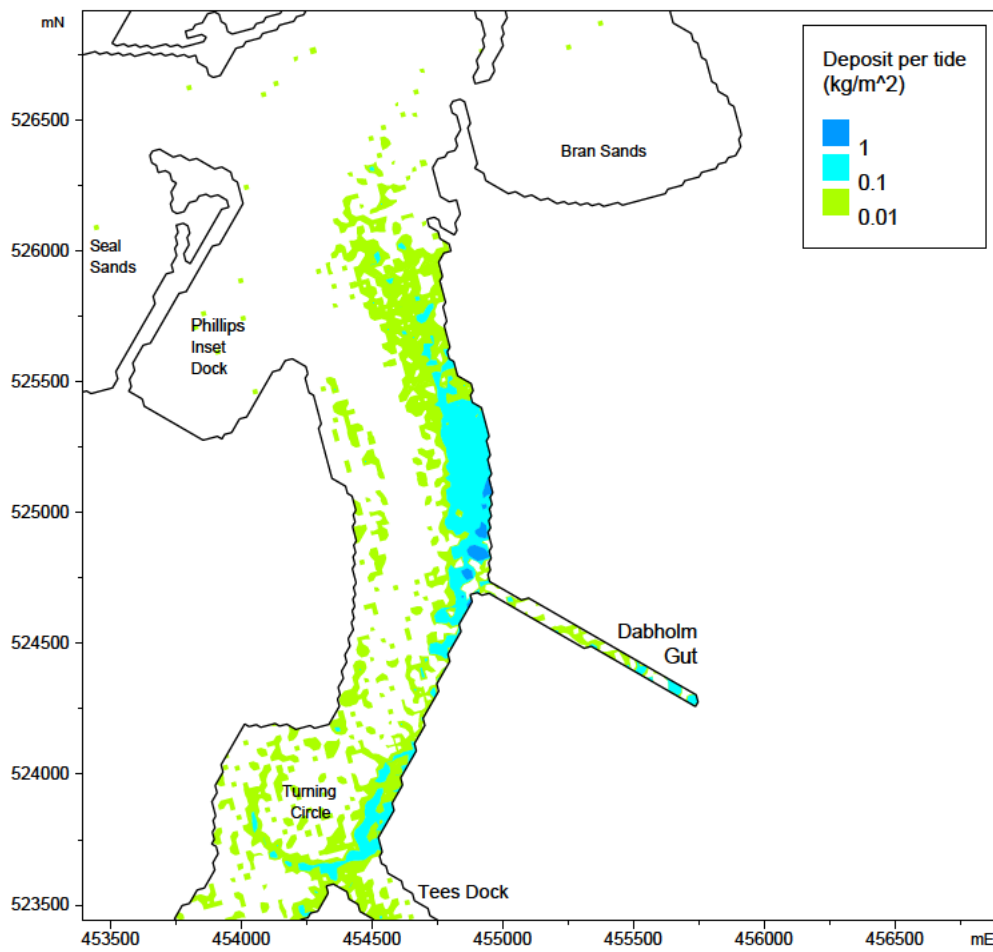


Figure 5.27 Increase in deposits over a tidal cycle – Proposed layout, spring tide, summer conditions

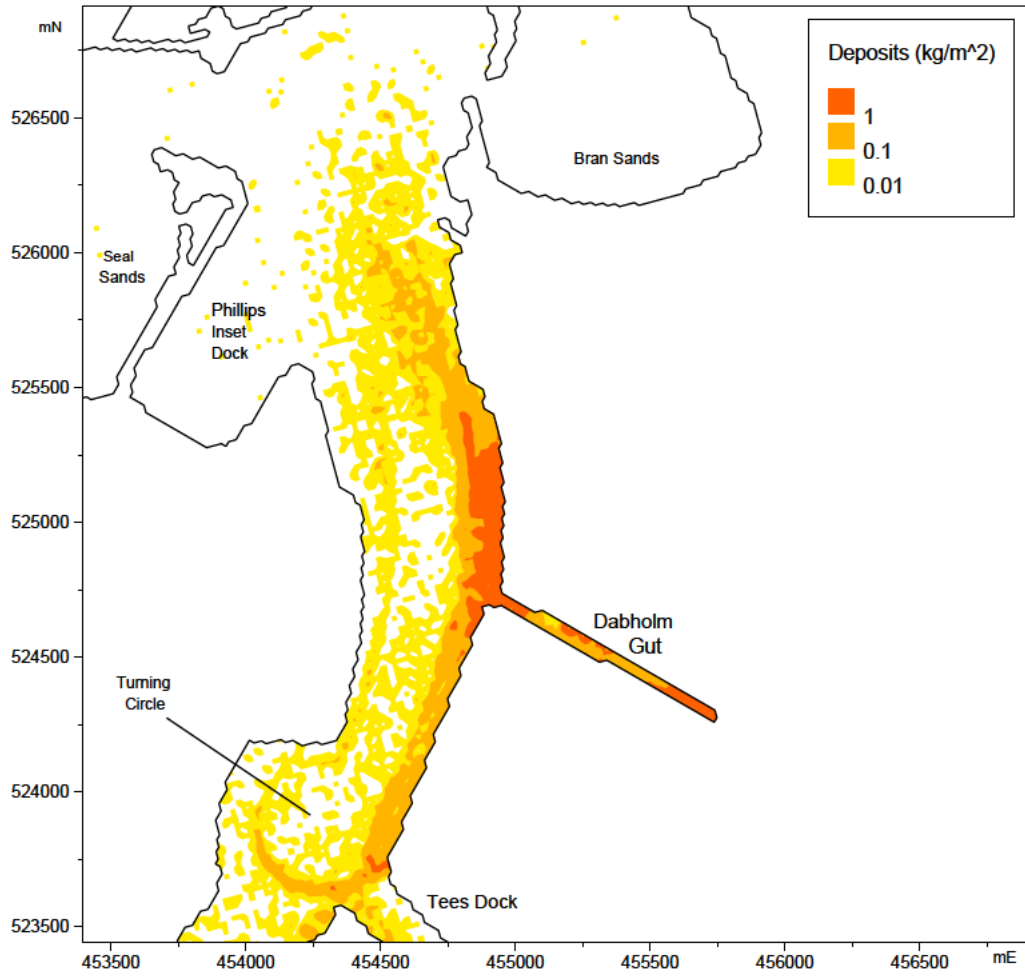


Figure 5.28 Distribution of maximum deposits over the tidal cycle. Proposed layout, spring tide, summer conditions

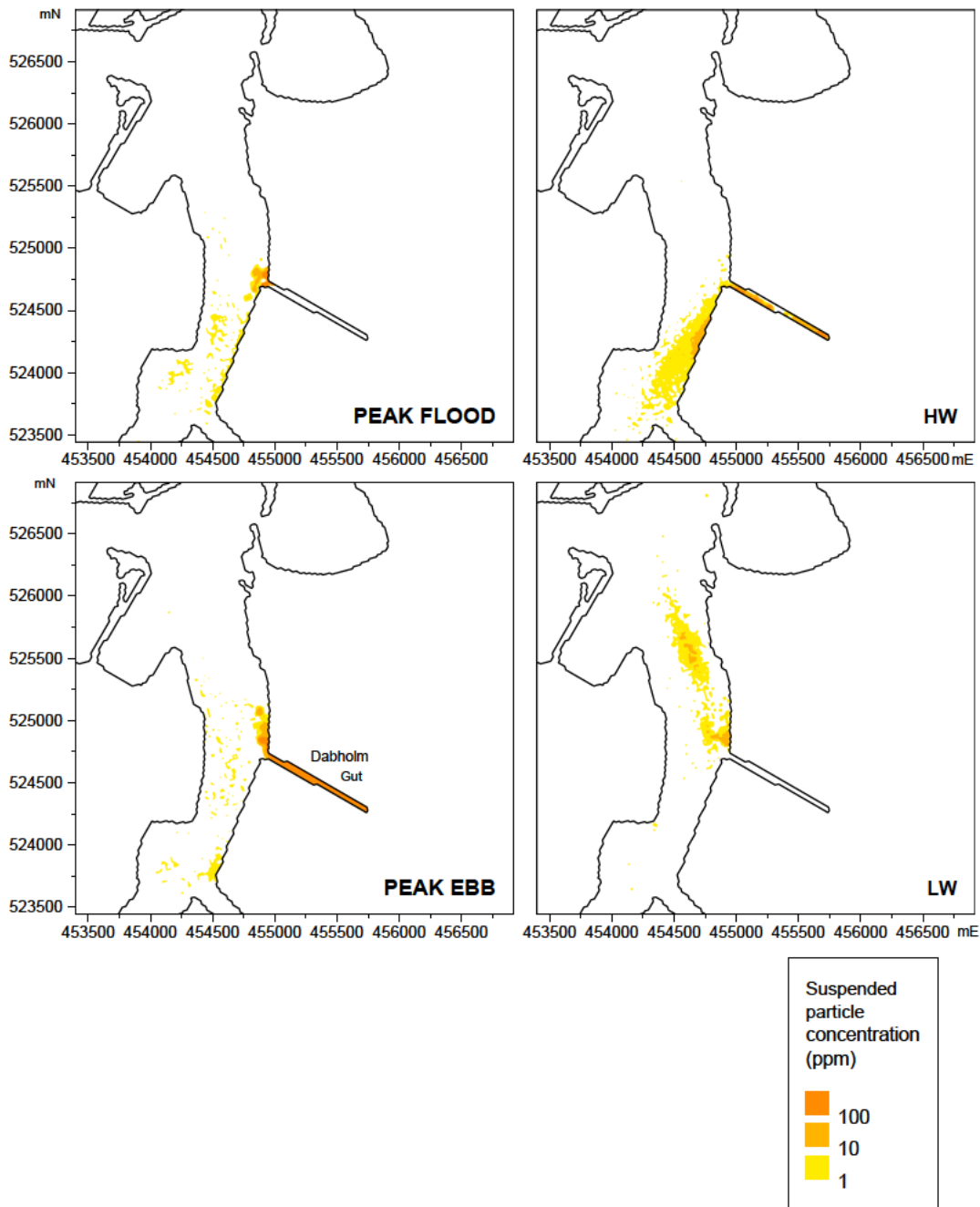


Figure 5.29 Depth-averaged suspended particle concentrations, proposed layout, spring tide, winter condition

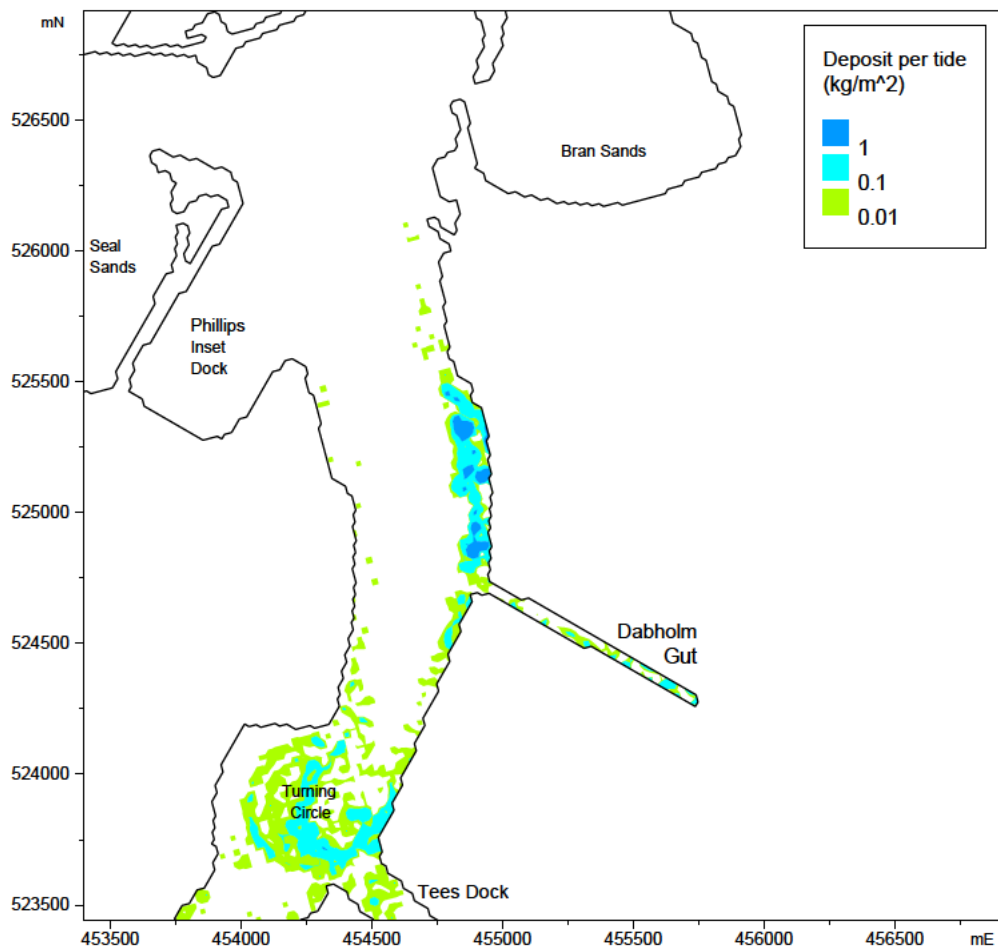


Figure 5.30 Increase in deposits over a tidal cycle – Proposed layout, spring tide, winter conditions

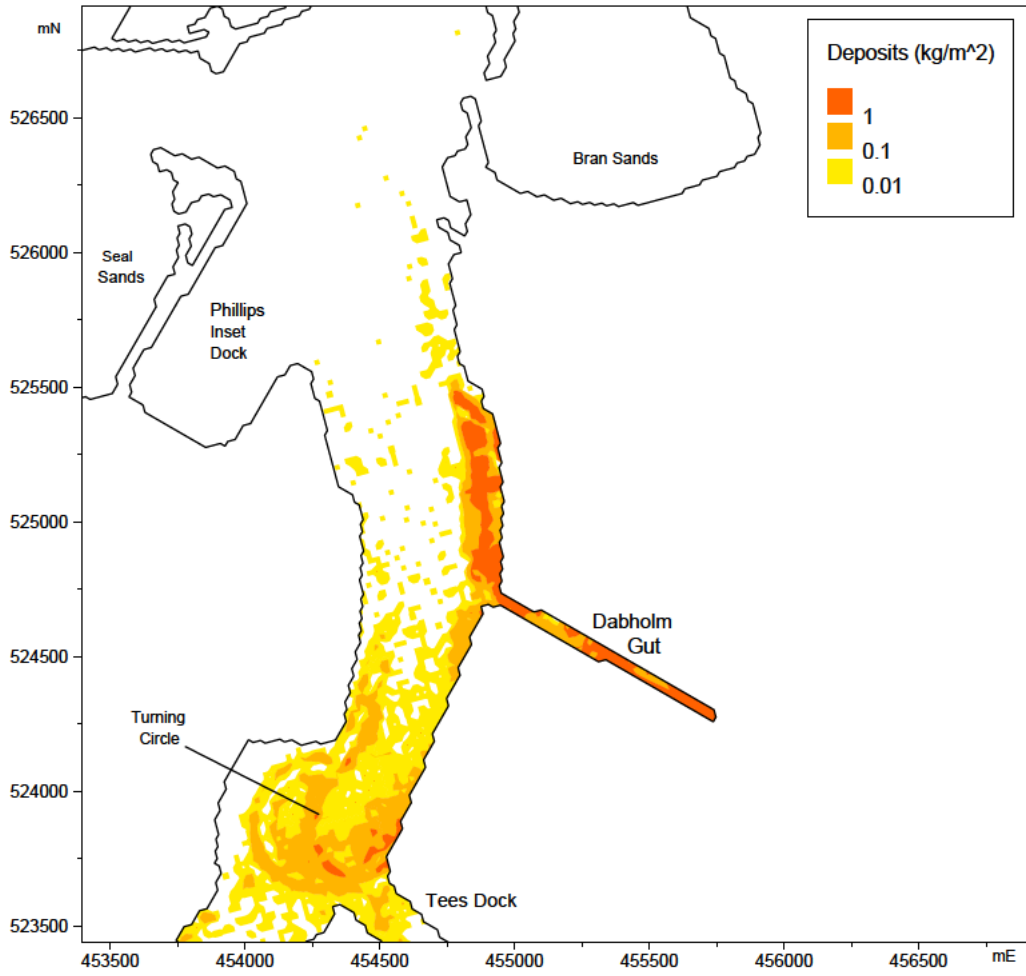


Figure 5.31 Distribution of maximum deposits over the tidal cycle. Proposed layout, spring tide, winter conditions

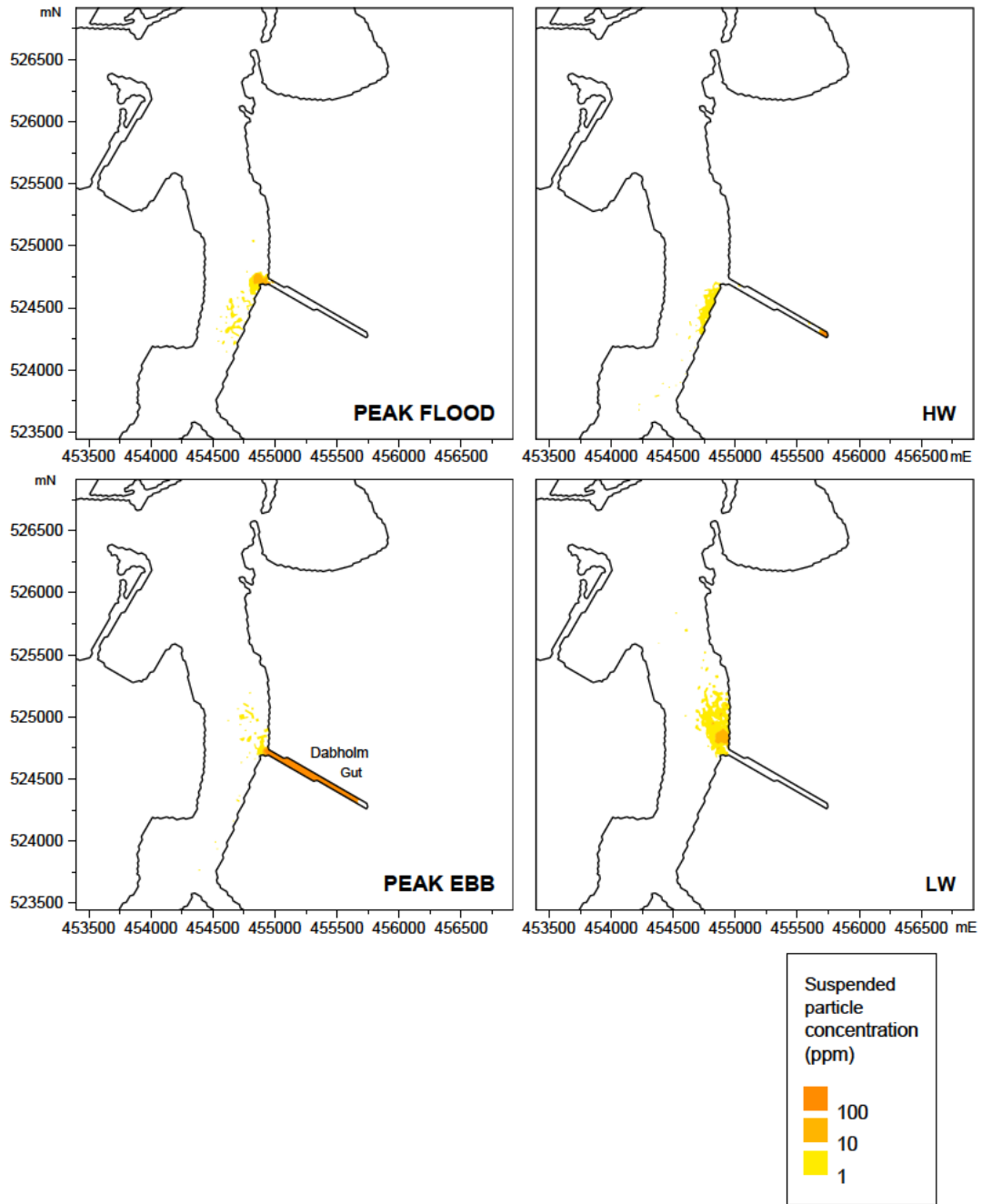


Figure 5.32 Depth-averaged suspended particle concentrations. Proposed layout, neap tide, summer condition

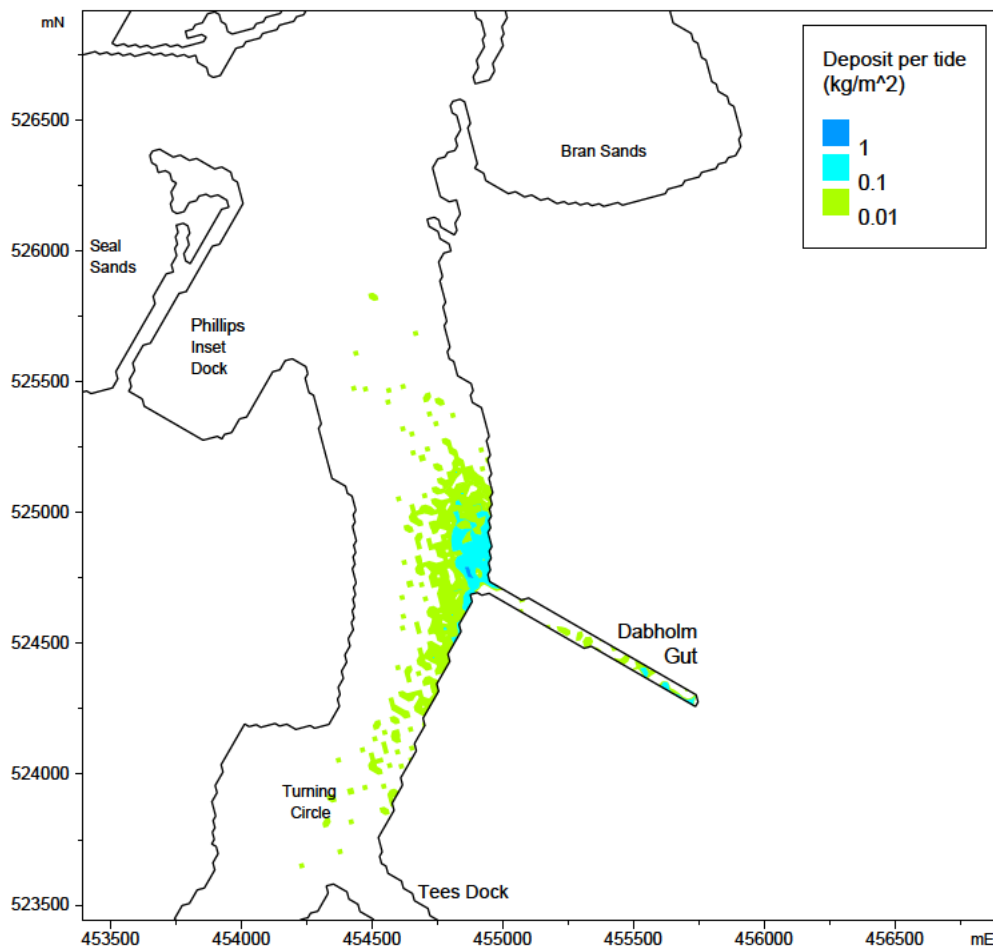


Figure 5.33 Increase in deposits over a tidal cycle – Proposed layout, neap tide, summer conditions

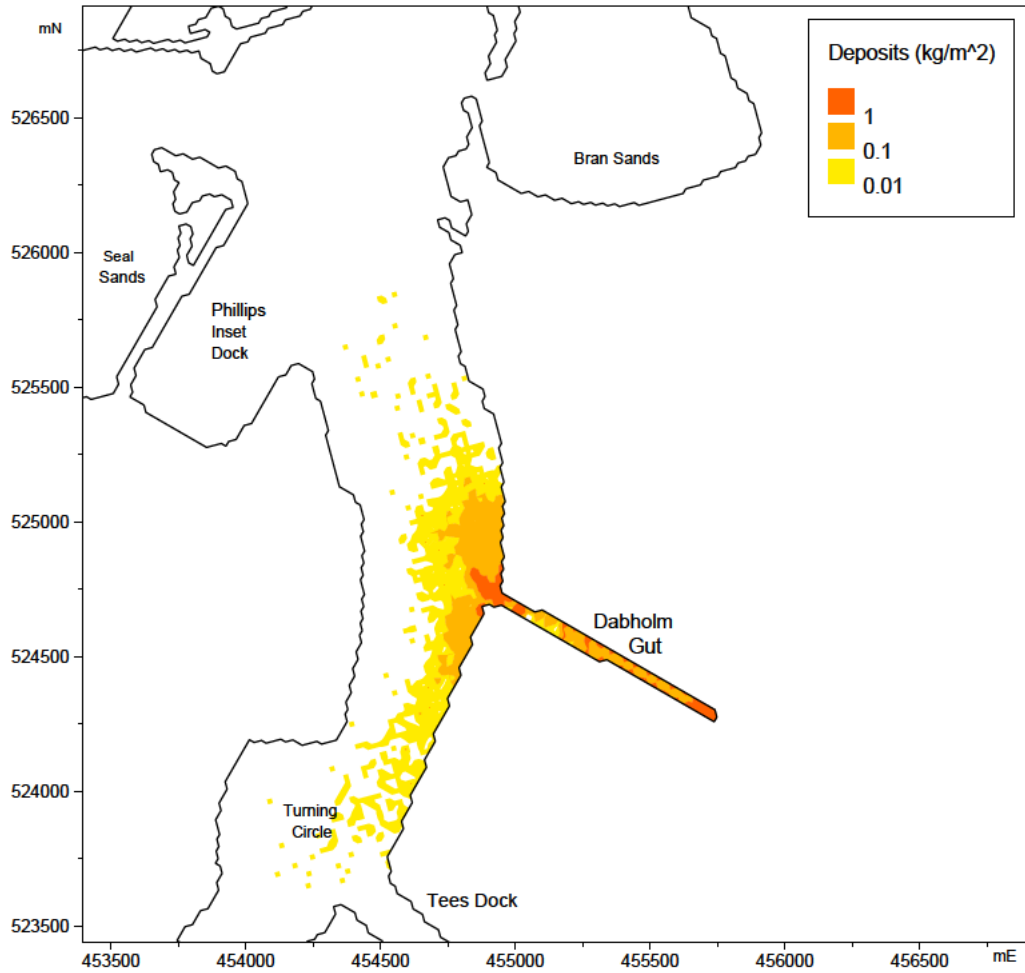


Figure 5.34 Distribution of maximum deposits over the tidal cycle. Proposed layout, neap tide, summer conditions

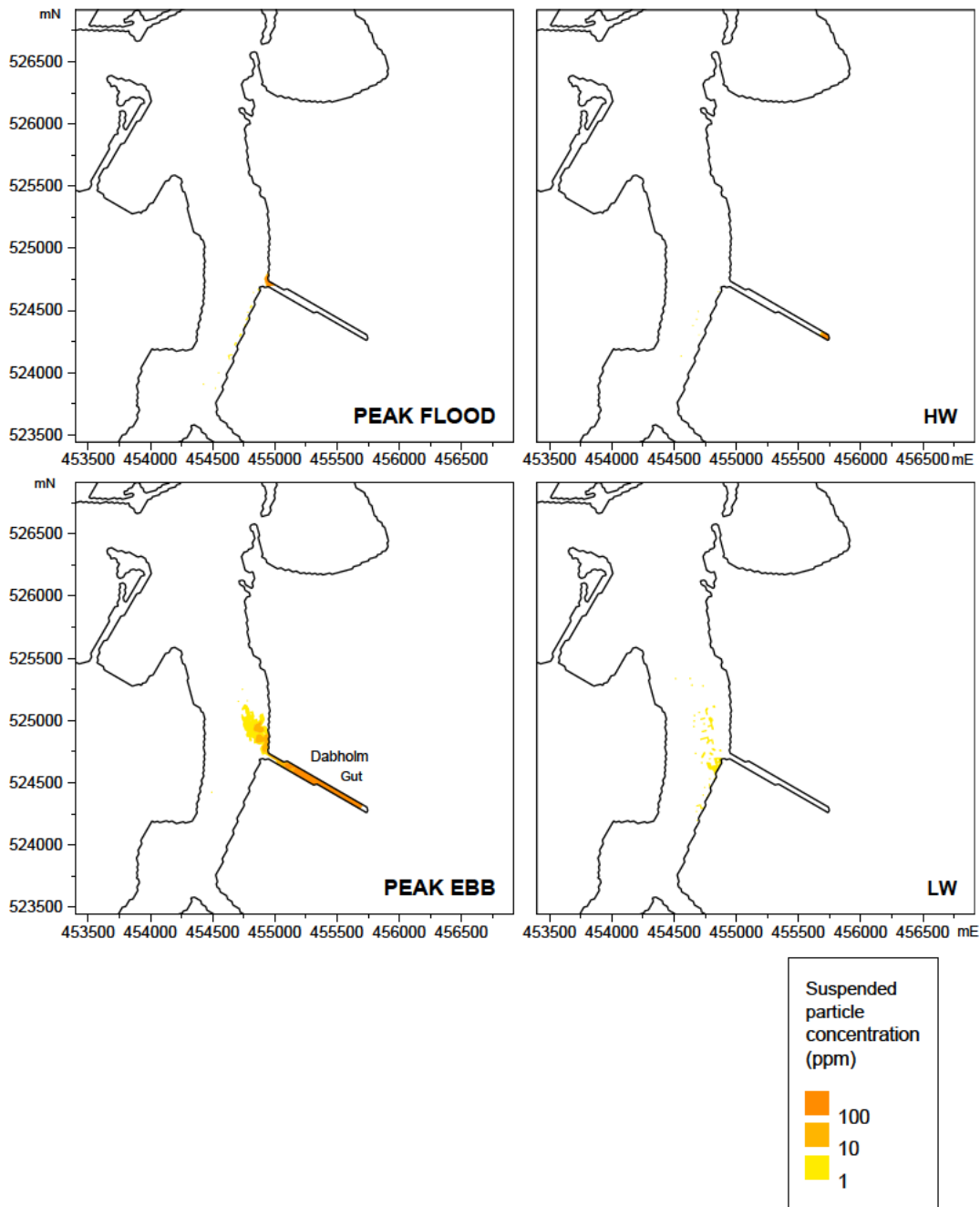


Figure 5.35 Depth-averaged suspended particle concentrations. Proposed layout, neap tide, winter conditions

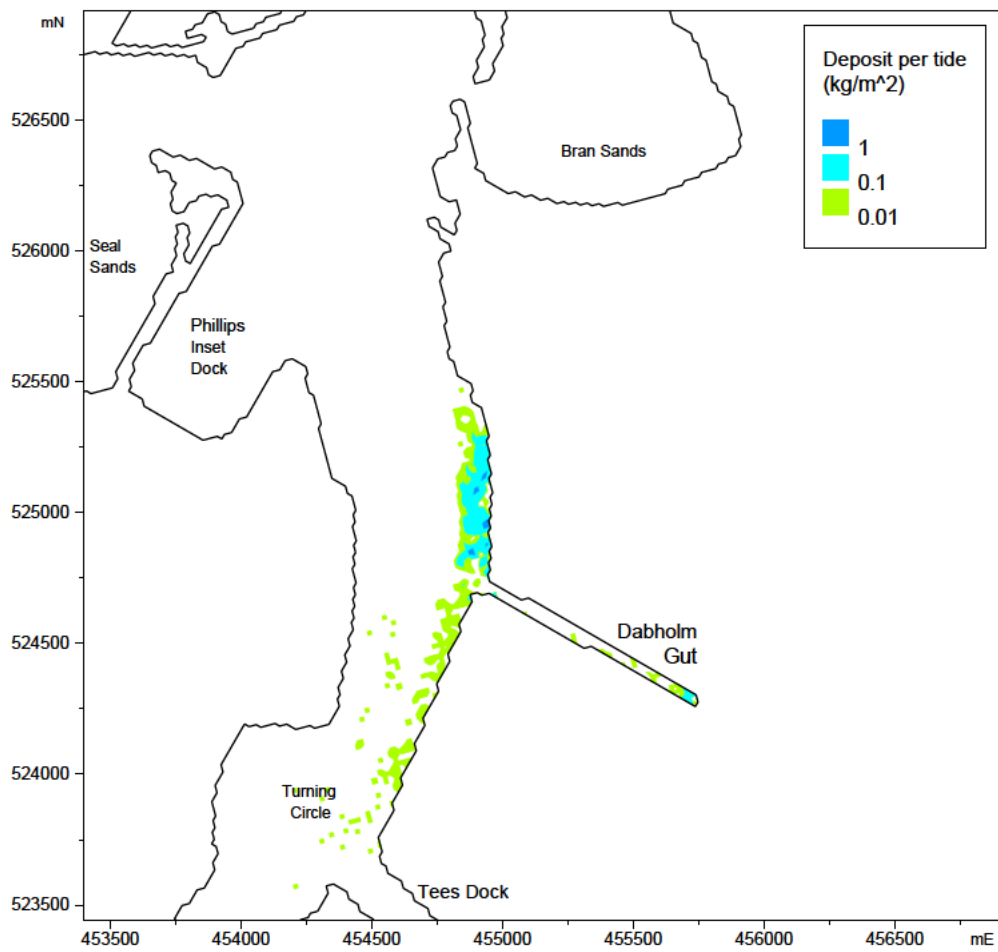


Figure 5.36 Increase in deposits over a tidal cycle – Proposed layout, neap tide, winter conditions

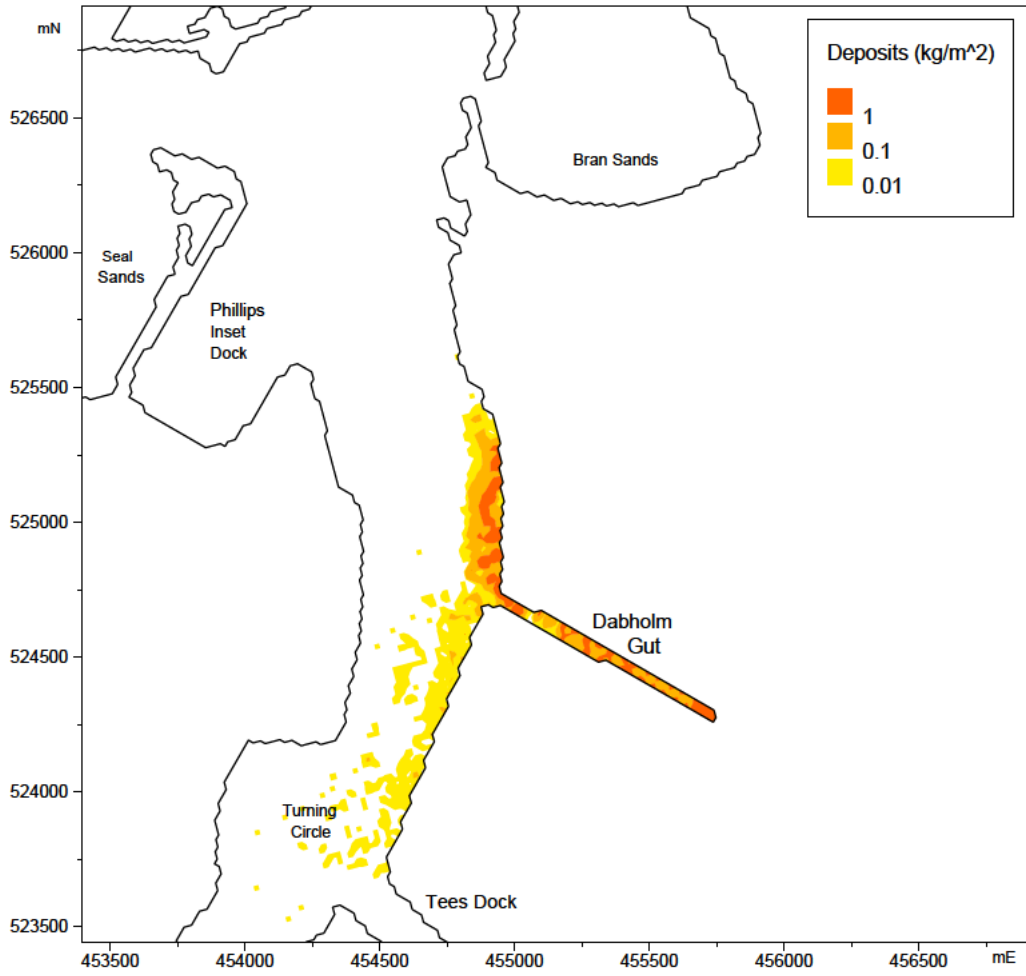


Figure 5.37 Distribution of maximum deposits over the tidal cycle. Proposed layout, neap tide, winter conditions

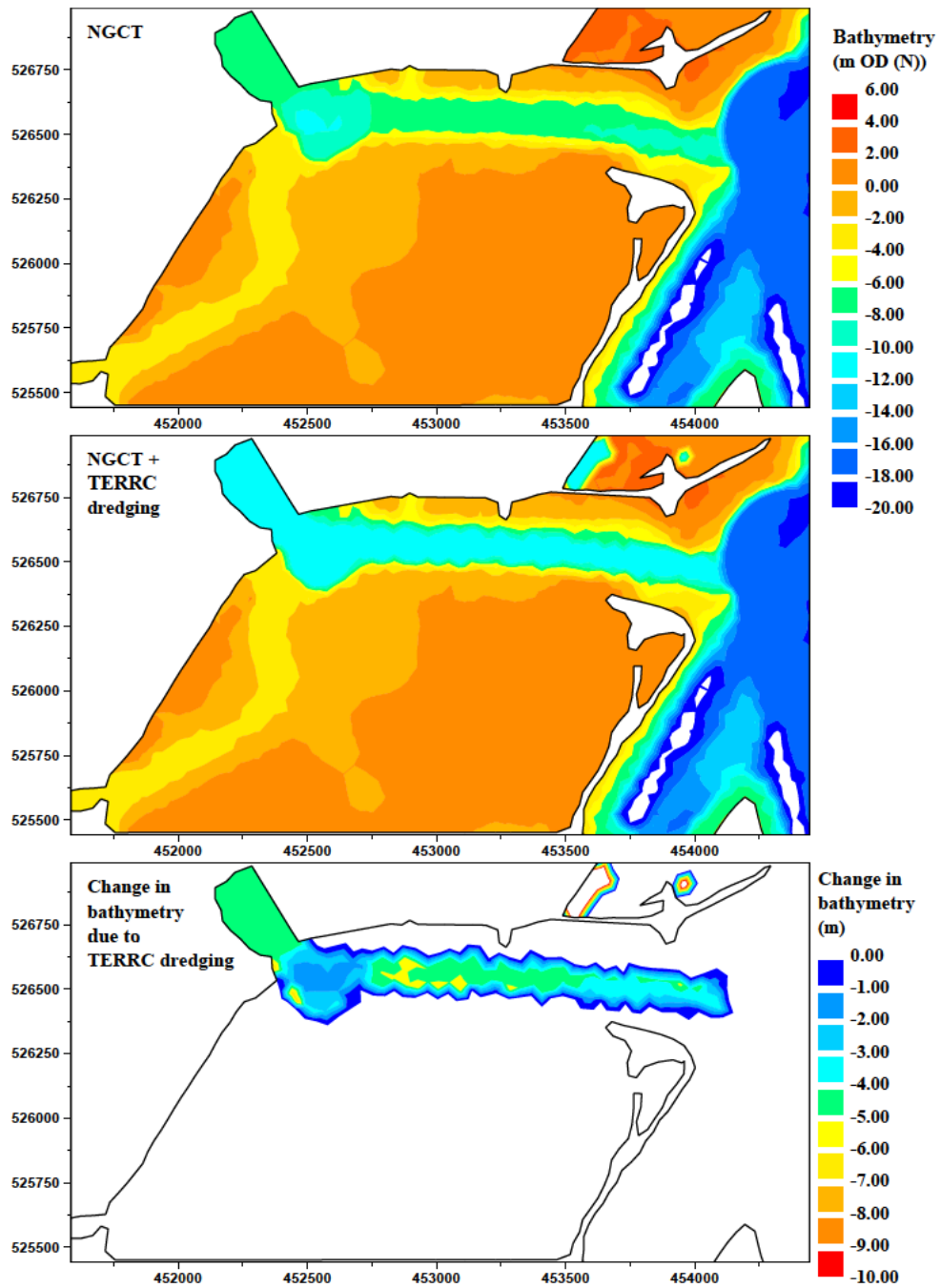


Figure 6.1 Model bathymetry for in-combination test

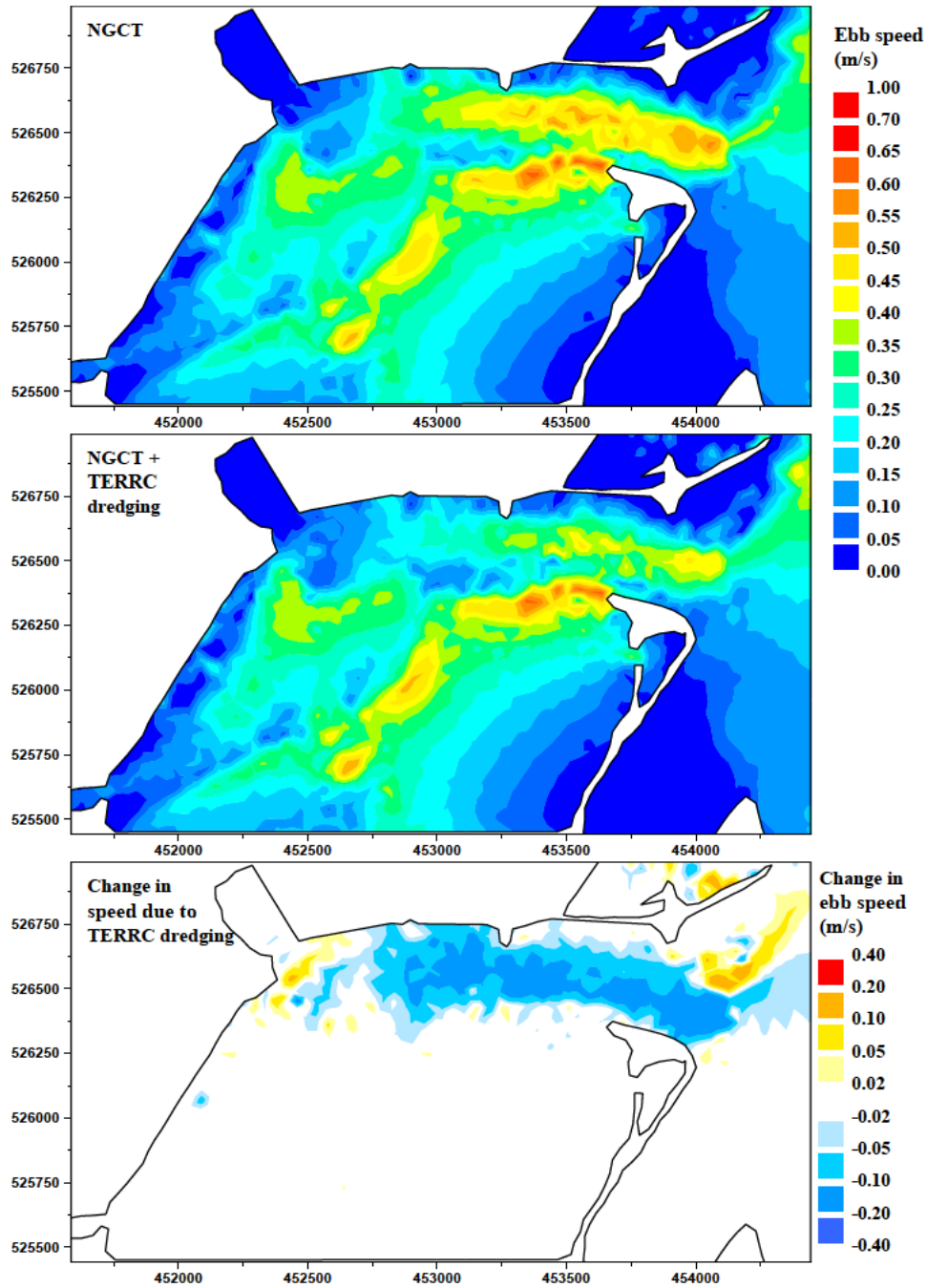


Figure 6.2 Peak ebb tidal currents before and after Seaton Channel deepening

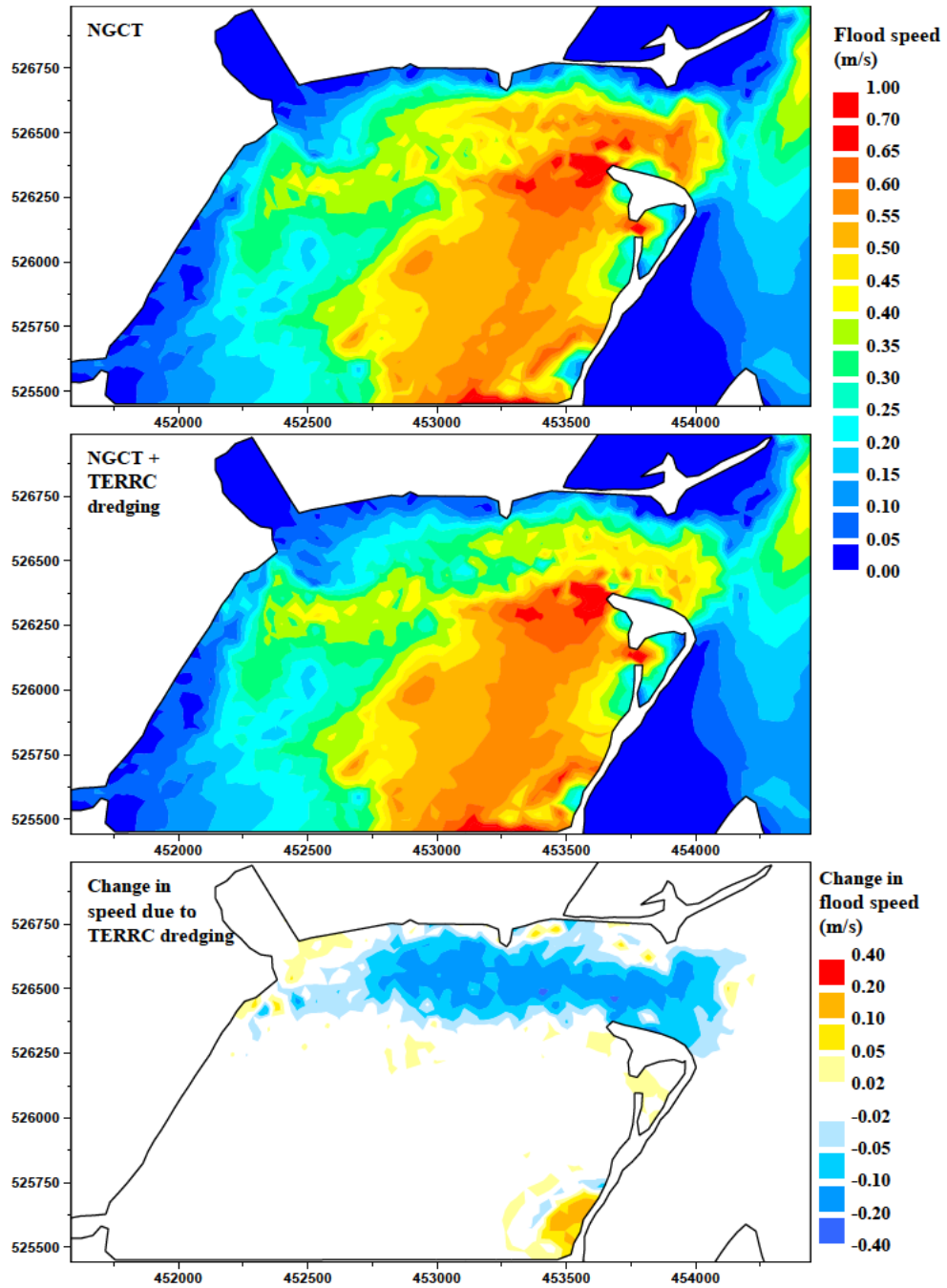


Figure 6.3 Peak flood tidal currents before and after Seaton Channel deepening

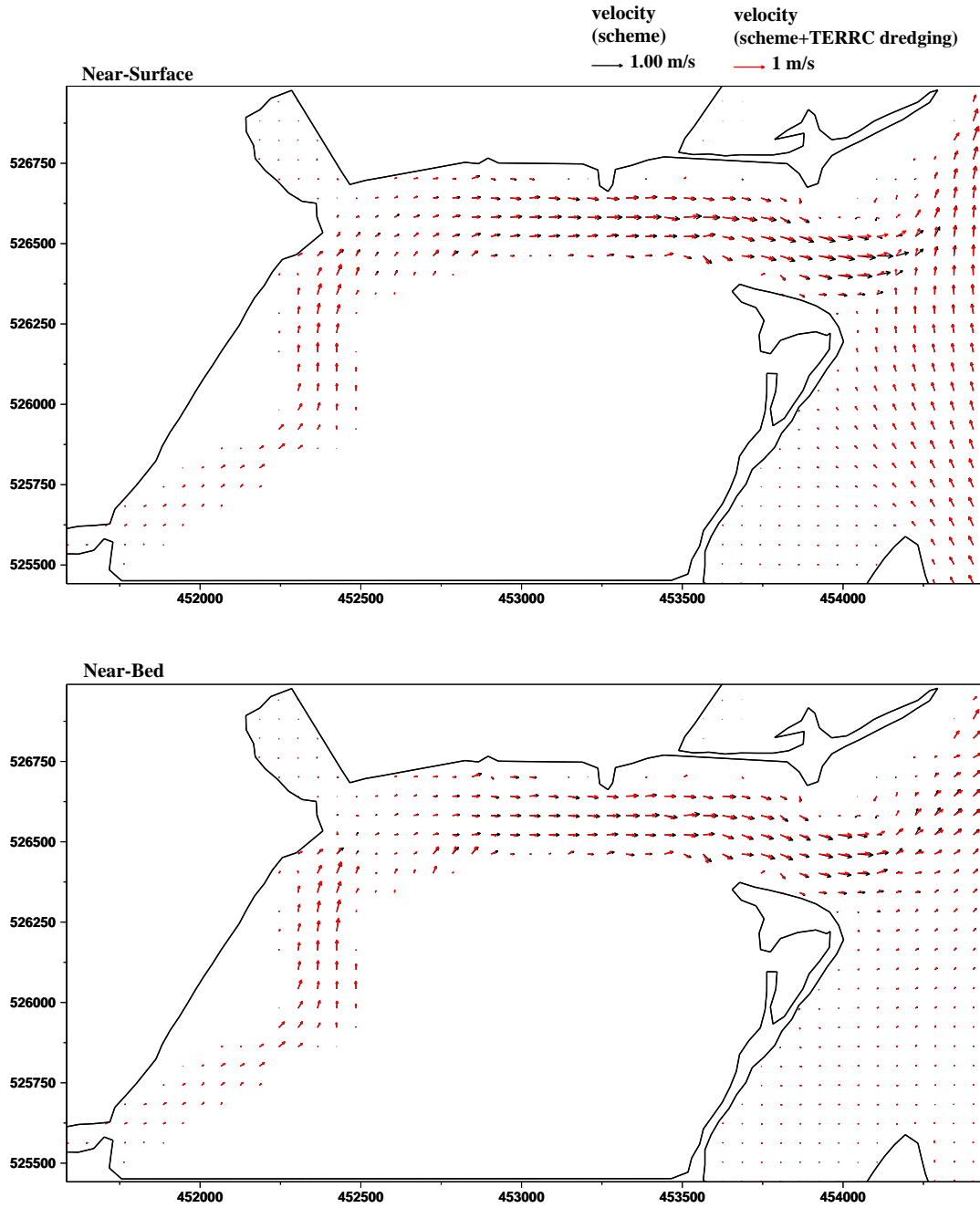


Figure 6.4 Peak ebb tidal current patterns before and after Seaton Channel deepening

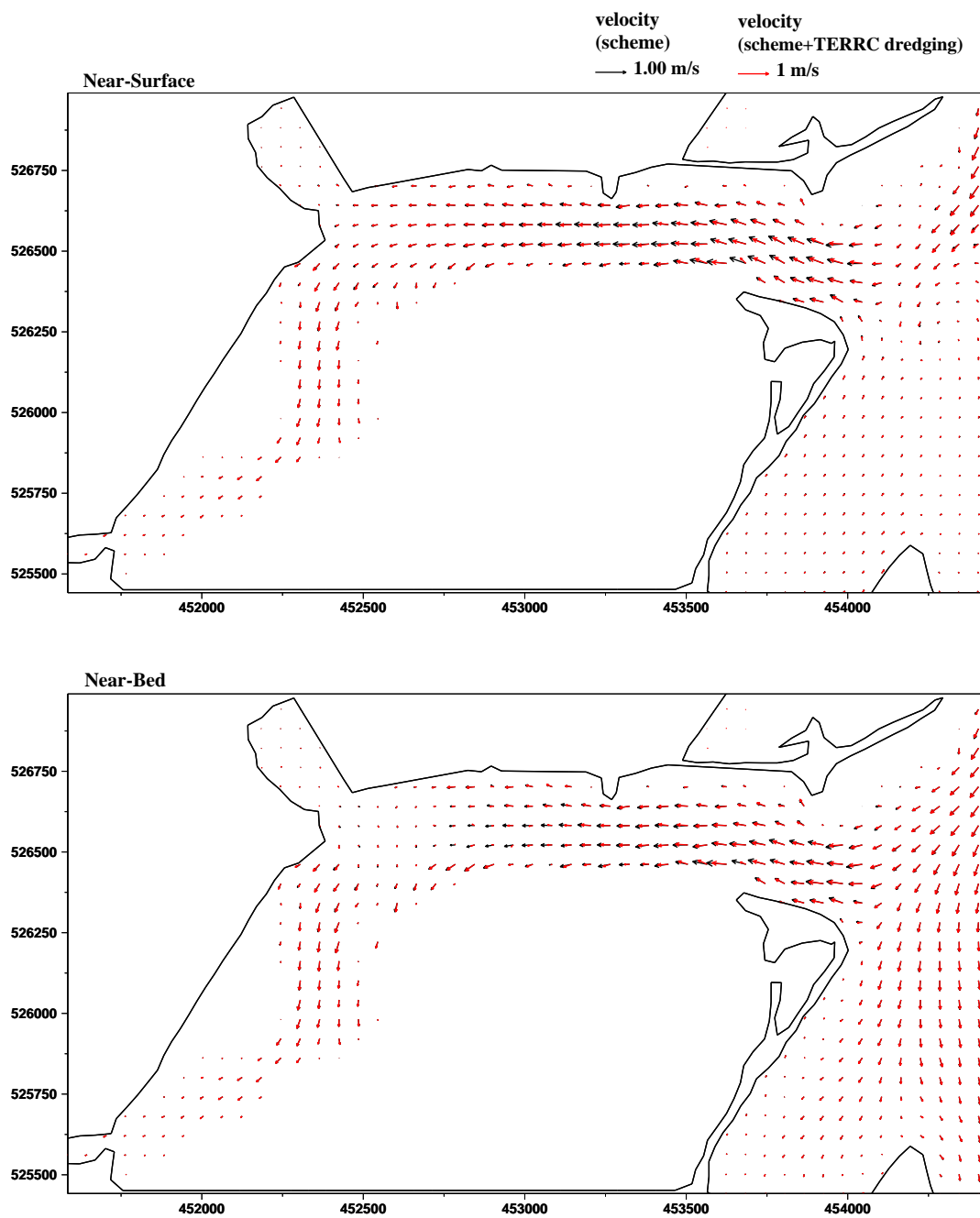


Figure 6.5 Peak flood tidal current patterns before and after Seaton Channel deepening

Location: Seaton 2
Model runs: schme_sp_wet/schme+terrc_sp_wet
Layout = scheme/scheme+TERRC dredging
Tide = mean spring
Discharge = 60 cumecs

Scheme speed *Scheme+TERRC dredging* speed
 ◊ direction ◊ direction

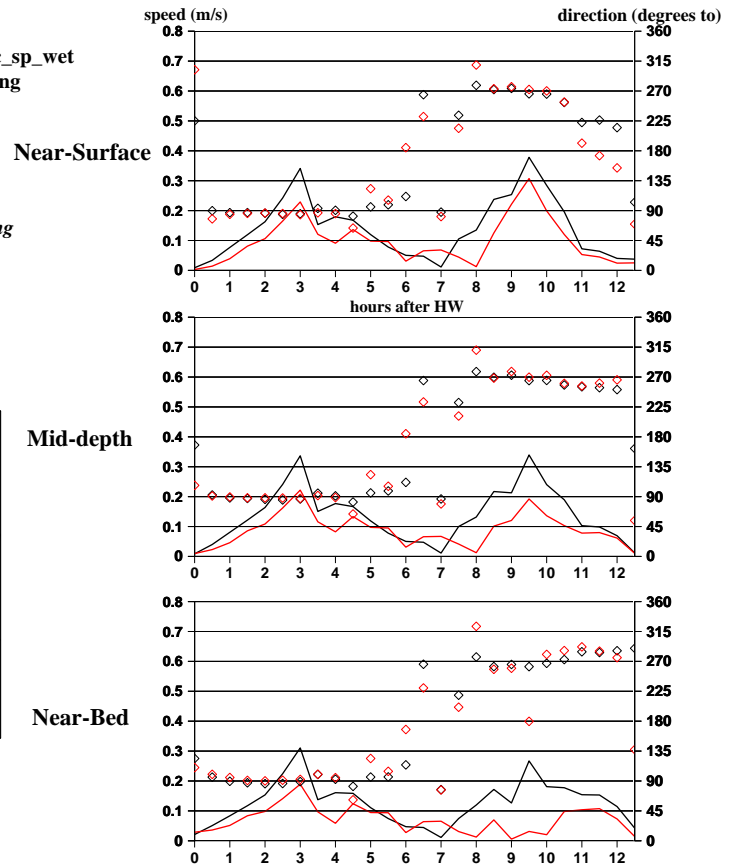
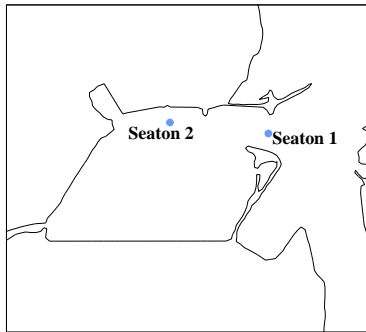


Figure 6.7 Time series of 3D currents near power station intake to Seaton Channel before and after Seaton Channel deepening

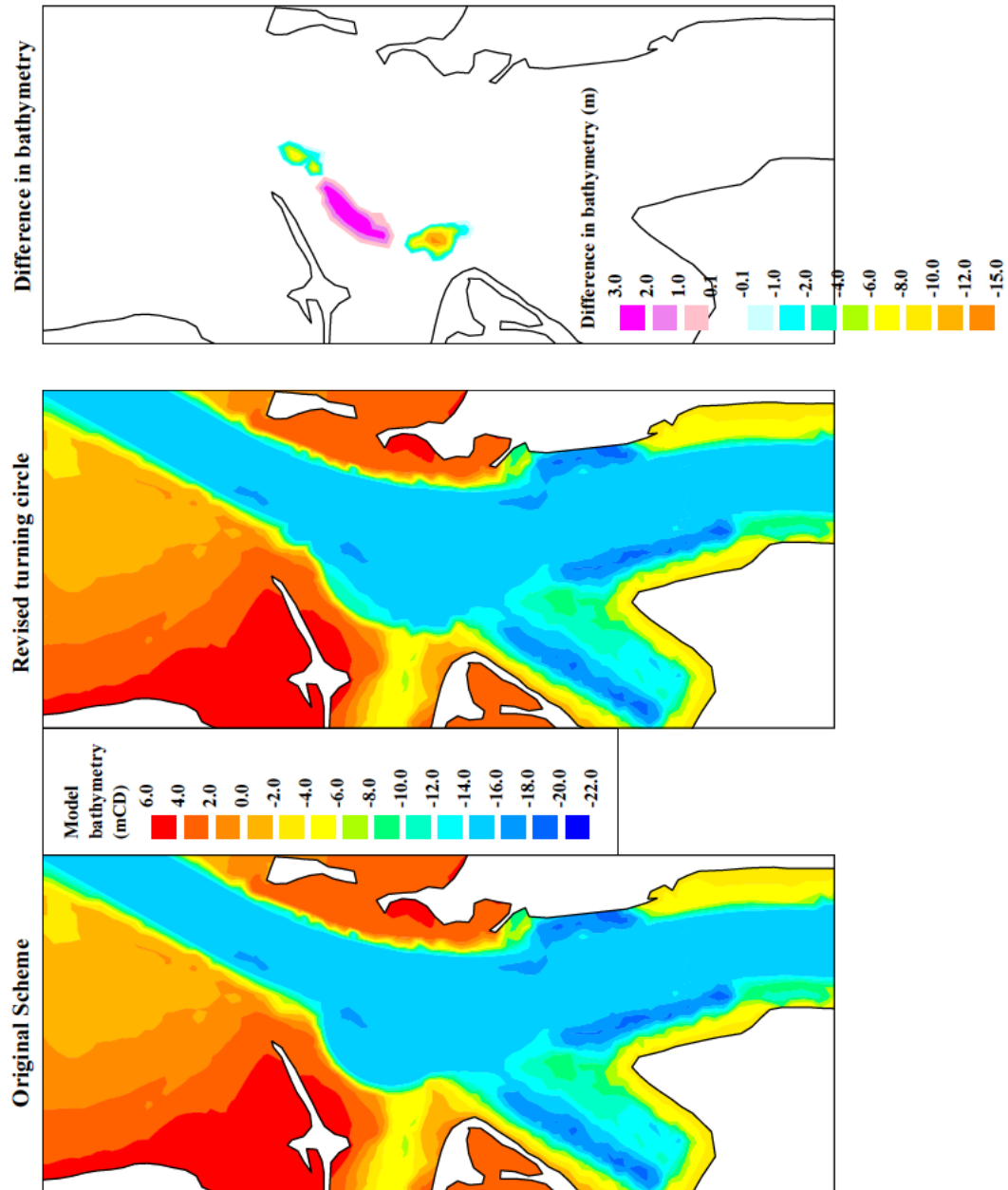


Figure 7.1 Model bathymetries used for sensitivity test

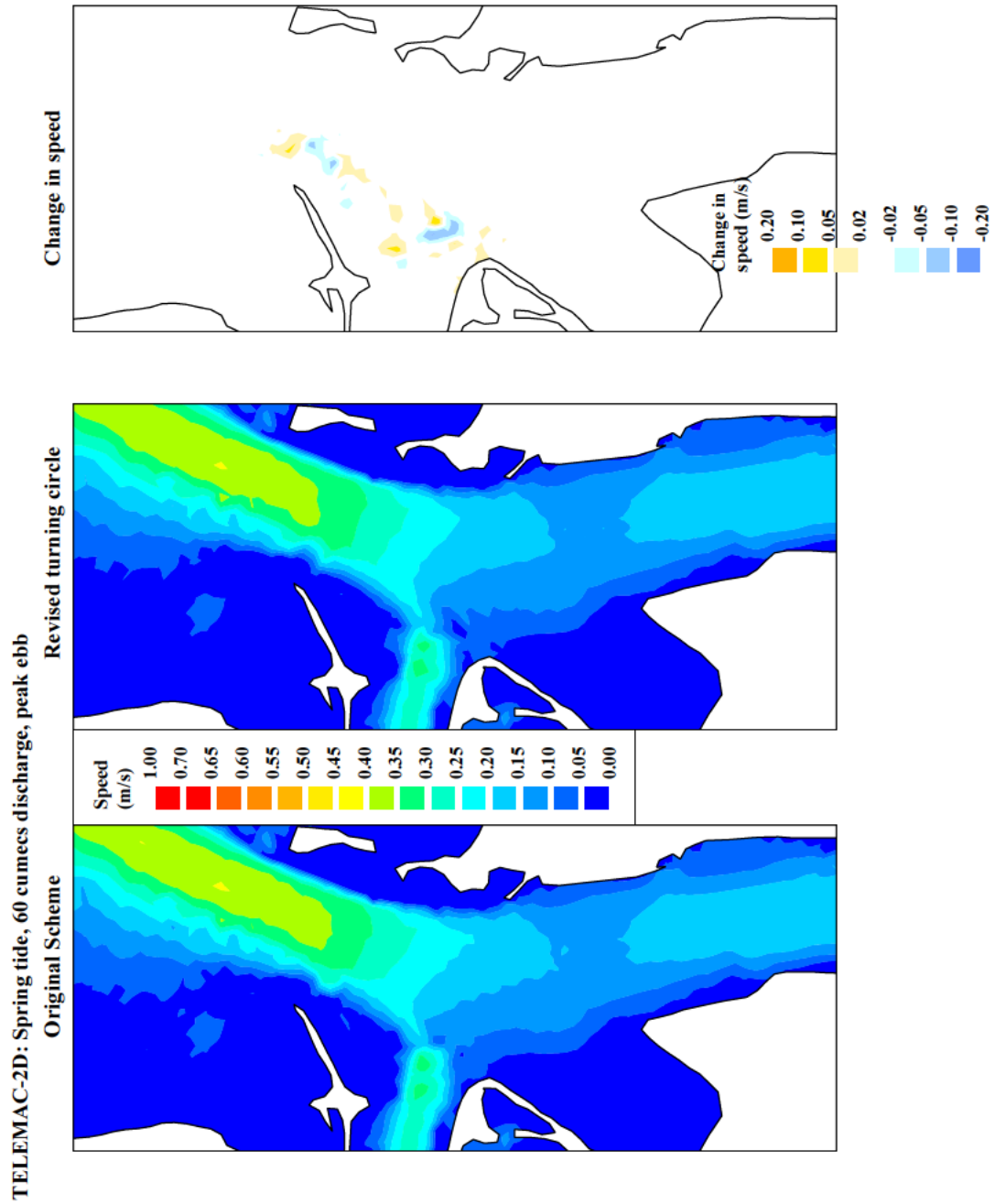


Figure 7.2 Sensitivity of peak ebb current magnitude to amended dredging

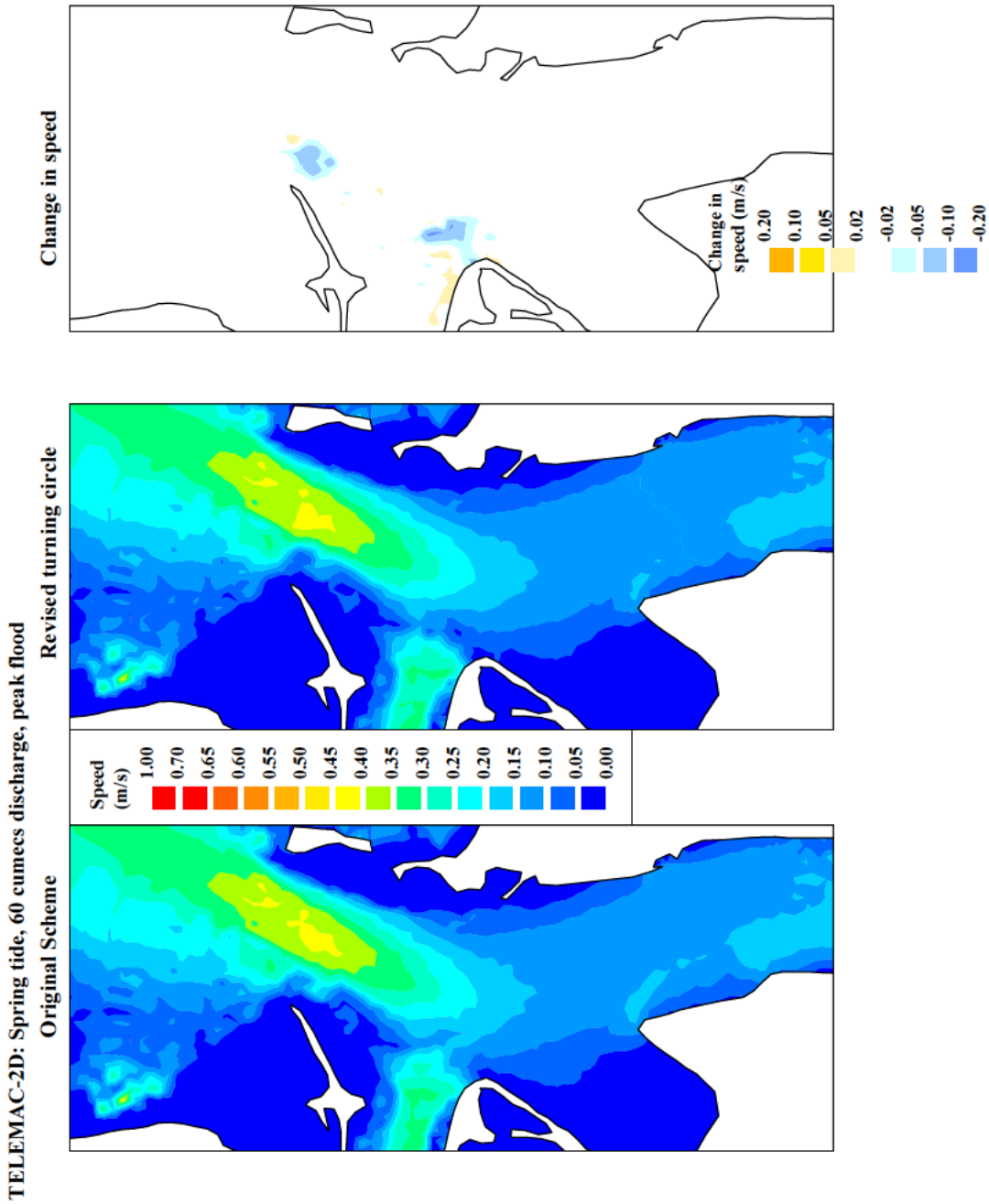


Figure 7.3 Sensitivity of peak flood current magnitude to amended dredging

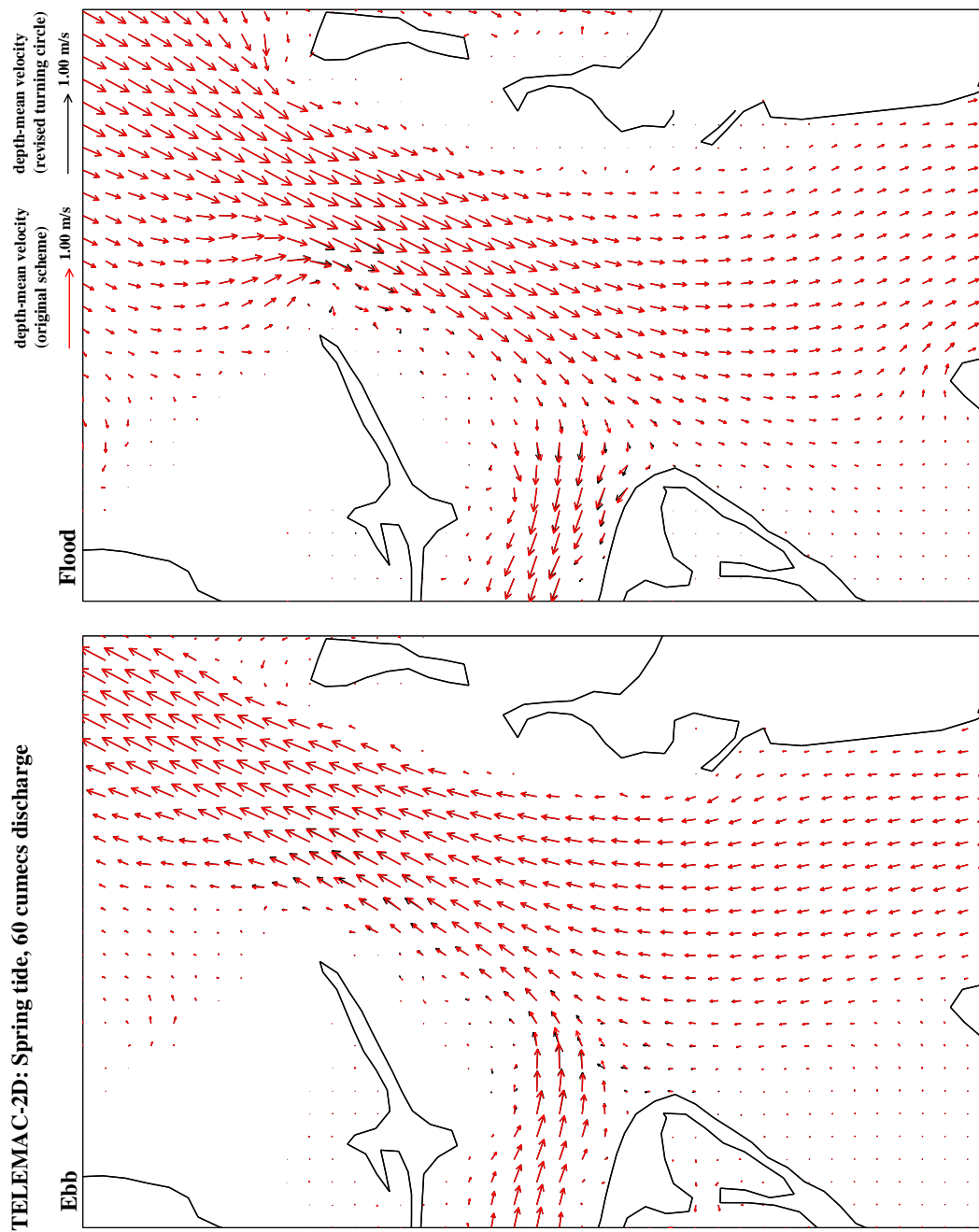


Figure 7.4 Sensitivity of peak tidal current pattern to amended dredging

